Morphologie und Entwicklung des Nervensystems der Cephalocarida (Crustacea) in Bezug auf Evolution und Phylogenie der Tetraconata

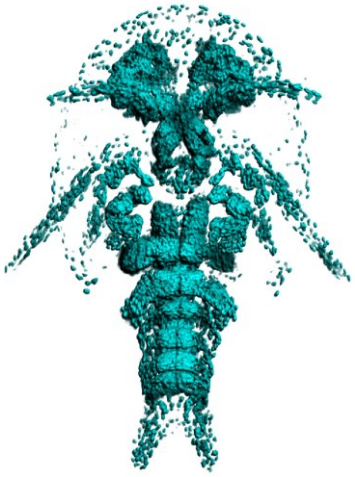

Kumulative Dissertation

zur Erlangung des Doktorgrades der Naturwissenschaften

an der Mathematisch-Naturwissenschaftlichen Fakultät

der Universität Rostock

vorgelegt durch

Martin Ernst Josef Stegner

Rostock 2014

urn:nbn:de:gbv:28-diss2016-0084-4

Gutachter

Prof. Dr. Stefan Richter (Betreuer), Universität Rostock, Institut für Biowissenschaften, Allgemeine & Spezielle Zoologie

Prof. Dr. Steffen Harzsch, Ernst-Moritz-Arndt-Universität Greifswald, Zoologisches Institut und Museum, Cytologie und Evolutionsbiologie

Datum der Einreichung: 24. Oktober 2014

Datum der Verteidigung: 12. Dezember 2014

Inhalt

Gliederung der Dissertation

Diese kumulative Dissertation besteht aus der zusammenfassenden Einleitung, dem Hauptteil aus insgesamt vier Publikationen sowie dem Schlussteil.

Die zusammenfassende Einleitung umfasst Kapitel 1 bis 9: Sie führt zunächst mit einer allgemeinen Vorstellung des Taxons der Cephalocarida (Kapitel 1) über deren evolutionsmorphologische und (neuro-)phylogenetische Bedeutung (Kapitel 2) zu den Zielen der Dissertation (Kapitel 3). Es folgt der Ergebnisteil aus Kapiteln 4 (Adultus) und 5 (Entwicklungsstadien), der die verschiedenen Publikationen zur Cephalocaridenart *Hutchinsoniella macracantha* Sanders, 1954 zusammenfasst. Dabei basiert die Beschreibung des adulten Gehirns (Kapitel 4.1) auf Stegner & Richter (2011; Kapitel 10) und Stegner et al. (2014a; Kapitel 11). Die allgemeine Übersicht zum Nervensystem zu Beginn des Kapitels 4 sowie die Beschreibung des adulten Bauchmarks (Kapitel 4.2) basieren auf Stegner et al. (2014b; Kapitel 12). Der Beschreibung der Entwicklung des Nervensystems der Cephalocarida (Kapitel 5.2) ist eine kurze Revision der Larvalentwicklung von *H. macracantha* vorangestellt, die im Zuge der Dissertation vorgenommen wurde (Kapitel 5.1), – beide Abschnitte basieren auf Stegner & Richter (2015; Kapitel 13). Im Diskussionsteil werden ausgewählte Merkmalskomplexe mit Blick auf die potentielle Homologien zwischen Cephalocarida und anderen Arthropoda verglichen (Kapitel 6) und schließlich die phylogenetische Bedeutung dieser Merkmale zusammenfassend dargestellt (Kapitel 7). Dabei werden die einzelnen Erkenntnisse und Hypothesen aus den vier Publikationen (Kapitel 10 bis 13) verknüpft und in einem allgemeinen evolutionären und phylogenetischen Zusammenhang beleuchtet. Die zusammenfassende Einleitung endet mit einem eigenen Abkürzungs- (Kapitel 8) und Literaturverzeichnis (Kapitel 9).

Den Hauptteil bilden die vier zugrundegelegten Publikationen (Kapitel 10 bis 13) und den Schlussteil akademischer Lebenslauf und Danksagung.

Nomenklatur und Präsentation der Daten

Nomenklatur

Die in dieser zusammenfassenden Einleitung verwendete Nomenklatur folgt weitgehend dem neuroanatomischen Glossar von Richter et al. (2010) sowie den nomenklatorischen Ergänzungen zum Zentralkomplex durch Stegner et al. (2014a). Die meisten Begriffe besitzen traditionelle deutsche Entsprechungen oder konnten problemlos eingedeutscht werden. ‚Bauchmark' steht hier für ‚ventral nerve cord' nach Richter et al. (2010).

Präsentation

Folgende wichtige Abkürzungen werden durchgängig im Text der zusammenfassenden Einleitung verwendet: (1) die Abkürzungen für spezifische neuroaktive Substanzen: **HI/HIR** – Immunreaktivität/immunreaktiv gegen histamin-artige Substanzen; **RFI/RFIR** – Immunreaktivität/immunreaktiv gegen RFamid-artige Substanzen; **SI/SIR** – Immunreaktivität/immunreaktiv gegen serotonin-artige Substanzen; (2) die Abkürzungen für Segmente: **Md, Mx1, Mx2** – Mandibel-, Maxillular-, Maxillarsegment; **Th1-Th9** – Thorakalsegment 1 bis 9, **Ab1-Ab10** – Abdominalsegment 1 bis 10; (3) die Abkürzungen für Entwicklungsstadien: **E1, E2** – Embryonalstadien 1 und 2; **L1-L23** – Larvalstadien 1 bis 23.

Wenn nicht anders angegeben, so liegt in allen Abbildungen die Dorsalseite bzw. das anteriore Ende oben. Alle spezifisch gefärbten Substanzen werden direkt in der Abbildung angegeben, in Abb. 8 ebenso das Entwicklungsstadium. Weitere Details zu Fixierung, Präparation, Immunhistochemie, Mikroskopie und Bildverarbeitungssoftware sind im Material- und Methodenteil der zugrundeliegenden Publikation angegeben, die in der Abbildungslegende vermerkt ist.

Zusammenfassende Einleitung

1. Einführung in die Cephalocarida

1.1. Einstieg in das Taxon

Gegen Mitte des zwanzigsten Jahrhunderts entdeckte der amerikanische Meeresbiologe Howard Sanders im Bodenschlamm des nordatlantischen Long-Island-Sunds einen blinden, nur 3 mm langen Krebs und beschrieb diesen als *Hutchinsoniella macracantha*, den ersten Vertreter des bis dahin unbekannten Taxons der Cephalocarida (Sanders 1954). Inzwischen wurden 13 marine Cephalocaridenarten in fünf Gattungen beschrieben, die sich morphologisch stark ähneln und über die ganze Welt verteilt sind. Aus evolutionsbiologischer Sicht war die Entdeckung des neuen Taxons eine Sensation, weisen doch Cephalocarida gleich mehrere äußere morphologische Merkmale auf, die innerhalb der rezenten Crustacea einzigartig sind und bis zum Vorfahren aller Crustacea, Mandibulata oder gar Arthropoda zurückverfolgt wurden. Anschauliche Beispiele sind der namensgebende hufeisenförmige Kopfschild – Cephalocarida werden auch als Hufeisengarnelen (horseshoe shrimp) bezeichnet – oder die thorakopodenförmige Maxilla (z. B. Sanders 1957; siehe Kapitel 2.1). Bereits in seiner Erstbeschreibung von *H. macracantha* prägte Sanders (1954) das Bild eines „extrem primitiven Krebses", welches sich später in verschiedenen Hypothesen zur Phylogenie und Evolution der Crustacea wiederfand (Sanders 1957; Hessler 1964; Hessler & Newman 1975; Lauterbach 1986) und in verändertem Wortlaut bis heute nachwirkt (Hessler 1984: „living fossil without a fossil record"; Hessler & Elofsson 1992, Read et al. 1994: „the most primitive living crustacean"; Addis et al. 2007: „ancient crustacean"). Zwar muss im Rahmen einer phylogenetischen Systematik dieses Bild als grobe Vereinfachung angesehen werden, schon aufgrund offenkundiger Autapomorphien der Cephalocarida wie der Augenlosigkeit (Sanders 1954) oder des Hermaphroditismus (Hessler et al. 1995; Ax 1999). Dennoch steht außer Zweifel, dass das Taxon bis heute eine Schlüsselrolle im kontroversen Diskurs um Phylogenie und Evolution der Arthropoda spielt (Sanders 1957; Hessler 1964; Lauterbach 1986; Scholtz & Edgecombe 2006; Olesen et al. 2011; von Reumont et al. 2012; Richter et al. 2013). Dem enormen evolutionsbiologischen Interesse steht eine auffällig geringe Zahl morphologischer und molekularer Studien gegenüber, die allesamt auf nur

wenigen Individuen basieren (zuletzt zusammengefasst durch Addis 2008; siehe zusätzlich Shimomura & Akiyama 2008; Stuardo & Vega 2011; Olesen et al. 2011). Der einfache Grund ist, dass die begehrten Tiere trotz ihrer weltweiten Verbreitung nur schwer zu finden sind. Obwohl die Habitate der 13 Arten vom Intertidal über das küstennahe Subtidal bis in die Tiefsee reichen und ökologisch entsprechend divers sind (Hessler & Sanders 1973), besiedeln Cephalocarida stets nur jene Meeresböden, in deren lockerer Oberschicht sich angeschwemmtes oder absinkendes organisches Material ablagern kann (siehe auch De Troch et al. 2000; Carcupino et al. 2006). Diese nährstoffreiche Schicht bietet auch zahlreichen anderen Bodenorganismen wie Polychäten, Muscheln oder Peracariden eine Lebensgrundlage und wird durch deren perturbierende Bewegungen locker, sauerstoffreich und trübe gehalten (Sanders 1963; De Troch 2000; Addis 2008). Die Sammelprozedur in diesem Substrat umfasst zeitintensive Hol-, Spül-, Siebe- und Ausleseschritte und wird zusätzlich durch eine auffällig niedrige Abundanz der Cephalocarida in den Proben verkompliziert (De Troch et al. 2000; Carcupino et al. 2006; auch bestätigt durch eigene Erfahrungen). Die über einhundert Exemplare von *H. macracantha*, die im Verlaufe dieser Dissertation gesammelt werden konnten, boten eine seltene Gelegenheit, das Taxon näher zu erforschen.

1.2. Äußere Morphologie

Der Körper der Cephalocarida ist in ein Cephalon (Kopf) und einen 19-segmentigen Rumpf gegliedert[1] (Abb. 1A; detailreich bei Sanders 1957, 1963; Carcupino et al. 2006; Olesen et al. 2011; Stuardo & Vega 2011). Das Cephalon trägt den Kopfschild, der die präantennale Region und die fünf vorderen extremitätentragenden Segmente (Antennula, Antenna, Mandibel, Maxillula, Maxilla) weiträumig überdeckt (Abb. 1A,B). Der Rumpf wird in einen 9-segmentigen Thorax mit weitgehend homonomen Thorakopoden und ein 10-segmentiges, extremitätenloses Abdomen untergliedert, das posterior im Telson (hier nicht als Segment gezählt) endet (Abb. 1A). Als Besonderheit der Cephalocarida gleicht die Maxilla weitgehend den auf sie folgenden

[1] Sanders'(1954) anfängliche Fehlinterpretationen, das Maxillarsegment gehöre zum Thorax und der Rumpf sei 18-segmentig, wurden rasch korrigiert (Sanders 1957).

Thorakopoden und bildet mit diesen einen Filterapparat, dessen metachroner Beinschlag sowohl dem Schwimmen als auch der Ernährung dient (Abb. 1A,B; Sanders 1963). Diese Doppelfunktion spiegelt sich auch im Aufbau der Extremitäten wider („Mixopodien" nach Sanders 1957): Der Protopodit trägt medial mehrere gnathale Endite, die Nahrungspartikel nach anterior durch die Nahrungsrinne (grauer Pfeil bzw. Stern in Abb. 1A,C) zum Mundbereich transportieren, welchen ein mächtiges Labrum überragt (Abb. 1B,C). Er trägt außerdem distal einen meist 6-gliedrigen Endopodit und einen 2-gliedrigen, paddelartigen Exopodit (Abb. 1B,C). Die genaue Insertionstelle des paddelartigen Pseudepipodits ist umstritten (Sanders 1963, Hessler & Elofsson 1992: am Protopodit; Richter 2002: am Epipodit), da er etwa in der lateralen Achsel zwischen Protopodit und Exopodit sitzt (angedeutet durch Strichlinie rechts auf Abb. 1C; ebenso nach Olesen et al. 2011: *Lightiella monniotae*). Die sukzessive Verkleinerung und Abwandlung der Thorakopoden in den posterioren Thorakalsegmenten wird ebenso wie die Beborstung taxonomisch herangezogen (Hessler & Sanders 1973; Carcupino et al. 2006). Der 9. Thorakopod ist zu einem kleinen Eiträger umgewandelt (Abb. 1A; Sanders 1957; Hessler et al. 1995), der ein großes Ei trägt.

1.3. Sinnesorgane und Nervensystem

Beinahe alle Kenntnisse der inneren Morphologie der Cephalocarida verdanken wir Untersuchungen der beiden Morphologen Robert Hessler und Rolf Elofsson an der Art *H. macracantha* (Hessler 1964: Skelettmuskulatur; Brown & Metz 1967: Spermien; Hessler et al. 1970, 1995; Addis et al. 2013: Reproduktionssystem; Hessler & Elofsson 1991, Elofsson & Hessler 1998: Drüsen; Elofsson et al. 1992: Verdauungssystem; Hessler & Elofsson 2001: Kreislaufsystem). Unter ihren Pionierstudien befinden sich auch die ersten Untersuchungen an Sinnesorganen und Nervensystem. Nachweisliche Sinnesorgane sind der Ästhetask der Antennula, die büschelartig angeordneten Setae auf Antennula und Antenna (Elofsson & Hessler 1991) sowie zahlreiche cilienassoziierte Setae und Poren auf Kopfschild und Rumpf (Elofsson & Hessler 1994), die in den entsprechenden Arbeiten allesamt als chemosensorisch interpretiert wurden. Die Beschreibung eines Komplexauges bei *H. macracantha* (Burnett 1981)

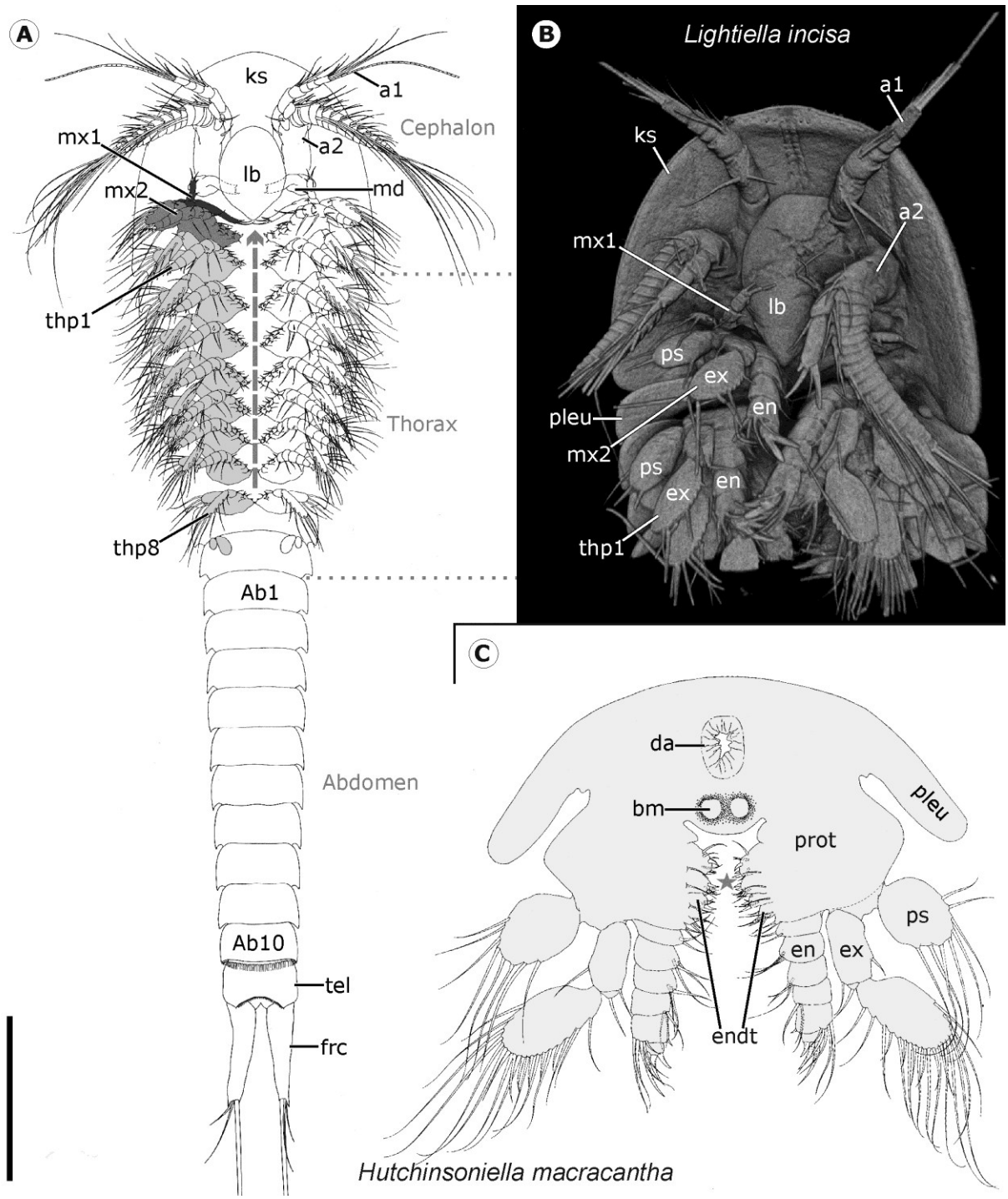

Abb. 1: Äußere Morphologie der Cephalocarida. A, C: Verändert nach Sanders (1963). B: Konfokale Autofluoreszenzmikrographie von *L. incisa*. A, B: Ventralansichten. Die Maxilla ist thorakopodenförmig. A: Pfeil zeigt Nahrungsrinne. C: Transversalansicht verdeutlicht Aufbau und Anordnung der Thorakopoden. Jeder Protopodit besitzt fünf bis sechs zur Nahrungsrinne (Stern) gerichtete, gnathobasische Endite. Die Insertionsstelle des Pseudepipodit ist umstritten – m. E. setzt er in der Achsel zwischen Exopodit und Protopodit an (Strichlinie rechts). Maßstab: 0,5 mm.

erwies sich als Fehlinterpretation (Elofsson & Hessler 1990; Stegner & Richter 2011). Elofssons und Hesslers (1990) vielbeachtete Pionierstudie des Zentralnervensystems von *H. macracantha* basiert auf Licht- und Transmissionselektronenmikroskopie. Demnach besitzt die Art zwar wie viele andere Crustaceen ein dreiteiliges Gehirn aus Proto-, Deuto-, Tritocerebrum und ein Bauchmark mit einem Unterschlundganglion und segmentalen Rumpfganglien. Die Autoren beschrieben aber auch erstmals die innerhalb der Crustacea einzigartige Organisation des olfaktorischen Systems und die Abdominalganglien bei *H. macracantha* – Strukturen, deren Komplexität nicht ins traditionelle Bild des „primitiven Krebses" passte und evolutionär schwer zu interpretieren war (Elofsson & Hessler 1990; siehe Kapitel 2.3). Elofsson (1992) wies erstmals einige serotonerge (SIRe) und FMRFamiderge (RFIRe) Neurone bei *H. macracantha* nach. Da er aber die Neurite dieser Neurone nicht verfolgen konnte, blieb ein verlässlicher Vergleich zu anderen Crustacea unmöglich (Elofsson 1992). Der bis zu dieser Dissertation letzte Beitrag zur Neuroanatomie der Cephalocarida, eine überarbeitete Lateralansicht des Nervensystems von *H. macracantha* (Hessler & Elofsson 1992), reicht nunmehr über zwanzig Jahre zurück. Die dramatischen Fortschritte auf den Gebieten der Neuroanatomie und Phylogenetik haben seither neue Fragen aufgeworfen, die eine grundlegende Neuuntersuchung des Cephalocariden-Nervensystems verlangen.

2. Cephalocarida in Evolutionsmorphologie und Phylogenetik

Angesichts einer Fülle unterstützender molekularer und morphologischer Daten wird im Rahmen dieser Dissertation davon ausgegangen, dass Arthropoda (Rota-Stabelli et al. 2011), Mandibulata (Edgecombe et al. 2003; Müller et al. 2003; Regier et al. 2010) und Tetraconata (Dohle 2001; Richter 2002; Ungerer & Scholtz 2008; von Reumont et al. 2012) monophyletische Taxa darstellen. Debatten um die Monophylie der drei Taxa wurden an anderer Stelle zusammengefasst (Fanenbruck 2005; Müller 2008). Unklar bleiben aber die phylogenetischen Beziehungen innerhalb der Tetraconata, also auch die Monophylie der Crustacea und die phylogenetische Stellung der Cephalocarida (Abb. 2; siehe auch Jenner 2010; von Reumont & Wägele

2014). Im Rahmen einer phylogenetischen Systematik kann ein Schwestergruppenverhältnis zwischen zwei Taxa nur durch gemeinsame Synapomorphien rekonstruiert werden (Sudhaus & Rehfeld 1992 nach Hennig 1966). Wie aber im Folgenden deutlich wird, sind potentielle Synapomorphien zwischen Cephalocarida und anderen Tetraconatentaxa selten und allesamt umstritten.

2.1. Morphologie-basierte Hypothesen (ohne Nervensystem)

Cephalocarida als Schwestergruppe der übrigen Crustacea. Frühe Morphologen sahen in den Cephalocarida die Schwestergruppe der übrigen Crustacea (Abb. 2A; z.B. Sanders 1957, 1963; Hessler 1964, 1984) und begründeten diese Stellung damit, dass viele Cephalocaridenmerkmale auf den Vorfahren aller Crustacea zurückgehen, so der Kopfschild, die thorakopodenförmige Maxilla (Sanders 1957; Lauterbach 1980); der Bau des „Mixopodiums" (nach Sanders 1957; Hessler & Newman 1975; Lauterbach 1979) oder die weitgehend homonomen Rumpfextremitäten (Sanders 1957; Hessler

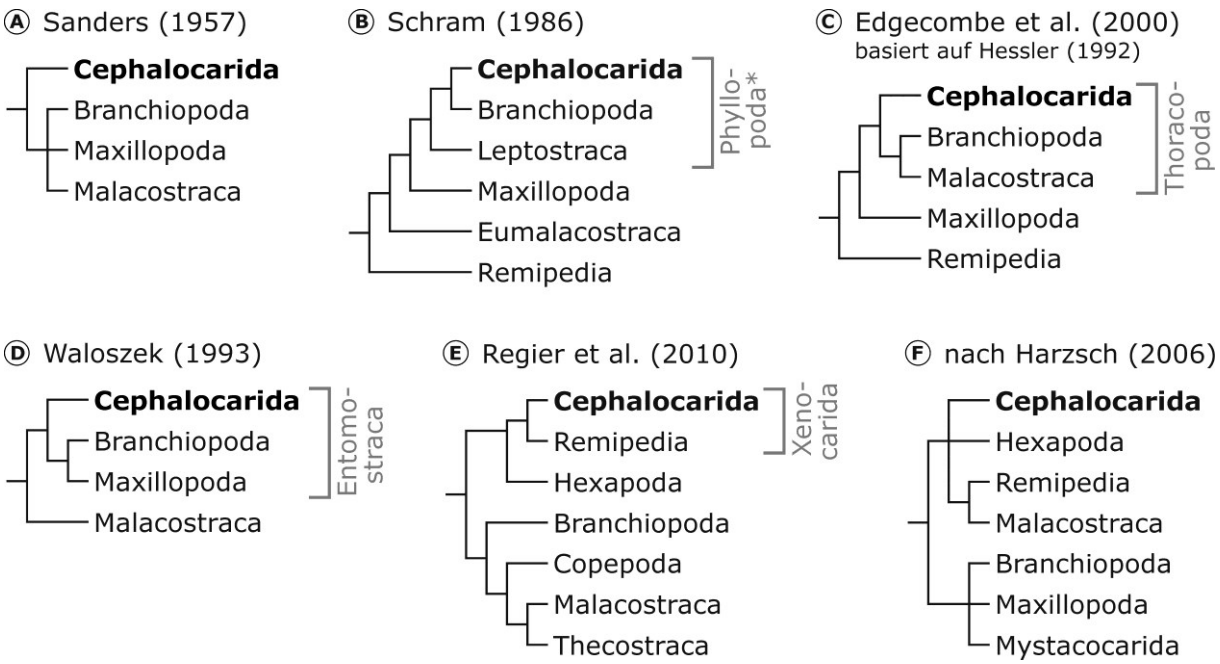

Abb. 2: Ausgewählte Hypothesen zur phylogenetischen Stellung der Cephalocarida innerhalb der Crustacea bzw. Tetraconata. Basierend auf extern-morphologischen (A-D), molekularen (E) sowie neuroanatomischen Daten (F). * Phyllopoda nach Schram (1986) nicht zu verwechseln mit dem gleichnamigen Branchiopodentaxon.

1984). Der heute viel umfangreichere Fossilbericht[2] legt nahe, dass mit Ausnahme des Pseudepipodits (s.u.) viele Cephalocariden-Merkmale tatsächlich von der Crustaceenstammart übernommene Plesiomorphien sind (Hessler 1992; Walossek 1993; Walossek & Müller 1998a; Scholtz & Edgecombe 2006; Haug et al. 2010). Allerdings treten all diese plesiomorphen Merkmale auch bei anderen Crustaceentaxa auf, wenn man auch fossile Vertreter wie *Rehbachiella* oder *Bredocaris* beachtet. So kann das Schwestergruppenverhältnis zwischen Cephalocarida und übrigen Crustacea durch keinerlei Synapomorphien gestützt werden. Dasselbe gilt für ein Schwestergruppenverhältnis zwischen Cephalocarida und übrigen Mandibulata nach Moura & Christofferson (1996), deren Studie die Maxilla falsch homologisiert.

Cephalocarida, Branchiopoda, Malacostraca und das Epipoditen-Problem. Frühe Einordnungen der Cephalocarida in die Nähe der Branchiopoda (Dahl 1956; Tiegs & Manton 1958; Siewing 1960) basierten auf Fehlinterpretationen der Maxilla (siehe Sanders 1963; Hessler 1984). Zahlreiche spätere Einordnungen basierten auf der bis heute umstrittenen Homologisierung des Pseudepipodits der Cephalocarida mit dem Epipoditen der Branchiopoda und Leptostraca. So begründete Schram (1986), der von einem remipedien-ähnlichen, zweiästigen Thorakopod in der Crustaceenstammart ausging (Schram 1983), das Monophylum Phyllopoda aus Cephalocarida, Branchiopoda und Leptostraca mit „vielästigen Blattbeinen" als Synapomorphie (Abb. 2B). Das ganz ähnliche Monophylum Thoracopoda (nach Hessler & Newman 1975), das zusätzlich die Eumalacostraca umfasst (Abb. 2C), wurde erstmals durch Hessler (1992) mit dem „Epipodit" als Synapomorphie begründet. Zwar präzisierte Ax (1999) diese Synapomorphie zu „Turgorextremitäten mit Epipoditen als Elemente eines thorakalen Filterapparats". Er klärte aber nicht, was genau mit „Filterapparat" gemeint sei – ein den Mundraum abschließendes Labrum (Labrophora nach Maas & Waloszek 2005) und weitgehend homonome Extremitäten mit gnathalen Enditen (Haug et al. 2010) könnten bereits in der Crustaceenstammart an einer anterograden Ernährung beteiligt gewesen sein. Die Homologie zwischen Epipodit auf der einen (Averof &

[2] Da unklar ist, wo die morphologisch stark abgeleiteten Hexapoda und Myriapoda von der/den Ahnenlinien der Crustacea abzweigten, lassen sich fossile Stammlinienvertreter der Mandibulata, Tetraconata und Crustacea schwer trennen (Richter 2002).

Cohen 1997; Olesen & Walossek 2000; Richter 2002; Pabst & Scholtz 2009) und Pseudepipodit auf der anderen Seite wurde bezweifelt, da sich die Beinglieder in ihrer Insertion (Protopodit vs. Exopodit) und Muskularisierung unterscheiden (diskutiert durch Olesen et al. 2011; siehe auch Richter 2002; Boxshall 2004). Maas et al. (2009) homologisierten zwar die Beinglieder der drei Taxa, allerdings auch epipoditen-ähnliche Strukturen bei anderen Taxa (siehe aber Boxshall 2004). Die Autoren vermuteten Epipoditen gar in der Crustaceenstammart (Maas et al. 2009), was sie als Synapomorphie der Thorakopoda ausschlösse. In zwei morphologisch-kladistischen Analysen wurden die Thoracopoda gestützt (Edgecombe et al. 2000; Bitsch & Bitsch 2004). Edgecombe et al. (2000) nannten als Apomorphien zusätzlich zum Epipodit anteriore Blindsäcke am Darm und den Verlust des präcoxalen Maxillula-Glieds. Nach Fanenbruck (2005) könnten die flagellenlosen Spermien der Cephalocarida, Branchiopoda und Malacostraca (basierend auf Brown & Metz 1967; Brown 1970; Wingstrand 1979) ein gemeinsames Reduktionsmerkmal der Thoracopoda darstellen, da andere Crustacea flagellierte Spermien besitzen. Insgesamt bleibt die Monophylie der Thoracopoda zweifelhaft.

Entomostraca. Walossek (1993) ordnete die Cephalocarida aufgrund ihres extremitätenlosen Abdomens den Entomostraca zu, worin sie die Schwestergruppe zu Maxillopoda + Branchiopoda bilden (Abb. 2D). Später bekräftigte der Autor die Entomostraca-Hypothese durch Merkmale der Mandibel, Maxillula und Maxilla, schwächte aber das Abdomen-Argument ab, weil beinlose Rumpfsegmente auch bei Leptostraca und diversen Fossilien außerhalb der Entomostraca vorkommen (Waloszek 2003).

Cephalocarida + Remipedia. Das mehrfach molekular gestützte Monophylum Xenocarida aus Cephalocarida und Remipedia (s. u.) erhielt bisher nur in einer morphologisch-kladistischen Analyse von Wheeler et al. (2004: ihre Abb. 17.3A,B) Zuspruch, Synapomorphien wurden aber nicht diskutiert. Kubrakiewicz et al. (2012) wiesen auf Übereinstimmungen in der Ovarienstruktur zwischen Cephalocarida (basierend auf Hessler et al. 1995) und Remipedia hin, deren phylogenetische Bedeutung aufgrund mangelnder Daten bei anderen Tetraconatentaxa aber unklar bleibt. Demnach ist bis heute keine morphologische Synapomorphie für Xenocarida bekannt.

2.2. Molekular-basierte Hypothesen

Gensequenzen liegen heute von den drei Cephalocaridenarten *H. macracantha*, *L. incisa* (nuklear und mitochondrial) und *L. magdalenina* (mitochondrial) vor (zusammengefasst durch Sanna et al. 2010). Bisherige molekularphylogenetische Analysen ergeben kein klares Bild: Sie zeigen Cephalocarida mal als Schwestergruppe zu den Malacostraca (Carapelli et al. 2007; Cook et al. 2005; Hassanin 2006); zu den Branchiopoda (von Reumont et al. 2009: ihre Abb. 3; Oakley et al. 2013: kombiniert mit morphologischen Daten); zu den Hexapoda (Lavrov et al. 2004; von Reumont et al. 2009: innerhalb der Hexapoda auf ihrer Abb. 4); zu den Remipedia (Abb. 2E nach Regier et al. 2010; Spears & Abele 1998; Giribet et al. 2001; Koenemann et al. 2010; Giribet & Edgecombe 2012); zu den Copepoda (Spears & Abele 1999; Hassanin 2006); oder in der Nähe der Cirripedia und Ostracoda (Giribet et al. 2005: ihre Abb. 5; Podsiadlowski & Bartolomaeus 2006: ihre Abb. 2). Thoracopoda werden durch molekulare Daten nicht gestützt, Entomostraca in nur einem Fall (Wheeler et al. 2004: ihre Abb. 17.6B kombiniert mit rezenten und fossilen morphologischen Daten). Schon Spears & Abele (1998) wiesen auf hohe Substitutionsraten in den Gensequenzen von Cephalocarida und Remipedia hin, welche in der phylogenetischen Rekonstruktion Artefakte wie Long Branch Attraction zur Folge haben. Vor diesem Hintergrund bleibt die „morphologisch unerwartete" (Giribet et al. 2001) Monophylie der Xenocarida auch von molekularer Seite her fraglich (kritisch diskutiert durch Koenemann et al. 2010; von Reumont et al. 2009, 2012; von Reumont & Wägele 2014). Auch an der durch Oakley et al. (2013) gestützten Verwandtschaft zwischen Cephalocarida und Branchiopoda bestehen Zweifel, da die morphologische Datenmatrix der Autoren mehrere fehlerhafte Codierungen[3] enthält. Gut gestützt ist heute eine nahe Verwandtschaft von Remipedia, Hexapoda und Branchiopoda, wobei unklar bleibt, in welchem Verhältnis Cephalocarida zu dieser Gruppe stehen

[3] Die Matrix liegt als Projekt 689 auf http://morphobank.org. Cephalocarida (*H. macracantha* und *Sandersiella* sp.) besäßen demnach z.B. Maxillipeden (Spalte 36), Komplexaugen (Spalte 47) oder einen Endopodit am 8. Thorakopoden (Spalte 56). Oakley et al. (2013) interpretieren den Pseudepipodit der Thorakopoden als Epipodit (Spalten 8, 127 sensu Hessler 1992, s. o.), nicht aber den dazu seriell homologen Pseudepipodit der Maxilla (Spalte 7).

(von Reumont et al. 2012). Nach Koenemann et al. (2010), die den Einfluss zahlreicher Rechenvariablen auf die Stabilität verschiedenster phylogenetischer Hypothesen prüften, stehen Cephalocarida den Hexapoda, Remipedia und Malacostraca näher als anderen Tetraconatentaxa.

2.3. Neurophylogenetische Hypothesen

Angesichts der bisherigen Schwierigkeiten, die phylogenetische Position der Cephalocarida mithilfe extern-morphologischer und molekularer Daten zu rekonstruieren, liegt es nahe, die innere Morphologie heranzuziehen. Das Nervensystem der Arthropoda wurde in den vergangenen zwei Jahrzehnten Gegenstand einer überwältigenden Anzahl vergleichend-morphologischer Studien (siehe Strausfeld et al. 1998; Harzsch 2006, 2007; Strausfeld & Andrew 2011; Loesel et al. 2013; Loesel & Richter 2014). Bedeutende methodische Fortschritte im Bereich der Immunhistochemie, Laser-Scanning-Mikroskopie und computergestützten Bildverarbeitung und das gewachsene phylogenetische Interesse an neuroanatomischen Daten bildeten die Grundlage für ein neues Forschungsfeld, für welches Harzsch (2006) den Begriff ‚Neurophylogeny' (Neurophylogenetik) prägte. Auch wenn Elofssons & Hesslers (1990) frühe Untersuchungen des Cephalocariden-Nervensystems außerhalb dieses Diskurses stattfanden, erlaubte ihr Detailgrad bereits einen ersten Vergleich mit anderen Taxa. Für die Autoren selbst stellte das erstaunlich komplexe olfaktorische System der Cephalocarida eine Spezialisierung der blinden Tiere in ihrem flokkulenten Substrat dar (Hessler & Elofsson 1992: S. 23), eine Interpretation, die in der Literatur weite Verbreitung findet (siehe aber Diskussion). Hessler & Elofssons (1992) Annahme, die (vermeintliche) Spezialisierung spreche für ein frühes Abzweigen der Cephalocarida vom Crustaceen-Stammbaum, ist phylogenetisch nicht stichhaltig. Harzsch (2006), der die Tetraconaten-Phylogenie aufgrund einer Fülle neuroanatomischer Daten rekonstruierte, schlug ein Monophylum aus Cephalocarida, Hexapoda, Remipedia und Malacostraca vor (Abb. 2F), überwiegend gestützt durch Merkmale des olfaktorischen Systems. Harzschs (2006) Interpretation erlangte besondere Aufmerksamkeit, als die nahe Verwandtschaft zwischen den besagten Taxa auch aus molekularer Sicht gestützt wurde (Koenemann et al. 2010, s. o.). Ein weiterer phylo-

genetischer Merkmalskomplex ist das segmentale Muster SIRer Neurone im Bauchmark, die sich aufgrund der Lage ihres Somas und ihres Neuritenverlaufs individuell identifizieren und zwischen Taxa vergleichen lassen (Harzsch & Waloszek 2000; Harzsch 2003; Harzsch et al. 2005). Harzsch et al. (2005) vermuteten, dass ein Muster von zwei anterioren und zwei posterioren SIRen Neuronen pro Hemiganglion im Grundmuster der Tetraconata steht. Nach Elofsson (1992) schien das SIRe Muster bei *H. macracantha* (siehe Abschnitt 1.3.) zwar im Einklang mit dieser Hypothese, mangels verlässlicher Daten zum Neuritenverlauf war aber kein detaillierter Vergleich mit anderen Arthropoden möglich (Harzsch et al. 2005). Die Lücken im Verständnis der Neuroanatomie der Cephalocarida machten sich auch in der Diskussion um andere phylogenetische Merkmalskomplexe bemerkbar, so beim optischen System (z. B. Strausfeld 2005; Strausfeld 2012), beim Zentralkomplex im Protocerebrum (Homberg 2008; Strausfeld 2012) und bei Aspekten der Nervensystementwicklung (z. B. Stollewerk & Simpson 2005). Viele Autoren regten daher an, das Nervensystem der Cephalocarida erneut zu untersuchen (Strausfeld et al. 1998; Harzsch & Waloszek 2000; Fanenbruck & Harzsch 2005; Schachtner et al. 2005; Homberg 2008).

Diese Dissertation ist Teil des Schwerpunktprogramms „Deep Metazoan Phylogeny“ der Deutschen Forschungsgemeinschaft (DFG-Projekt RI 837/10-1,2). Die intensive Förderung in diesem Rahmen erlaubte zum einen vier Sammelreisen an die nordatlantische Buzzards Bay (Massachusetts; USA), wo mithilfe vieler Unterstützer über 100 Vertreter der seltenen Art *H. macracantha* gesammelt werden konnten (gelistet durch Stegner & Richter 2015: ihre Tab. 1). Zum anderen erlaubte sie über den Austausch mit Fachkollegen die Weiterentwicklung der vergleichend-morphologischen Grundlagen der Neurophylogenetik durch eine vereinheitlichte Nomenklatur (Richter et al. 2010) und eine interaktive Merkmalsmatrix (Loesel & Richter 2014). Vor diesem günstigen Hintergrund wurden hier die Neuuntersuchung des Adultnervensystems und die Erstuntersuchung der Entwicklung des Nervensystems der Cephalocarida vorgenommen. Dies geschah mit modernsten neuroanatomischen Methoden (‚Material and Methods‘ in Kapitel 10-13) und einem vergleichend-morphologischen Blick auf die phylogenetisch wichtigen Merkmalskomplexe.

3. Ziele der Dissertation

Als Ziele der Dissertation ergeben sich:

(1) die Beschreibung von Morphologie und Entwicklung des Nervensystems des Cephalocariden *Hutchinsoniella macracantha* vermittels einer Kombination aus Semidünnschnitt, Immunhistochemie (acetyliertes α-Tubulin, Serotonin, RFamid, Histamin), Kernfärbungen, konfokaler Laserscanningmikroskopie und computergestützter 3D-Rekonstruktion (Kapitel 4 und 5.2);

→ aufgrund neuentdeckter Embryonal- und Larvenstadien ergab sich hier als Zwischenziel die Revision der bisherigen Beschreibung der Larvalentwicklung von *H. macracantha* (Kapitel 5.1);

(2) der Vergleich des Nervensystems der Cephalocarida mit dem anderer Arthropoda im Hinblick auf potentiell homologe Merkmale sowie deren evolutionsmorphologische Interpretation anhand aktueller phylogenetischer Hypothesen (für ausgewählte Merkmalskomplexe zusammengefasst in Kapitel 6);

(3) die neurophylogenetische Auswertung der Daten im Hinblick auf die Phylogenie der Tetraconata (Kapitel 7).

4. Das adulte Nervensystem der Cephalocarida

Wie bei anderen Crustacea gliedert sich das Zentralnervensystem der Cephalocarida in ein dreiteiliges Gehirn aus Proto-, Deuto- und Tritocerebrum sowie ein Bauchmark, das sich vom Mandibularsegment bis ins Telson erstreckt und perlschnurartig aufgereihte segmentale Ganglien trägt (Abb. 3). Dabei sind Mandibular-, Maxillular- und Maxillarneuromer zum Unterschlundganglion (Abb. 6A) mit einheitlichem Somacortex verschmolzen, während die neun Thorakalganglien sowie die Abdominalganglien 1 bis 8 durch somafreie Konnektive miteinander verbunden sind (Abb. 6B-G). Die paarigen Neuropile jedes Ganglions sind innerhalb des Somacortex über segmentale Kommissuren transversal verbunden (z.B. Abb. 6E), sodass Konnektive und Kommissuren wie bei vielen anderen Crustaceen strickleiterartig angeordnet sind (Abb. 3, 6A,B; ‚rope-ladder-like nervous system' sensu Richter et al. 2010).

Das unpaare mediane Neuritenbündel liegt parallel längs zwischen den Hauptsträngen des Bauchmarks und ist mit den meisten segmentalen Kommissuren verbunden (Abb. 3, 6A,B,E,G). Das periphere Nervensystem umfasst neben den zahlreichen segmentalen und intersegmentalen Nerven auch mehrere Neuritenbündel, welche hier dem stomatogastrischen Nervensystem zugeordnet wurden, da sie mit dem Darm oder am Darm ansetzenden Muskeln assoziiert sind. Dazu gehört das unpaare dorsomediane Neuritenbündel, welches vom Labralneuropil aus auf der Dorsalseite des umbiegenden Ösophagus bis in den Unterschlundbereich zieht (Abb. 3, 6H). Dort gibt es nach jeder Seite ein dorsolaterales Neuritenbündel ab, das lateral zum Filtermagen auf ein lockeres Neuritengeflecht trifft (Abb. 3, 6H). An diesem Geflecht ist maßgeblich das laterale Neuritenbündel beteiligt, welches sich in Längsrichtung lateral am Darm vom Tritocephalon bis ins Telson erstreckt (Abb. 3). In jedem Thorakalsegment ist das laterale Neuritenbündel über ein anteriores und ein posteriores transversales Neuritenbündel mit dem medianen Neuritenbündel verbunden (Abb. 3).

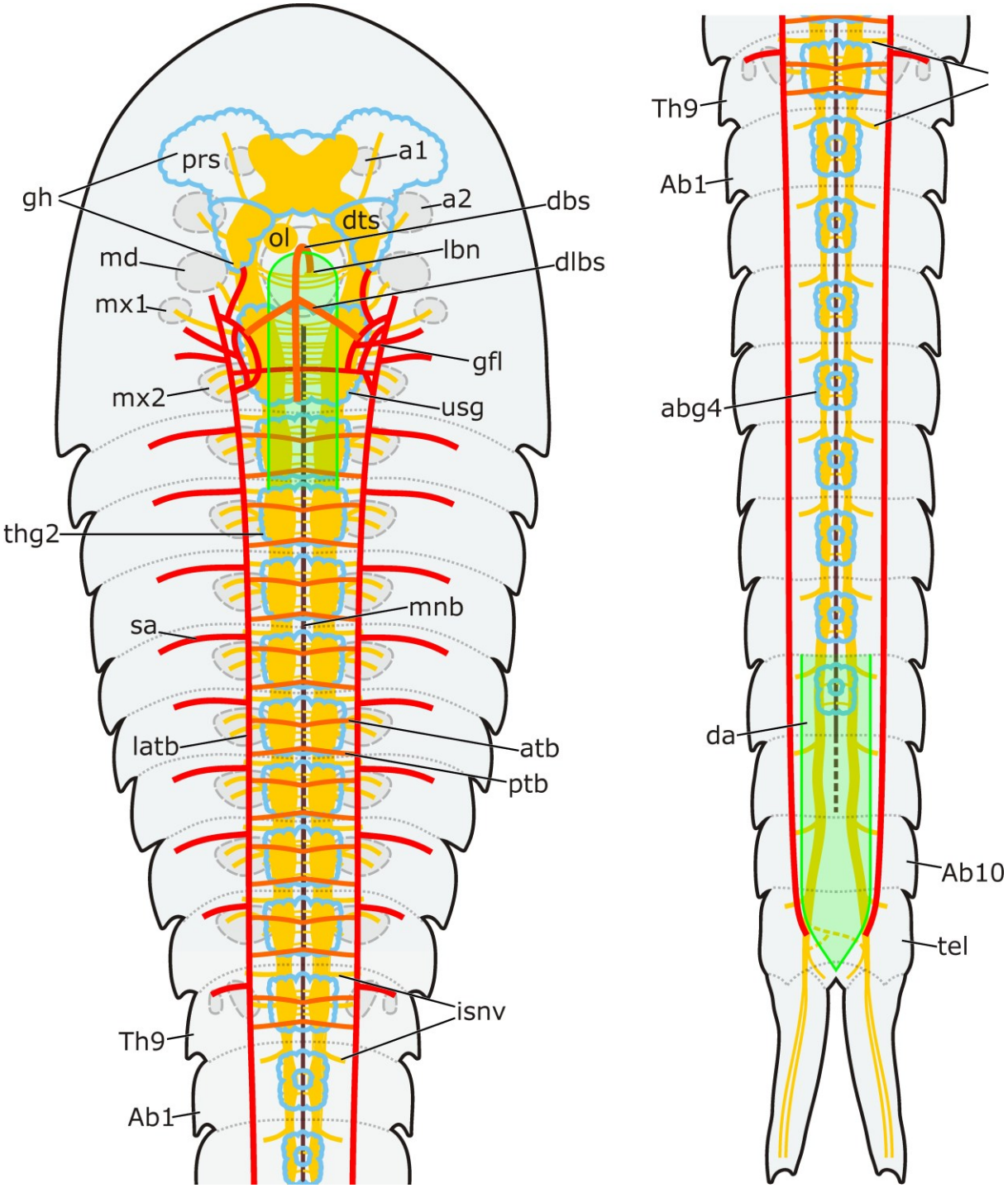

Abb. 3: Dorsaler Überblick des Nervensystems von *H. macracantha*. Extremitätenansatzstellen durch Strichlinien angedeutet, Darm von Th2 bis Ab7 ausgeblendet. Das Zentralnervensystem umfasst das dreiteilige Gehirn (Proto-, Deuto-, Tritocerebrum) und das Bauchmark. Letzteres besteht aus einem Paar Hauptstränge und einem dazwischenliegenden, medianen Neuritenbündel, welche longitudinal das dreiteilige Unterschlundganglion (Neuromere von Md, Mx1, Mx2) sowie die segmentalen Rumpfganglien durchziehen. Das periphere Nervensystem umfasst neben den Nerven (hier stark vereinfacht) das stomatogastrische Nervensystem (dbs, dlbs), zu dem hier auch die mit dem Darm assoziierten lateralen Neuritenbündel (latb) samt ihrer lateralen (sa) und medialen Seitenverbindungen (atb, ptb) gerechnet werden. Nach Stegner et al. (2014b).

4.1. Gehirn

4.1.1. Genereller Aufbau. Das unpaare Protocerebrum liegt anterior, die paarigen Hälften des Deuto- und Tritocerebrums anterolateral bzw. lateral zum Ösophagus. Aus jeder Hälfte des Deutocerebrums ragt ventral ein markanter olfaktorischer Lobus hervor (Abb. 4B,C). Eine mächtige unpaare protocerebrale Somaansammlung umschließt das protocerebrale Neuropil und reicht nach lateral weit in den Kopfschild hinein (Abb. 3, 4A-C,E,F, 5A,C). Hingegen sind die meisten Somata des Deuto- und Tritocerebrums auf jeder Seite zu einer einheitlichen deuto-tritocerebralen Somaansammlung zusammengefasst (Abb. 4A,C, 5C). Eine separate ventrale Somaansammlung befindet sich posteroventral in jedem olfaktorischen Lobus (Abb. 4C).

4.1.2. Nerven und Kommissuren. Die proximal zweigeteilte Wurzel des Antennulanervs sitzt lateral am Deutocerebrum (Abb. 4A,C): Ihr ventraler Teil zieht direkt in den olfaktorischen Lobus, ihr dorsaler Teil in das deutocerebrale Hauptneuropil (Abb. 5E). Der Antennanerv sitzt lateral am Tritocerebrum (Abb. 4A). Sowohl von Deutocerebrum als auch vom Tritocerebrum zieht jeweils ein Tegumentärnerv ans Kopfschild (siehe Stegner & Richter 2011). Die paarigen Hälften des Deutocerebrums sind durch eine präösophageale Kommissur verbunden (Abb. 4F, 5B), die des Tritocerebrums durch zwei postösophageale Kommissuren und eine Labralkommissur (Abb. 4E, 5B), die in ihrem Scheitelpunkt das unpaare Labralneuropil trägt (Abb. 4A).

4.1.3. Neuropile und assoziierte Neuritenbündel. Die Neuropile des Protocerebrums sind in zwei Clustern angeordnet: dem multilobierten Komplex (s. u.) und dem posterodorsalen Neuropilcluster (Abb. 4F). Im Deutocerebrum fällt das olfaktorische Neuropil im olfaktorischen Lobus durch seine besondere innere Organisation auf (s.u.). Im Tritocerebrum fehlen distinkte Neuropile.

Der multilobierte Komplex füllt das protocerebrale Neuropil dorsal beinahe vollständig aus (Abb. 4D,E). Er besteht aus den drei unpaaren Neuropilen 1, 2 und 11 und acht Neuropilpaaren, nummeriert von 3 bis 10, welche untereinander über paarige Trakte oder direkt verbunden sind. Der mächtigste Trakt ist der Pedunkulus, der sich auf jeder Körperseite transversal zwischen den Neuropilen 10 und 3 erstreckt und

auch mit den Neuropilen 4 bis 6 in Verbindung steht (Abb. 4D,E). Zahlreiche Neuriten des Pedunkulus entspringen lateral zum Neuropil 10 aus einer Gruppe vergleichsweise kleiner, dicht gedrängter Globulizellsomata (Division ‚iv' in Abb. 4E,F). Der multilobierte Komplex stellt als funktionelle Einheit das sekundäre olfaktorische Zentrum dar. Auf jeder Körperseite ist das Neuropil 8 über einen ipsilateralen olfaktorio-globulären Trakt mit dem olfaktorischen Lobus verbunden (Abb. 4D), welcher das primäre olfaktorische Zentrum darstellt.

Das Neuropil jedes olfaktorischen Lobus ist in sieben bis acht säulenartige vertikale Stapel gegliedert (z.B. Abb. 4G). Dabei liegt jeweils ein größerer anteromedialer Stapel etwas abseits im Lobus (roter Stern in Abb. 4G-I, 5B), während die gleichgroßen übrigen Stapel in einem Ring angeordnet sind (gelbe Sterne). Jeder Stapel besteht aus zahlreichen, übereinander getürmten olfaktorischen Glomeruli (schwarze und gelbe Pfeile in Abb. 4G,H), deren Form aufgrund ihrer dichten Packung unklar bleibt. Transversalschnitte und RFI legen eine längliche Form nahe (Abb. 4G,H), wohingegen virtuelle Horizontalschnitte und Elofssons & Hesslers (1990) TEM-Daten auf scheibenförmige Glomeruli hindeuten. Nach dorsal geht das Neuropil des olfaktorischen Lobus in ein mächtiges Neuritenbündel über (Pfeilspitze in Abb. 4C,G, 5A), welches die ventrale Wurzel des Antennulanervs, den olfaktorio-globulären Trakt und Neuriten aus der deuto-tritocerebralen Somaansammlung umfasst.

4.1.4. Neuroaktive Substanzen. Auf jeder Seite des Gehirns lassen sich etwa 35 SIRe (Abb. 5C), mindestens 200 RFIRe (Abb. 4H,I, 5E) und etwa 25 HIRe Neurone (z.B. Abb. 5F) immunhistochemisch anfärben und in vielen Fällen individuell identifizieren. Ihre Somata senden spezifisch-immunoreaktive Neurite aus den peripheren Somaansammlungen des Gehirns ins Innere des Neuropils, wo sich die Neurite aufzweigen und an distinkten, spezifisch-immunreaktiven Domänen beteiligt sind (Abb. 5C-G). Diese Domänen werden – anders als Neuropile – nur aufgrund ihrer spezifischen Immunoreaktivität vom umgebenden Neuropil abgegrenzt (‚domain' nach Stegner et al. 2014a: ihre S. 365). Im Gehirn von *H. macracantha* lassen sich insgesamt sieben SIRe, sieben RFIRe und fünf HIRe Domänen relativ klar unterscheiden (z.B. Abb. 5C-F). Mehrere zusätzliche kleinere, weniger distinkte SIRe, RFIRe und HIRe

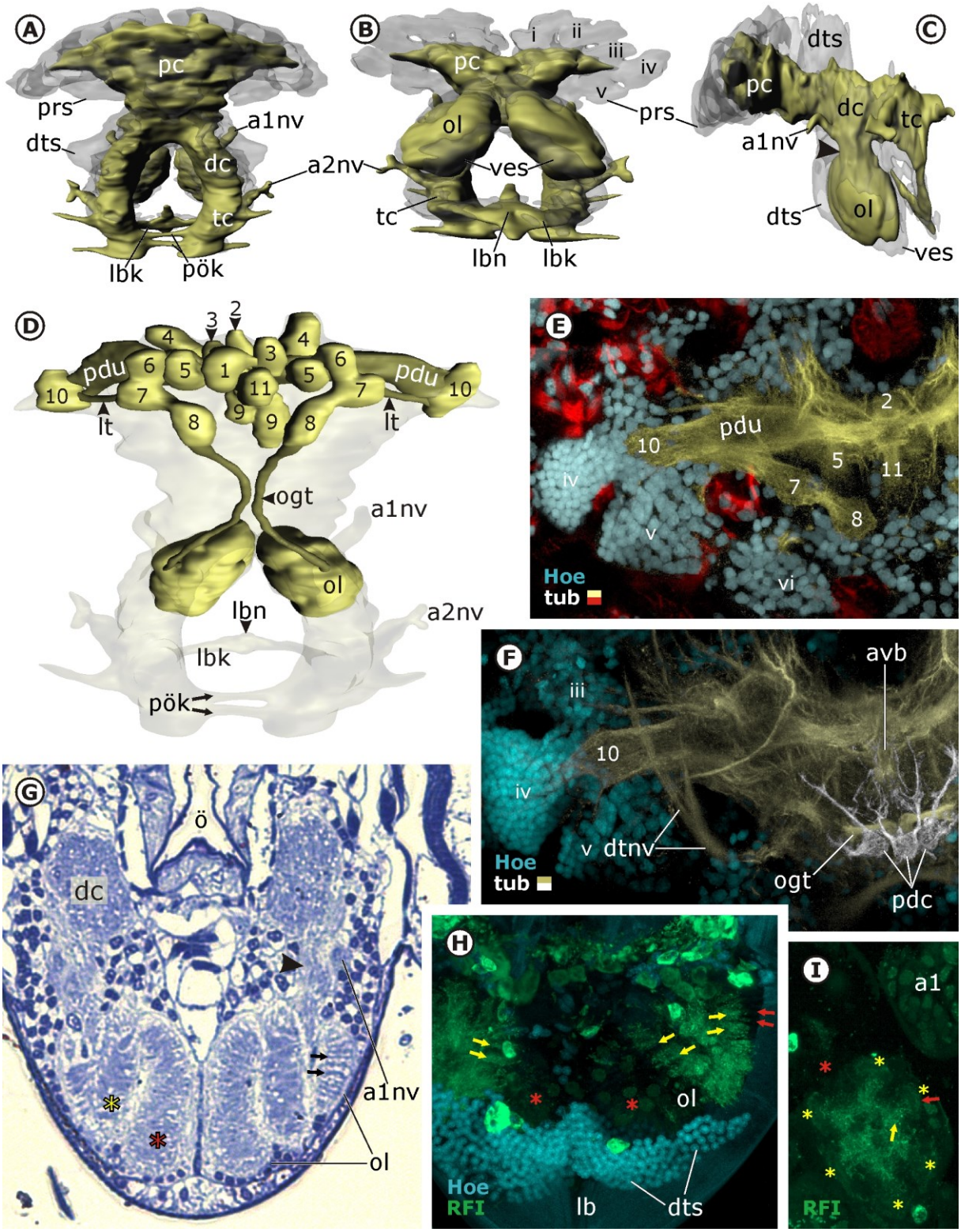

Abb. 4: Morphologie des Gehirns von *H. macracantha*. A-D: Semidünnschnittbasierte 3D-Rekonstruktionen. E, F, H, I: Konfokale Mikrografien. G: Semidünnschnitt. A-C: Dorsale, ventrale und laterale Übersicht über Somaansammlungen (halbtransparent) und Neuropile, Nervenwurzeln und Kommissuren (gelb). B, E, F: Division iv der protocerebralen Somaansammlung besteht aus relativ kleinen, dicht gedrängten Globulizellsomata, die an das Neuropil 10 grenzen. D, E: Dorsale Ansicht des multilobierten Komplexes. Der transversale Pedunkulus (pdu) verbindet zahlreiche lobenartige Neuropile.

Domänen befinden sich über das Gehirn verteilt (z.B. Abb. 5D). Die drei unpaaren Domänen sd1, rfd1 und hd2, die angesichts der ungeklärten Evolution des Zentralkomplexes (Kapitel 2.3, 6, 7) von besonderem Interesse sind, überlappen sich weder gegenseitig, noch mit unpaaren Mittellinienneuropilen sensu Richter et al. (2010). Die unpaare SIRe Domäne sd1, welche anteroventral im protocerebralen Neuropil liegt, wird von anterior durch kolumnäre Neurite der SIRen Neurone s1 innerviert (Abb. 5C,D) – die Neurite bilden dabei ein auffälliges Chiasma (Pfeil).

Die olfaktorischen Glomeruli weisen eine deutliche Zonierung auf: im zentralen Bereich jedes olfaktorischen Lobus konzentrieren sich die Neuriten RFIRer (Abb. 4H,I) und SIRer Interneurone (Abb. 5B), im peripheren Bereich die Neuriten HIRer Interneurone (siehe Stegner & Richter 2011). Die SIRe Innervation geht jeweils auf zwei individuell identifizierbare Neurone der deuto-tritocerebralen Somaansammlung zurück (s8 in Abb. 5A,C).

4.2. Bauchmark

4.2.1. Segmentale Muster in den vier Regionen des Bauchmarks. Das Bauchmark lässt sich in vier Regionen einteilen, innerhalb derer das segmentale Muster der beteiligten Neuromere (Somacortex, Nerven, Kommissuren, SIRe Neurone) weitgehend übereinstimmt (Abb. 3). Diese Regionen sind: (1) das Unterschlundganglion; (2) die Thorakalganglien 1 bis 9; (3) die Abdominalganglien 1 bis 8; sowie (4) der ganglionfreie Bereich des Bauchmarks, der sich durch Ab9 und Ab10 bis ins Telson erstreckt. Das Unterschlundganglion unterscheidet sich von den Thorakalganglien besonders durch seine drei verschmolzenen Neuromere sowie durch sein abweichendes Muster von insgesamt 13 segmentalen Kommissuren (Md: 3, Mx1: 4; Mx2: 6; siehe Abb. 6A). Im Vergleich dazu besitzt jedes Thorakalganglion vier Kommissuren (anterodorsale,

---

D: Ein ipsilateraler olfaktorio-globulärer Trakt (ogt) verbindet den olfaktorischen Lobus (ol) mit dem multilobierten Komplex. G-I: Jeder olfaktorische Lobus besteht aus einem anteromedialen größeren Stapel (roter Stern) und sechs bis sieben gleichgroßen Stapeln (gelbe Sterne) aus olfaktorischen Glomeruli (Pfeile). Die Glomeruli der gleichgroßen Stapel sind im zentralen Bereich RFIR (gelbe Pfeile), nicht aber im peripheren (rote Pfeile). C,G: Ein dickes Neuritenbündel (Pfeilspitze) verbindet den olfaktorischen Lobus mit dem übrigen Gehirn. Nach Stegner & Richter (2011).

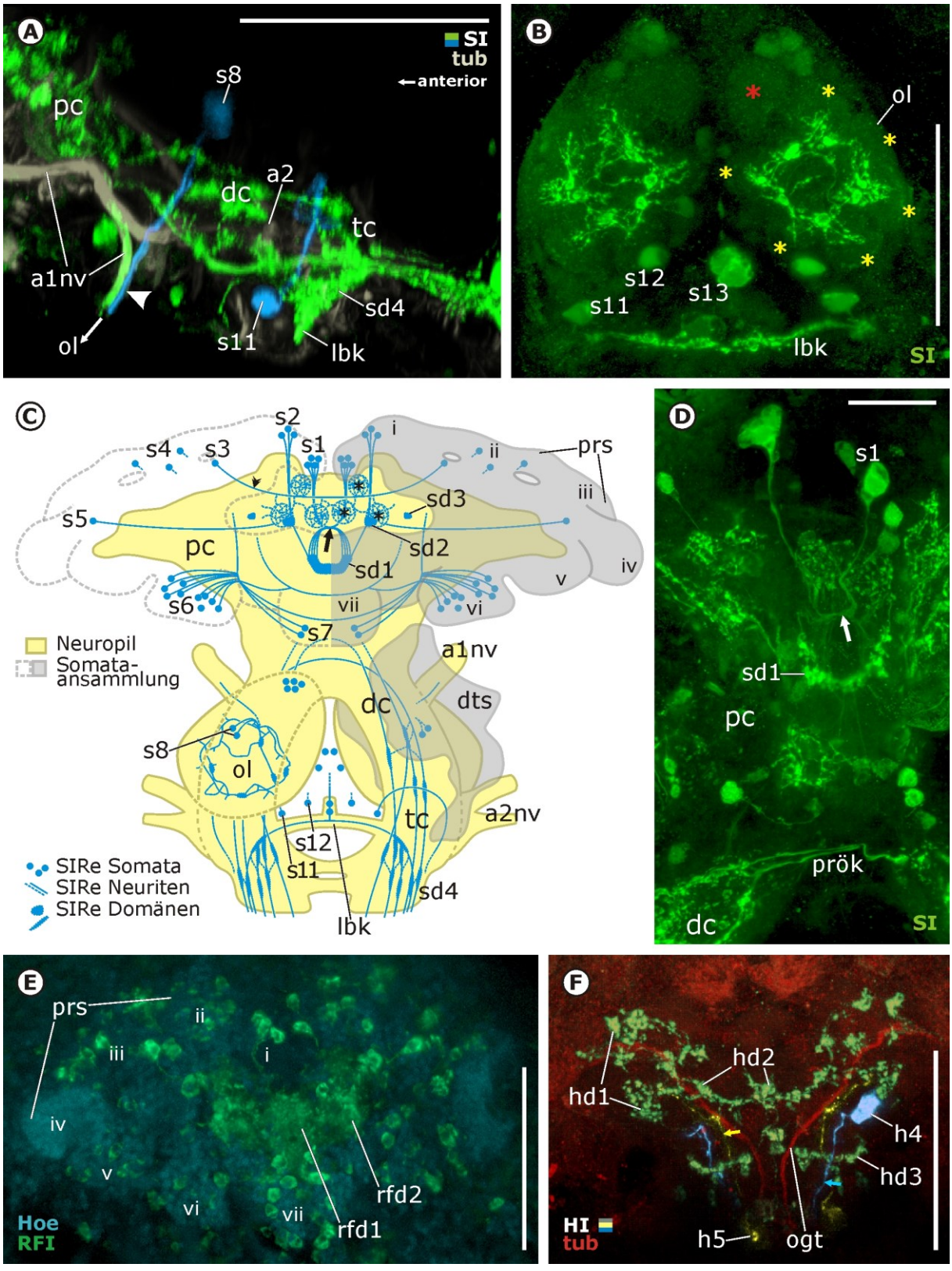

Abb. 5: Serotonin-artige Immunreaktivität (SI) im Gehirn von *H. macracantha*. Konfokale Mikrografien. **A:** Lateralansicht des Gehirns. Die untere Wurzel des Antennulanervs zieht direkt in den olfaktorischen Lobus, als Teil eines dicken Neuritenbündels, das auch andere Neuriten umfasst (Pfeilspitze). **B.** Ventralansicht des anterioren Labrums. **A, B:** Die Neurite der beiden SIRen lokalen Interneurone s8 innervieren die gleichgroßen vertikalen Kolumnen des olfaktorischen Lobus (gelbe Ster-

anteroventrale, erste posteriore und zweite posteriore Kommissur; Abb. 6B). Hingegen stimmen die jeweils drei Extremitätennerven (Exopodit-, Endopodit-, Posterolateralnerv) von Md bis Th9 weitgehend überein (Abb. 6A,B; Th9 ohne Endopoditnerv). Das komplexe Muster SIRer Neurone zeigt intersegmentale Übereinstimmungen, aber auch Unterschiede zwischen Md und Th9 (s. u. im Detail). Vergleichsweise einfacher gebaut sind die Abdominalganglien von Ab1 bis Ab8, die keine segmentalen Nerven, nur zwei segmentale Kommissuren (ak, pk entsprechen adk und 1pk im Thorax, vgl. Abb. 6B,E) und zwei SIRe Neurone pro Seite (s27 und s28 entsprechen s16 und s19 im Thorax) besitzen (vgl. Abb. 6C,F; nur ein SIRes Neuron in Ab8). Die Thorax/Abdomen-Grenze spiegelt sich also deutlich im Nervensystem wider. Dem ganglionfreien Ende des Bauchmarks fehlen Kommissuren und SIRe Neurone (siehe Stegner et al. 2014b). Übereinstimmend zwischen allen Regionen des Bauchmarks entspringt an jeder Segmentgrenze zwischen Tritocephalon und Ab10 ein Intersegmentalnerv lateral aus dem Konnektiv bzw. Längsstrang (Abb. 3, 6A,B,G). Der Intersegmentalnerv ist proximal mit dem lateralen Neuritenbündel verbunden und spaltet sich distal auf, um Tergit und Pleura zu innervieren (Stegner et al. 2014b; Stegner & Richter 2015).

4.2.2. Serotonin-artige Immunoreaktivität (SI). Die hohe Anzahl von fünf bis acht segmentalen SIRen Neuronen pro Hemineuromer von Md bis Th8 bei *H. macracantha* ist innerhalb der Crustacea einzigartig. Viele SIRe Neurone konnten aufgrund der Lage ihres Somas (relativ im Neuromer) sowie aufgrund ihres Neuritenverlaufs *individuell identifiziert* werden (theoretische Grundlage bei Stegner et al. 2014b) – und somit intersegmental verglichen, da ihre Neuriten spezifisch zu ausgedehnten SIRen Domänen im Ganglion sowie zu Kommissuren und Konnektiven beitragen (Abb. 6B,C,H). Diese wurden hier mit den Labels s14-s20 (Md bis Th9, z. B. Abb. 6C,D) bzw. s27 und s28 versehen (Ab1 bis Ab8, Abb. 6F). SIRe Neurone, deren Neuriten-

---

ne), nicht aber die größere, anteromediale Kolumne (roter Stern). **C:** Übersicht von dorsal über alle SIRen Neurone, Neurite und Domänen im Gehirn. **D.** Dorsalansicht der medianen Protocerebralregion. **C, D:** Die unpaare SIRe Domäne sd1 wird durch sich median kreuzende (Pfeil) Neurite der SIRen Neurone s1 innerviert. **E, F:** Dorsalansichten des Protocerebrums zeigen paarige und unpaare RFIRe (E) und HIRe Domänen (F). Nach Stegner & Richter (2011).

verlauf unklar blieb, wurden hier nur aufgrund der Lage ihres Somas identifiziert und mit vorläufigen Labels s21?-s26? versehen.

Ein gewisser Grad an intraspezifischer Variabilität zwischen drei untersuchten Tieren kann nicht darüber hinwegtäuschen, dass das Muster SIRer Neurone in den einzelnen Neuromeren des Bauchmarks innerhalb der Art *H. macracantha* weitgehend konstant ist. Nicht nur zwischen den homonomen Abdominalsegmenten Ab1 bis Ab7, sondern auch zwischen den extremitätentragenden Segmenten Md bis Th9 finden sich intersegmentale Übereinstimmungen im SIRen Muster. So entsprechen die sechs individuell identifizierten SIRen Neurone von Mx2 (nicht gezeigt) vollständig denen von Th1 (siehe Fig. 6C). Abgesehen davon, dass die cephalen Neuromere von Md, Mx1 und Mx2 ein Unterschlundganglion bilden, spiegelt sich die Kopf/Thorax-Grenze also nicht im Nervensystem wider.

Keines der Neuromere von Md bis Th9 beinhaltet alle individuell identifizierten SIRen Neurone von s14 bis s20. Ebenso kommt keines der Neurone s14 bis s20 übereinstimmend in allen Neuromeren von Md bis Th9 vor. Zum Beispiel stimmen zwar auch bei Th1 und Th6 die vier SIRen Neurone s15a, s15b, s16 und s17 überein, jedoch kommen s14 und s19 nur bei Th1 vor und s18 und s20 nur bei Th6 (Abb. 6C,D).

Im Gegensatz zum homonomen Muster segmentaler Nerven und Kommissuren darf das Muster segmentaler SIRer Neurone *als Gesamtheit* im Thorax nicht als homonom betrachtet werden. Die serielle Homologie der individuell identifizierten SIRen Neuronen bleibt aber davon unberührt. So ist eine phylogenetisch zentrale Aussage unserer Daten (Stegner et al. 2014b), dass die SIRen Neurone s14 bis s20 in jedem untersuchten Tier gefunden wurden, trotz intersegmentaler Unterschiede und intraspezifischer Variabilität. Die Neurone s14 bis s20 können also ganz segmentunabhängig als konstantes Merkmal von *H. macracantha* betrachtet werden.

Abb. 6: Bauchmark und stomatogastrisches Nervensystem von *H. macracantha*. A: Unterschlundganglion in Ventralansicht. **B-H:** Konfokale Mikrografien verschiedener Regionen des Bauchmarks in dorsaler Ansicht. **A, B:** Trotz einiger Abweichungen im Unterschlundganglion (A) konnten dessen 13 Kommissuren mit den vier segmentalen Kommissuren im Thorax (B) homologisiert werden. **C, D:** Die Segmente des Thorax weisen in ihrem Muster individuell identifizierter SIRer Neurone Gemeinsam-

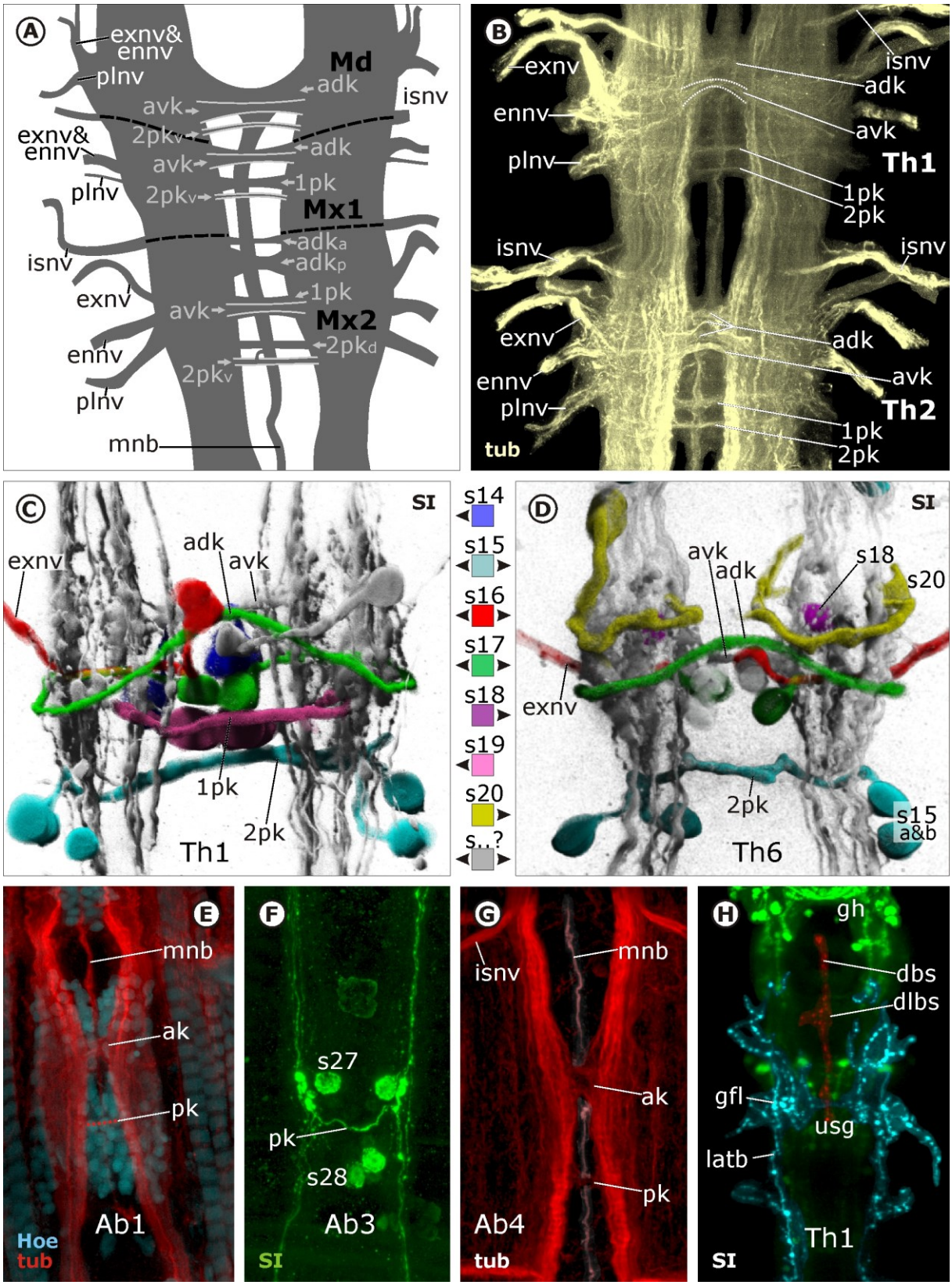

keiten (hier z. B. s15a, s15b, s16, s17), aber auch Unterschiede auf. **E-G:** Die Abdominalganglien 1 bis 7 besitzen je zwei Kommissuren und zwei SIRe Neurone, aber keine segmentalen Nerven. **G:** Medianes Neuritenbündel manuell maskiert (weiß). **H:** Neuritenbündel des stomatogastrischen Nervensystems liegen konzentriert um den muskularisierten Ösophagus. Nach Stegner et al. (2014b).

5. Entwicklung des Nervensystems der Cephalocarida

5.1. Entwicklungsstadien von *H. macracantha*

Die Entdeckung von bisher unbekannten zwei Embryonal- (E1, E2) und fünf Larvalstadien (L6, L7, L12, L13, L18) erforderte eine Revision der bisherigen Beschreibung der Larvalentwicklung von *H. macracantha* (Sanders 1963; Abb. 7). Der früheste gefundene Embryo (E1) besitzt einen schwach entwickelten Kopfschild, Anlagen der drei naupliaren Extremitäten Antennula, Antenna und Mandibel sowie eine kurze Maxillula-Knospe. Andere Extremitätenanlagen oder separate Rumpfsegmente sind noch nicht ausgebildet. Das Telson trägt eine kurze Furca und bleibt während der gesamten Embryonalphase nach ventral umgeklappt. E2 ähnelt äußerlich bereits weitgehend dem Metanauplius des ersten Larvenstadiums L1: Der Kopfschild ist deutlich hufeisenförmig ausgeprägt, die Extremitätenanlagen umfassen nun auch die der Maxilla, der Rumpf weist zwei separate, beinlose Segmente auf, die Furcaläste sind deutlich verlängert. Mit dem Schlupf beginnt eine Larvalentwicklung aus insgesamt 23 Stadien (Abb. 7). Dabei wächst der Rumpf zunächst um zwei Segmente pro Häutung (L1 bis L5), später nur noch um ein Segment pro Häutung (L5 bis L13 bzw. L14 bis L15). Während der anamorphen Anfangsphase der Entwicklung können die Stadien L1 bis L12 leicht anhand ihrer unterschiedlichen Rumpfsegmentzahl unterschieden werden. Die Thorakopoden entwickeln sich sukzessive von anterior nach posterior, weitaus langsamer als die neuen Segmente. In L15 ist die vollständige Anzahl von 19 Rumpfsegmenten erreicht, aber erst drei von neun Thorakopoden sind vollständig ausgebildet (Sanders 1963; Abb. 7). Die Larvalstadien mit 18 (L13, L14) bzw. 19 Rumpfsegmenten (L15-L23) werden nach dem Entwicklungsgrad ihrer Thorakopoden unterschieden (Legende von Abb. 7). Möglicherweise umfasst die Larvalentwicklung weitere, bislang unentdeckte Stadien.

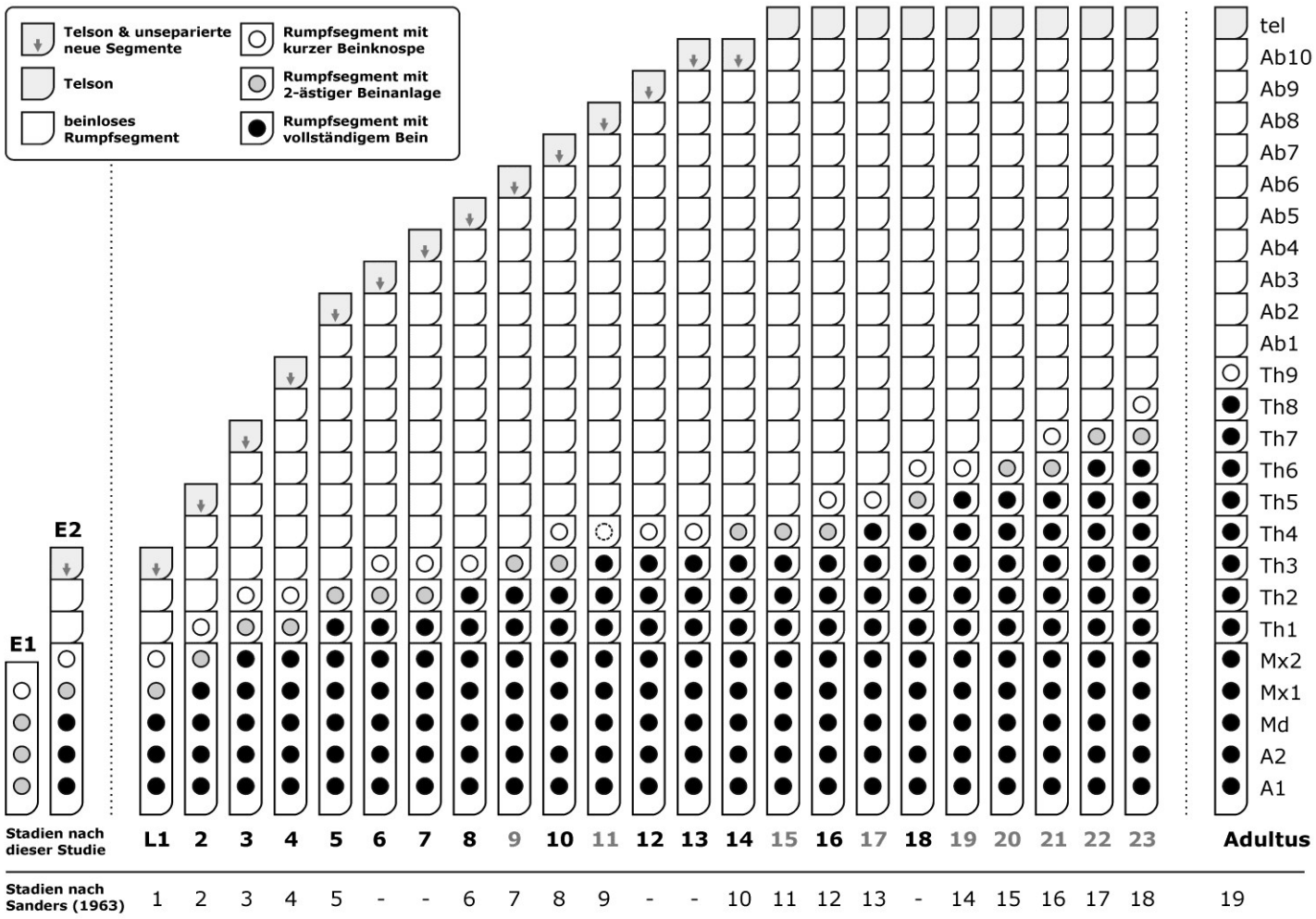

Abb. 7: Übersicht über die revidierten Entwicklungsstadien von *H. macracantha.* Soweit möglich basieren die abgebildeten Daten auf selbst untersuchten Stadien (schwarz, fett). Hier fehlende Stadien (grau, fett) wurden nach Sanders (1963) ergänzt. In der anamorphen Anfangsphase der Entwicklung werden zunächst zwei, später ein Segment pro Häutung zum Rumpf hinzuaddiert. Die Differenzierung Thorakopoden erfolgt vergleichsweise langsamer und wird abgeschlossen, mehrere Stadien nachdem die vollständige Segmentzahl erreicht ist. Nach Stegner & Richter (2015).

5.2. Entwicklung des Nervensystems

Embryonalphase. Bereits im frühsten untersuchten Embryonalstadium E1 bilden die Anlagen von Proto-, Deuto- und Tritocerebrum einen circumösophagealen Neuritenring aus zwei prä- und zwei postösophagealen Kommissuren und den verbindenden parösophagealen Neuritenbündeln (vgl. im Folgenden Abb. 8A). Das Bauchmark besteht lediglich aus einem Paar dünner longitudinaler Neuritenbündel, die im Mandibularsegment durch eine anterodorsale Kommissur verbunden sind und posterior bis ins Maxillularsegment reichen. Jeweils ein segmentaler Nerv zieht aus den vier Extremitätenanlagen nach proximal – im Deutocerebrum, Tritocerebrum und Mandibelneuromer, nicht aber im Maxillularneuromer, trifft der Nerv auf eine schwach ausgeprägte segmentale Neuropilanlage. An den (insgesamt vier) Segmentgrenzen zwischen Protocerebrum und Mx1 entspringt auf jeder Seite jeweils ein Intersegmentalnerv – die beiden anterioren entsprechen den deuto- und tritocerebralen Tegumentärnerven späterer Stadien. Das Gehirn des späten Embryos E2 ähnelt in seiner Form und relativen Größe bereits weitgehend dem adulten Gehirn (siehe Stegner & Richter 2015). Der olfaktorische Lobus ist voll entwickelt und sendet einen olfaktorioglobulären Trakt ins Protocerebrum, welches sämtliche Trakte des multilobierten Komplexes beinhaltet, aber noch keine distinkten Neuropile. Die meisten SIRen Neurone und die ersten beiden SIRen Domänen sd1 und sd4 sind in E2 ausgeprägt. Das Bauchmark zieht erstmals vom Mandibularneuromer bis zum Telson durch. Das Rumpfende zeigt zwei wichtige Neuerungen gegenüber E1: Erstens findet sich im mittleren Telsonbereich auf jeder Seite eine Gruppe großer Somata (farbig markiert in Abb. 8B), von denen mehrere longitudinale Neuriten des Bauchmarks entsprin-

---

Abb. 8: Aspekte der Entwicklung des Nervensystems von *H. macracantha*. Konfokale Mikrografien. **A:** Ventralansicht auf die hier manuell maskierten Neuritenbündel im frühen Embryo. Die naupliaren Neuromere bilden einen charakteristischen, circumösophagealen Neuritenring. Auch die postnaupliare Anlage des Maxillularnervs ist vorhanden. **B:** Ventralansicht verschiedener manuell maskierter Zellen im Telson. Zellen in gelb, grün, rot und blau erinnern an posteriore Pionierneurone, die ihre Neuriten nach anterior ins Bauchmark senden. **C, D:** Ventral- und Sagittalansicht des posterioren Rumpfendes. Die schmale Wachstumszone (maskiert in gelb) proliferiert nach anterior neue Zellen, die sich rasch differenzieren und das Thorakalganglion 5 bilden (maskiert in grün). **E:** Die beobachtete Anordnung einer großen apikalen Zelle (Stern) und einer angrenzenden Reihe aus drei kleineren Zelle (Pfeile) erinnert an Neuroblasten und Ganglienmutterzellen bei anderen Crustaceen. **F:** Apikale Zellen anterior zur Wachstumszone sind meist kleiner, mitunter abgeflacht (rote Markierung). **G, H:** Die Bil-

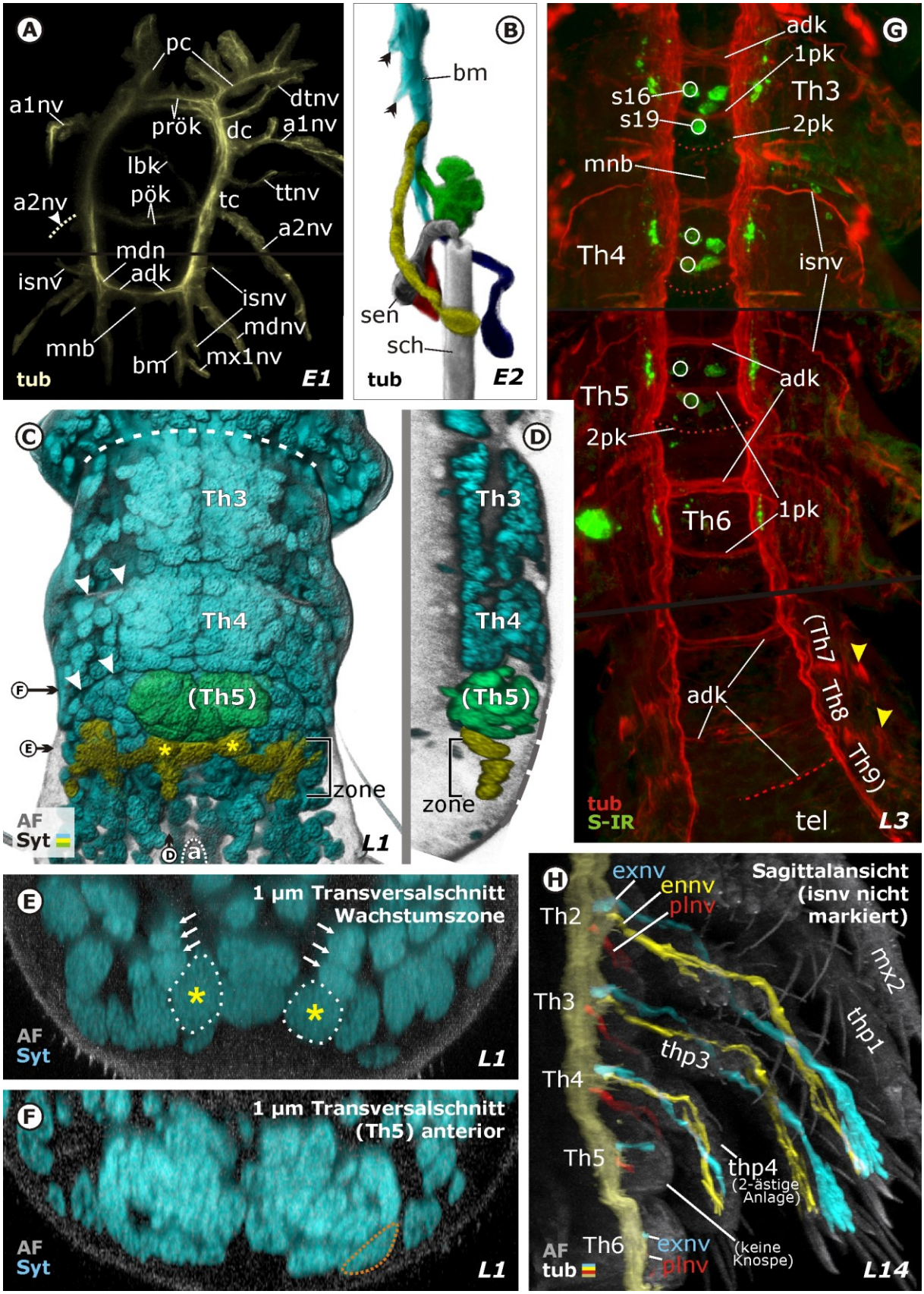

dung der segmentalen Strukturen und Muster erfolgt sukzessive von anterior nach posterior. **H:** Dabei erscheinen die Wurzeln des Exopodit- und Posterolateralnervs (maskiert in blau und rot) vor der Beinanlage, die Wurzel des Endopoditnervs (maskiert in gelb) mit ihr. Nach Stegner & Richter (2015).

gen. Einige dieser Somata erinnern an posteriore Pionierneurone, wie sie bei anderen Crustaceen die ersten durchgängigen longitudinalen Neurite zwischen Mandibelneuromer und Telson. Zweitens findet sich erstmals in E2 anterior zum Telson die schmale Wachstumszone, die während der anamorphen Entwicklungsphase stetig neue Zellen von posterior nach anterior proliferiert (Abb. 8C-E). Indem sich diese Zellen von anterior nach posterior ausdifferenzieren, bilden sie sukzessive neue Rumpfsegmente – einschließlich ihrer Neuromere.

Larvalphase. In der frühen Larvalphase vervollständigen sich die Strukturen und Muster des Gehirns (siehe Stegner & Richter 2015): Bereits in L1 besitzt der multilobierte Komplex beinahe alle Neuropile, und sämtliche SIRen Neurone sind vorhanden. In L2 vervollständigen sich die SIRen Domänen des Gehirns, in L3 das posterodorsale Neuropilcluster. In L4 sind alle Strukturen und Muster des Gehirns ausdifferenziert. Wenn die Entstehung der Rumpfneuromere auch nicht direkt beobachtet werden konnte, so gibt es doch interessante Indizien bei *H. macracantha*, die an die Neuroblasten und Ganglienmutterzellen der Malacostraca und Branchiopoda erinnern (Abschnitt 6.4.5.). Auch in der Wachstumszone eines Schlüpflings von *H. macracantha* wurde auf jeder Seite eine große apikale Zelle (neuroblastenähnlich) beobachtet, die offenbar eine Reihe von drei kleineren Zellen nach innen abgibt (ganglienmutterzellenähnlich; Abb. 8E). Die neuronale Differenzierung im Rumpf erfolgt außerordentlich früh: Noch bevor sich ein neues Segment äußerlich vom Rumpfende absetzt, ist das zugehörige Neuromer mit einem eigenen Somacortex (Abb. 8C,D,F), einem Paar segmentaler Neuropile, verbunden durch eine anterodorsale bzw. anteriore Kommissur, sowie den anterior und posterior angrenzenden Intersegmentalnerven ausgestattet (Abb. 8G). Auch wenn die segmentalen Ganglien rasch ihr äußeres Erscheinungsbild erreichen, sei hier betont, dass die Ausbildung der restlichen Strukturen und Muster jedes Neuromers nur allmählich von anterior nach posterior erfolgt (Neuromere in Abb. 8G). Zwischen allen Segmenten des Rumpfes stimmt die Entwicklungssequenz von Nerven, Kommissuren, SIRen Neuronen und Beinen (sofern vorhanden) weitgehend überein. Von insgesamt 16 hier untersuchten nervensystembezogenen Ereignissen sind elf konsistent durch alle Thorakalsegmente hinweg mit der Entwicklung der Beine korreliert. Interessanterweise

treten im Thorax zuerst jene Kommissuren (adk, 1pk) bzw. SIRe Neurone (s16, s19) auf, deren serielle Homologa (ak, pk bzw. s27, s28) auch im beinlosen adulten Abdomen vorkommen (Abb. 8G). In den meisten Thorakalsegmenten treten der Exopoditnerv und Posterolateralnerv bereits vor der Beinknospe auf, wohingegen der Endopoditnerv stets erst gemeinsam mit der zweiästigen Beinanlage auswächst (vgl. die Segmente innerhalb Abb. 8H). Intersegmentale Unterschiede in der Entwicklungssequenz betreffen nur fünf von 16 untersuchten, nervensystembezogenen Ereignissen und nur wenige Thorakalsegmente (Stegner & Richter 2015; Abb. 9). Während die adulte Neuroanatomie die Thorax/Abdomen-Grenze klar widerspiegelt, gibt es nur einen einzigen intersegmentalen Unterschied in der Entwicklungssequenz, der mit der Thorax/Abdomen-Grenze korrelieren könnte: die Reihenfolge, in welcher der Intersegmentalnerv und die anterodorsale/anteriore Kommissur erscheinen. Allerdings wurde diese Reihenfolge nicht in allen Rumpfsegmenten aufgelöst und könnte auch mit einer anderen Segmentgrenze korrelieren (Stegner & Richter 2015).

6. Morphologischer Vergleich des Nervensystems zwischen Cephalocarida und anderen Taxa

Das verbesserte neuroanatomische Verständnis der Cephalocarida erlaubt einen detaillierten Vergleich zu anderen Arthropodentaxa, welcher immens davon profitiert, dass im Verlaufe dieser Dissertation auch die neuroanatomische Literatur zu anderen Arthropodentaxa beträchtlich anwuchs. Im Folgenden wird für ausgewählte Merkmalskomplexe geprüft, inwiefern neuroanatomische Übereinstimmungen zwischen verschiedenen Taxa als homolog betrachtet werden müssen, und wo der evolutionäre Ursprung dieser Merkmale zu vermuten ist. Wie eingangs erwähnt, wird hier von der Monophylie der Arthropoda, Mandibulata und Tetraconata ausgegangen (Kapitel 2). Der Vergleich konzentriert sich auf die Tetraconata – ggf. unter Rückgriff auf Myriapoda, Chelicerata und Onychophora als Außengruppen.

6.1. Olfaktorisches System

Viele Komponenten des olfaktorischen Systems der Cephalocarida konnten mit entsprechenden Strukturen anderer Arthropoda homologisiert werden (in Abb. 9 durch gleiche Farben dargestellt). So trägt die Antennula verschiedener Mandibulata olfaktorische Rezeptororgane, die ihre sensorischen Axone über den Antennalnerv in das Deutocerebrum senden (Cephalocarida: Elofsson & Hessler 1991; Remipedia: Fanenbruck & Harzsch 2005; Malacostraca: Scholtz & Richter 1995, Gleeson et al. 1996; Hexapoda: Shanbhag et al. 1999; Branchiopoda: Hallberg et al. 1997; Chilopoda: Ernst et al. 2013; Diplopoda: Sombke & Ernst 2014). Bei verschiedenen Tetraconaten und Myriapoda befindet sich dort ein olfaktorischer Lobus, der aus distinkten Neuropil-Untereinheiten, den olfaktorischen Glomeruli zusammengesetzt ist (Cephalocarida: Stegner & Richter 2011; Remipedia: Fanenbruck & Harzsch 2005; Malacostraca, Hexapoda: Schachtner et al. 2005; Branchiopoda: Fritsch & Richter 2012; Diplopoda: Duy-Jacquemin & Arnold 1991; Chilopoda: Sombke et al. 2012. Bei Cephalocarida (Stegner & Richter 2011), Remipedia (Stemme et al. 2012), vielen Malacostraca (Schmidt & Ache 1997), Hexapoda (Dacks et al. 2006), aber auch Chilopoda (persönliche Mitteilung von Andy Sombke, Greifswald) werden die Glomeruli durch SIRe lokale Interneurone innerviert, was die Homologie der olfaktorischen Loben innerhalb der Mandibulata stützt. Zwischen Cephalocarida, Hexapoda und Malacostraca wird diese Homologie zusätzlich durch RFIRe und HIRe lokale Interneurone gestützt (diskutiert durch Stegner & Richter 2011). Die taxonomische Verbreitung kugelförmiger olfaktorischer Glomeruli (Remipedia: Fanenbruck et al. 2004; Malacostraca: Harzsch et al. 2011, Kenning et al. 2013; Hexapoda: Böhm et al. 2012, Hanström 1940, Schachtner et al. 2005; Pleurostigmophora: Sombke et al. 2012; Diplopoda: Duy-Jacquemin & Arnold 1991) spricht dafür, dass kugelförmige Glomeruli im Grundmuster der Mandibulata stehen (Abb. 9; Schachtner et al. 2005; Stegner & Richter 2011). Somit wären die einzigartig gestapelten Glomeruli der Cephalocarida (Abb. 9) wie die länglichen Glomeruli der Scutigeromorpha (Sombke et al. 2012) und Decapoda (Harzsch & Hansson 2008) unabhängig abgeleitet (Stegner & Richter 2011).

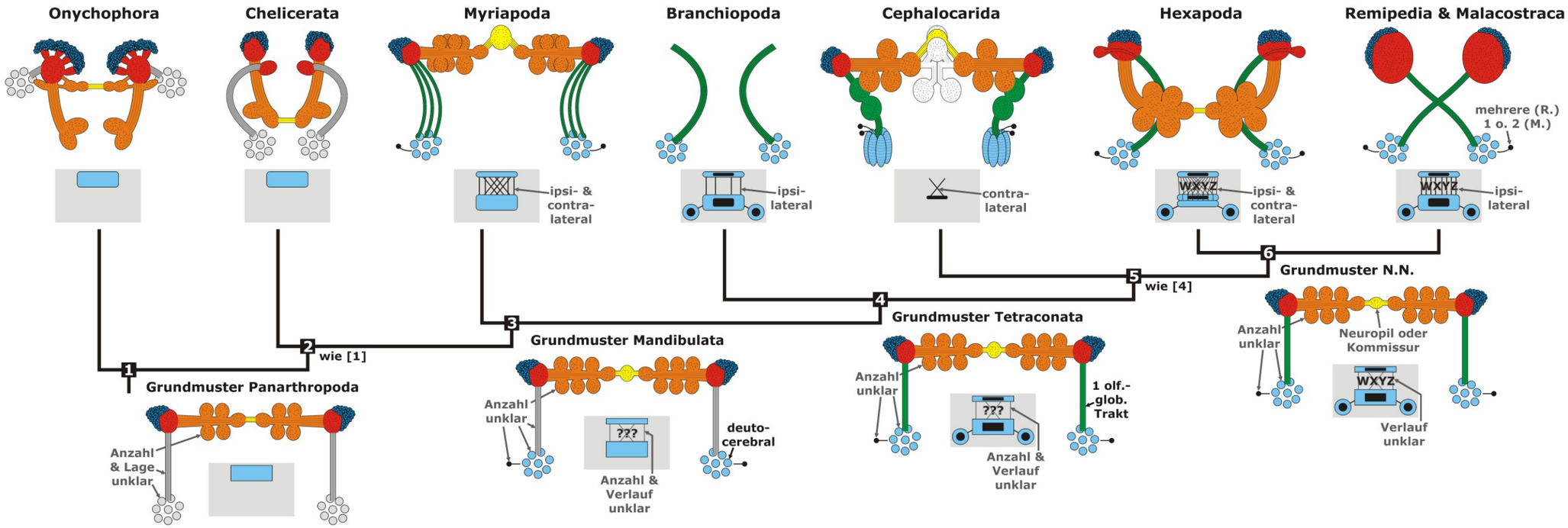

Abb. 9: Hypothese zur Evolution des olfaktorischen Systems (OS) und Zentralkomplexes (ZX) innerhalb der Arthropoda. Ungeachtet der hier veränderten Polarität einiger Merkmale eignet sich die zugrundegelegte Phylogenie der Tetraconata nach Harzsch (2006) bestens zur Veranschaulichung der Merkmalstransformationen. Das Schema fasst eine von mehreren möglichen sparsamsten Interpretationen der vorliegenden Daten zum OS (nach Stegner & Richter 2011) und ZX zusammen (nach Stegner et al. 2014a). Die dargestellten Merkmale aller terminalen Taxa außerhalb der Cephalocarida wurden aus Studien an verschiedenen Arten kombiniert, stets aber so, dass nach meiner Ansicht Merkmale aus dem Grundmuster der jeweiligen Taxa dargestellt sind. Bei den hier nicht abgebildeten „Maxillopoda" wurden OS und ZX entweder weitgehend reduziert, oder es fehlen verlässliche Daten.

Farbcode: OS: hellgrau und dunkelgrau: olfaktorische Glomeruli und olfaktorio-globulärer Trakt der Onychophora und Chelicerata (Homologie unklar, da Position innerhalb der Chelicerata variabel). hellblau: deutocerebrale olfaktorische Glomeruli. grün: olfaktorio-globulärer Trakt zwischen Deuto- und Protocerebrum. dunkelblau: Globulizellsomata. rot: mit den Globulizellen und den olfaktorio-globulären Trakt assoziiertes Neuropil. orange: Pedunkulus mit mehreren lobenartigen Neuropilen. gelb: mediane Verbindung zwischen beiden Pedunkuli. weiß: nicht homologisierte Strukturen des multilobierten Komplexes. schwarz: SIRe Interneurone. **ZX:** hellblau: Arcuate Body bei Onychophora und Chelicerata, Protocerebralbrücke, Zentralkörper und laterale akzessorische Loben bei Mandibulata (Homologie unklar, siehe Text). schwarze Flächen: SIRe Domänen im ZX. schwarze Linien und WXYZ: ausgewählte am ZX beteiligte Trakte.

Ausgewählte Transformationsschritte: [1→Onychophora], [1→2], [2→Chelicerata]: Keine Veränderungen rekonstruierbar (Position der olfaktorischen Glomeruli variabel innerhalb der Chelicerata). **[2→3]:** Olfaktorische Glomeruli auf das Deutocerebrum beschränkt und innerviert durch lokale SIRe Interneurone; unpaares medianes Neuropil verbindet beide Pedunkuli; Protocerebralbrücke und Zentralkörper. **[3→Myriapoda]:** Keine Veränderungen rekonstruierbar. **[3→4]:** ZX nun mit lateralen akzessorischen Loben sowie anteriorer, zentraler und lateraler SIRer Domäne; auch der einzelne olfaktorio-globuläre Trakt in [4] könnte eine Apomorphie sein (Zustand der entsprechenden Trakte in [3] unklar). **[4→Branchiopoda]:** Die SIRen Interneurone im Deutocerebrum und das sekundäre olfaktorische Zentrum wurden reduziert. **[4→5]:** Keine Veränderungen rekonstruierbar. **[5→Cephalocarida]:** Zwei zusätzliche mediane Neuropile (weiß) verbinden beide Pedunkuli, olfaktorio-globulärer Trakt durchdringt Neuropile (grün) des multilobierten Komplexes, olfaktorische Glomeruli in vertikalen Kolumnen angeordnet; Verlust aller Neuropile sowie der anterioren und lateralen SIRen Domäne im ZX. **[5→6]:** Distinkte W-, X-, Y- und Z-Trakte zwischen Protocerebralbrücke und Zentralkörper. **[6→Hexapoda]:** Zentralkörper in Fan-Shaped Body und Ellipsoid Body untergliedert. Das mediane unpaare Neuropil zwischen beiden Pedunkuli wird wieder zur Kommissur. **[6→Remipedia & Malacostraca]:** Gegenüberliegende olfaktorio-globuläre Trakte bilden Chiasma.

Zugrundegelegte Literatur: Onychophora, Chelicerata (Strausfeld et al. 2006); Myriapoda (OS: Holmgren 1916, Duy-Jacquemin and Arnold 1991, Strausfeld et al. 1995, Sombke et al. 2012, pers. Mitteil. durch A. Sombke, Greifswald: SIRe Neurone; ZX: Hanström 1928, Loesel et al. 2002, Sombke et al. 2011), Cephalocarida (Stegner & Richter 2011), Branchiopoda (OS: Fritsch & Richter 2012; ZX: Stegner et al. 2014a), Hexapoda (OS: Hanström 1940, Schachtner et al. 2005, Farris 2005a, b, Dacks et al. 2006, Strausfeld et al. 2009, Böhm et al. 2012; ZX: Kollmann et al. 2011, Homberg & Hildebrand 1991), Remipedia (Fanenbruck & Harzsch 2005, Stemme et al. 2012), Malacostraca (OS: Schachtner et al. 2005; ZX: Utting et al. 2000, Harzsch & Hansson 2008, Kenning et al. 2013).

Übereinstimmend verbindet bei vielen Tetraconata ein distinkter olfaktorio-globulärer Trakt vom Deuto- ins Protocerebrum (Cephalocarida: Stegner & Richter 2011; Remipedia: Fanenbruck & Harzsch 2005; Malacostraca: Kenning et al. 2013; Branchiopoda: Fritsch & Richter 2012; Hexapoda: Strausfeld 2009, Strausfeld et al. 2009), sodass er für den gemeinsamen Vorfahren dieser Taxa angenommen wird (Abb. 9). Da die entsprechenden Neurite der Myriapoda vereinzelt vorliegen (Strausfeld et al. 1995; Sombke et al. 2012) und Chelicerata aufgrund der abweichenden Lage ihrer olfaktorischen Glomeruli nicht vergleichbar sind (Strausfeld & Reisenmann 2009), bleibt hinsichtlich der Traktbündelung das Grundmuster der Mandibulata unklar (Abb. 9). Cephalocarida stimmen mit vielen Arthropoden darin überein, dass ihr olfaktorio-globulärer Trakt ipsilateral bleibt (Chelicerata: Strausfeld et al. 2006; Myriapoda: Sombke et al. 2012; Hexapoda: Strausfeld et al. 2009; Branchiopoda: Fritsch & Richter 2012), was innerhalb der Mandibulata und Tetraconata wahrscheinlich den plesiomorphen Zustand darstellt (Abb. 9). Das einzigartige Chiasma der Trakte bei Remipedia und Malacostraca kann demnach weiterhin als Synapomorphie dieser beiden Taxa interpretiert werden (Harzsch 2006; Abb.9). Wie Abbildung 9 zeigt, trifft der olfaktorio-globuläre Trakt vieler Arthropoda im Protocerebrum auf ein distinktes sekundäres olfaktorisches Zentrum, das je nach Taxon als Pilzkörper (Onychophora, Chelicerata, Myriapoda, Hexapoda), multilobierter Komplex (Cephalocarida) oder Hemiellipsoidkörper (Malacostraca, Remipedia) bezeichnet wird (ausführlich bei Stegner & Richter 2011; Literaturauswahl in Abb. 9). Eine zentrale Entdeckung dieser Dissertation war , dass im multilobierten Komplex der Cephalocarida ein mächtiger Pedunkulus vorhanden ist, der mehrere lobuläre Neuropile trägt (orange in Abb. 9) – ebenso wie der Pedunkulus im Pilzkörper der Onychophora, Chelicerata (Strausfeld et al. 2006), diverser Hexapoda (z. B. Farris 2005a, b; Strausfeld et al. 2009) und Lithobiomorpha (Holmgren 1916; Strausfeld et al. 1995). Ein nach dorsal gerichtetes, medianes Neuropil, wie es bei Cephalocarida und Lithobiomorpha (Holmgren 1916) beide Pedunkuli mittig verbindet, wurde durch Stegner & Richter (2011) homologisiert und zum Mandibulata-Grundmuster zurückverfolgt (vgl. gelb in Abb. 9). Da aber ein kommissur-ähnlicher Trakt, wie er stattdessen die Pedunkuli bei Onychophora und

Chelicerata verbindet (Hanström 1928; Strausfeld et al. 2006), inzwischen auch bei einem Vertreter der Hexapoda nachgewiesen wurde (Böhm et al. 2012: Diplura), ist heute ebenso wahrscheinlich, dass das mediane Neuropil bei Cephalocarida und Lithobiomorpha konvergent ist.

Bisherige Beschreibungen einzelner Komponenten eines olfaktorischen Systems bei Ostracoda, Cirripedia (Hanström 1928) und Copepoda (Andrew et al. 2012) bleiben zweifelhaft (siehe Schachtner et al. 2005; Harzsch 2006). Bei Mystacocarida fehlt das olfaktorische System (Brenneis & Richter 2010). In jedem Fall ist das olfaktorische System mehrerer Tetraconatentaxa (exemplarisch für Branchiopoda in Abb. 9; Harzsch & Glötzner 2002; Fritsch & Richter 2010, 2012) teilweise oder vollständig reduziert worden.

6.2. Zentralkomplex

Der Zentralkomplex ist ein protocerebrales Neuropilcluster aus einem unpaaren Zentralkörper, einer unpaaren Protocerebralbrücke, einem Paar lateraler akzessorischer Loben und ihren verbindenden Trakten. Die Neuropile wurden in übereinstimmender Lage bei Copepoda und Ostracoda (unsichere Nachweise, s. u.), Malacostraca (Utting et al. 2000; Kenning et al. 2013), Remipedia (Fanenbruck & Harzsch 2005; Stemme et al. 2012), Branchiopoda (Harzsch & Glötzner 2002; Fritsch & Richter 2010, 2012) und Hexapoda beschrieben (Williams 1975; Pfeiffer & Homberg 2014). Auf dieser Basis schlug Harzsch (2006) den Zentralkomplex als Synapomorphie der Tetraconata vor (siehe bereits Hanström 1928), wurde doch bei den Außengruppen Onychophora, Chelicerata und Myriapoda meist nur ein unpaares Mittellinienneuropil beschrieben (Loesel et al. 2002; Loesel 2004). Jedoch fehlen Zentralkomplexneuropile bei Cephalocarida (Elofsson & Hessler 1990; bestätigt durch Stegner & Richter 2011), Mystacocarida (Brenneis & Richter 2010), Cirripedia (Semmler et al. 2008), Branchiura (Overstreet et al. 1992), und möglicherweise auch bei Copepoda und Ostracoda (Stegner et al. 2014a; aber siehe Andrew et al. 2012; Aramant & Elofsson 1976).

Im Rahmen dieser Dissertation wurde daher die alternative Hypothese diskutiert, dass der Zentralkomplex erst innerhalb der Tetraconata entstanden sei – als Synapo-

morphie nur einer Teilgruppe der Tetraconata (Stegner et al. 2014a). Dazu wurden auch die Crustaceentaxa ohne Zentralkomplexneuropile hinsichtlich mehrerer feinstruktureller Merkmale verglichen, die im Zentralkomplex der Hexapoda, Malacostraca, Remipedia und Branchiopoda vorkommen (Strausfeld et al. 2006; Stemme et al. 2012; Stegner et al. 2014a). Auffälligerweise besitzen Cephalocarida (Stegner et a. 2014a), Mystacocarida (Brenneis & Richter 2010) und Cirripedia (Semmler et al. 2008) trotz fehlender Zentralkomplexneuropile mindestens eine längliche SIRe Domäne (sd1 bei *H. macracantha*) im Zentrum des Protocerebrums, wie sie auch bei Malacostraca (Langworthy et al. 1997; Harzsch & Hansson 2008), Remipedia (Stemme et al. 2012); Hexapoda (Homberg & Hildebrand 1991; Homberg 2002) und einigen Branchiopoda mit dem Zentralkörper überlappt (Harzsch & Glötzner 2002; Fritsch & Richter 2010). Die Domänen bei Cephalocarida und Mystacocarida (Brenneis & Richter 2010) werden durch SIRe kolumnäre Neurone (s1 bei *H. macracantha*) innerviert, die bei Cirripedia (Semmler et al. 2008) durch SIRe tangentiale Neurone – beides Muster, die auch bei einigen Tetraconata *mit* Zentralkörper beschrieben wurden (ausführlicher bei Stegner et al. 2014a). Ein ähnliches Chiasma, wie es die kolumnären Neuriten der Neurone s1 bei *H. macracantha* bilden, kommt auch zwischen Protocerebralbrücke und Zentralkörper der Hexapoda vor (z. B. Boyan & Williams 2011) sowie anterior zum zentralen Neuropil der Myriapoda (Loesel et al. 2002: ihre Abb. 2B).

Vor diesem Hintergrund wird hier die Homologie der SIRen zentralkörperähnlichen Domäne innerhalb der Tetraconata angenommen (nach Stegner et al. 2014a). Demnach muss eine solche Domäne schon beim Vorfahren der Cephalocarida, Branchiopoda, Remipedia, Hexapoda, Malacostraca, Mystacocarida und Cirripedia vorhanden gewesen sein. Nach allen aktuellen phylogenetischen Hypothesen (z. B. Regier et al. 2010) – und im Einklang mit Harzsch (2006) – stünde eine solche Domäne bereits im Grundmuster der Tetraconata (Stegner et al. 2014a; Abb. 9). Das Fehlen distinkter Zentralkomplexneuropile bei Cephalocarida, Mystacocarida, Cirripedia und anderen Crustaceen wäre sekundär und mehrfach unabhängig erfolgt.

Inwiefern der Zentralkomplex aber tatsächlich eine Synapomorphie der Tetraconata darstellt, bleibt fraglich. Die verbreitete Annahme eines einzelnen Mittellinienneuropils in der Außengruppe Myriapoda (Loesel 2004; Harzsch 2006; Homberg 2008) stützt sich allein auf Untersuchungen des Hundertfüßers *Scolopendra (*Loesel et al. 2002). Studien anderer Autoren an Myriapoda (Holmgren 1916; Hanström 1928; Joly & Descamps 1987; Sombke et al. 2011: ihre Abb. 2C) legen hingegen nahe, dass sowohl Zentralkörper als auch Protocerebralbrücke bereits im Grundmuster der Mandibulata stehen (Abb. 9). Eine detailliertere Untersuchung der Myriapoda, auch hinsichtlich ihrer SI und potentieller kolumnärer und tangentialer Neurone im Protocerebrum, ist unabdingbar für das Verständnis der Evolution des Zentralkomplexes.

6.3. Segmentale SIRe Neurone im Bauchmark

Basierend auf Studien an verschiedenen Taxa (Crustacea: Harzsch & Waloszek 2000, Harzsch 2003; Hexapoda: Harzsch 2002; Chilopoda, Diplopoda, Chelicerata: Harzsch 2004), formulierten Harzsch et al. (2005; in Anlehnung an Harzsch 2004) ein umfassendes Evolutionsszenario für das segmentale Muster SIRer Neurone innerhalb der Arthropoda. Demnach besaß der Vorfahr aller Tetraconata pro Hemineuromer eine anteriore und eine posteriore Gruppe aus jeweils zwei SIRen bipolaren Neuronen, wie rezent durch die Anostraca repräsentiert (Abb. 10A; Harzsch et al. 2005). Die neuen Beschreibungen des SIRen Musters bei Remipedia (Stemme et al. 2013) und Cephalocarida erlaubten eine Überarbeitung dieses Szenarios – auf Basis eines detaillierten Vergleichs jedes einzelnen SIRen Neurons (Stegner et al. 2014b). Die an anderen Tetraconata vorgenommene Unterscheidung in anteriore, zentrale und posteriore SIRe Neurone nach der Position des Somas im Hemineuromer (Harzsch 2002; Stemme et al. 2012) lässt sich nur begrenzt auf *H. macracantha* übertragen. Hier wird s20 als anteriores Neuron, s18 als zentrales, und s15a und 15b als posteriore Neurone interpretiert, während s14, s16, s17 und s19 mit ihrem ambivalenten anteromedialen Soma mit anterioren *und* zentralen Neuronen anderer Taxa verglichen werden müssen (siehe 10B; Stegner et al. 2014b). Die Klassifikation SIRer Neurone nach ihrer Neuritenmorphologie nach Harzsch & Waloszek (2000) lässt sich problemlos auf *H. macracantha* übertragen (Abb. 10B): Demnach umfasst Typ A bi-

polare Neurone mit kontra- und ipsilateralem Neurit (fehlen bei *H. macracantha*), Typ B monopolare Neurone, deren Primärneurit sich in einen kontra- und einen ipsilateralen Neurit aufteilt (s14 bei *H. macracantha*), Typ C monopolare Neurone mit kontralateralem Neurit (s15a, s15b, s17, s19) und Typ D monopolare Neurone mit ipsilateralem Neurit (s18, s20). Auf dieser Basis wurden die SIRen Neurone s14 bis s20 mit der Literatur zu anderen Tetraconata verglichen (ausführlich bei Stegner et al. 2014b).

Zwei SIRe anteriore Neurone, ähnlich s14 und s17 bei *H. macracantha*, kommen bei mehreren Tetraconatentaxa vor und senden dort ihre Neuriten durch die anteriore Kommissur (Harzsch & Waloszek 2000; Harzsch 2002; Fritsch & Richter 2010; Harrison et al. 1995). Dies stützt zwar Harzschs et al. (2005) Hypothese, nach der zwei anteriore Neurone im Grundmuster der Tetraconata stehen. Dass diese Neurone beide von Typ B sind (Harzsch et al. 2005), wäre zwar im Einklang mit dem Fund des Typ-B-Neurons s14 bei *H. macracantha*, bleibt aber angesichts der Disparität der Neuritentypen anteriorer Neurone innerhalb der Tetraconata rein spekulativ (Stegner et al. 2014b). Zwei SIRe anterolaterale Neurone, vergleichbar mit s20 bei *H. macracantha*, wurden zwar bei Myriapoda beschrieben, fehlen aber allen anderen Vertretern der Tetraconata. Im Einklang mit Harzsch (2004) wird hier angenommen,

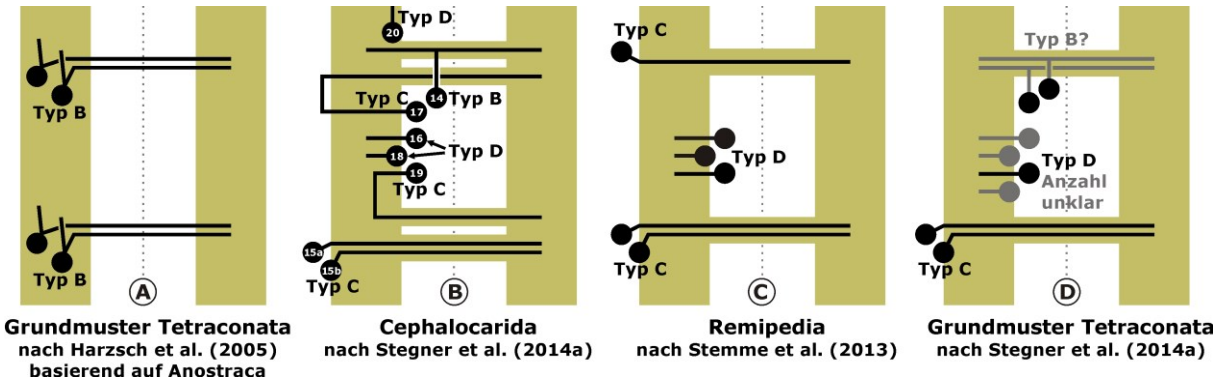

Abb. 10: Segmentale SIRe Neurone im Bauchmark der Cephalocarida und Remipedia und alternative Tetraconata-Grundmusterhypothesen. Nach Harzsch et al. (2005) wären „zentrale" Typ-D-Neurone bei Cephalocarida, Remipedia und evtl. Zygentoma (Harzsch 2002) eine potentielle Synapomorphie. Nach Stegner et al. (2014b) wären sie eine Plesiomorphie vom Grundmuster der Mandibulata und Tetraconata – unter der Annahme, dass homologe zentrale Typ-D-Neurone auch bei Myriapoda vorkommen.

dass im Grundmuster der Tetraconata keine vergleichbaren Neurone vorhanden waren. Basierend auf Harzschs et al. (2005) Tetraconata-Grundmuster (Abb. 10) wurden die SIRen zentralen Typ-D-Neuronen bei Cephalocarida (Stegner et al. 2014b: zwei Neurone; Abb. 10B), Zygentoma (Harzsch 2002: ein Neuron) und Remipedia (Abb. 10C: drei Neurone) als mögliche Synapomorphie diskutiert (Stemme et al. 2013). Diese Hypothese ist insofern interessant, als eine nahe Verwandtschaft der drei Taxa auch von molekularer Seite her Unterstützung erhält (Koenemann et al. 2010; Regier et al. 2010). Allerdings wurden auch bei Chilopoda und Diplopoda bis zu vier zentrale SIRe Neurone pro Hemineuromer beschrieben (Harzsch 2002: Typ D in seiner Abb. 5C,D; Harzsch 2004). Vor diesem Hintergrund liegt es näher, zentrale Typ-D-Neurone nicht nur für das Grundmuster der Mandibulata anzunehmen (Harzsch et al. 2005), sondern ebenso – als Plesiomorphie –für das Grundmuster der Tetraconata (Stegner et al. 2014b). Zwei posteriore Typ-B-Neurone wurden für das Grundmuster der Tetraconata angenommen (Harzsch et al. 2005). Angesichts der beiden posterioren Typ-C-Neurone bei *H. macracantha*, Remipedia, Cirripedia, Hexapoda und Chilopoda, ist wahrscheinlicher, dass zwei posteriore Typ-C-Neurone im Grundmuster der Tetraconata und Mandibulata stehen. Andere Neuronentypen wie bei Branchiopoda wären davon abgeleitet.

6.4. Aspekte der Entwicklung des Nervensystems

6.4.1. Nervensystementwicklung im Vergleich mit anderen Crustaceen. Trotz der enormen Vielfalt an Entwicklungsmodi innerhalb der Crustacea (Martin et al. 2014), stimmen Cephalocarida mit allen untersuchten Crustacea darin überein, dass Proto-, Deuto-, Tritocerebrum, und Mandibelneuromer, die als ‚naupliare Neuromere' zusammengefasst werden – zeitlich vor den postnaupliaren Neuromeren angelegt werden (Branchiopoda: Fritsch & Richter 2010, 2012; Malacostraca: Vilpoux et al. 2006, Fischer & Scholtz 2010, Ungerer et al. 2011b; Copepoda: Lacalli 2009; Cirripedia: Semmler et al. 2008). Weiterhin stimmen Cephalocarida mit anderen Crustacea darin überein, dass ihre postnaupliaren Neuromere aus ektodermalen Stammzellen einer Wachstumszone (sensu Scholtz & Wolff 2013) anterior zum Telson hervorgehen (vgl. z. B. Malacostraca: Dohle 1972; Branchiopoda: Williams et

al. 2012). Trotz dieser generellen Übereinstimmungen ist *H. macracantha* der einzige bekannte Krebs, in dessen Thorakalsegmenten sich noch vor den Beinanlagen Ganglien mit Somacortex, Exopodit- und Posterolateralnerv und mindestens zwei Kommissuren entwickeln. Bei allen anderen untersuchten Krebsen entwickelt sich hingegen das Ganglion nach der Beinanlage oder simultan mit ihr (Branchiopoda: Fritsch & Richter 2010, 2012; Malacostraca: Harzsch 2003; Fischer & Scholtz 2010; Ungerer et al. 2011b). Die extrem frühe Ganglienbildung bei Cephalocarida darf nicht darüber hinwegtäuschen, dass wie bei anderen Crustacea auch die Nervensystemstrukturen jedes Segments sukzessive, in starker Korrelation mit den Beinen gebildet werden (vgl. Branchiopoda: Fritsch & Richter 2010, 2012; Malacostraca: Ungerer et al. 2011b). Während der Rumpfentwicklung aller Arthropoda sind die *Proliferation* neuer Zellen von posterior und die *Differenzierung* dieser Zellen innerhalb metamerer Einheiten (Parasegmente, Segmente) von anterior zwei unabhängige Prozesse (Williams et al. 2012; Scholtz & Wolff 2013). Der wesentliche Unterschied von *H. macracantha* zu anderen Arthropoda ist (z. B. Anostraca: Frase 2012; Malacostraca: Dohle & Scholtz 1997), dass viele Neurektodermzellen bereits unmittelbar nach ihrer Proliferation, in direkter Nachbarschaft zur Wachstumszone mit ihrer neuronalen Differenzierung beginnen und Ganglien beginnen.

6.4.2. Thorax und Abdomen der Cephalocarida im Vergleich ihrer Entwicklungssequenzen. Olesen et al. (2011) deuteten als Besonderheit der Cephalocarida darauf, dass alle Rumpfsegmente während ihrer Entwicklung eine rundliche, mit spitzen Pleuren besetzte Form aufweisen, welche äußerlich der von Abdominalsegmenten entspricht. Erst nach Durchlaufen dieser nach Olesen et al. (2011) „abdomen-artigen" Form entwickeln Thorakalsegmente ihre adulte abgeflachte Form mit flügelartige Pleuren. Zudem sind Cephalocarida und Mystacocarida innerhalb der Crustacea einzigartig, da sie adult nicht nur im Thorax sondern auch im beinlosen Abdomen segmentale Ganglien aufweisen (Brenneis & Richter 2010; Stegner et al. 2014b). Unsere serielle Homologisierung von Nerven, Kommissuren und SIRen Neuronen über die Thorax/Abdomen-Grenze von *H. macracantha* hinweg erlaubte hier einen Vergleich der verschiedenen Rumpfsegmente hinsichtlich ihrer Nervensystementwicklung (im Thorax unter Berücksichtigung der Beinentwicklung). Der erste Nerv (Intersegmen-

talnerv), die ersten beiden Kommissuren und die ersten beiden SIRen Neurone, die während der Entwicklung auftreten, sind in allen Rumpfsegmenten – thorakal wie abdominal – stets dieselben. Im Abdomen (Ab1 bis Ab7) werden diese frühen Nervensystemmerkmale bis in das Adultstadium beibehalten. In den Thorakalsegmenten treten diese frühen Nervensystemmerkmale treten stets vor den Beinanlagen auf. Da sich hier aber sukzessive zusätzliche Nerven, Kommissuren und SIRe Neurone herausbilden, zeigt kein einziges Thorakalsegment während seiner Entwicklung eine „abdomen-artige" Neuroanatomie, abweichend von Olesens et al. (2011) auf externer Morphologie basierter Hypothese.

6.4.3. Neurogenese. Übereinstimmend werden bei Hexapoda, Malacostraca und Branchiopoda die Neuronen aus einzelnen, distinkten Vorläuferzellen, den Neuroblasten gebildet (z. B. Scholtz & Wolff 2013). Bei Hexapoda wandert der Neuroblast aus der apikalen Zellschicht nach innen und vergrößert sich, bevor er sich inäqual teilt (Hartenstein et al. 1994; Bossing et al. 1996; Wheeler et al. 2003). Bei Malacostraca (Ungerer & Scholtz 2008) und Branchiopoda (Ungerer et al. 2011b) behält der Neuroblast hingegen weitgehend seine Größe und Position in der apikalen Zellschicht; er teilt sich inäqual und gibt so mehrere kleinere Ganglionmutterzellen nach innen ab, die später durch äquale Teilungen die Neuronen (Ganglienzellen) bilden. Das hier in der Wachstumszone eines Schlüpflings von *H. macracantha* beobachtete Anordnungsmuster einer großen apikalen Zelle und dreier nach innen gerichteter kleinerer Zellen entspricht eher dem Muster der Malacostraca und Branchiopoda (Abb. 8E).

7. Beitrag zur Phylogenetik der Tetraconata

Zusammenfassend ergibt der Vergleich mit anderen Arthropoden, dass das Nervensystem der Cephalocarida hauptsächlich Merkmale aufweist, die entweder als Autapomorphien oder als Plesiomorphien vom Grundmuster der Tetraconata, Mandibulata bzw. Arthropoda interpretiert werden (Abb. 9, 10).

Für zwei wichtige Merkmalskomplexe – nämlich das olfaktorische System und das segmentale Muster SIRer Neurone im Bauchmark – wird auf Grundlage dieser Dis-

sertation eine umgekehrte Polarität in der evolutionären Merkmalsabfolge vorgeschlagen (Transformationsserie nach Richter & Wirkner 2014). Viele homologe Übereinstimmungen im olfaktorischen System bzw. SIRen Muster, die von früheren Autoren als Synapomorphien nur weniger Tetraconatentaxa aufgefasst wurden (Abb. 2F; Harzsch 2006; Harzsch et al. 2005; Stemme et al. 2012), müssen vielmehr als Symplesiomorphien gegenüber dem Grundmuster der Mandibulata (olfaktorisches System) bzw. Tetraconata (SIRes Muster) angesehen werden. Das bringt mit sich, dass das erwähnte Fehlen von Komponenten des olfaktorischen Systems ebenso wie das Fehlen zentraler SIRer Neurone bei zahlreichen Crustaceentaxa (z. B. Anostraca; Abb. 10) als sekundäre Reduktionen innerhalb der Tetraconata interpretiert werden müssen. Zentralkörper und Protocerebralbrücke werden hier für das Grundmuster der Mandibulata angenommen, sodass das Fehlen der beiden unpaaren Neuropile bei Cephalocarida und vielen anderen Crustaceentaxa sekundär wäre (siehe auch Stegner et al. 2014a). Entsprechend wird die SIRe Domäne der Cephalocarida als Relikt eines früheren Zentralkörpers mit SIRer Domäne interpretiert (Abb. 9; Stegner et al. 2014a). Hingegen ist durchaus denkbar, dass laterale akzessorische Loben und distinkte W-, X-, Y-, Z-Trakte bei Cephalocarida primär fehlen und erst innerhalb der Tetraconata entstanden. Dann könnten diese Merkmale als Synapomorphien herangezogen werden (Abb. 9). Die Evolution des Zentralkomplexes bleibt unsicher, solange die Myriapoda (Zitate in Abb. 9) nicht besser untersucht sind.

Bei einem ersten Vergleich mit den Entwicklungssequenzen der Branchiopoda (z. B. Fritsch et al. 2013) bzw. Malacostraca (z. B. Ungerer et al. 2011a; Jirikowski et al. in Vorbereitung) stellte sich die frühe neuronale Differenzierung und Rumpfganglionbildung bei Cephalocarida als einzigartig heraus. Eine evolutionäre oder phylogenetische Interpretation dieses bemerkenswerten Befunds bleibt jedoch unmöglich, solange umfassende Daten zu anderen Crustaceentaxa fehlen. Gleiches gilt für die evolutionäre und phylogenetische Interpretation der übereinstimmenden Anordnung von Neuroblasten und Ganglionmutterzellen bei Branchiopoda und Malacostraca (Stollewerk & Simpson 2005; Scholtz & Wolff 2013; Brenneis et al. 2013), für die es hier zwar erstmals einen schwachen Hinweis bei Cephalocarida gibt, die aber bisher bei keinem anderen Crustaceen nachgewiesen wurden.

Diese Dissertation liefert einen wichtigen Beitrag zum Verständnis der Evolution des Nervensystems innerhalb der Arthropoda. So birgt gerade das olfaktorische System der Cephalocarida, das wegen seiner für Crustacea ungewöhnlichen Komplexität als hochspezialisiert galt (Hessler & Elofsson 1992; Strausfeld et al. 1998; Fanenbruck & Harzsch 2005), offenbar Merkmale, die bis zum Vorfahren aller Arthropoda zurückreichen (z. B. Böhm et al. 2012; Wolff & Strausfeld 2012). Andere Merkmale des Cephalocariden-Nervensystems sind wahrscheinlich abgeleitet, wie die Reduktion des optischen Systems und der Neuropile des Zentralkomplexes. Keineswegs sind die Tiere „lebende Fossilien". Das Rätsel um die phylogenetische Position der Cephalocarida konnte hier nicht gelöst werden – im adulten Nervensystem fehlen überzeugende Synapomorphien mit anderen Tetraconatentaxa, und für eine phylogenetische Interpretation der Entwicklungsdaten sind noch Studien an vielen anderen Crustaceentaxa nötig. Cephalocarida bleiben phylogenetisch schwer zu fassen.

8. Abkürzungen

1-11	Neuropile 1-11
1pk, 2pk	erste und zweite posteriore Kommissur (Thorax)
$2pk_d$, $2pk_v$	dorsaler und ventraler Teil von 2pk
A1, A2	Deuto- und Tritocephalon
a1, a2	Antennula und Antenna
a1nv, a2nv	Antennula- und Antennanerv
Ab1-Ab10	Abdominalsegmente 1-10
abg4	Abdominalganglion 4
adk	anterodorsale Kommissur (Thorax)
adk_a, adk_p	anteriorer und posteriorer Teil von adk
AF	Autofluoreszenz
ak	anteriore Kommissur (Ab1-Ab8)
atb	anteriores transversales Neuritenbündel
avb	anteroventrales Neuritenbündel
avk	anteroventrale Kommissur (Thorax)
bm	Bauchmark
da	Darm
dbs, dlbs	dorsomedianes und dorsolaterales Neuritenbündel
dc	Deutocerebrum
dtnv	deutocerebraler Tegumentärnerv
dts	deuto-tritocerebrale Somaansammlung
E1, E2	Embryonalstadien 1 und 2
en	Endopodit
endt	gnathale Enditen
ennv	Endopoditnerv
ex, exnv	Exopodit, Exopoditnerv
frc	Furca
gfl	periösophageales Neuritengeflecht
gh	Gehirn
h4, h5	HIRe Neurone 4 und 5
hd1-hd3	HIRe Domänen 1-3
HI, HIR	histamin-artige Immunreaktivität, histamin-artig immunreaktiv
Hoe	Hoechst-Kernfärbung
isnv	Intersegmentalnerv
i-vii	Divisionen i-vii von prs
ks	Kopfschild
L1-L23	Larvalstadien 1-23
latb	laterales Neuritenbündel
lb	Labrum
lbk	Labralkommissur
lbn	Labralneuropil
lt	lateraler Trakt
md	Mandibel
mnb	medianes Neuritenbündel
Mx1, Mx2	Maxillular- und Maxillarsegment
mx1, mx2	Maxillula und Maxilla
ö	Ösophagus
ogt	olfaktorio-globulärer Trakt
ol	olfaktorischer Lobus
pc	Protocerebrum
pdc	posterodorsales Neuropilcluster
pdu	Pedunkulus
pk	posteriore Kommissur (Ab1-Ab8)
pleu	abgeflachte Pleura
plnv	Posterolateralnerv
pök	postösophageale Kommissur
prök	präösophageale Kommissur
prs	protocerebrale Somaansammlung
ps	Pseudepipodit
ptb	posteriores transversales Neuritenbündel
rfd1, rfd2	RFIRe Domänen 1 und 2
RFI, RFIR	RFamid-artige Immunreaktivität, RFamid-artig immunreaktiv
s1-s28	SIRe Neurone 1-28
sa	Seitenast von latb
sd1-sd4	SIRe Domänen 1-4
SI, SIR	serotonin-artige Immunreaktivität, serotonin-artig immunreaktiv
Syt	Sytox-Kernfärbung
tc	Tritocerebrum
tel	Telson
Th1-Th9	Thorakalsegmente 1-9
thg2	Thorakalganglion 2
thp1-thp9	Thorakopoden 1-9
tub	Tubulin-Färbung
usg	Unterschlundganglion
ves	ventrale Somaansammlung

9. Literatur der zusammenfassenden Einleitung

Addis A. 2008. Distribution and biology of *Lightiella magdalenina* (Crustacea, Cephalocarida). Dissertation. Università di Sassari. 89 S.

Addis A, Biagi F, Floris A, Puddu E, Carcupino M. 2007. Larval development of *Lightiella magdalenina* (Crustacea, Cephalocarida). Marine Biology 152:733-744.

Andrew DR, Brown SM, Strausfeld NJ. 2012. The minute brain of the copepod *Tigriopus californicus* supports a complex ancestral ground pattern of the tetraconate cerebral nervous systems. Journal of Comparative Neurology 520:3446-3470.

Aramant R, Elofsson R. 1976. Distribution of monaminergic neurons in the nervous system of non-malacostracan crustaceans. Cell and Tissue Research 166:1-24.

Averof M, Cohen SM. 1997. Evolutionary origin of insect wings from ancestral gills. Nature 385:627-630.

Ax P. 1999. Das System der Metazoa II. Ein Lehrbuch der phylogenetischen Systematik. Stuttgart, Jena, Lübeck, Ulm: Gustav Fischer Verlag.

Bitsch C, Bitsch J. 2004. Phylogenetic relationships of basal hexapods among the mandibulate arthropods: a cladistic analysis based on comparative morphological characters. Zoologica Scripta 33:511-550.

Böhm A, Szucsich NU, Pass G. 2012. Brain anatomy in Diplura (Hexapoda). Frontiers in Zoology 9.

Bossing T, Udolph G, Doe CQ, Technau GM. 1996. The embryonic central nervous system lineages of *Drosophila melanogaster*. 1. Neuroblast lineages derived from the ventral half of the neuroectoderm. Developmental Biology 179:41-64.

Boxshall GA. 2004. The evolution of arthropod limbs. Biological Reviews 79:253-300.

Boyan G, Williams L. 2011. Embryonic development of the insect central complex: Insights from lineages in the grasshopper and *Drosophila*. Arthropod Structure & Development 40:334-348.

Brenneis G, Richter S. 2010. Architecture of the nervous system in Mystacocarida (Arthropoda, Crustacea): An immunohistochemical study and 3D-reconstruction. Journal of Morphology 271:169-189.

Brenneis G, Stollewerk A, Scholtz G. 2013. Embryonic neurogenesis in *Pseudopallene* sp. (Arthropoda, Pycnogonida) includes two subsequent phases with similarities to different arthropod groups. EvoDevo 4:1-36.

Brown GG. 1970. Some comparative aspects of selected crustacean spermatozoa and crustacean phylogeny. In: Baccetti B (Hrsg). Comparative spermatology. New York: Academic Press. S. 183-205.

Brown GG, Metz CB. 1967. Ultrastructural studies on the spermatozoa of two primitive Crustaceans *Hutchinsoniella macracantha* and *Derocheilocaris typicus*. Zeitschrift für Zellforschung und Mikroskopische Anatomie 80:78-92.

Burnett BR. 1981. Compound eyes in the cephalocarid crustacean *Hutchinsoniella macracantha*. Journal of Crustacean Biology 1:11-15.

Carapelli A, Liò P, Nardi F, van der Wath E, Frati F. 2007. Phylogenetic analysis of mitochondrial protein coding genes confirms the reciprocal paraphyly of Hexapoda and Crustacea. BMC Evolutionary Biology 7(Suppl 2).

Carcupino M, Floris A, Addis A, Castelli A, Curini-Galletti M. 2006. A new species of the genus *Lightiella*: The first record of Cephalocarida (Crustacea) in Europe. Zoological Journal of the Linnean Society 148:209-220.

Cook CE, Yue Q, Akam M. 2005. Mitochondrial genomes suggest that hexapods and crustaceans are mutually paraphyletic. Proceedings of the Royal Society B: Biological Sciences 272:1295-1304.

Dacks AM, Christensen TA, Hildebrand JG. 2006. Phylogeny of a serotonin-immunoreactive neuron in the primary olfactory center of the insect brain. Journal of Comparative Neurology 498:727-746.

Dahl E. 1956. On the differentiation of the topography of the crustacean head. Acta Zoologica 37:123-193.

De Troch M, Fiers F, Vincx M. 2000. Range extension and microhabitat of *Lightiella incisa* (Cephalocarida). Journal of Zoology 251:199-204.

Dohle W. 1972. Über die Bildung und Differenzierung des postnauplialen Keimstreifs von *Leptochelia* spec. (Crustacea, Tanadaicea). Zoologische Jahrbücher Abteilung für Anatomie und Ontogenie der Tiere 89:503-566.

Dohle W, Scholtz G. 1997. How far does cell lineage influence cell fate specification in crustacean embryos? Seminars in Cell & Developmental Biology 8:379-390.

Dohle W. 1976. Die Bildung und Differenzierung des postnauplialen Keimstreifs von *Diastylis rathkei* (Crustacea, Cumacea). II. Die Differenzierung und Musterbildung des Ektoderms. Zoomorphologie 84:235-277.

Dohle W. 2001. Are the insects terrestrial crustaceans? A discussion of some new facts and arguments and the proposal of the proper name Tetraconata for the monophyletic unit Crustacea + Hexapoda. Annales de la Société Entomologique de France 37:85-103.

Duy-Jacquemin MN, Arnold G. 1991. Spatial organization of the antennal lobe in *Cylindroiulus puctatus* (Leach) (Myriapoda Diplopoda). International Journal of Insect Morphology and Embryology 20:205-214.

Edgecombe GD, Richter S, Wilson GDF. 2003. The mandibular gnathal edges: Homologous structures throughout Mandibulata? African Invertebrates 44:115-135.

Edgecombe GD, Wilson GDF, Colgan DJ, Gray MR, Cassis G. 2000. Arthropod Cladistics: Combined Analysis of Histone H3 and U2 snRNA Sequences and Morphology. Cladistics 16:155-203.

Elofsson R. 1992. Monoaminergic and peptidergic neurons in the nervous system of *Hutchinsoniella macracantha* (Cephalocarida). Journal of Crustacean Biology 12:531-536.

Elofsson R, Hessler RR. 1990. Central nervous system of *Hutchinsoniella macracantha* (Cephalocarida). Journal of Crustacean Biology 10:423-439.

Elofsson R, Hessler RR. 1991. Sensory morphology in the antennae of the cephalocarid *Hutchinsoniella macracantha*. Journal of Crustacean Biology 11:345-355.

Elofsson R, Hessler RR. 1994. Sensory structures associated with the body cuticle of *Hutchinsoniella macracantha* (Cephalocarida). Journal of Crustacean Biology 14:454-462.

Elofsson R, Hessler RR. 1998. Tegumental glands of *Hutchinsoniella macracantha* (Cephalocarida). Journal of Crustacean Biology 18:42-56.

Elofsson R, Hessler RR, Hessler AY. 1992. Digestive system of the cephalocarid *Hutchinsoniella macracantha*. Journal of Crustacean Biology 4-571.

Ernst A, Hilken G, Rosenberg J, Voigtländer K, Sombke A. 2013. Structure and distribution of antennal sensilla in the centipede *Scolopendra oraniensis* (Lucas, 1846) (Chilopoda, Scolopendromorpha). Zoologischer Anzeiger 252:217-225.

Fanenbruck M, Harzsch S. 2005. A brain atlas of *Godzilliognomus frondosus* Yager, 1989 (Remipedia, Godzilliidae) and comparison with the brain of *Speleonectes tulumensis* Yager, 1987 (Remipedia, Speleonectidae): Implications for arthropod relationships. Arthropod Structure & Development 34:343-378.

Fanenbruck M, Harzsch S, Wägele JW. 2004. The brain of the Remipedia (Crustacea) and an alternative hypothesis on their phylogenetic relationships. Proceedings of the National Academy of Sciences of the United States of America 101:3868-3873.

Fanenbruck M. 2003. Die Anatomie des Kopfes und des cephalen Skelett-Muskelsystems der Crustacea, Myriapoda und Hexapoda - Ein Beitrag zum phylogenetischen System der Mandibulata und zur Kenntnis der Herkunft der Remipedia und Tracheata. Dissertation. Ruhr-Universität Bochum. 436 S.

Farris SM. 2005a. Developmental organization of the mushroom bodies of *Thermobia domestica* (Zygentoma, Lepismatidae): Insights into mushroom body evolution from a basal insect. Evolution & Development 7:150-159.

Farris SM. 2005b. Evolution of insect mushroom bodies: Old clues, new insights. Arthropod Structure & Development 34:211-234.

Fischer AHL, Scholtz G. 2010. Axogenesis in the stomatopod crustacean *Gonodactylaceus falcatus* (Malacostraca). Invertebrate Biology 129:59-76.

Frase, T. 2012. Evolution und Entwicklung des Nervensystems der Anostraca. Diplomarbeit. Universität Rostock. 82 S.

Fritsch M, Bininda-Emonds ORP, Richter S. 2013. Unraveling the origin of Cladocera by identifying heterochrony in the developmental sequences of Branchiopoda. Frontiers in Zoology 10.

Fritsch M, Richter S. 2010. The formation of the nervous system during larval development in *Triops cancriformis* (Bosc) (Crustacea, Branchiopoda): An immunohistochemical survey. Journal of Morphology 271:1457-1481.

Fritsch M, Richter S. 2012. Nervous system development in Spinicaudata and Cyclestherida (Crustacea, Branchiopoda): Comparing two different modes of indirect development by using an event pairing approach. Journal of Morphology 273:672-695.

Giribet G, Edgecombe GD. 2012. Reevaluating the arthropod tree of life. Annual Review of Entomology 57:167-186.

Giribet G, Richter S, Edgecombe GD, Wheeler WC. 2005. The position of crustaceans within Arthropoda: Evidence from nine molecular loci and morphology. In: Koenemann S, Jenner RA (Hrsg). Crustacea and Arthropod Relationships. Boca Raton, London, New York, Singapore: Tailor Francis Group. S. 307-352.

Giribet G, Edgecombe GD, Wheeler WC. 2001. Arthropod phylogeny based on eight molecular loci and morphology. Nature 413:157-161.

Giribet G, Richter S, Edgecombe GD, Wheeler WC. 2004. The position of Crustacea within Arthropoda: evidence from nine molecular loci and morphology. Crustacean Issues 16:307-352.

Gleeson RA, McDowell LM, Aldrich HC. 1996. Structure of the aesthetasc (olfactory) sensilla of the blue crab, *Callinectes sapidus*: Transformations as a function of salinity. Cell and Tissue Research 284:279-288.

Hallberg E, Johansson KUI, Wallén R. 1997. Olfactory sensilla in crustaceans: morphology, sexual dimorphism, and distribution patterns. International Journal of Insect Morphology and Embryology 26:173-180.

Hanström B. 1928. Vergleichende Anatomie des Nervensystems der wirbellosen Tiere unter Berücksichtigung seiner Funktion. Berlin, Heidelberg, New York: Julias Springer. 623 S.

Hanström, B. 1940. Inkretorische Organe, Sinnesorgane und Nervensystem des Kopfes einiger niederer Insektenordnungen. Stockholm, Almqvist & Wiksells Boktryckeri-A.-B. Kungliga Svenska Vetenskapsakademiens Handlingar Tredje serien 8:1-266.

Harrison PJ, Macmillan DL, Young HM. 1995. Serotonin immunoreactivity in the ventral nerve cord of the primitive crustacean *Anaspides tasmaniae* closely resembles that of crayfish. Journal of Experimental Biology 198:531-535.

Hartenstein V, Younossihartenstein A, Lekven A. 1994. Delamination and division in the *Drosophila* neurectoderm: Spatiotemporal pattern, cytoskeletal dynamics, and common control by neurogenic and segment polarity genes. Developmental Biology 165:480-499.

Harzsch S. 2001. Neurogenesis in the crustacean ventral nerve cord: Homology of neuronal stem cells in Malacostraca and Branchiopoda? Evolution & Development 3:154-169.

Harzsch S. 2002. Neurobiologie und Evolutionsforschung: „Neurophylogenie“ und die Stammesgeschichte der Euarthropoda. Neuroforum 4/02:267-273.

Harzsch S. 2003. Evolution of identified arthropod neurons: The serotonergic system in relation to engrailed-expressing cells in the embryonic ventral nerve cord of the American lobster *Homarus americanus* Milne Edwards, 1873 (Malacostraca, Pleocyemata, Homarida). Developmental Biology 258:44-56.

Harzsch S. 2004. Phylogenetic comparison of serotonin-immunoreactive neurons in representatives of the Chilopoda, Diplopoda, and Chelicerata: Implications for arthropod relationships. Journal of Morphology 259:198-213.

Harzsch S. 2006. Neurophylogeny: Architecture of the nervous system and a fresh view on arthropod phyologeny. Integrative and Comparative Biology 46:162-194.

Harzsch S. 2007. The architecture of the nervous system provides important characters for phylogenetic reconstructions: Examples from the Arthropoda. Species, Phylogeny and Evolution 1:33-57.

Harzsch S, Glötzner J. 2002. An immunohistochemical study of structure and development of the nervous system in the brine shrimp *Artemia salina* Linnaeus, 1758 (Branchiopoda, Anostraca) with remarks on the evolution of the arthropod brain. Arthropod Structure & Development 30:251-270.

Harzsch S, Hansson BS. 2008. Brain architecture in the terrestrial hermit crab *Coenobita clypeatus* (Anomura, Coenobitidae), a crustacean with a good aerial sense of smell. BMC Neuroscience 9.

Harzsch S, Müller CHG, Wolf H. 2005. From variable to constant cell numbers: Cellular characteristics of the arthropod nervous system argue against a sister-group relationship of Chelicerata and ''Myriapoda'' but favour the Mandibulata concept. Development Genes and Evolution 215:53-68.

Harzsch S, Rieger V, Krieger J, Seefluth F, Strausfeld NJ, Hansson BS. 2011. Transition from marine to terrestrial ecologies: changes in olfactory and tritocerebral neuropils in land-living isopods. Arthropod Structure & Development 40:244-257.

Harzsch S, Waloszek D. 2000. Serotonin-immunoreactive neurons in the ventral nerve cord of Crustacea: A character to study aspects of arthropod phylogeny. Arthropod Structure & Development 29:307-322.

Hassanin A. 2006. Phylogeny of Arthropoda inferred from mitochondrial sequences: Strategies for limiting the misleading effects of multiple changes in pattern and rates of substitution. Molecular Phylogenetics and Evolution 38:100-116.

Haug JT, Waloszek D, Haug C, Maas A. 2010. High-level phylogenetic analysis using developmental sequences: The Cambrian dagger *Martinssonia elongata*, dagger *Musacaris gerdgeyeri* gen. et sp. nov. and their position in early crustacean evolution. Arthropod Structure & Development 39:154-173.

Hennig W. 1966. Phylogenetic Systematics. Urbana: University of Illinois Press. 263 S.

Hessler AY, Hessler RR, Sanders HL. 1970. Reproductive system of *Hutchinsoniella macracantha*. Science 168:1464.

Hessler RR. 1964. The Cephalocarida: Comparative skeletomusculature. Memoirs of the Connecticut Academy of Arts & Sciences XVI:1-97.

Hessler RR. 1984. Cephalocarida: Living fossil without a fossil record. In: Eldredge N, Stanley SM (Hrsg). Living fossils. New York: Springer. S. 181-186.

Hessler RR. 1992. Reflections on the phylogenetic position of the Cephalocarida. Acta Zoologica 73:315-316.

Hessler RR, Elofsson R. 1991. Excretory system of *Hutchinsoniella macracantha* (Cephalocarida). Journal of Crustacean Biology 11:356-367.

Hessler RR, Elofsson R. 1992. Cephalocarida. In: Harrison FW (Hrsg). Microscopic Anatomy of Invertebrates. New York: Wiley-Liss. S. 9-24.

Hessler RR, Elofsson R, Hessler AY. 1995. Reproductive system of *Hutchinsoniella macracantha* (Cephalocarida). Journal of Crustacean Biology 15:493-522.

Hessler RR, Sanders HL. 1973. Two new species of *Sandersiella* (Cephalocarida), including one from the deep sea. Crustaceana 24:181-196.

Hessler RR, Elofsson R. 2001. The circulatory system and an enigmatic cell type of the cephalocarid crustacean *Hutchinsoniella macracantha*. Journal of Crustacean Biology 21:28-48.

Holmgren N. 1916. Zur vergleichenden Anatomie des Gehirns von Polychæten, Onychophoren, Xiphosuren, Arachniden, Crustaceen, Myriapoden und Insekten. Kungliga Svenska Vetenskapsakademiens Handlingar 56.

Homberg U. 2002. Neurotransmitters and neuropeptides in the brain of the locust. Microscopy Research and Technique 56:189-209.

Homberg U. 2008. Evolution of the central complex in the arthropod brain with respect to the visual system. Arthropod Structure & Development 37:347-362.

Homberg U, Hildebrand JG. 1991. Histamine-immunoreactive neurons in the midbrain and subesophageal ganglion of the sphinx moth *Manduca sexta*. Journal of Comparative Neurology 307:647-657.

Jenner RA. 2010. Higher-level crustacean phylogeny: Consensus and conflicting hypotheses. Arthropod Structure & Development 39:143-153.

Joly R, Descamps M. 1987. Histology and ultrastructure of the myriapod brain. In: Gupta A (Hrsg). Arthropod brain – its evolution, development, structure, and functions. New York, Chichester, Brisbane, Toronto, Singapore: John Wiley & Sons. S. 135-157.

Kenning M, Müller CHG, Wirkner CS, Harzsch S. 2013. The Malacostraca (Crustacea) from a neurophylogenetic perspective: New insights from brain architecture in *Nebalia herbstii* Leach, 1814 (Leptostraca, Phyllocarida). Zoologischer Anzeiger.

Koenemann S, Jenner RA, Hoenemann M, Stemme T, von Reumont BM. 2010. Arthropod phylogeny revisited, with a focus on crustacean relationships. Arthropod Structure & Development 39:88-110.

Kollmann M, Huetteroth W, Schachtner J. 2011. Brain organization in Collembola (springtails). Arthropod Structure & Development 40:304-316.

Kubrakiewicz J, Jaglarz MK, Iliffe TM, Bilinski SM, Koenemann S. 2012. Ovary structure and early oogenesis in the remipede, *Godzilliognomus frondosus* (Crustacea, Remipedia): phylogenetic implications. Zoology 115:261-269.

Lacalli TC. 2009. Serial EM analysis of a copepod larval nervous system: Naupliar eye, optic circuitry, and prospects for full CNS reconstruction. Arthropod Structure & Development 38:361-375.

Langworthy K, Helluy S, Benton J, Beltz B. 1997. Amines and peptides in the brain of the American lobster: Immunocytochemical localization patterns and implications for brain function. Cell and Tissue Research 288:191-206.

Lauterbach K-E. 1980. Schlüsselereignisse in der Evolution des Grundplans der Mandibulata (Arthropoda). Abhandlungen aus dem Gebiete der Naturwissenschaften, Naturwissenschaftlicher Verein Hamburg 23:105-161.

Lauterbach K-E. 1986. Zum Grundplan der Crustacea. Verhandlungen des naturwissenschaftlichen Vereins Hamburg 28:27-63.

Lauterbach K-E. 1979. Über die mutmaßliche Herkunft der Epipodite der Crustacea. Zoologischer Anzeiger 202:33-50.

Lavrov DV, Brown WM, Boore JL. 2004. Phylogenetic position of the Pentastomida and (pan)crustacean relationships. Proceedings of the Royal Society of London, Series B : Biological Sciences 271:537-544.

Loesel R. 2004. Comparative morphology of central neuropils in the brain of arthropods and its evolutionary and functional implications. Acta Biologica Hungarica 55:39-51.

Loesel R, Nassel DR, Strausfeld NJ. 2002. Common design in a unique midline neuropil in the brains of arthropods. Arthropod Structure & Development 31:77-91.

Loesel R, Richter S. 2014. Neurophylogeny: From description to character analysis. In: Wägele JW, Bartolomaeus T (Hrsg). Deep metazoan phylogeny: The backbone of the Tree of Life. Berlin: de Gruyter. S. 505-514.

Loesel R, Wolf H, Kenning M, Harzsch S, Sombke A. 2013. Architectural principles and evolution of the arthropod central nervous system. In: Minelli A, Boxshall G, Fusco G (Hrsg). Arthropod biology and evolution - molecules, development, morphology. Heidelberg, New York, Dordrecht, London: Springer. S. 299-342.

Maas A, Haug C, Haug JT, Olesen J, Zhang X, Waloszek D. 2009. Early crustacean evolution and the appearance of epipodites/gills. Arthropod Systematics & Phylogeny 67:255-273.

Maas A, Waloszek D. 2005. Phosphatocopina – ostracode-like sister group of Eucrustacea. Hydrobiologia 538:139-152.

Martin JW, Olesen J, Hoeg JT. 2014. Atlas of crustacean larvae. Baltimore: John Hopkins University Press. 384 S.

Moura G, Christoffersen ML. 1996. The system of the mandibulate arthropods: Tracheata and Remipedia as sister groups, "Crustacea" non-monophyletic. Journal of Computational Biology 1:96-113.

Müller C. 2008. Vergleichend-ultrastrukturelle Untersuchungen an Augen ausgewählter Hundertfüßer (Mandibulata: Chilopoda) und zur Bedeutung von Augenmerkmalen für die phylogenetische Rekonstruktion der Euarthropoda. Göttingen: Cuvillier Verlag. 276 S.

Müller CHG, Rosenberg J, Richter S, Meyer-Rochow VB. 2003. The compound eye of *Scutigera coleoptrata* (Linnaeus, 1758) (Chilopoda: Notostigmophora): An ultrastructural reinvestigation that adds support to the Mandibulata concept. Zoomorphology 122:191-209.

Oakley TH, Wolfe JM, Lindgren AR, Zaharoff AK. 2013. Phylotranscriptomics to bring the understudied into the fold: Monophyletic Ostracoda, fossil placement, and pancrustacean phylogeny. Mol Biol Evol 30:215-233.

Olesen J, Haug JT, Maas A, Waloszek D. 2011. External morphology of *Lightiella monniotae* (Crustacea, Cephalocarida) in the light of Cambrian 'Orsten' crustaceans. Arthropod Structure & Development 40:449-478.

Olesen J, Walossek D. 2000. Limb ontogeny and trunk segmentation in *Nebalia* species (Crustacea, Malacostraca, Leptostraca). Zoomorphology 120:47-64.

Overstreet RM, Dyková I, Hawkins WE. 1992. Branchiura. In: Harrison FW, Humes AG (Hrsg). Microscopic Anatomy of Invertebrates Vol. 9. New York: Wiley-Liss Inc. S. 385-413.

Pabst T, Scholtz G. 2009. The development of phyllopodous limbs in Leptostraca and Branchiopoda. Journal of Crustacean Biology 29:1-12.

Pfeiffer K, Homberg U. 2014. Organization and functional roles of the central complex in the insect brain. Annual Review of Entomology, Vol 59, 2014 59:165-U787.

Podsiadlowski L, Bartolomaeus T. 2006. Major rearrangements characterize the mitochondrial genome of the isopod *Idotea baltica* (Crustacea : Peracarida). Molecular Phylogenetics and Evolution 40:893-899.

Read AT, Hessler RR, Govind CK. 1994. Muscle and nerve terminal fine structure of a primitive crustacean, the cephalocarid *Hutchinsoniella macracantha*. Biological Bulletin 187:16-22.

Regier JC, Shultz JW, Zwick A, Hussey A, Ball B, Wetzer R, Martin JW, Cunningham CW. 2010. Arthropod relationships revealed by phylogenomic analysis of nuclear protein-coding sequences. Nature 463:1079-1U98.

Richter S. 2002. The Tetraconata concept: Hexapod-crustacean relationships and the phylogeny of Crustacea. Organisms Diversity & Evolution 2:217-237.

Richter S, Loesel R, Purschke G, Schmidt-Rhaesa A, Scholtz G, Stach T, Vogt L, Wanninger A, Brenneis G, Doring C, Faller S, Fritsch M, Grobe P, Heuer CM, Kaul S, Møller OS, Müller CHG, Rieger V, Rothe BH, Stegner MEJ, Harzsch S. 2010. Invertebrate neurophylogeny: Suggested terms and definitions for a neuroanatomical glossary. Frontiers in Zoology 7.

Richter S, Stein M, Frase T, Szucsich NU. 2013. The arthropod head. In: Minelli A, Boxshall GA, Fusco G (Hrsg). Arthropod biology and evolution. Berlin, Heidelberg: Springer-Verlag. S. 223-240.

Richter S, Wirkner CS. 2014. A research program for Evolutionary Morphology. Journal of Zoological Systematics and Evolutionary Research 52:338-350.

Rota-Stabelli O, Campbell L, Brinkmann H, Edgecombe GD, Longhorn SJ, Peterson KJ, Pisani D, Philippe H, Telford MJ. 2011. A congruent solution to arthropod phylogeny: Phylogenomics, microRNAs and morphology support monophyletic Mandibulata. Proceedings of the Royal Society B-Biological Sciences 278:298-306.

Sanders HL. 1954. The Cephalocarida, a new subclass of Crustacea from Long Island Sound. Proceedings of the National Academy of Sciences of the United States of America 41:61-66.

Sanders HL. 1957. The Cephalocarida and crustacean phylogeny. Systematic Zoology 6:112-148.

Sanders HL. 1963. The Cephalocarida. Memoirs of the Connecticut Academy of Arts & Sciences 15:1-80.

Sanna D, Addis A, Carcupino M, Francalacci P. 2010. Molecular data on two mitochondrial genes of a newly discovered crustacean species (*Lightiella magdalenina*, Cephalocarida). Journal of the Marine Biological Association of the United Kingdom 90:827-829.

Schachtner J, Schmidt M, Homberg U. 2005. Organization and evolutionary trends of primary olfactory brain centers in Tetraconata (Crustacea plus Hexapoda). Arthropod Structure & Development 34:257-299.

Schmidt M, Ache BW. 1997. Immunocytochemical analysis of glomerular regionalization and neuronal diversity in the olfactory deutocerebrum of the spiny lobster. Cell and Tissue Research 287:541-563.

Scholtz G. 1992. Cell lineage studies in the crayfish *Cherax destructor* (Crustacea, Decapoda): Germ band formation, segmentation, and early neurogenesis. Rouxs Archives of Developmental Biology 202:36-48.

Scholtz G, Edgecombe GD. 2006. The evolution of arthropod heads: Reconciling morphological, developmental and palaeontological evidence. Development Genes and Evolution 216:395-415.

Scholtz G, Richter S. 1995. Phylogenetic systematics of the reptantian Decapoda (Crustacea, Malacostraca). Zoological Journal of the Linnean Society 113:289-328.

Scholtz G, Wolff C. 2013. Arthropod embryology: Cleavage and germ band development. In: Minelli A, Boxshall GA, Fusco G (Hrsg). Arthropod biology and evolution: Molecules, development, morphology. Heidelberg, New York, Dordrecht, London: Springer. S. 63-90.

Schram FR. 1986. Crustacea. New York, Oxford: Oxford University Press. 606 S.

Schram FR. 1983. Remipedia and crustacean phylogeny. In: Schram FR (Hrsg). Crustacean Phylogeny. Rotterdam: A.A. Balkema. S. 23-28.

Semmler H, Wanninger A, Hoeg JT, Scholtz G. 2008. Immunocytochemical studies on the naupliar nervous system of *Balanus improvisus* (Crustacea, Cirripedia, Thecostraca). Arthropod Structure & Development 37:383-395.

Shanbhag SR, Müller B, Steinbrecht RA. 1999. Atlas of olfactory organs of *Drosophila melanogaster*. 1. Types, external organization, innervation and distribution of olfactory sensilla. International Journal of Insect Morphology & Embryology 28:377-397.

Shimomura M, Akiyama T. 2008. Description of a new species of Cephalocarida, *Sandersiella kikuchii*, and redescription of *S. acuminata* Shiino based upon the type material. Journal of Crustacean Biology 28:572-579.

Siewing R. 1960. Neuere Ergebnisse der Verwandtschaftsforschung bei den Crustaceen. Wissenschaftliche Zeitschrift der Universuität Rostock 9:343-358.

Sombke A, Ernst A. 2014. Structure and distribution of antennal sensilla in Oranmorpha guerinii (Gervais, 1837) (Diplopoda, Polydesmida). Arthropod Structure & Development 43:77-86.

Sombke A, Lipke E, Kenning M, Müller CHG, Hansson BS, Harzsch S. 2012. Comparative analysis of deutocerebral neuropils in Chilopoda (Myriapoda): Implications for the evolution of the arthropod olfactory system and support for the Mandibulata concept. BMC Neuroscience 13:1-17.

Sombke A, Rosenberg J, Hilken G. 2011. Chilopoda: Nervous system. In: Minelli A (Hrsg). Treatise on Zoology - Anatomy, Taxonomy, Biology. The Myriapoda, Volume 1. Leiden, Boston: Brill. S. 217-234.

Spears T, Abele LG. 1998. Crustacean phylogeny inferred from 18S rDNA. In: Fortey RA, Thomas RH (Hrsg). Arthropods relationships. London: Chapman & Hall. S. 169-187.

Spears T, Abele LG. 1999. Phylogenetic relationships of crustaceans with foliaceous limbs: An 18s rDNA study of Branchiopoda, Cephalocarida, and Phyllocarida. Journal of Crustacean Biology 19:825-843.

Stegner MEJ, Brenneis G, Richter S. 2014a. The ventral nerve cord in Cephalocarida (Crustacea): New insights into the ground pattern of Tetraconata. Journal of Morphology 275:269-294.

Stegner MEJ, Fritsch M, Richter S. 2014b. The central complex in Crustacea. In: Wägele JW, Bartolomaeus T (Hrsg). Deep metazoan phylogeny: The backbone of the Tree of life. Berlin: de Gruyter. S. 361-384.

Stegner MEJ, Richter S. 2011. Morphology of the brain in *Hutchinsoniella macracantha* (Cephalocarida, Crustacea). Arthropod Structure & Development 40:221-243.

Stegner MEJ, Richter S. 2015. Development of the nervous system in Cephalocarida – Early neuronal differentiation and successive patterning. Zoomorphology 134:183-209.

Stemme T, Iliffe TM, Bicker G, Harzsch S, Koenemann S. 2012. Serotonin immunoreactive interneurons in the brain of the Remipedia: New insights into the phylogenetic affinities of an enigmatic crustacean taxon. BMC Evolutionary Biology 12:168.

Stemme T, Iliffe TM, von Reumont BM, Koenemann S, Harzsch S, Bicker G. 2013. Serotonin-immunoreactive neurons in the ventral nerve cord of Remipedia (Crustacea): Support for a sister group relationship of Remipedia and Hexapoda? BMC Evolutionary Biology 13:119.

Stollewerk A, Simpson P. 2005. Evolution of early development of the nervous system: A comparison between arthropods. Bioessays 27:874-883.

Strausfeld CM, Buschbeck EK, Gomez RS. 1995. The arthropod mushroom body: Its functional roles, evolutionary enigmas and mistaken identities. In: Breidbach O, Kutsch W (Hrsg). The nervous system of invertebrates: An evolutionary and comparative approach. Basel, Boston, Berlin: Birkhäuser. S. 349-381.

Strausfeld N. 2012. Arthropod brains: Evolution, functional elegance, and historical significance. Cambridge, MA: Harvard University Press. 830 S.

Strausfeld N, Reisenman CE. 2009. Dimorphic olfactory lobes in the Arthropoda. International Symposium on Olfaction and Taste 1170:487-496.

Strausfeld NJ. 2005. The evolution of crustacean and insect optic lobes and the origins of chiasmata. Arthropod Structure & Development 34:235-256.

Strausfeld NJ. 2009. Brain organization and the origin of insects: An assessment. Proceedings of the Royal Society B-Biological Sciences 276:1929-1937.

Strausfeld NJ, Andrew DR. 2011. A new view of insect-crustacean relationships I. Inferences from neural cladistics and comparative neuroanatomy. Arthropod Structure & Development 40:276-288.

Strausfeld NJ, Hansen L, Li YS, Gomez RS, Ito K. 1998. Evolution, discovery, and interpretations of arthropod mushroom bodies. Learning & Memory 5:11-37.

Strausfeld NJ, Sinakevitch I, Brown SM, Farris SM. 2009. Ground plan of the insect mushroom body: Functional and evolutionary implications. Journal of Comparative Neurology 513:265-291.

Strausfeld NJ, Strausfeld CM, Loesel R, Rowell D, Stowe S. 2006. Arthropod phylogeny: Onychophoran brain organization suggests an archaic relationship with a chelicerate stem lineage. Proceedings of the Royal Society B-Biological Sciences 273:1857-1866.

Stuardo JR, Vega R. 2011. SEM study of *Sandersiella chilenica* sp. nov. (Cephalocarida), with a review of the integumentary structures and functional adaptations in the group. Gayana (Concepción) 1:99-122.

Sudhaus W, Rehfeld K. 1992. Einführung in die Phylogenetik und Systematik. Berlin: Spektrum Akademischer Verlag. 241 S.

Tiegs OW, Manton SM. 1958. The evolution of the Arthropoda. Biological Reviews of the Cambridge Philosophical Society 33:255-337.

Ungerer P, Eriksson BJ, Stollewerk A. 2011a. Neurogenesis in the water flea *Daphnia magna* (Crustacea, Branchiopoda) suggests different mechanisms of neuroblast formation in insects and crustaceans. Developmental Biology 357:42-52.

Ungerer P, Geppert M, Wolff C. 2011b. Axogenesis in the central and peripheral nervous system of the amphipod crustacean *Orchestia cavimana*. Integrative Zoology 6:28-44.

Ungerer P, Scholtz G. 2008. Filling the gap between identified neuroblasts and neurons in crustaceans adds new support for Tetraconata. Proceedings of the Royal Society B-Biological Sciences 275:369-376.

Utting M, Agricola HJ, Sandeman R, Sandeman D. 2000. Central complex in the brain of crayfish and its possible homology with that of insects. Journal of Comparative Neurology 416:245-261.

Vilpoux K, Sandeman R, Harzsch S. 2006. Early embryonic development of the central nervous system in the Australian crayfish and the Marbled crayfish (Marmorkrebs). Development Genes and Evolution 216:209-223.

von Reumont BM, Jenner RA, Wills MA, Dell'Ampio E, Pass G, Ebersberger I, Meyer B, Koenemann S, Iliffe TM, Stamatakis A, Niehuis O, Meusemann K, Misof B. 2012. Pancrustacean phylogeny in the light of new phylogenomic data: Support for Remipedia as the possible sister group of Hexapoda. Molecular Biology and Evolution 29:1031-1045.

von Reumont BM, Meusemann K, Szucsich NU, Dell'Ampio E, Gowri-Shankar V, Bartel D, Simon S, Letsch HO, Stocsits RR, Luan Y-X, Wägele JW, Pass G, Hadrys H, Misof B. 2009. Can comprehensive background knowledge be incorporated into substitution models to improve phylogenetic analyses? A case study on major arthropod relationships. BMC Evolutionary Biology 9:119.

von Reumont BM, Wägele JW. 2014. Advances in molecular phylogeny of crustaceans in the light of phylogenomic data. In: Wägele JW, Bartolomaeus T (Hrsg). Deep Metazoan Phylogeny: The backbone of the Tree of Life. Berlin: de Gruyter. S. 385-398.

Walossek D. 1993. The Upper Cambrian *Rehbachiella kinnekullensis* and the phylogeny of Branchiopoda and Crustacea. Fossils & Strata 32:1-202.

Walossek D, Müller KJ. 1998. Cambrian 'Orsten'-type arthropods and the phylogeny of Crustacea. In: Fortey RA, Thomas RH (Hrsg). Arthropod relationships. London: Chapman Hall. S. 139-153.

Waloszek D. 2003. Cambrian 'Orsten'-type preserved arthropods and the phylogeny of Crustacea. Proceedings of the 18th International Congress of Zoology 69-87.

Wheeler SR, Carrico ML, Wilson BA, Brown SJ, Skeath JB. 2003. The expression and function of the achaete-scute genes in *Tribolium castaneum* reveals conservation and variation in neural pattern formation and cell fate specification. Development 130:4373-4381.

Williams JLD. 1975. Anatomical studies of the insect central nervous system: A ground-plan of the midbrain and an introduction to the central complex in the locust, *Schistocerca gregaria* (Orthoptera). Journal of Zoology 176:67-86.

Williams T, Blachuta B, Hegna TA, Nagy LM. 2012. Decoupling elongation and segmentation: Notch involvement in anostracan crustacean segmentation. Evolution & Development 14:372-382.

Wingstrand KG. 1978. Comparative Spermatology of the Crustacea Entomostraca 1. Subclass Branchiopoda. Biologiske Skrifter 22:1-67.

Wolff G, Harzsch S, Hansson BS, Brown S, Strausfeld N. 2012. Neuronal organization of the hemiellipsoid body of the land hermit crab, *Coenobita clypeatus*: Correspondence with the mushroom body ground pattern. Journal of Comparative Neurology 520:2824-2846.

Publikationen der Dissertation

10. Morphology of the brain in *Hutchinsoniella macracantha* (Cephalocarida, Crustacea). Stegner MEJ, Richter S (2011): Arthropod Structure and Development 40:221-243

Arthropod Structure & Development 40 (2011) 221–243

Contents lists available at ScienceDirect

Arthropod Structure & Development

journal homepage: www.elsevier.com/locate/asd

Morphology of the brain in *Hutchinsoniella macracantha* (Cephalocarida, Crustacea)

Martin E.J. Stegner*, Stefan Richter

Institut für Biowissenschaften, Abteilung Allgemeine und Spezielle Zoologie, Universität Rostock, Universitätsplatz 2, 18055 Rostock, Germany

ARTICLE INFO

Article history:
Received 1 October 2010
Accepted 18 April 2011

Keywords:
Neurophylogeny
Homology
Immunolabeling
3D-reconstruction
Multi-lobed complex
Olfactory lobe
Immunoreactive domains

ABSTRACT

External morphological features of Cephalocarida have long been interpreted as plesiomorphic with regard to those of other crustaceans. Based on transmission electron microscopy and light microscopy, however, the brain in the cephalocarid *Hutchinsoniella macracantha* has been shown to contain a number of structures that are more difficult to interpret in an evolutionary context. These include the multi-lobed complex, a unique cluster of neuropils associated with the olfactory lobes. To establish a well-founded comparison of phylogenetically relevant, neuroanatomical data from Cephalocarida to other arthropods, we investigated the brain in *H. macracantha* using immunolabeling (acetylated α-tubulin, serotonin, RFamide, histamine) and nuclear counter stains of whole mounts and vibratome sections analyzing specimens with confocal laser scanning microscopy and computer-aided 3D-reconstruction. Other 3D-reconstructions were based on serial 1 μm semi-thin sections. The multi-lobed complex features a pedunculus and shows detailed homologies with the mushroom bodies of certain Insecta and Lithobiomorpha (Chilopoda), suggesting that the hemiellipsoid bodies in Remipedia and Malacostraca have derived from a cephalocarid-like pattern. Like the corresponding tracts in Insecta, the olfactory globular tracts linking the multi-lobed complex to the olfactory lobes are ipsilateral, probably constituting the plesiomorphic pattern from which the decussating tracts in Remipedia and Malacostraca have evolved. The olfactory lobes in *H. macracantha* are uniquely organized into vertical stacks of olfactory glomeruli whose exact shape could not be identified. Similarly to Malacostraca and Insecta, the olfactory glomeruli in *H. macracantha* are innervated by serotonin-like, RFamide-like, and histamine-like immunoreactive interneurons. This suggests homology of the olfactory lobes across Tetraconata, despite the different morphological organization. Although *H. macracantha* lacks elongated, unpaired midline neuropils known from the protocerebrum of other Arthropoda, the possible rudiment of a central-body-like neuropil that receives decussating fibers from anterior somata was revealed by the serotonin-like immunoreactive pattern.

1. Introduction

In addition to Malacostraca, Branchiopoda, Remipedia, and "Maxillopoda", Cephalocarida constitute one of the five higher taxa of Crustacea. The first species, *Hutchinsoniella macracantha*, was discovered only in 1954 by Howard Sanders (Sanders, 1954), and it has since been the basis for most morphological studies in Cephalocarida. *H. macracantha* has a length of about 3 mm and occurs in the upper, flocculent layer of the benthic zone in the Northwestern Atlantic. The low abundance of this species, and the slurry consistency of the detritus-rich sediment, make the collection time-consuming and restrict the number of *H. macracantha* available for research. Today, a total of 11 species of Cephalocarida have been described from marine coasts all over the world (Carcupino et al., 2006).

Several external anatomical and behavioral features of Cephalocarida – such as the thoracopod-like second maxilla or the general function of the appendages, which are used for swimming and feeding at the same time – have been interpreted as plesiomorphic with respect to the ground pattern of Crustacea, Mandibulata, or Euarthropoda (e.g., Sanders, 1957, 1963; Hessler, 1964, 1992; Lauterbach, 1974, 1983, 1986; Walossek, 1993). Yet, even if Cephalocarida might externally suggest "living fossils", they are not in all respects plesiomorphic. Their hermaphroditism was suggested to be an autapomorphy by Ax, (1999, based on Hessler et al., 1995). Also, the cephalocarid nervous system features a number of

* Corresponding author. Tel.: +49 381 4986263; fax: +49 381 4986262.
E-mail address: martin.stegner@uni-rostock.de (M.E.J. Stegner).

1467-8039/$ – see front matter © 2011 Elsevier Ltd. All rights reserved.
doi:10.1016/j.asd.2011.04.001

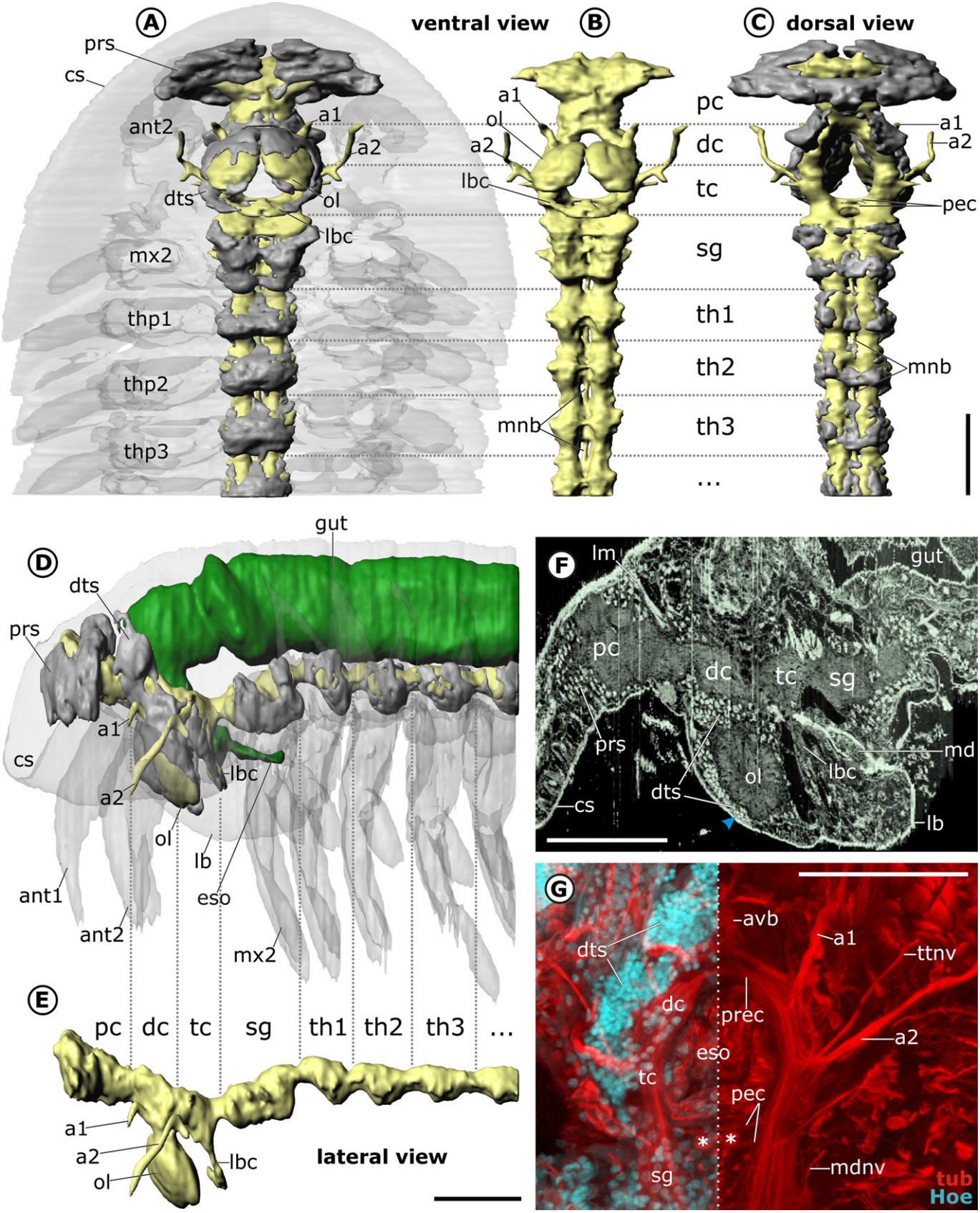

Fig. 1. Position and general morphology of the brain. A–E: 3D-reconstructions of somata (grey) and neuropil (yellow) in relation to body contours (semitransparent) and the gut (green), based on semi-thin sections. Smaller nerves omitted. F: Virtual sagittal section through an image stack based on semi-thin sections. A group of small-diameter somata (blue arrowhead) lies anteriorly in the olfactory lobe (ol), which is situated ventral to the rest of the deutocerebrum (dc). G: Confocal laser scan of a whole mount showing the circumesophageal region in ventral view. Imaris surpass view. The two post-esophageal commissures (pec) are separated from each other by muscles (asterisks). Abbreviations:

structures that have been considered derived from the ground pattern of Crustacea.

The first detailed study of Cephalocarida was based on transmission electron (TEM) and light microscopy (LM) and concentrated on the anterior portion of the nervous system of *H. macracantha* (Elofsson and Hessler, 1990). The study revealed that the brain contains an intricate cluster of interconnected neuropils. Elofsson and Hessler (1990) termed this cluster 'mushroom bodies', but emphasized structural differences with respect to mushroom bodies found in other arthropods. To avoid drawing premature homologies, we here follow Fanenbruck's and Harzsch's (2005) suggestion to instead use the more descriptive term 'multilobed complex' rather than 'mushroom body'. Elofsson and Hessler (1990) showed that the multi-lobed complex is associated with a pair of large (deutocerebral) olfactory lobes situated in the labrum. Due to their unusual internal organization, the olfactory lobes of *H. macracantha* were erroneously interpreted as compound eyes in an earlier description by Burnett (1981). The first immunolabeling of the nervous system in *H. macracantha* was undertaken by Elofsson (1992), at that time without the benefits of confocal laser scanning microscopy. This author identified approximately 60 serotonin-like immunoreactive (SL-ir) and approximately 80 RFamide-like immunoreactive (RFL-ir) neurons on each body side, including three SL-ir and eleven RFL-ir neurons in the brain. Apart from a schematic drawing of the yet undepicted posterior portion of the nervous system added by Hessler and Elofsson (1992), no further studies of the cephalocarid nervous system have been undertaken.

Interest in arthropod neuroanatomy has grown significantly in the past two decades, particularly with respect to the use of neural structures for inferring phylogeny, a field of study coined 'neurophylogeny' by Harzsch (2006, 2007), based on the term 'neural phylogeny' introduced by Paul (1989). Recent neuroanatomical studies combine a comparative, phylogenetic approach with present-day methods such as confocal laser scanning microscopy and computer-based 3D-reconstruction. While detailed insights into the neuroanatomy of Insecta (e.g., Farris, 2005b; Strausfeld et al., 2009; Galizia and Rössler, 2009) and Malacostraca (e.g., Schachtner et al., 2005; Harzsch and Hansson, 2008; Krieger et al., 2010) have improved our picture on the evolution of the nervous system, as have investigations of long-neglected arthropod taxa such as Remipedia (Fanenbruck et al., 2004), Anostraca (Harzsch and Glötzner, 2002), Notostraca (Fritsch and Richter, 2010), and Mystacocarida (Brenneis and Richter, 2010), several authors have expressed the need for more detailed data on the nervous system in Cephalocarida (e.g., Strausfeld et al., 1998; Harzsch and Waloszek, 2000; Fanenbruck and Harzsch, 2005; Schachtner et al., 2005; Harzsch, 2006; Homberg, 2008).

The phylogenetic position of Cephalocarida is difficult to reconstruct, because possible synapomorphies with other Crustacea are elusive. Based mainly on limb morphology and fossil evidence, Sanders (1963) suggested that Cephalocarida are the sister-group to all other Crustacea. In Walossek's (1993) view, Cephalocarida are the sister-group to Branchiopoda + Maxillopoda, together with those two constituting the monophylum Entomostraca. Following Hessler (1992), Cephalocarida, Branchiopoda, and Malacostraca form together the monophylum Thoracopoda, with their epipods as a synapomorphy (see also Ax, 1999; Edgecombe et al., 2000; Richter, 2002). Based only on neuroanatomical characters, Harzsch (2006: his Fig. 6) suggested a monophylum composed of Cephalocarida, Hexapoda, and Remipedia + Malacostraca. Concerning the exact position of Cephalocarida, none of these hypotheses was supported by molecular data. Instead, molecular analyses imply Cephalocarida as a sister-group candidate to Copepoda (Spears and Abele, 1999), Cirripedia + Ostracoda (Giribet et al., 2005: their Fig. 5, combining molecular with morphological data) and, most recently, Remipedia (Regier et al., 2010; Koenemann et al., 2010). Apart from being representatives of the Tetraconata (which includes by definition all crustaceans and hexapods, see Richter, 2002), we have to admit the phylogenetic position of cephalocarids is still unknown, which obviously makes any discussion on evolutionary transformations difficult.

Elofsson's and Hessler's (1990) report of complexity in the brain of *H. macracantha* encouraged a reinvestigation using present-day methods to resolve morphological characters that could prove helpful for phylogenetic and evolutionary discussion. Using a combination of semi-thin sectioning, immunolabeling, confocal laser scanning microscopy, and computer-aided 3D-reconstruction, the present paper expands Elofsson's and Hessler's (1990) pioneering TEM and LM study as well as Elofsson's (1992) observations of serotonin-like and RFamide-like immunoreactivity.

2. Material and methods

2.1. Collection, fixation, and storage

Adults, juveniles, and larvae of the cephalocarid species *H. macracantha* were collected in September 2007, September 2008, and July 2009 at different spots in Buzzards Bay, Massachusetts (USA). Samples of benthic mud were collected by boat from depths of 5–25 m using a dredge or diving. The animals were separated from the sieved samples using fine forceps or pipettes. Three different fixation methods were required for procedures used for this study. (1) For semi-thin sectioning, one adult animal was fixed and stored in Bouin's fixative (Mulisch and Welsch, 2010) whose salinity had been increased to 3% by adding NaCl. (2) For immunolabeling of acetylated α-tubulin as well as serotonin-like and RFamide-like proteins, animals were fixed with a 4% 'saline paraformaldehyde solution' (16% PFA stem solution [Electron Microscopy Sciences, Hatfield, PA: N° CAS #30525-89-4] diluted in 'saline PBS solution' which was produced by dilution of 10 × PBS stock solution in filtered water from Buzzards Bay) for 30 min to 1 h. Fixed specimens were transferred to 100% methanol for storage at 4 °C. (3) For immunolabeling of histamine-like proteins, animals were fixed in a 4% 'saline carbodiimid solution' (400 mg of carbodiimid [Sigma–Aldrich, St. Louis, MO: N° E1769] in 10 ml of filtered water from Buzzards Bay) for 24 h at 4 °C. Hereafter, specimens were postfixed with a 4% 'saline paraformaldehyde solution' for 1 h and stored in 'saline PBS solution' at 4 °C. All animals used for this study were adults, except that (a) serotonin-like immunoreactivity in the olfactory lobes could best be visualized in a juvenile, and (b) as we only had three adults fixed for histamine-like staining, our data on this neurotransmitter are mainly based on larval stages.

2.2. Pretreatment of whole mounts for immunolabeling

After a dilution series from their storage medium into PBS, specimens were exposed to short pulses (<1 s with 35 kHz) in

a1 – antennular nerve. a2 – antennal nerve. ant1 – antennule. ant2 – antenna. avb – anteroventral fiber bundle. cs – cephalic shield. dc – deutocerebrum. dts – deuto-tritocerebral somata assemblage. eso – esophagus. gut – gut. lb – labrum. lbc – labral commissure. lm – labral muscles 1 and 2. md – mandible. mdnv – mandible nerve. mnb – median fiber bundle. mx2 – maxilla 2. ol – olfactory lobe. pc – protocerebrum. pec – post-esophageal commissures. prs – protocerebral somata assemblage. prec – pre-esophageal commissure. sg – subesophageal ganglion. tc – tritocerebrum. th1-3 – thoracic ganglia 1-3. thp1-3 – thoracopods 1-3. ttnv – tritocerebral tegumentary nerve. Scale bars: 100 μm.

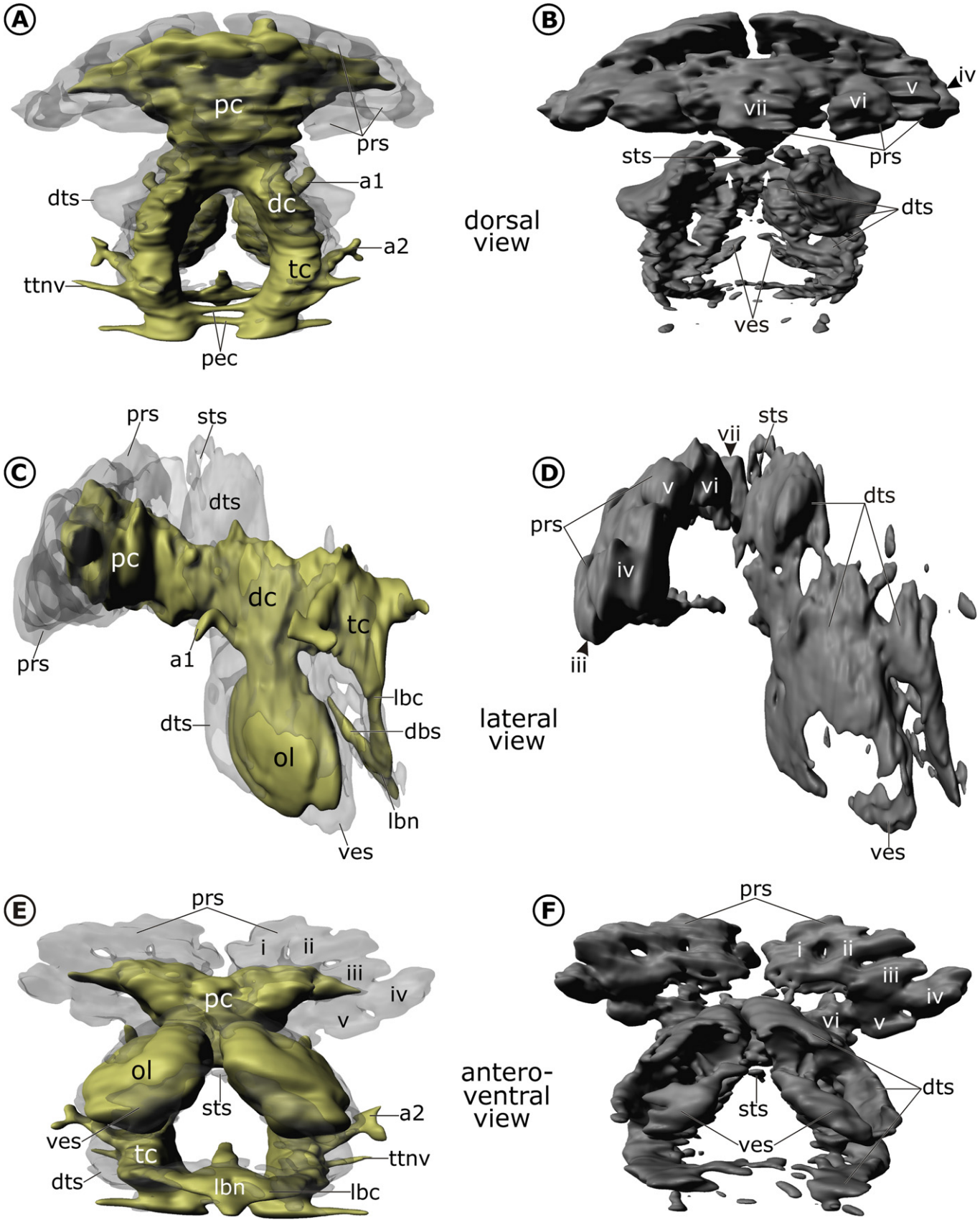

Fig. 2. Somata assemblages in relation to the neuropil of the brain. A,C,E: 3D-reconstructions of the somata assemblages (semitransparent) and neuropil based on semithin-sections. B,D,F: 3D-reconstructions of somata assemblages. B,D: Several muscles split the posterodorsal region of the protocerebral somata assemblage (prs) into three divisions (from lateral: v-vii). White arrows in B indicate the horizontal connection between the two halves of the deuto-tritocerebral somata assemblage (dts). E,F: The anteroventral region

a bath-ultrasonicator (Elma, Singen, Germany: Elmasonic One). Between pulses, specimens were investigated with a stereomicroscope to check for any visible signs of external or internal damage due to treatment. Ultrasonication permeabilized the cuticle in PFA-fixed specimens, but this treatment destroyed carbodiimid/PFA-fixed specimens already at the first pulse. In some specimens, the distal portions of the cephalic appendages, the cephalic shield, or the labrum were removed using dissecting instruments such as forceps, needles, or a small razorblade segment attached to the tip of a glass Pasteur pipette. The two pretreatment procedures were often combined and facilitated the penetration of antibodies. Dissection of the labrum allowed scanning more deeply into the brain from ventral direction.

2.3. Vibratome sectioning for immunolabeling

Specimens chosen for vibratome sectioning first underwent a dilution series from their storage medium into PBS. Then they were put on a glass plate, patted dry with a tissue, and covered by a drop of Poly-L-Lysin (Sigma–Aldrich, St. Louis, MO: N° P8920) to increase the affinity to the embedding medium. After a few seconds in Poly-L-Lysin, specimens were patted dry again and completely sunken in 3% agarose. The hardened block was cut off the glass plate with a razor blade and glued onto the working disk of a Hyrax V50 vibratome (Carl Zeiss Jena GmbH, Jena, Germany). Vibratome sections between 50 and 150 μm thick were cut in transverse, horizontal, and sagittal planes, removed with a soft brush, and stored in PBS at 4 °C until needed for immunolabeling.

2.4. Immunolabeling and mounting

Both vibratome sections and whole mounts underwent the same immunolabeling procedures. Antibody incubation was conducted in PBT (PBS with 0.5% bovine serum albumin, 0.3% Triton X-100, 1.5% dimethylsulfoxide) containing 5% Normal Goat Serum (Calbiochem, Merck KGaA, Darmstadt, Germany: N° NS02L). Labeling of the cytostructural protein acetylated α-tubulin was performed with a primary monoclonal mouse antibody (anti-ac-α-tub IgG 2b Isotype, clone 6–11B-1, Sigma–Aldrich, St. Louis, MO: N° T6793 [dilution 1:100]) and a Cy-3-coupled secondary goat antibody (anti-mouse IgG (H + L), Jackson/Dianova, Hamburg, Germany: N° 115-001-003 [dilution 1:200]). For labeling of the neuropeptide RFamide and the biogenic amines serotonin and histamine, polyclonal rabbit antisera were used (Neuromics, Edina, MN: N°: 20002 [dilution 1:1000]; Immunostar, Hudson, WI: N° 20080 [dilution 1:100]; and Progen, Heidelberg, Germany: N° 16043 [dilution 1:100], respectively). An Alexa 488-coupled secondary goat antibody (anti-rabbit IgG (H + L), Invitrogen Molecular Probes, Darmstadt, Germany: N° A11008, dilution 1:500) was applied for visualization. Labeling of nuclei was accomplished with Hoechst (Invitrogen Molecular Probes, Darmstadt, Germany: N° H33342, 1 μg/ml in PBS). Incubations were carried out overnight at 4 °C, each time followed by thorough washing in PBT on a horizontal shaker (neoLab, Heidelberg, Germany: DOS-20S) at 50 rpm. The use of polyclonal antisera against serotonin, RFamide, and histamine does not exclude the possibility of labeling related neuroactive substances. This holds in particular for the neuropeptide RFamide, which is a member of a large neuropeptide family that is characterized by a shared RFamide motif (Zajac and Mollereau, 2006 for short overview). Therefore, we refer to serotonin-like, RFamide-like, and histamine-like immunoreactivity (SLI, RFLI, HLI). Stained whole mounts were mounted in Vectashield Mounting Medium (Vector Laboratories Inc., Burlingame, CA), after placing tiny pieces of plasticine as spacers at the corners of the cover slips. Stained vibratome sections were mounted in Mowiol 4–88 (Roth, Karlsruhe, Germany: N° 0713) between two cover slips, enabling scanning from both sides.

2.5. Laser scanning microscopy

Stained specimens were scanned using a DM IRE2 confocal laser scanning microscope (UV: 405 nm; Arg/Kr: 488 nm, HeNe: 543 nm) equipped with a TCS SP2 AOBS laser scanning unit (Leica Microsystems GmbH, Wetzlar, Germany) at step sizes of 0.4–0.7 μm between successive scanning planes. Alternatively, a DMI 6000 CS confocal laser scanning microscope (Arg/Kr: 488 nm, HeNe: 543 nm) equipped with a TCS SP5 II laser scanning unit (Leica Microsystems GmbH, Wetzlar, Germany) was used at same step sizes.

2.6. Semi-thin sectioning and digitization

The specimen fixed in 'saline Bouin's fixative' (see above) was dehydrated in a graded ethanol series and, after an intermediate step of epoxypropane, embedded in araldite epoxy resin under vacuum. Serial semi-thin sections (2160 × 1 μm) were made in the transverse plane with an RM 2165 microtome (Leica Microsystems GmbH, Wetzlar, Germany), using glass knives. The sections were stained with a mixture of 1% azure II blue and 1% methylene blue in aqueous 1% borax solution for approximately 20–35 s at 80–90 °C. The histological sections were digitized with an AxioCam ICc 3 digital camera mounted on an Axio Scope Imager.M1 microscope (Carl Zeiss Jena GmbH, Jena, Germany). Sections were digitized in 20× magnification yielding an overall image of the whole brain in relation to other organ systems. Using 40× magnifications yielded a more detailed image of its substructures. Digitized sections were aligned and combined to a 3D virtual stack using the software AutoAligner (Bitplane AG, Zurich, Switzerland), respectively. A congruent alignment was guaranteed by referring to the following structures from anterior to posterior (see Hessler, 1964: his Fig. 2): the cephalic shield cuticle, cephalic pleural muscles cp1+2, labral muscles lm1+2, and the ventral longitudinal muscles vlm.

2.7. Analysis and 3D-reconstruction

All analyses and 3D-reconstructions of the 3D virtual stacks derived from laser scanning microscopy and histological sectioning were built using the software Imaris (Bitplane AG, Zurich, Switzerland: versions 6.0.2, 6.4.0 and 7.0). The 'surpass view' is used to display the complete data set, whereas the 'extended section mode' of this program generates virtual sections of individually definable thickness, achieved by including a variable number of images. The 'blend' option renders scanned structures opaque, thus allowing an evaluation of a structure's surface and external shape. In some cases, for a better 3D presentation of data, the 'contour surface' tool was used to highlight specific structures artificially or to mask structures that obscure viewing the nervous system. All figure plates were created and labeled using the

of the protocerebral somata assemblage (prs) is split into four divisions (from medial: i-iv). Abbreviations: a1 – antennular nerve. a2 – antennal nerve. dbs – dorsal fiber bundle of the stomatogastric nervous system. dc – deutocerebrum. dts – deuto-tritocerebral somata assemblage. i-vii – divisions i-vii of the protocerebral somata assemblage. lbc – labral commissure. lbn – labral neuropil. ol – olfactory lobe. pc – protocerebrum. pec – post-esophageal commissures. prs – protocerebral somata assemblage. sts – stomatogastric somata. tc – tritocerebrum. ttnv – tritocerebral tegumentary nerve. ves – ventral somata assemblage.

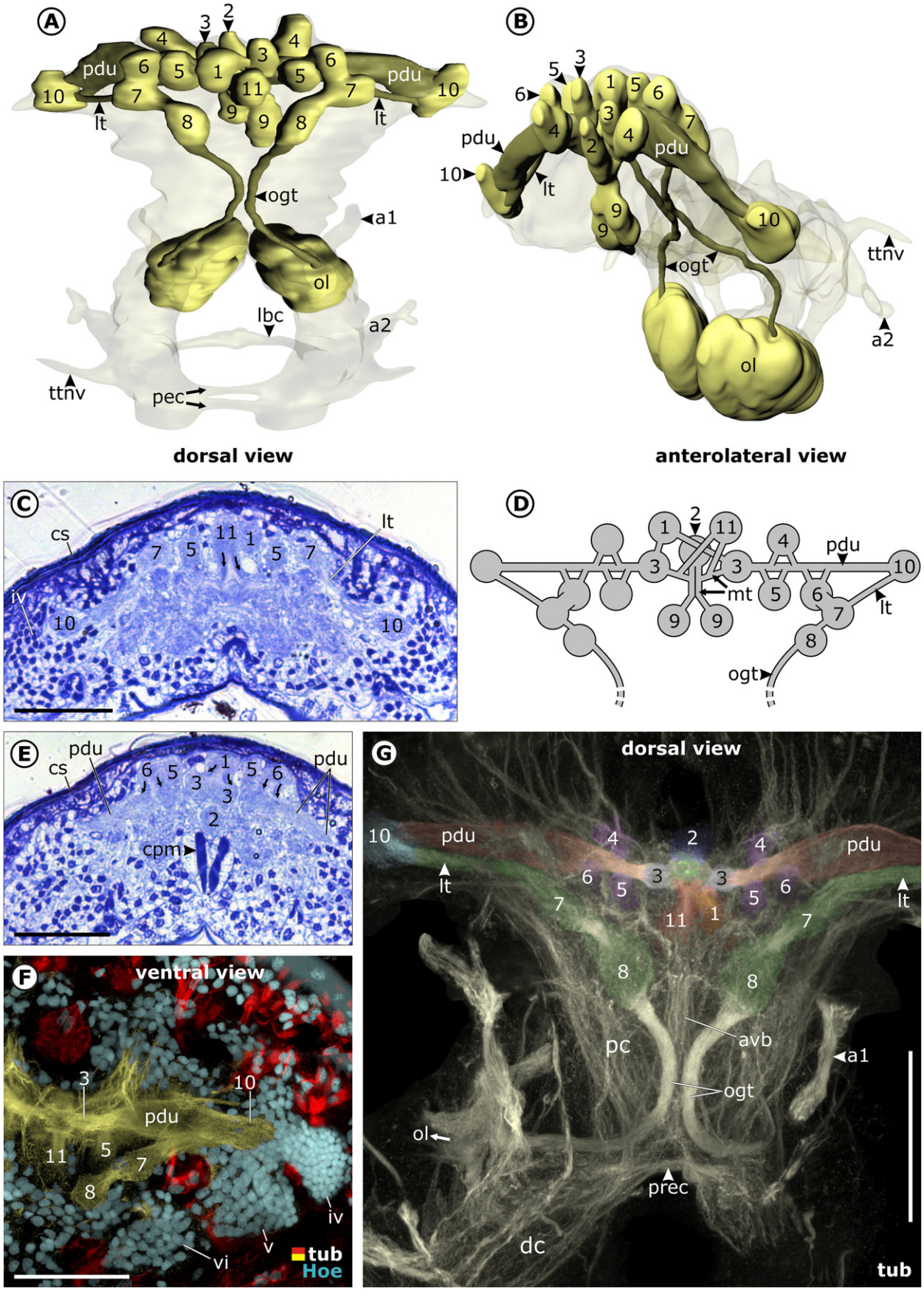

software Corel Draw X3. Bitmap images were edited unselectively using the software Corel PhotoPaint X3.

2.8. Presentation of data and terminology

For a better visualization of the 3D-reconstructions, the Supplementary material provides a number of red/cyan anaglyph stereograms, which are best viewed using a pair of red/cyan 3D glasses. (A practicable alternative is a pair of green/red 3D glasses with the red glass over the left eye.) We widely use the neuroanatomical terminology proposed by Richter et al. (2010). Morphological descriptions of spatially extended structures can require coordinates and directional terms, such as 'extend into' or 'project anteriorly'. These do not carry physiological, ontogenetic, or evolutionary inferences. All positions (such as 'anterior' or 'dorsal') refer to the body axis. In all figures showing immunolabeling results, the presumed labeled molecules are indicated within the corresponding figure and are abbreviated as follows: acetylated α-tubulin (tub); Hoechst (Hoe); serotonin-like, RFamide-like, and histamine-like immunoreactivity (SLI, RFLI, HLI). The corresponding adjectives serotonin-like, RFamide-like, and histamine-like immunoreactive have here been abbreviated to SL-ir, RFL-ir, and HL-ir, respectively. We use the term olfactory glomerulus (*Latin* glomerulus – 'little ball') in a wider sense to include also olfactory neuropils that are geometrically distinct from ball-shaped elements, as practiced by many other morphologists (e.g., Hanström, 1928, 1947; Elofsson and Hessler, 1990; Sandeman et al., 1992; Sullivan and Beltz, 2004; Schachtner et al., 2005; Krieger et al., 2010).

3. Results

3.1. General anatomy of the brain and associated nerves

Traditionally, the brain in Euarthropoda is conceived as a syncerebrum, i.e., the entity of the three anteriormost subunits of the nervous system: the protocerebrum, deutocerebrum, and tritocerebrum (see Scholtz and Edgecombe, 2006; Richter et al., 2010). In *H. macracantha*, the protocerebrum (pc) is unpaired and situated anterior to the esophagus (eso), while the deutocerebrum (dc) and the tritocerebrum (tc) occur as paired halves situated anterolateral and lateral to the esophagus, respectively (Fig. 1).

3.1.1. Protocerebrum

The protocerebral neuropil (pc) is distinct from the deutocerebral neuropil (dc, Figs. 1B,E,F, 2A,C, 3G), connected to the latter on each side of the brain by the olfactory globular tract (ogt) and by an unpaired anteroventral fiber bundle (avb; Figs. 1G, 3G, 4A,B). Optic lobes are absent. The distinction of the protocerebrum (pc) from the deutocerebrum (dc) is indicated by a transition zone that lacks somata (Fig. 1A,C,D,F) and shows less SLI, RFLI, and HLI than either the protocerebral (pc) or deutocerebral neuropil (dc, Figs. 5C, 6G, 9H).

3.1.2. Deutocerebrum

On each side of the brain, the deutocerebrum gives rise laterally to the root of the antennular nerve (a1, Figs. 1A–E,G, 2A,C, 4F). Because the basal segment of the antennule (ant1) is anterodorsal to this root, the incoming antennular nerve (a1) describes an upward arc before entering the deutocerebrum (Figs. 1D,E, 2C, 6A). Proximally, the root (a1) bifurcates, with the dorsal part proceeding into the main part of the deutocerebral neuropil (dc) and the ventral part proceeding into one olfactory lobe (arrows, ol, Fig. 6A,B). Both olfactory lobes (ol) are situated distinct from, and ventral to the rest of the deutocerebral neuropil (dc), connected to the latter via a thick fiber bundle (Figs. 1A,B,D-F, 2C, 4D). Their location in this position suggests a bulge of the brain extruding out into the base of the labrum. But this should not conceal the fact that the olfactory lobes are deutocerebral structures. The root of one deutocerebral tegumentary nerve resides immediately dorsal to the root of the antennular nerve. From there, the deutocerebral tegumentary nerve (dtnv) extends anterodorsally (Fig. 5A), passes the dorsal side of the protocerebrum, and terminally splits up into a number of thin bundles, all of which project ipsilaterally to the anterior cephalic shield. The paired halves of the deutocerebral neuropil (dc) are interconnected anteroventrally by a pre-esophageal commissure (prec, Figs. 1G, 3G, 4F). Different from the intervening gap between the proto- and deutocerebrum, a distinct border between the deuto- and tritocerebrum is not apparent: most deutocerebral and tritocerebral somata are arranged as one somata assemblage on each side of the brain (dts, Figs. 1F,G, 2). Thus, the deutocerebrum is denoted only by the antennular nerve entering it.

3.1.3. Tritocerebrum

The tritocerebral neuropil (tc) gives rise to a pair of antennal nerves (a2) as well as a pair of the tritocerebral tegumentary nerves (ttnv, Figs. 1G, 6A). The latter originate dorsal to the antennal nerves and, like the deutocerebral tegumentary nerves, divide distally into a number of thin bundles that extend out to the anterolateral cephalic shield. Two post-esophageal commissures (pec), one anterior and one posterior, connect the two halves of the tritocerebrum (tc, Figs. 1G, 2A). Near the midline, the commissures are separated by a few dorsoventrally oriented muscles (asterisks, Fig. 1G). The root of the anterior post-esophageal commissure lies directly posterodorsal to the root of the labral commissure (lbc), which connects the two halves of the tritocerebrum ventrally (tc, Figs. 1A,B,D–F, 2C,E). This connection sags downwards at its vertex, which is connected to the stomatogastric nervous system (see below). Posteriorly, a pair of post-tritocerebral connectives link the tritocerebrum (tc) with the subesophageal ganglion (sg, Figs. 1C–G, 6A,B). Although a border between deutocerebral and tritocerebral

Fig. 3. Multi-lobed complex. A,B: 3D-reconstructions of the multi-lobed complex neuropils (yellow) and tracts (dark yellow) in relation to the brain neuropil (semitransparent). A: Neuropil 1, 2, and 11 are the only unpaired neuropils in the multi-lobed complex. Due to space restrictions in the cephalon, neuropil 1 and 11 are displaced from the midline. C: Transverse semi-thin section through the posterior region of the multi-lobed complex. Neuropil 11 has a bulbous shape and a pair of tracts (arrows) leaving it ventrally. D: Schematic interpretation of the connectivity among the multi-lobed complex neuropils in posterodorsal view. For presentability, the positional relationships between the neuropils were slightly distorted. E: Transverse semi-thin section through the anterior region of the multi-lobed complex. Here, neuropil 2 lies amidst the less distinctly structured neuropil of the ventral protocerebrum and between a pair of cephal pleural muscles (cpm). Neuropil 6 is connected to the pedunculus (pdu) via two tracts (arrows) leaving ventrally. Similarly, neuropil 1 is connected to a pair of neuropils 3 via short tracts (arrows). F: Confocal laser scan focussing the left part of the protocerebrum. Imaris extended section view. Nervous tissue (yellow) and muscle tissue (red) artificially highlighted using the Imaris contour surface tool. Small-diameter globuli cell somata (iv, v) lie densely packed lateral to neuropil 10. G: Confocal laser scan of a vibratome section showing the protocerebral neuropil (pc) in dorsal view. Imaris surpass view. Multi-lobed complex neuropils (1-11) artificially highlighted using the Imaris contour surface tool. The ipsilateral olfactory globular tract (ogt) connects the olfactory lobe (indicated by ol) to neuropil 8. Abbreviations: 1-11 – multi-lobed complex neuropils 1-11. a1 – antennular nerve. a2 – antennal nerve. avb – anteroventral fiber bundle. cpm – cephal pleural muscle 1. cs – cephalic shield. dc – deutocerebrum. iv-vi – divisions iv-vi of the protocerebral somata assemblage. lbc – labral commissure. lt – lateral tract. mt – medial tracts. ogt – olfactory globular tract. ol – olfactory lobe. pc – protocerebrum. pdu – pedunculus. pec – post-esophageal commissures. prec – pre-esophageal commissure. ttnv – tritocerebral tegumentary nerve. Scale bars: 50 μm.

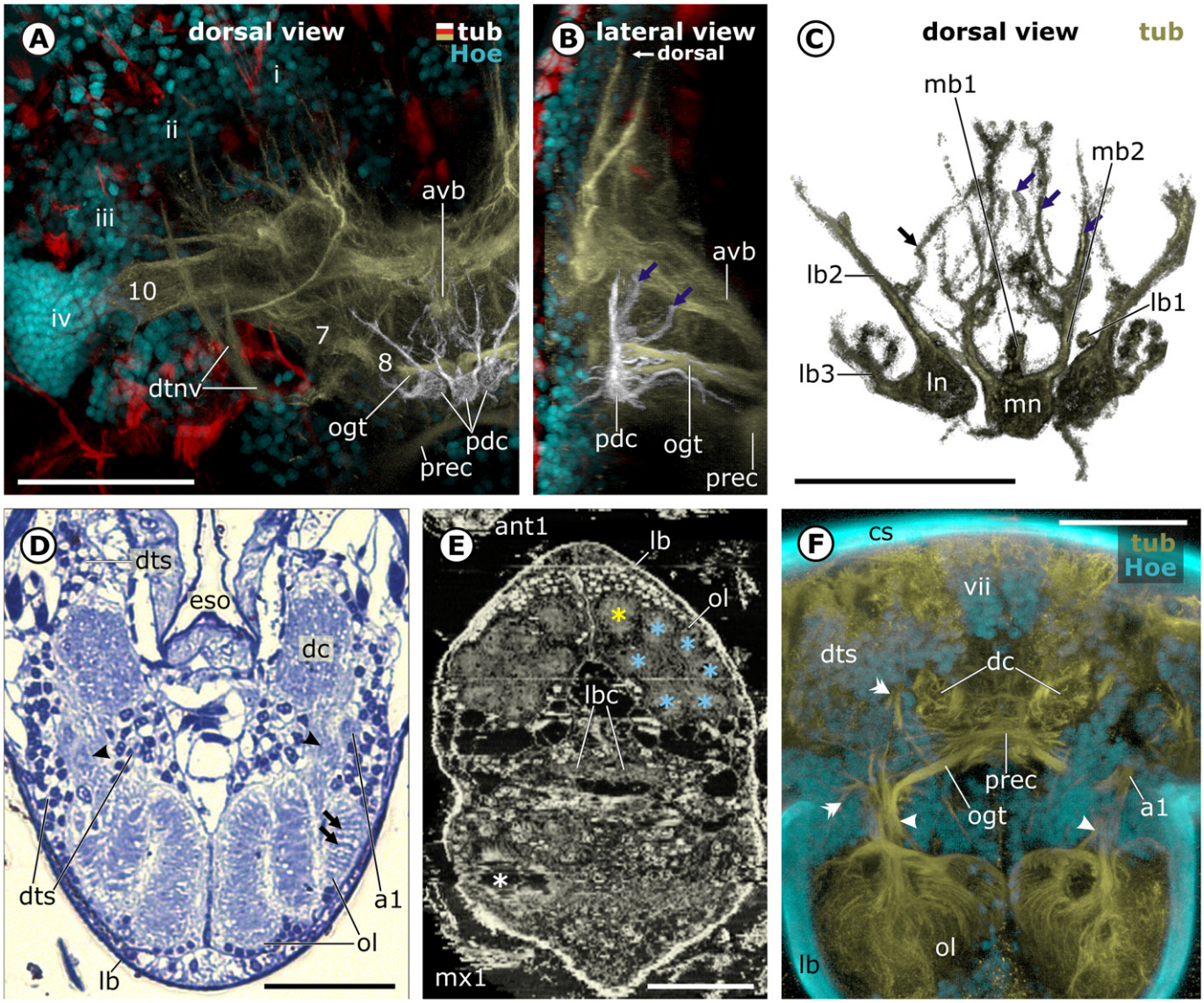

Fig. 4. Posterodorsal neuropil cluster (A–C) and olfactory lobes (D–F). A,B: Confocal laser scan of a whole mount showing the left part of the protocerebrum. Imaris extended section view. Muscles (red), posterodorsal neuropil cluster (pdc, white), and rest of nervous tissue (yellow) artificially highlighted using the Imaris contour surface tool. The posterodorsal neuropil cluster (pdc) lies posteromedial to the olfactory globular tract (ogt) and is connected to the large unpaired anteroventral fiber bundle (avb) via several processes (blue arrows). C: Same data set as in A,B. Imaris surpass view. Structures surrounding the posterodorsal neuropil cluster were artificially removed using the Imaris contour surface tool. Several larger fiber bundles (mb1-2, lb1-3) branch (blue and black arrows) to connect the posterodorsal neuropil cluster with different regions of the nervous system. D: Transverse semi-thin section through the anterior labrum. The olfactory lobe (ol) is composed of vertical stacks of olfactory glomeruli (arrows). A thick fiber bundle (arrowheads) leaves each olfactory lobe (ol) dorsally and connects it to different regions of the nervous system. E: Virtual horizontal section through an image stack based on transverse semi-thin sections. Each olfactory lobe (ol) consists of six even-sized (blue asterisks) and one slightly larger vertical stack (yellow asterisk) of olfactory glomeruli. The white asterisk marks the furrow tangent to the dorsal edge of the left mandible. F: Confocal laser scan of a transverse vibratome section through the anterior labrum. Imaris extended section view. The thick fiber bundle (arrowheads) dorsally splits up into the antennular nerve (a1), the olfactory globular tract (ogt), and a few thinner fiber bundles (double arrowheads) associated to the deuto-tritocerebral somata assemblage (dts). Abbreviations: 7-10 – multi-lobed complex neuropils 7-10. a1 – antennular nerve. ant1 – antennule. avb – anteroventral fiber bundle. cs – cephalic shield. dc – deutocerebral neuropil. dtnv – deutocerebral tegumentary nerve. dts – deuto-tritocerebral somata assemblage. eso – esophagus. i-vii – divisions i-vii of the protocerebral somata assemblage. lb – labrum. lb1-3 – lateral fiber bundles 1-3 (starting from the lateral neuropil). lbc – labral commissure. ln – lateral neuropil of the posterodorsal neuropil cluster. mb1,2 – median fiber bundles 1 and 2 (starting from the median neuropil). mn – median neuropil of the posterodorsal neuropil cluster. mx1 – maxilla 1. ogt – olfactory globular tract. ol – olfactory lobe. pdc – posterodorsal neuropil cluster. prec – pre-esophageal commissure. Scale bars: A,B,D–F: 50 μm. C: 25 μm.

neuropil is not indicated by immunoreactivity, a strongly SL-ir domain (sd4) is present at the root of the labral commissure (lbc). This marks the position of the tritocerebrum, just as does the antennal nerve entering it (Fig. 6A,B).

3.1.4. Neuraxis

The neuraxis of *H. macracantha*, which is the axis of the central nervous system, as defined by its arrangement of segmental ganglia irrespective of any curvature, runs directly posteriorly from the protocerebrum (pc) through the tritocerebrum (tc). The neuraxis trajectory in the brain is slightly deflected from the body axis (Fig. 1D–F). Posterior to the tritocerebrum, the neuraxis bends slightly upwards to parallel the gut through all segments as far as the furca (Fig. 1D–F).

3.2. Somata assemblages

The majority of neurons in the brain are unipolar (e.g., Fig. 5B: s5). Somata are arranged in altogether four distinct somata assemblages (two unpaired and one pair), clearly separated from

each other in the periphery of the brain, with the neuropil situated centrally (Fig. 2).

3.2.1. Protocerebral somata assemblage

Different from Decapoda, where the protocerebral somata are arranged in a number of distinct somata assemblages (Sandeman et al., 1992), all protocerebral somata in *H. macracantha* are arranged as one contiguous unpaired protocerebral somata assemblage (prs), which is situated anteroventral, posterodorsal, and lateral to the protocerebral neuropil and extends into the cephalic shield (prs, Figs. 1A,C,D,F, 2A,C,E). The ventral, anterior, anterodorsal, and posterior surface of the protocerebral neuropil is not covered by somata, however. The protocerebral somata assemblage (prs) is traversed dorsoventrally by about ten muscles on each side of the brain (see hollows in Fig. 2E,F). These are conspicuous landmarks, by which the protocerebral somata assemblage can be subdivided into different partitions, although these are not strictly separated from each other. In other words, these partitions are purely topological: they do not represent structural entities but facilitate morphological description, especially when it comes to locating immunoreactive somata (see below). Anteroventrally, the protocerebral somata assemblage is split into four partitions on each side of the brain (from medial to lateral: partition i, ii, iii, iv; Figs. 2E,F, 4A, 6E). Two further partitions on each side (from lateral to medial: v, vi), and one unpaired partition in the midline (vii), are situated posterodorsally (Figs. 2B,D,F, 3F, 6E). Somata in partition iv and in a small region of partition v have a smaller diameter and are more densely packed than somata in any other partition (prs, Figs. 3C,F, 4A, 6E). These especially small somata are here referred to as globuli cell somata.

3.2.2. Deuto-tritocerebral somata assemblage

The deuto-tritocerebral somata assemblage (dts) is situated dorsal, lateral, and ventral to the deutocerebral neuropil (dc), anteriorly in the olfactory lobe (ol), and lateral to the tritocerebral neuropil (tc, Figs. 1D,F,G, 2, 4D,F, 8E). Ventral to the tritocerebral neuropil, it also extends along the labral commissure (lbc, Figs. 1A, 2E,F). A thin row of somata situated anteroventral to the deutocerebral neuropil merges the two large halves of the assemblage across the midline (white arrows, dts, Fig. 2B). The largest extension of the deuto-tritocerebral somata assemblage (dts) occurs dorsal to the deutocerebral neuropil (dc) on each side of the brain (Figs. 1D, 2C,D). Acetylated α-tubulin and nuclear staining suggests that most (if not all) somata in this region send their neurites (double arrowheads) ipsilaterally into the olfactory lobe (ol) via a thick bundle (arrowhead, Fig. 4F).

3.2.3. Ventral somata assemblage

A small isolated ventral somata assemblage (ves) is situated at the ventral margin of each olfactory lobe (ol; Fig. 2B–F).

In addition, the dorsal fiber bundle belonging to the stomatogastric nervous system (described below) is associated with a diffuse group of stomatogastric somata, anterior to the esophagus (sts, Fig. 2B–F).

3.3. Neuropils and associated fiber bundles

H. macracantha's protocerebrum and deutocerebrum reveal a number of spatially and structurally distinctive neuropils (e.g., 1, 5, 7, Fig. 3C). Due to their comparatively high density and their distinctive boundaries, these can be identified in semi-thin sections and in acetylated α-tubulin stains. In the protocerebrum, these dense neuropils are arranged in two clusters: the multi-lobed complex and the posterodorsal neuropil cluster. The neuropil of the deutocerebral olfactory lobe is also clearly distinguished by virtue of its internal organization (see below). The tritocerebrum lacks discrete neuropils.

3.3.1. Multi-lobed complex

The multi-lobed complex is situated dorsally in the protocerebral neuropil and constitutes the most prominent feature of the brain, comprising altogether 19 neuropils (three unpaired neuropils, labeled 1, 2, and 11, and eight pairs of neuropils, labeled 3-10) and a pair of pedunculi (pdu, Fig. 3). All neuropils of the multi-lobed complex have a bulbous shape and are approximately of uniform size. Neuropils 1, 2, 4, 5, 6, and 11 are distinguished by having two tracts that initially extend in the same direction and then diverge. This is illustrated in Fig. 3C where neuropil 11 gives rise to two smaller tracts (indicated by arrows) that initially run parallel with each other ventrally, before one tract bends to the left and the other to the right (compare also neuropils 1 and 6 in Fig. 3E). Crucially, all 19 neuropils of the multi-lobed complex are linked by tracts and thus form one coherent structural unit (Fig. 3D). The exact anatomy of the multi-lobed complex can be best understood starting from its posterior end. This is where the protocerebral portion of the olfactory globular tract (ogt: see below), which ascends from the olfactory lobes from a posteroventral direction, enters neuropil 8. On each side of the brain, the olfactory globular tract (ogt), and neuropils 8, 7, and 10 form together one diagonal axis (Fig. 3A,D,G). Neuropil 8 is linked to neuropil 7 via a short tract, and a longer lateral tract (lt) links neuropil 7 to neuropil 10 (Fig. 3A,C,D,G). Neuropil 7 is furthermore fused anteriorly to neuropil 6 (Fig. 3A,B,D). Laterally, neuropil 10 is immediately associated with the globuli cell somata in partitions iv and v of the protocerebral somata assemblage (Fig. 3F). Medially, neuropil 10 is linked to the pedunculus of the multi-lobed complex (pdu), which extends to neuropil 3 (Fig. 3A,B,F,G). Compared to the lateral tract and the olfactory globular tract, the pedunculus's diameter is much wider. Its fibers lie parallel to one another but are more loosely packed than those found in other tracts and neuropils. Medially, the pedunculus (pdu) gives rise to neuropils 6 and 5 from its posterodorsal side and to neuropil 4 from its anterior side (Fig. 3). Neuropil 3 is connected via a short tract to neuropil 1 (Fig. 3A,D,E), but not to neuropil 11. Moreover, a medial tract (mt) leaves the medial side of neuropil 3 to extend ventrally to neuropil 9, which is situated in the anteroventral protocerebrum (Fig. 3B,D). Although the medial tracts in both sides of the brain touch at the midline, no processes could be shown to extend across the midline. Two unpaired neuropils are connected to the medial tracts each via a pair of fiber bundles pointing ventrally; neuropil 2 (Fig. 3A,B,D,G) is situated anterodorsal and neuropil 11 (Fig. 3A–D,G) posterodorsal to the medial tracts (mt). Given the different connectivity of neuropil 1 and 11, their immediate lateral neighborhood must not give the impression that the neuropils form a bilaterally symmetrical pair. Rather, neuropil 1 and 11 are simply displaced from the midline, due to space restrictions within the cephalon. Our data suggest that the unpaired neuropils 1, 2, and 11 are the only structures of the multi-lobed complex that span the midline (Fig. 3A,C–E).

3.3.2. Posterodorsal neuropil cluster

The posterodorsal neuropil cluster (pdc) is situated posterodorsally in the protocerebral neuropil (Fig. 4A,B) and comprises three neuropils: an unpaired median neuropil (mn) and a pair of lateral neuropils (ln, Fig. 4C). All three are about the same size, are bulbous and have a high density of processes. Anterolaterally, each side of the posterodorsal neuropil cluster (pdc) is flanked by the olfactory globular tract (ogt) and by neuropil 8 of the multi-lobed complex (Fig. 4A,B). Each of the three neuropils sends a number of fiber bundles to different regions of the nervous system (mb1,2, lb1-3 in Fig. 4C; arrows in Fig. 4B,C).

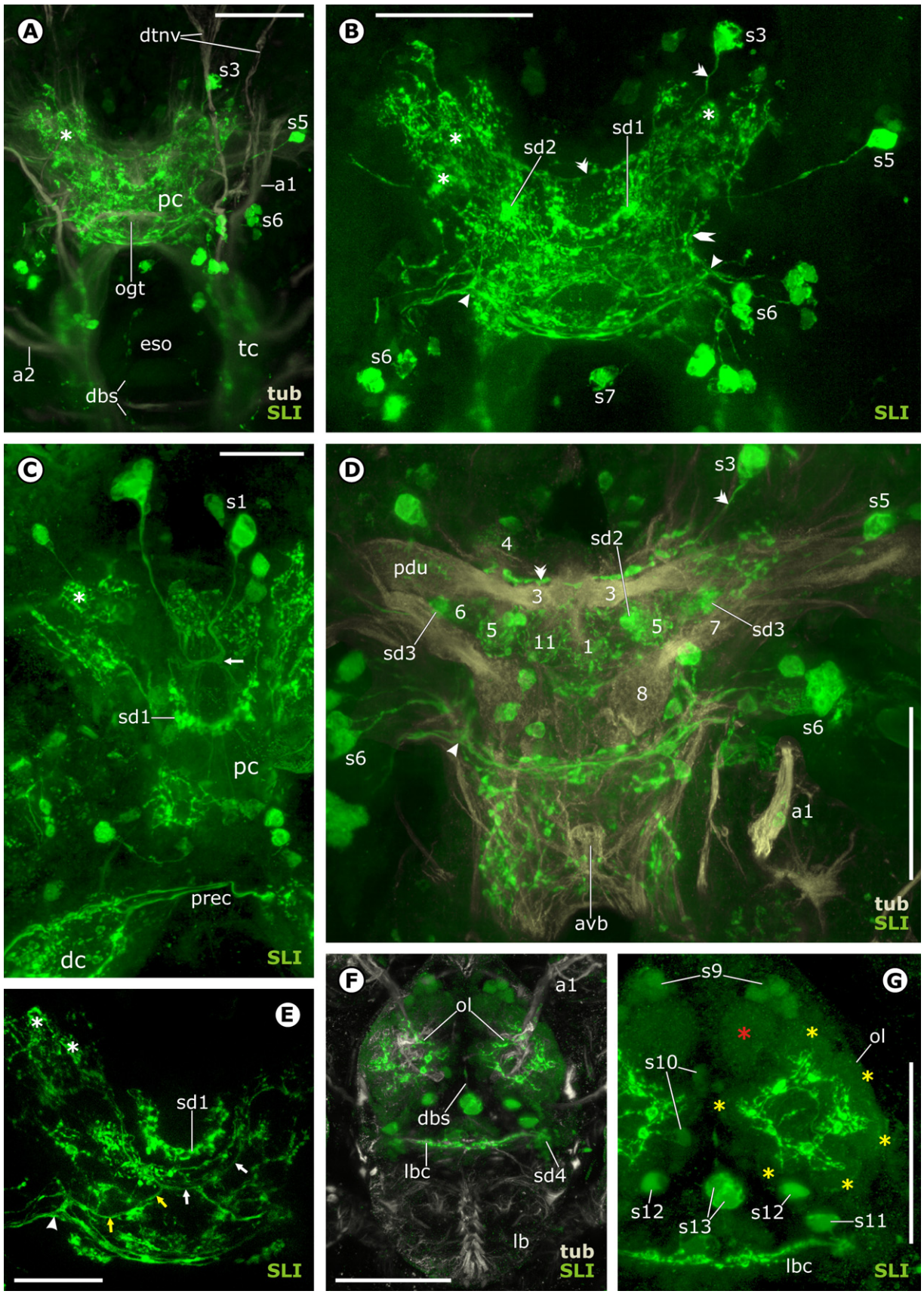

Fig. 5. Serotonin-like immunoreactivity in the protocerebrum and the labrum. A–G: Confocal laser scans. A,B,E–G: Whole mounts in Imaris surpass view. C,D: Vibratome sections in Imaris extended section view. A–C,E: The asterisks show several indistinct SL-ir domains. A: Dorsal view on the overall SL-ir pattern in the brain. B: Dorsal view on the protocerebrum. SL-ir soma (s3) sends a long commissure (double arrowheads) through the anterior protocerebrum. SL-ir somata (s6) send neurites into a posterolateral convergence

3.3.3. Olfactory lobes

A pair of olfactory lobes (ol) are located ventral to the rest of the deutocerebral neuropil (Figs. 1D,F, 4D–F). The neuropil of each olfactory lobe is organized into seven vertical stacks (ol, Fig. 4D, and asterisks in Fig. 4E, see also Figs. 5G, 9G), each composed by olfactory glomeruli (*sensu lato*) lying on top of each other (black arrows, Fig. 4D). The density of the olfactory glomeruli complicates their individual identification. While horizontal semi-thin sections suggest that the olfactory glomeruli have a discoid shape (Fig. 4E), transverse semi-thin sections and RFLI rather suggest an elongated shape (black arrows in Fig. 4D, see also Fig. 8E). Six stacks have the same size and are arranged in a ring (blue asterisks, Fig. 4E). The seventh stack (yellow asterisk) is slightly wider than the others (blue asterisks) and lies somewhat distant from them anteromedially (ol, Fig. 4E). On each side of the brain, one thick fiber bundle (arrowheads) enters the olfactory lobe (ol) from a dorsal direction (Fig. 4D,F). The bundle is composed of three parts: the proximoventral part of the antennular nerve (a1); the ventral part of the olfactory globular tract (ogt), which extends from here to the neuropil 8 of the multi-lobed complex; and several bundles of neurites (double arrowheads) originating from different groups of somata in the deuto-tritocerebral somata assemblage (dts, Fig. 4F).

3.4. Stomatogastric nervous system

The labral commissure (lbc) interconnects the two halves of the tritocerebrum (tc) and extends across the labrum (lb) as a ventral arc (Figs. 1A,B,D–F, 2C,E, 4E), the vertex of which is directly ventral to the esophagus (eso, Fig. 1D). The labral commissure (lbc) is connected to the unpaired labral neuropil (lbn, Fig. 2C,E). The labral neuropil (lbn) stretches along the midline and gives rise to the dorsal fiber bundle (dbs) of the stomatogastric nervous system, which, initially, runs anteriorly along the ventral side of the esophagus (Fig. 2C,E). As the esophagus bends upwards (compare Fig. 1D), the bundle (dbs) is also deflected up and around to extend posteriorly along the dorsal side of the gut (gut, Fig. 6C). In the mandibular segment, a dorsolateral bundle (dlbs) branches off from each side of the dorsal bundle (dbs) to run posterolaterally, whereas the latter continues posteriorly (Fig. 8I).

3.5. Distribution of neuroactive substances

A number of somata were found to be SL-ir, RFL-ir, or HL-ir. Their immunoreactive neurites extend into the brain neuropil where they are associated with domains of immunoreactive processes. We have avoided calling such immunoreactive domains 'neuropils' (Section 3.3.), because whereas *neuropils* are recognized in semi-thin sections and acetylated α-tubulin stains by their density and by their spatial and structural separation from the surrounding brain neuropil, *immunoreactive domains* stand out from the surrounding neuropil solely because of their pattern of immunoreactivity.

3.5.1. Serotonin-like immunoreactivity

3.5.1.1. SLI in the protocerebrum. About 24 SL-ir neurons (s1-7) on each side of the brain have their SL-ir somata distributed over the protocerebral somata assemblage (prs, Figs. 5A–D, 7). All somata (s1-7) send their SL-ir neurites into the protocerebral neuropil, which contains an intricate network of interconnected SL-ir fiber bundles linking SL-ir domains. This SL-ir network also includes SL-ir processes that envelop or extend into the multi-lobed complex neuropils 1, 4, 5, and 11 (Fig. 5D). An unpaired, and conspicuously sickle-shaped SL-ir domain (sd1), is situated ventrally in the protocerebral neuropil, directly posterior to an anteroventral fiber bundle (Figs. 5B,C,E, 7), and has a characteristic association with the SL-ir somata (s1). Each side of the brain all SL-ir neurites that extend from SL-ir somata (s1) unite into one bundle that first extends posteriorly into the protocerebral neuropil, passing by the multi-lobed complex neuropil 9. Still anterior to the anteroventral fiber bundle, this bundle then turns medially to project across the midline, forming a decussation (arrow) with its counterpart from the other side of the brain (Figs. 5C, 7). The bundle then turns again posteriorly and extends into the SL-ir domain (sd1, Figs. 5B,C,E, 7). There are two strongly SL-ir spherical domains (sd2, sd3, Figs. 5B,D, 7) on each side of the protocerebrum and a number of less conspicuous SL-ir domains loosely embedded within the SL-ir network, such as in the anterolateral region of the protocerebrum (asterisks, Fig. 5A–C,E).

3.5.1.2. SLI in the deutocerebrum. On each side of the brain about nine SL-ir somata (s8-10) are distributed in the deutocerebral part of the deuto-tritocerebral somata assemblage (Figs. 5G, 7). Two somata (s8) lie dorsal to the deutocerebral neuropil (Figs. 6A,B, 7), five others (s9) lie anterior to the olfactory lobe (Figs. 5G, 7) and two more (s10) lie medial to the olfactory lobe (Figs. 5G, 7). The somata (s8) send their neurites anteroventrally (Fig. 7, marked in blue in Fig. 6A,B) to supply a loose spherical network of SL-ir processes that pervades the six even-sized stacks of each olfactory lobe (ol, Figs. 5F,G, 7). As the network also establishes SL-ir interconnections between neighboring stacks of the olfactory lobe, it appears clearly ring-shaped in ventral or dorsal view (Figs. 5F,G, 7). Glomeruli do not contain SL-ir processes throughout, however. Rather, immunoreactive processes are concentrated near each glomerulus's inner margin (ol, Fig. 5G). Neither the seventh larger stack (red asterisk), nor the center of the olfactory lobe shows SLI (Fig. 5G). A few SL-ir longitudinal fibers (arrowheads) extend posteriorly from the protocerebral neuropil (pc) into the deutocerebral neuropil (dc) to project into more posterior regions of the nervous system (e.g., tc, sg, Figs. 6A,B, 7). En route, they are joined by a few SL-ir fibers originating from the pre-esophageal commissure (prec, Figs. 5C, 6A, 7). A few, somewhat diffuse, SL-ir domains occur along these SL-ir longitudinally oriented fibers (Figs. 6A,B, 7). The ventral part of the incoming antennular nerve (a1), which turns ventrally to run directly into the olfactory lobe (ol), shows SLI only in its proximal portion (Figs. 6A,B, 7).

3.5.1.3. SLI in the tritocerebrum. Altogether, six SL-ir neurons have their somata distributed over the tritocerebrum. Two somata occur on each side of the brain (s11, s12), and two unpaired somata (s13) occur at the midline (Fig. 7). The SL-ir neurite of soma (s11, Figs. 5G, 7, marked in blue in Fig. 6A,B) takes an interesting course: it first runs dorsally along the medial side of the tritocerebral neuropil

region (arrowhead). From here an SL-ir fiber bundle (rocket) runs into the anterolateral protocerebrum which features several indistinct SL-ir domains (asterisks). C: Neurites from somata (s1) form a decussation (arrow), before they run contralaterally into the sickle-shaped SL-ir domain (sd1). D: Within the multi-lobed complex, strongest SLI is shown in neuropils 1, 4, 5, and 11. Arrowhead and double arrowheads as in B. E: Dorsal view. An SL-ir fiber bundle (yellow arrow) coming from the posterolateral convergence region (arrowhead) runs ventromedially to join one out of many SL-ir commissures (white arrows) in the protocerebrum. F,G: Ventral view on the labrum of a juvenile. G: A network of SL-ir processes pertrudes the six even-sized vertical stacks (yellow asterisks) of olfactory glomeruli but not the seventh larger stack (red asterisk). Abbreviations: a1 – antennular nerve. a2 – antennal nerve. avb – anteroventral fiber bundle. dbs – dorsal fiber bundle of the stomatogastric nervous system. dc – deutocerebrum. dtnv – deutocerebral tegumentary nerve. eso – esophagus. lb – labrum. lbc – labral commissure. ogt – position of olfactory globular tract. ol – olfactory lobe. pc – protocerebrum. pdu – pedunculus. prec – pre-esophageal commissure. s1-13 – SL-ir somata 1-13. sd1-4 – SL-ir domain 1-4. tc – tritocerebrum. Scale bars: A,B,D,F,G: 50 μm. C,E: 25 μm.

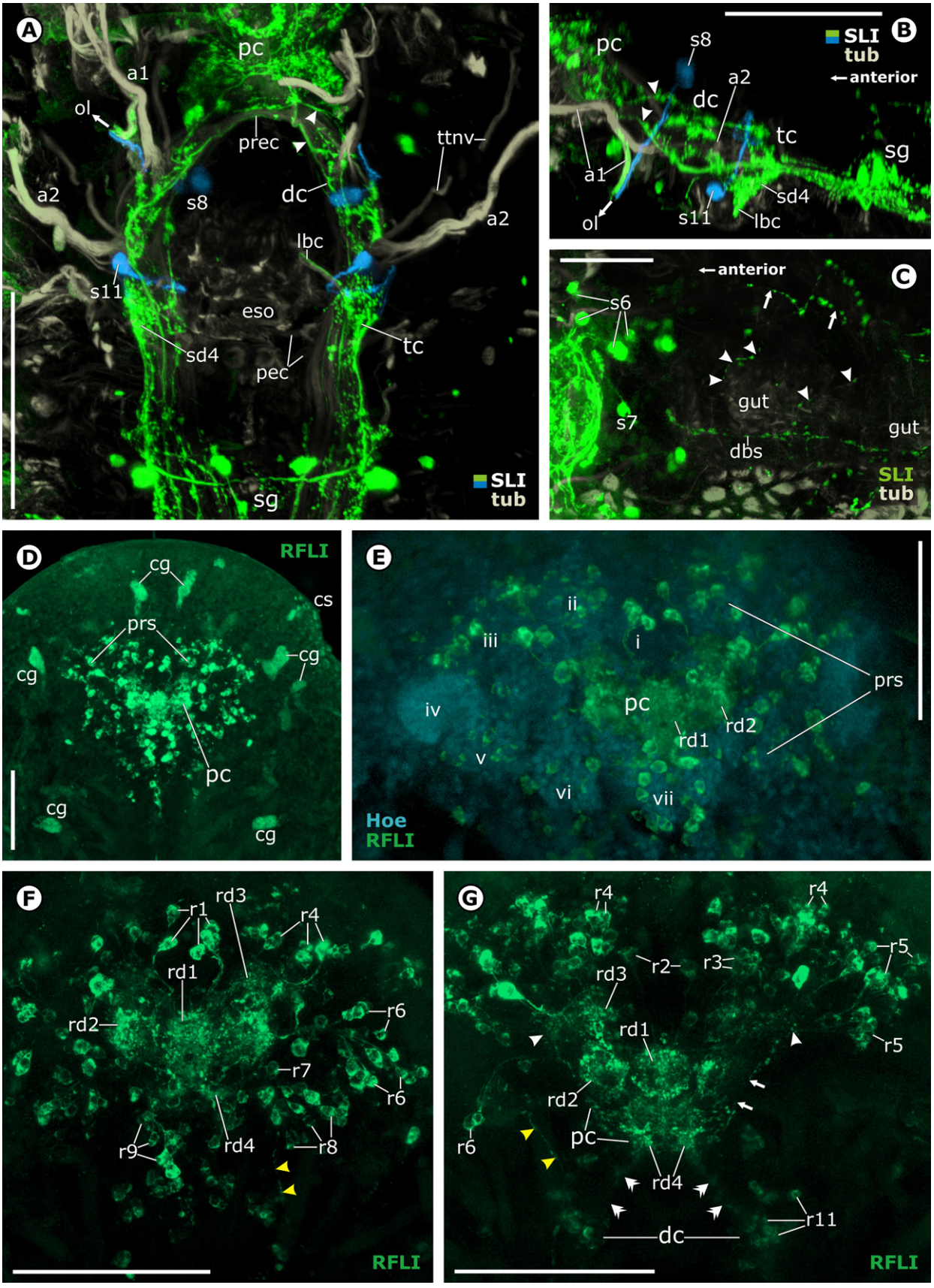

Fig. 6. Serotonin-like immunoreactivity in the posterior brain (A–C) and RFamide-like immunoreactivity in the protocerebrum (D–G). A–G: Confocal laser scans of whole mounts. A,B: Imaris surpass view. A: Dorsal and B: lateral view on deutocerebrum (dc) and tritocerebrum (tc). SL-ir somata (s8) and (s11) and their neurites were artificially highlighted using the Imaris contour surface tool. The arrow points towards the olfactory lobe (ol), which was removed together with the labrum. Arrowheads show a few SL-ir fibers

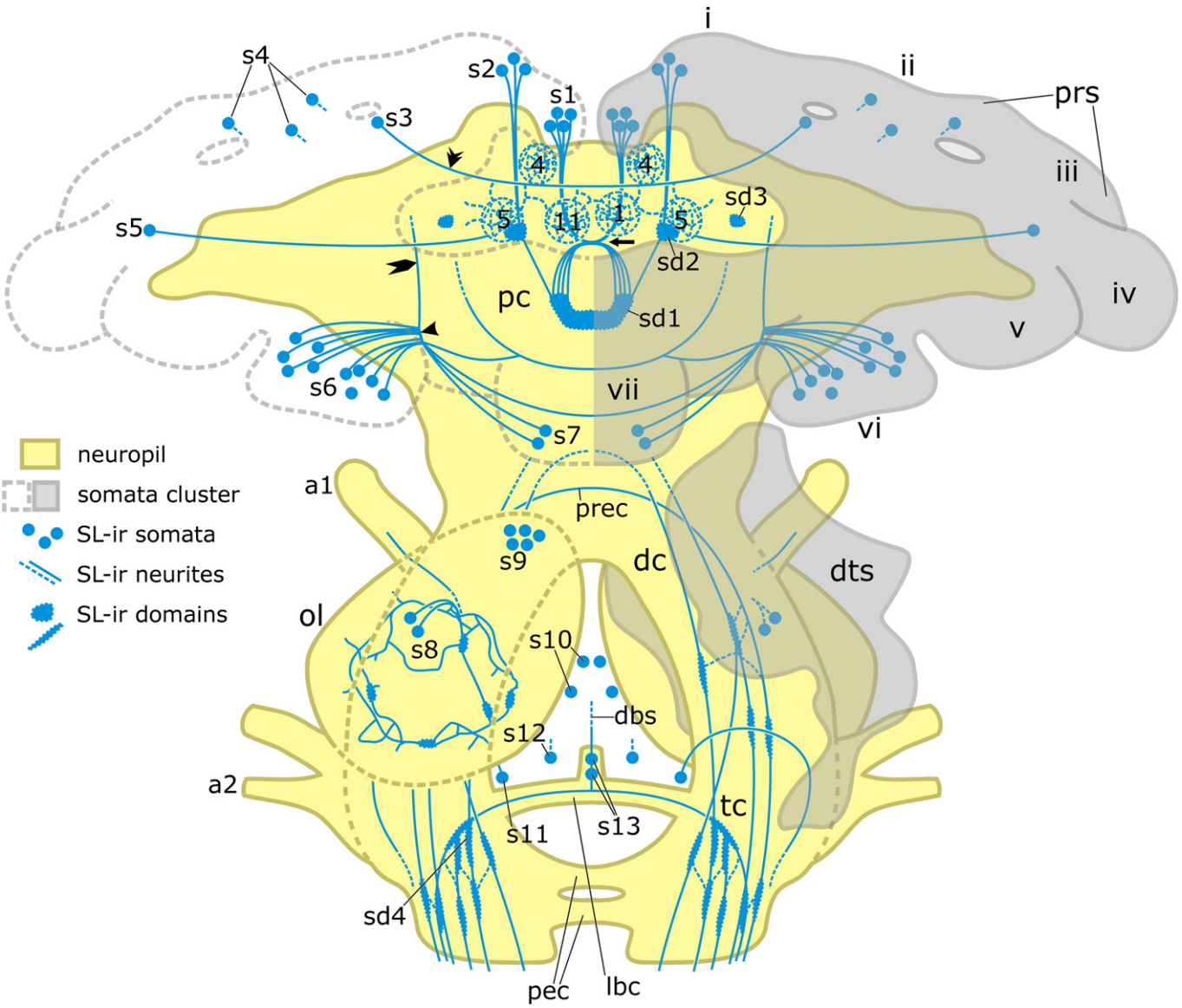

Fig. 7. Schematic drawing of the serotonin-like immunoreactivity in the brain. The right half of the scheme shows a dorsal view on the complete brain. In the left half of the scheme, part of the deutocerebrum and tritocerebrum is removed to show the interior of the olfactory lobe. On each body side, over 20 SL-ir somata (s1-13) are distributed over the three partitions of the brain. This scheme only shows those fibers and domains which are directly related to the SL-ir somata in the protocerebral somata assemblage, whereas other domains, e.g., in the anterolateral protocerebrum, are omitted. The neurites from somata (s1) form a decussation (arrow) before entering a sickle-shaped SL-ir domain (sd1). The process from SL-ir soma (s3) forms a long commissure (double arrowhead) passing the multi-lobed complex. Neurites from SL-ir somata (s6) enter an SL-ir posterolateral convergence region (arrowhead) from which one bundle runs into the anterolateral protocerebrum (rocket) and others contribute to different commissures. Abbreviations: 1-11 – multi-lobed complex neuropils 1-11. a1 – antennular nerve. a2 – antennal nerve. dbs – dorsal fiber bundle of the stomatogastric nervous system. dc – deutocerebrum. dts – deuto-tritocerebral somata assemblage. i-vii – divisions i-vii of the protocerebral somata assemblage. lbc – labral commissure. ol – olfactory lobe. s1-13 – SL-ir somata 1-13. sd1-4 – SL-ir domains 1-4. pc – protocerebrum. pec – post-esophageal commissures. prec – pre-esophageal commissure. prs – protocerebral somata assemblage. tc – tritocerebrum.

connecting the protocerebrum (pc) to the deutocerebrum. Note the distinct SL-ir domain (sd4) around the root of the labral commissure (lbc). C: Imaris surpass view. Dorsal view on the region posterior to the protocerebrum. The SL-ir dorsomedian fiber bundle (dbs) of the stomatogastric nervous system runs along the dorsal side of the gut (gut) and successively sends off several weakly SL-ir bundles (arrowheads) laterally. Arrows show an SL-ir lateral fiber bundle of unclear origin. D,E: Imaris surpass view. D: Overall pattern of RFLI in the protocerebrum. Note that the cuticular gland-like structures (cg) are larger than any RFL-ir somata (prs). E: RFLI is present in all divisions of the protocerebral somata assemblage (prs) with the exception of division iv. F,G: Imaris extended section view. F shows a more dorsal horizontal section and G a more ventral horizontal section through the protocerebrum. Four different RFL-ir domains (rd1-4) are shown in the protocerebrum: the unpaired domain (rd1) and the lateral domain (rd2) are most prominent. Arrows show the fiber bundle connecting an RFL-ir convergence region in the lateral protocerebrum (arrowhead) to the RFL-ir domain (rd4). Double arrowheads indicate the course of RFL-ir longitudinal fiber bundles in the deutocerebrum. Yellow arrowheads indicate the course of an RFL-ir lateral fiber bundle with unclear origin. Abbreviations: a1 – antennular nerve. a2 – antennal nerve. cg – cuticular gland-like structures. cs – cephalic shield. dbs – dorsal fiber bundle of the stomatogastric nervous system. dc – deutocerebrum. eso – esophagus. gut – gut. i-vii – divisions i-vii of the protocerebral somata assemblage. lbc – root of the labral commissure. ol – olfactory lobe. pc – protocerebrum. pec – position of non-SL-ir post-esophageal commissures. prec – pre-esophageal commissure. prs – protocerebral somata assemblage. r1-11 – RFL-ir somata 1-11. rd1-4 – RFL-ir domain 1-4. s6-11 – SL-ir somata 6-11. sg –subesophageal ganglion. sd4 – SL-ir domain 4. tc – tritocerebrum. ttnv – tritocerebral tegumentary nerve. Scale bars: A,B,D–G: 100 μm. C: 50 μm.

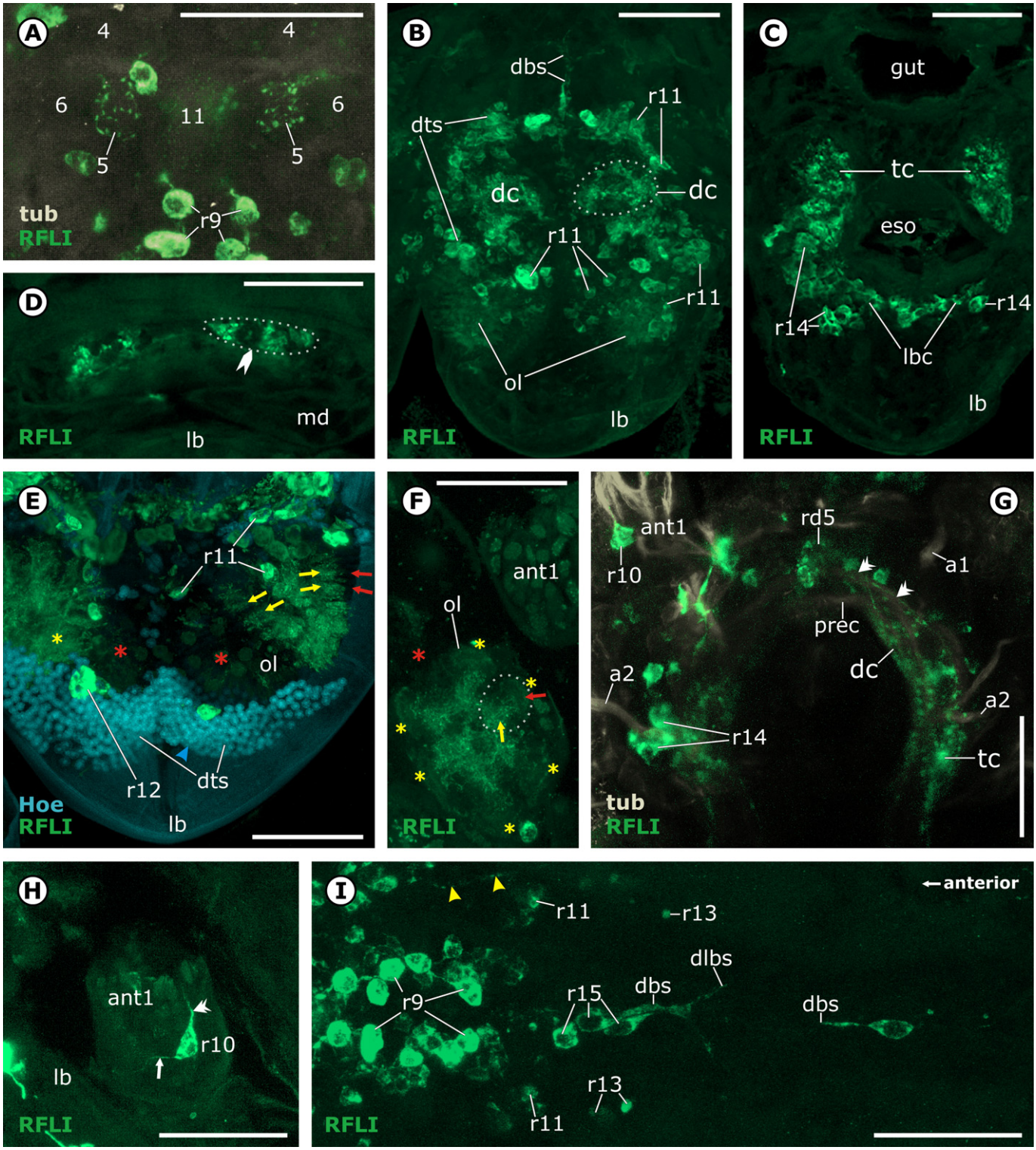

Fig. 8. RFamide-like immunoreactivity in multi-lobed complex, deutocerebrum, and tritocerebrum. Confocal laser scans of whole mounts (A,G–I) and transverse vibratome sections (B–F). A: Imaris extended section view. Dorsal view on the multi-lobed complex in which only neuropil 5 shows moderate RFLI and neuropil 11 shows very weak RFLI (compare to non-RFL-ir neuropils 4 and 6). B–D: Imaris surpass view. B-D are a series of transverse vibratome sections reaching from the deutocerebrum (B) through the tritocerebrum (C) to the post-tritocerebral connectives (D). A considerable number of RFL-ir somata are distributed (B: r11) around the deutocerebral neuropil (dc) and (C: r14) around the root of the RFL-ir labral commissure (lbc). D: RFL-ir processes continue posteriorly through the post-tritocerebral connectives (rocket). E,F: Imaris extended section view. E shows a transverse and F a horizontal section through the olfactory lobe (ol). Only six vertical stacks (yellow asterisks) of each olfactory lobe show RFLI, whereas the seventh stack (red asterisk) does not. The olfactory glomeruli in the six stacks show RFLI only in their central half (yellow arrows) but not in their peripheral half (red arrows). The blue arrowhead points at small-diameter somata in the deuto-tritocerebral somata assemblage. G: Imaris extended section view. Dorsal view on deutocerebrum and tritocerebrum. Double arrowheads show one out of several longitudinal RFL-ir fiber bundles which proceed from the protocerebral into the deutocerebral neuropil. H: Imaris surpass view. Ventral view on the proximal segment of the antennule, from where RFL-ir soma (r10) sends one neurite distally (double arrowhead) and one neurite proximally (arrow). I: Imaris surpass view. Dorsal view on the region posterior to the protocerebrum showing several RFL-ir somata (r15) associated with the weakly RFL-ir dorsomedian fiber bundle of the stomatogastric nervous system (dbs). Yellow

(Figs. 6A,B, 7). Then it loops laterally, to finally extend posteriorly (Figs. 6A, 7). As in the deutocerebral neuropil, a few diffuse SL-ir domains are associated with the SL-ir longitudinal processes (tc, Figs. 6A,B, 7). In each side of the tritocerebrum, a dense SL-ir domain (sd4) is situated at the root of the SL-ir labral commissure (lbc, Figs. 5F, 6A,B, 7). The dorsal fiber bundle of the stomatogastric nervous system (dbs, Figs. 5F, 7) shows weak SLI. As it extends along the gut (gut), it gives rise to other weakly SL-ir processes that run laterally (indicated by arrowheads in Fig. 6C). On each side, an SL-ir fiber bundle of undetermined origin is situated lateral to the gut and runs posteriorly into the trunk (arrows, Fig. 6C). The post-esophageal commissures show no SLI (Fig. 6A).

3.5.2. RFamide-like immunoreactivity

While the present study identified RFLI in the protocerebrum, there are only sparse data for the deutocerebrum and tritocerebrum. A few RFL-ir cuticular gland-like structures (cg) are attached to the interior side of the dorsal cephalic shield, fairly distant from the protocerebrum (pc, Fig. 6D). Their size clearly exceeds that of any somata in the brain. At least one of these structures is connected to the tegumentary nerve of the deutocerebrum.

3.5.2.1. RFLI in the protocerebrum. Each side, about a hundred RFL-ir neurons (r1-9) are distributed over partitions i-iii and v-vii of the protocerebral somata assemblage (prs, Fig. 6D,E). In comparison, there are no RFL-ir somata among globuli cell somata (iv, v, Fig. 6E). RFL-ir somata (r1-9) send neurites into the protocerebral neuropil, which contains a dense network of RFL-ir processes (pc, Fig. 6E,G). This network includes one unpaired RFL-ir domain (rd1) and three pairs of RFL-ir domains (rd2-4; Fig. 6E–G). The unpaired RFL-ir domain (rd1) is situated at the center of the protocerebral neuropil, directly ventral to the multi-lobed complex neuropils 1 and 11 (Fig. 6F,G), where it is intersected by a non-RFL-ir part of the anteroventral fiber bundle. Another unpaired RFL-ir domain (rd5, Fig. 8G) is situated in the transitional zone between the protocerebral and deutocerebral neuropil, posterior to the RFL-ir domain (rd4). It is traversed both by the olfactory globulary tract and by the unpaired anteroventral fiber bundle. The latter has only a few RFL-ir processes at this level and shows no RFLI anteriorly. All the RFL-ir domains (rd1-5) are located in the more diffuse part of the protocerebrum, ventral to the multi-lobed complex. Within the multi-lobed complex, moderate RFLI is present in neuropil 5 and weakly in neuropils 1 and 11 (Fig. 8A). Connections between the multi-lobed complex and the surrounding RFL-ir processes could not be identified. The posterodorsal neuropil cluster and the olfactory globulary tract are not RFL-ir. An RFL-ir longitudinal lateral fiber bundle (yellow arrowheads) arises from within the ventral region of partition vi to project posteriorly into the trunk (Figs. 6F,G, 8I) where it runs parallel to the gut.

3.5.2.2. RFLI in the deutocerebrum. A considerable number of RFL-ir somata (r10-12) are distributed over the deutocerebrum. A unique bipolar soma (r10) is situated in the proximal segment of each antennule and sends one neurite distally into the appendage and another neurite proximally to an unidentified destination (Fig. 8G,H). Most RFL-ir somata (r11) are situated dorsal, lateral, and medial to the non-glomerular deutocerebral neuropil (dc) as well as anterior and medial to the olfactory lobe (ol, Fig. 8B). A few, more strongly RFL-ir somata (r12) are situated anteromedially in the olfactory lobe (ol, Fig. 8E). Several weakly stained RFL-ir longitudinal fibers from RFL-ir domains (rd4, rd5) project posteriorly through the deutocerebrum (dc) into the tritocerebrum (tc) and further into more posterior ganglia (indicated by double arrowheads in Figs. 6G and 8G). The olfactory lobe shows RFL-ir only in six stacks (yellow asterisks), but not in the seventh larger stack (red asterisk, Fig. 8E,F). Olfactory glomeruli within the six even-sized stacks are RFL-ir only in their centrally oriented (yellow arrows), but not in their peripherally oriented half (red arrows, Fig. 8E,F). Neither the pre-esophageal commissure (prec, Fig. 8G) nor the olfactory globular tract is RFL-ir.

3.5.2.3. RFLI in the tritocerebrum. Several RFL-ir somata (r13-15) are distributed over the tritocerebrum. On each side of the brain, two somata (r13) – one large and one small – are situated in the deuto-tritocerebral somata assemblage, dorsal to the tritocerebral neuropil (Fig. 8I). Most RFL-ir somata (r14) are situated directly ventral to the root of the antennal nerve (a2) as well as along the labral commissure (lbc, Fig. 8C). Three unpaired RFL-ir somata (r15) are associated with the dorsal fiber bundle (dbs) of the stomatogastric nervous system (Fig. 8I). The labral commissure (lbc, Fig. 8C) and the dorsal (dbs) and dorsolateral fiber bundle (dlbs) of the stomatogastric nervous system are RFL-ir (Fig. 8B,I) whereas the post-esophageal commissures are not.

3.5.3. Histamine-like immunoreactivity

Like data on RFLI, our results are incomplete for HLI in the deutocerebrum and tritocerebrum, because the labrum hindered staining and scanning. Furthermore, due to the restricted availability of adults fixed for histamine-like staining, our results on HLI in the brain of *H. macracantha* are mainly based on larval whole mounts (larval stages 'nauplius 1–3' *sensu* Sanders, 1963).

3.5.3.1. HLI in the protocerebrum. About a dozen HL-ir somata (h1–h6) are distributed over each side of the protocerebrum. One (h1) is anteromedial, six (h2) are anterolateral, and about five others (h3-6) are situated posteriorly in the protocerebral somata assemblage. The largest and most strongly HL-ir soma (h4) sends its neurite ventrally into the deutocerebral neuropil (dc, Fig. 9A–D,H). The other HL-ir somata (h1-3, h5-6) send their neurites into the protocerebral neuropil, to contribute to a loose network of HL-ir processes and altogether four somewhat diffuse HL-ir domains (hd1-3). The HL-ir domain (hd1) lies anterolateral on each side of the brain, whereas both the median HL-ir domain (hd2) and the more posterior HL-ir domain (hd3) are unpaired (Fig. 9B). Domain (hd1) is connected medially to HL-ir domain (hd2) via one HL-ir fiber bundle (arrowheads; Fig. 9B). An unpaired HL-ir fiber bundle (arrows) extends ventrally into the deutocerebral neuropil from domain (hd2, Fig. 9A–D). It is not known whether this belongs to the anteroventral fiber bundle, because acetylated α-tubulin is only weakly labeled in the few carbodiimid-fixed specimens. The HL-ir domain (hd3, Fig. 9B) is divided into several small subdomains (Fig. 9B,H). Neither the olfactory globular tract (ogt) nor any of the neuropils in the multi-lobed complex (asterisks) are HL-ir (Fig. 9D).

3.5.3.2. HLI in the deutocerebrum. An extensive dorsolateral region within the deuto-tritocerebral somata assemblage (dts, h7) shows weak HLI (Fig. 9E,H,I). However, this may be artefactual, because

arrowheads indicate the course of the RFL-ir lateral fiber bundle. Abbreviations: 4-11 – neuropils 4-11 of the multi-lobed complex. a1 – antennular nerve. a2 – antennal nerve. ant1 – antennule. dbs – dorsomedian fiber bundle of the stomatogastric nervous system. dc – deutocerebral neuropil. dlbs – dorsolateral fiber bundle of the stomatogastric nervous system. dts – deuto-tritocerebral somata assemblage. eso – esophagus. gut – gut. lb – labrum. lbc – labral commissure. md – mandible. ol – olfactory lobe. prec – pre-esophageal commissure. r9-15 – RFL-ir somata 9-15. rd5 – RFL-ir domain 5. tc – tritocerebral neuropil. Scale bars: 50 μm.

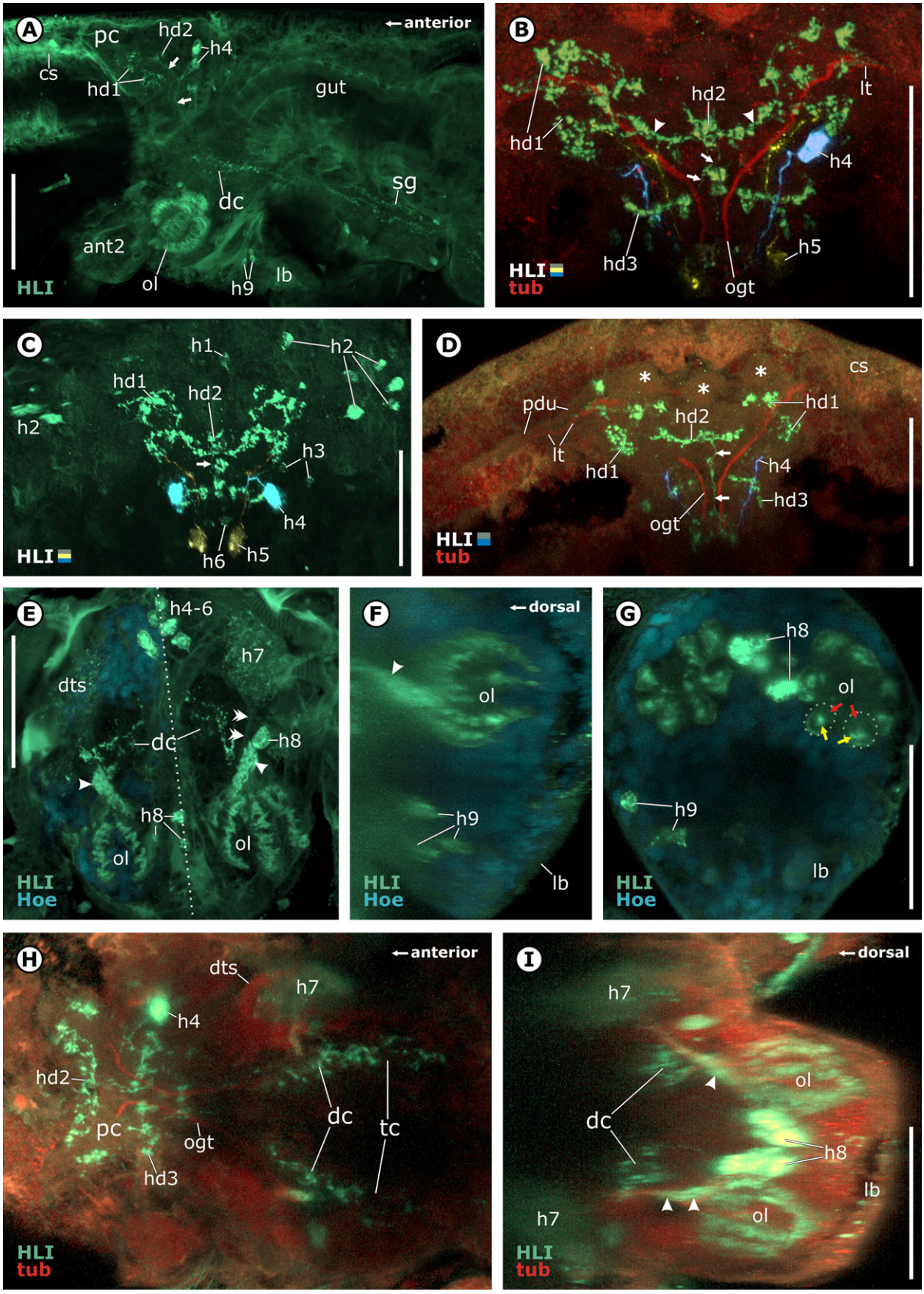

unlike other HL-ir somata the labeled epitope is not concentrated within the somata, but is spread amongst them. Borders between single somata are not distinguished by the HL-ir signal (compare h7 to the distinct signal from h4-6, Fig. 9E). A fiber bundle, indicated by double arrowheads in Fig. 9E, projects ventromedially from this dorsolateral region of somata (h7) into a strongly HL-ir thick fiber bundle (arrowheads). About five additional HL-ir somata (h8) were found anteromedially in each olfactory lobe (ol, Fig. 9E,G). The HL-ir pattern in the thick bundle (arrowheads) that enters dorsally into each olfactory lobe (ol) is HL-ir (Fig. 9E,F,I), suggesting that both HL-ir and non-HL-ir fibers interweave in a plait-like manner. HLI ends abruptly in the more dorsal part of the bundle (arrowheads: Fig. 9E). Ventrally, the bundle (arrowheads) splits up into seven HL-ir branches, each of which runs into one of the vertical stacks of the olfactory lobe (ol, Fig. 9E–G). HLI is strongest in the middle of each olfactory glomerulus (yellow arrows), weaker in the peripherally oriented part and absent in the centrally oriented part (red arrows, Fig. 9G. In contrast to SLI and RFLI, which are absent in the seventh anteromedial stack, the HL-ir pattern described here occurs in all the stacks. Several longitudinal HL-ir fibers extend through the deutocerebral (dc) into the tritocerebral neuropil (tc) and, from there to more posterior ganglia (Fig. 9A,H,I).

3.5.3.3. HLI in the tritocerebrum. Two pairs of HL-ir somata (h9) are situated in the posterolateral labrum (Fig. 9A,F,G).

4. Discussion

This discussion focuses on structures central to debates about the phylogeny and evolution of neuroanatomical features of Arthropoda. These include unpaired midline neuropils and immunoreactive domains (e.g., reviewed by Loesel et al., 2002; Harzsch, 2006, 2007; Homberg, 2008), as well as the olfactory system comprising the olfactory lobes (Schachtner et al., 2005), the olfactory globular tracts, and second order olfactory centers such as the hemiellipsoid bodies (Fanenbruck and Harzsch, 2005), mushroom bodies (Strausfeld et al., 2009; Loesel and Heuer, 2010) and, in *H. macracantha*, the multi-lobed complex. Here, the respective neuroanatomical structures and immunoreactive patterns in *H. macracantha* will first be compared with the neuroanatomy of other arthropods. Next, these aspects are discussed in an evolutionary context. Because of unresolved phylogenetic relationships within Tetraconata, we have not plotted neuroanatomical characters onto divergent cladograms. The lack of optic neuropils in *H. macracantha* has been discussed extensively by Elofsson and Hessler (1990) and will not be discussed here.

4.1. Unpaired midline neuropils

Strausfeld et al. (2006a) suggested an elongate, horizontally oriented, unpaired midline neuropil in the protocerebrum to be part of the ground pattern of Arthropoda, which evolved independently into different structures. These are: the arcuate body, an unpaired midline neuropil described in Chelicerata, and Onychophora (Strausfeld, 1998; Loesel, 2004; Strausfeld et al., 2006a,b), and the central complex (reviewed by Homberg, 2008), a cluster of neuropils (i.e., central body, protocerebral bridge, paired lateral accessory lobes) and tracts described in Malacostraca (Utting et al., 2000; Harzsch and Hansson, 2008), Insecta (Williams, 1975; Loesel et al., 2002), certain Branchiopoda (Harzsch and Glötzner, 2002; Kirsch and Richter, 2007), and Remipedia (Fanenbruck et al., 2004). The single unpaired midline neuropil found in Chilopoda (Loesel et al., 2002) shows more correspondences to the central body in Insecta than to the arcuate body in Onychophora and Chelicerata (see also Strausfeld et al., 2006a; Homberg, 2008).

Neither the unpaired midline neuropils described by Elofsson and Hessler (1990: i.e., neuropils 1 and 2) nor those described in this study (i.e., neuropil 11 and the median neuropil of the posterodorsal neuropil cluster) resemble the arcuate body or neuropils of the central complex. Unpaired midline neuropils in the protocerebrum are also completely missing in Mystacocarida (Brenneis and Richter, 2010). The description of a bulbous “central body” in certain Copepoda and Ostracoda (Aramant and Elofsson, 1976) does not suffice for a comparison with other taxa.

Even though *H. macracantha* lacks the distinctive neuropils of a central complex, the unpaired immunoreactive domain (sd1) can be related to the central body in other taxa. Because we could not test whether the stained epitopes in *H. macracantha* are homologous across compared taxa, our suggestions regarding homology of immunoreactive patterns across taxa must be viewed as preliminary. Like the SL-ir central body in Malacostraca (Sandeman et al., 1988; Utting et al., 2000; Harzsch and Hansson, 2008) and Insecta (Homberg, 1991), the SL-ir domain (sd1) in *H. macracantha* occupies a central position within the protocerebral neuropil. Another interesting correspondence is that the decussating neurites (s1) that enter this midline SL-ir domain are reminiscent of a decussation described for Insecta. There, neurites of columnar neurons run from their associated somata across the midline to the other side of the brain before they enter the central body (Williams, 1975; Williams and Boyan, 2008). Similar decussations of neurites were described in the arcuate body of Chelicerata (Loesel, 2004), and are suggested in the unpaired midline neuropil of Chilopoda by Loesel’s et al. (2002) Fig. 2B, although the latter authors state that the dorsal protocerebrum lacks chiasmal axons. The small SL-ir domain in the protocerebrum of Mystacocarida corresponds to the SL-ir domain (sd1) in *H. macracantha* with respect to its size and position, but receives uncrossed neurites from its SL-ir anterior somata (Brenneis and Richter, 2010).

None of the other three unpaired immunoreactive domains (rd1, hd2, hd3) in *H. macracantha* correspond to neuropils of the central complex.

4.1.1. Evolutionary interpretations

If we base our assumptions on Harzsch’s (2006) hypothesis that a central complex (central body, protocerebral bridge and paired

Fig. 9. Histamine-like immunoreactivity in the brain. A–J: Confocal laser scans in adult vibratome sections (A,E) and larval whole mounts (B-D,F-I). A: Sagittal vibratome section. An unpaired process (arrows) runs from the HL-ir domain (hd2) into the deutocerebrum (dc). From there (dc), a few HL-ir longitudinal fibers run posteriorly through the tritocerebrum (not shown) into the subesophageal ganglion (sg). B–D: HL-ir neurons (h4) and (h5) artificially highlighted using the Imaris contour surface tool. HL-ir domain (hd2) is connected to the deutocerebrum via an HL-ir process (arrows). B: Imaris surpass view. Dorsal view of the HL-ir pattern in the protocerebral neuropil. HL-ir domains (hd1) and (hd2) are interconnected via a pair of HL-ir fiber bundles (arrowheads). C: Imaris surpass view. Overall dorsal view on the protocerebrum showing all HL-ir somata (h1-6) in the protocerebral somata assemblage. D: Imaris extended section view. Dorsal view of only a slim virtual horizontal section through the middle of the protocerebrum. Neuropils of the multi-lobed complex (asterisks) lack HLI. E: Transverse vibratome section through the labrum. Imaris extended section view. The thick fiber bundle (arrowheads) shows HLI only in its ventral section. A thin non-HL-ir bundle (indicated by double arrowheads) connects the thick bundle (arrowhead) to the weakly HL-ir somata (h7). F,G: Imaris extended section view. Sagittal (F) and horizontal (G) virtual section through the labrum showing HLI in the vertical stacks of the olfactory lobe (ol). F: Arrowhead shows the thick fiber bundle. G: The yellow arrows point at the strongly HL-ir middle of two vertical stacks of olfactory glomeruli, while the red arrows point at the part directed towards the center which shows no HLI. H,I: Imaris extended section view. H: Horizontal virtual section through deutocerebrum (dc) and tritocerebrum (tc). I: Transverse virtual section through deutocerebrum (dc) with olfactory lobe (ol). Arrowheads show the thick fiber bundle. Abbreviations: ant2 – antenna. cs – cephalic shield. dc – deutocerebrum. dts – deuto-tritocerebral somata assemblage. gut – gut. h1-9 – HL-ir somata 1-9. hd1-3 – HL-ir domain 1-3. lb – labrum. lt – lateral tract of the multi-lobed complex. ogt – olfactory globular tract. ol – olfactory lobe. pc – protocerebrum. pdu – pedunculus. sg – subesophageal ganglion. tc – tritocerebrum. Scale bars: A: 100 μm. B–I: 50 μm.

accessory lobes) is part of the tetraconate ground pattern, then the absence of comparable neuropils in Cephalocarida must be due to a reduction and loss. We suggest that both the SL-ir domain (sd1) in Cephalocarida and the SL-ir domain in Mystacocarida constitute rudiments of an SL-ir central body precursor in the tetraconate stem species. With respect to unresolved phylogenetic relationships across Tetraconata, however, we leave the question open whether originally also a protocerebral bridge was present in the ancestors of these two taxa. Also the decussation of neurites from somata (s1) in *H. macracantha* may be a plesiomorphy with respect to the ground pattern of Tetraconata. As convincingly demonstrated by Strauss (2002) and Bender et al. (2010), all the evidence points to the central complex having a cardinal role in controlling motor actions, irrespective whether this is in response to visual (Triphan et al., 2010) or to tactile stimuli (Harley and Ritzmann, 2010). The comparably simple, metachronic movement of homonomous appendages in *H. macracantha* (see Sanders, 1963) suggests why Cephalocarida do not require unpaired midline neuropils for coordination of complex multijoint movements.

4.2. The multi-lobed complex

Elofsson and Hessler (1990) described neuropils 1-9 of the multi-lobed complex in *H. macracantha* as "a number of paired and unpaired lobular structures, visibly connected by tracts" and termed them 'mushroom bodies 1-9'. Based on TEM, Elofsson and Hessler (1990) reported that neuropils 1-9 are "areas of synaptic contact between neurons", while their borders are covered by a "thin glial envelope", which supports the hypothesis that the multi-lobed complex is a functional unit. Also, Elofsson and Hessler (1990) described neuropil 10 as an "unstructured neuropil" which is pervaded by a lateral tract originating from neuropil 7 and ending near a spherical clump of "Kenyon cells". The authors discovered "striations" in the distal part of the lateral tract and interpreted them as being rather due to membrane thickenings of an axon-glial connection than due to synapses. In contrast, our data reveal that both the lateral tract and the pedunculus are associated with neuropil 10, implying that fibers of the lateral tract and the pedunculus form synapses there. Other than this one disagreement, our study confirms Elofsson's and Hessler's (1990) description of neuropils 1-10 and the lateral tract, and adds two additional structures: neuropil 11 and the pedunculus. The last is crucial to an understanding of the spatial relationships and interconnections of the multi-lobed complex.

Here, Fig. 10 will serve as a reference throughout this part of the discussion. Like *H. macracantha*, many arthropods have neuropils in the protocerebrum connected to first order olfactory neuropils in the deutocerebrum. Such protocerebral neuropils include the hemiellipsoid bodies in Remipedia and Malacostraca, the mushroom bodies and lateral horn in Insecta (i.e., ectognath Hexapoda, comprising Archaeognatha, Zygentoma, and Pterygota), and the mushroom bodies in *Lithobius* (Chilopoda), which are compared to the multi-lobed complex below. Mushroom bodies have also been described in Onychophora (Schürmann, 1987; Strausfeld et al., 2006a,b), Chelicerata (e.g., Holmgren, 1916; Babu, 1985; Strausfeld and Barth, 1993; Fahrenbach, 1977, 1979), other Chilopoda (see below), and even in polychaetes (Holmgren, 1916; Heuer et al., 2010).

4.2.1. Comparison with the hemiellipsoid bodies (see Fig. 10A,B)

A pair of neuropils termed hemiellipsoid bodies occurs in the lateral protocerebrum of Remipedia (Fanenbruck et al., 2004) and Malacostraca (e.g., Hanström, 1928; Sullivan and Beltz, 2004). Fanenbruck and Harzsch (2005: p. 359) suggested that "parts of the cephalocaridan multi-lobed complex are equivalent to the terminal medulla with the hemiellipsoid bodies". The term 'terminal medulla' comprises all neuropils in the lateral protocerebrum other than the hemiellipsoid bodies (e.g., Hanström, 1947; Sullivan and Beltz, 2001a). Especially in Remipedia, the hemiellipsoid bodies show indeed certain correspondences to the multi-lobed complex neuropil 10. Both share an overall spherical shape and stand out from the surrounding nervous tissue by a comparably dense and overall unstructured neuropil whose processes show no overall parallel arrangement (Fanenbruck et al., 2004: "fine, dense texture"), as does, for example, the pedunculus in *H. macracantha*. In contrast, the hemiellipsoid bodies in Stomatopoda (Sullivan and Beltz, 2004) and Decapoda are organized into several layers (e.g., Harzsch and Hansson, 2008; Krieger et al., 2010). Since hemiellipsoid bodies in other Malacostraca such as Anaspidacea, Euphausiacea, Mysidacea are apparently more simply organized (Hanström, 1928, 1947), the malacostracan ground pattern cannot be reconstructed. In addition, Sullivan and Beltz (2001a,b, 2004) pointed out that the protocerebral part of the olfactory globular tract in Stomatopoda and Decapoda is not exclusively associated with the hemiellipsoid body, like the tract in Remipedia, but additionally with the terminal medulla. Yet only the hemiellipsoid body, but not the terminal medulla is associated with globuli cell somata as is neuropil 10 in *H. macracantha*. Thus, while we are well aware of the structural variations across Malacostraca, we suggest homology of neuropil 10 with the hemiellipsoid bodies in Remipedia and Malacostraca.

4.2.2. Comparison with the mushroom body and the lateral horn in Insecta (see Fig. 10A,C)

The protocerebrum of dicondylic Hexapoda contains a pair of mushroom bodies (Farris and Sinakevitch, 2003; Farris, 2005b; Strausfeld et al., 2009). Each mushroom body is composed of a group of globuli cell somata (referred to as Kenyon cells) and, usually, an adjacent neuropil, which is divided into one or two calyces, a pedunculus, and two or more lobes (Farris and Sinakevitch, 2003). In some Dicondylia (Zygentoma + Pterygota), the calyces are overall spherical, as is neuropil 10 in *H. macracantha*, in others they are cap-like or cup-like. The parallel arrangement of fibers in the pedunculus of Dicondylia corresponds to the parallel organization of fibers in the pedunculus of *H. macracantha*. The number and arrangement of lobes along the pedunculus varies within Dicondylia (Farris, 2005b; Strausfeld et al., 2009). The closest similarity with the pedunculus in *H. macracantha* is in the Lepismatidae (Zygentoma), Heteroptera and Ephemeroptera, in which the pedunculus gives rise to several globe-like neuropils, which have been termed 'trauben' (e.g., Hanström, 1940; Pohl, 1958; Farris, 2005a; Strausfeld et al., 2009). Their grape-like arrangement is clearly reminiscent of the successive arrangement of neuropils 4, 5, and 6 along the pedunculus in *H. macracantha*. Unpaired median neuropils which might interconnect the pedunculi of both body sides, similarly to neuropil 1, 2, and 11 in *H. macracantha*, were not identified in Dicondylia, although trauben from both body sides closely touch in the midline and have been described as being connected by at least two commissures (Hanström, 1940; Pohl, 1958). The absence of mushroom bodies in Archaeognatha remains enigmatic both from a functional and evolutionary point of view. Their presence in entognathous Hexapoda needs further validation, although some indications for mushroom bodies exist in Diplura (Hanström, 1940) and Collembola (Kollmann et al., 2011).

The 'lateral horn' is situated separately from the calyx in the lateral protocerebrum of Insecta (Strausfeld, 1976). Fanenbruck and Harzsch (2005) homologized the lateral horn with the hemiellipsoid bodies in Remipedia and Malacostraca, because both are associated via tracts with the deutocerebral antennal lobes. Despite

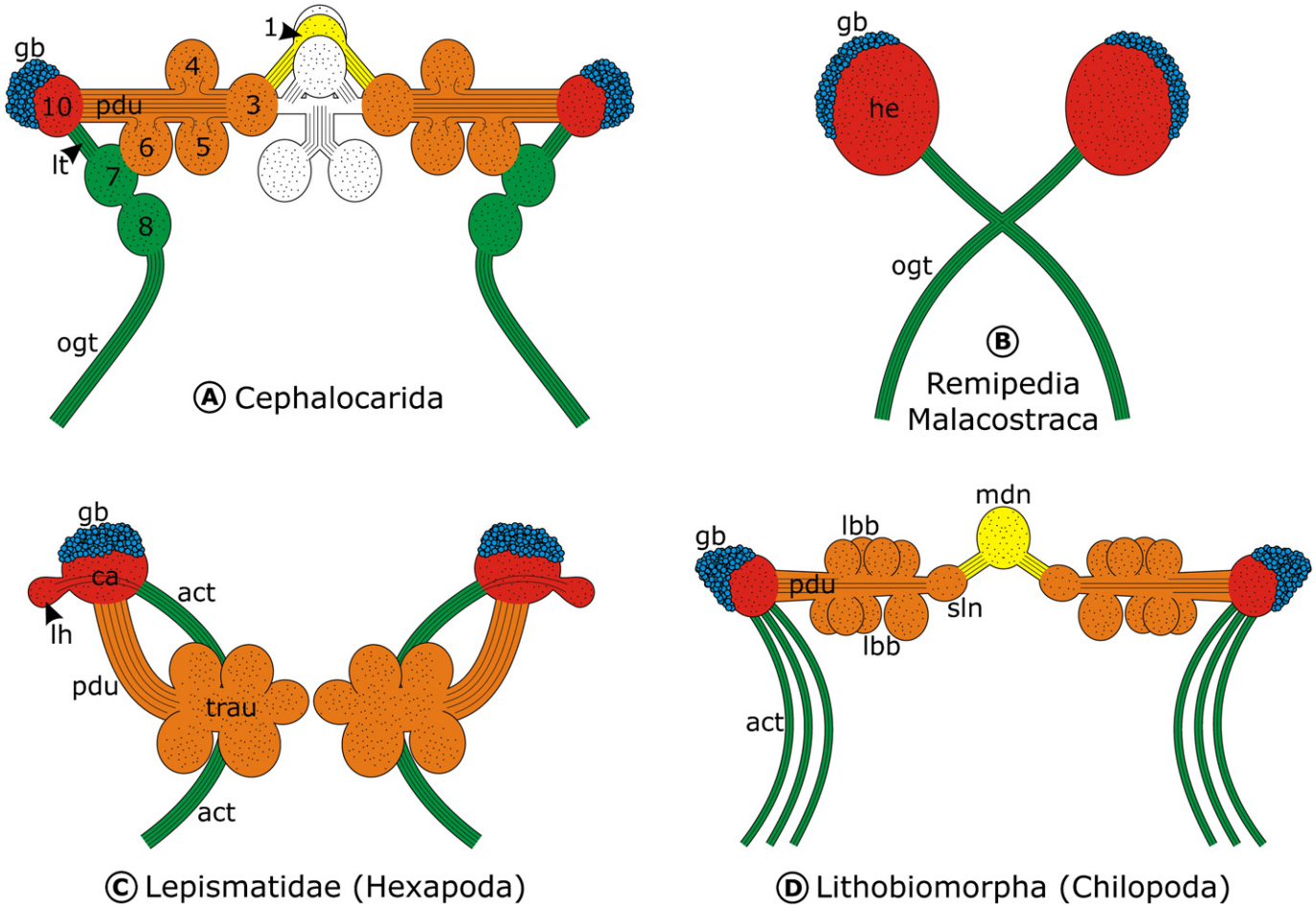

Fig. 10. Schematic overview of neuropils in the protocerebrum associated to the olfactory or antennal lobe in different arthropods. A: Multi-lobed complex in Cephalocarida. B: Hemiellipsoid bodies in Remipedia (based on Fanenbruck and Harzsch, 2005) and Malacostraca (based on Sandeman et al., 1992). C: Mushroom bodies in Lepismatidae (Hexapoda) with trauben-bearing pedunculus, based on Strausfeld et al. (2009). D: Mushroom bodies in Lithobiomorpha (Chilopoda), based on Holmgren (1916) and Strausfeld et al. (1995). Abbreviations: 1-10 – multi-lobed complex neuropils 1-10. act – antennocerebral tract(s). ca – calyx. gb – globuli cell somata. he – hemiellipsoid body. lbb – lobed body. lh – lateral horn. lt – lateral tract. mdn – median neuropil. ogt – olfactory globular tract. pdu – pedunculus. sln – small lateral neuropil. trau – trauben.

this correspondence, the lateral horn is not associated with globuli cell somata (N.J. Strausfeld, personal communication) and thus might not correspond to neuropil 10 in *H. macracantha*.

4.2.3. Comparison to the mushroom bodies in Lithobius (Chilopoda; see Fig. 10A,D)

A similar arrangement of neuropils and tracts was described in the protocerebrum of *Lithobius* (species name not given), based on Golgi and methylene-blue staining (Holmgren, 1916: "Das Globulussystem", pp. 183–185), composed of globuli cell somata, an associated neuropil, a pedunculus giving rise to several spherical neuropils, a small medial neuropil and an unpaired median neuropil. Although the last-mentioned unpaired median neuropil is missing in Insecta, we refer to the mentioned arrangement in *Lithobius* as mushroom bodies, following later authors (Hanström, 1928: "corpora pedunculata", Strausfeld et al., 1995). Like in *H. macracantha*, the pedunculus is a thick bundle of parallel fibers originating from the globuli cell somata and is oriented horizontally (Holmgren, 1916). Laterally, the pedunculus is associated with a neuropil that lies directly underneath the globuli cell somata (Holmgren, 1916; Strausfeld et al., 1995), a position that corresponds to that of neuropil 10 in *H. macracantha* and the calyx of the insect mushroom body. In *Lithobius variegatus*, this neuropil receives three separate tracts from the deutocerebrum (Strausfeld et al., 1995). Medially, and mainly from its anterior and dorsal side, the pedunculus in *Lithobius* gives rise to a number of spherical neuropils that together constitute what Holmgren (1916) and Hanström (1928) referred to as the lobed body ("lobierter Körper"; Strausfeld et al., 1995: "glomerulus-like outswellings"). This organization corresponds to that of the pedunculus and neuropils 4, 5, and 6 in *H. macracantha*. As a difference from *H. macracantha*, both the medialmost neuropil of the lobed body and the pedunculus are connected with their respective counterparts on the other side of the brain via commissures (Holmgren, 1916). Neuropils corresponding to the unpaired midline neuropils 2 and 11 in *H. macracantha* do not occur in *Lithobius*. A pair of horizontally oriented pedunculi and median neuropils similar to those in *H. macracantha* and *Lithobius*, but no lobed body, was also reported in *Julus* (Diplopoda; Holmgren, 1916; Hanström, 1928), although these findings certainly need validation using modern techniques.

4.2.4. Evolutionary interpretations

Here, we propose homology of neuropil 10 in *H. macracantha* with the remipede and malacostracan hemiellipsoid bodies, and with the calyces of dicondylic Hexapoda. As discussed above, these correspondences are revealed by their protocerebral location as well as by their supply by globuli cell somata and the olfactory globular tract. We propose that the pedunculus in *H. macracantha*

and Dicondylia is homologous, as are its offbranching neuropils (neuropils 4–6, lobes, trauben, respectively), based on structural correspondences. If Hexapoda, Cephalocarida, Malacostraca, and Remipedia form a monophyletic clade with the latter two as sister-groups (Harzsch, 2006: Fig. 6), its last common ancestor probably had, on each side of the brain, a second order olfactory center featuring a group of globuli cells, an adjacent neuropil which received an olfactory globular tract from the olfactory lobe, and a pedunculus with several offbranching neuropils. The comparatively simpler hemiellipsoid body in Remipedia and Malacostraca, lacking a pedunculus with offbranching neuropils, would be apomorphic. The structural correspondences between the second order olfactory center in *Lithobius* and *H. macracantha* (and, with the exception of median neuropils, also in Insecta) suggest that a myriapod/cephalocarid-like second order olfactory center with at least one median neuropil might have been part of the ground pattern of Mandibulata. This implies the loss of such complex system in various crustaceans, the exact number of losses, however, depend on the phylogenetic relationships (e.g., considering Regier et al., 2010, four times, i.e., in Oligostraca, Branchiopoda, Copepoda and Thecostraca).

4.3. Olfactory globular tracts

4.3.1. Connectivity between proto- and deutocerebrum

A single olfactory globular tract on each side of the brain connects the olfactory lobe to the multi-lobed complex in *H. macracantha* (Elofsson and Hessler, 1990, this study) and to the hemiellipsoid body in Malacostraca (Sandeman et al., 1992, 1993) and Remipedia (Fanenbruck et al., 2004), respectively. Recently, a single ipsilateral tract between deuto- and protocerebrum was also found in certain Copepoda (Strausfeld and Andrews, 2011), Spinicaudata, Laevicaudata, and Cyclestherida (M. Fritsch, personal communication). All other studied crustacean taxa apparently lack an olfactory globular tract (e.g., Harzsch and Glötzner, 2002; Kirsch and Richter, 2007; Brenneis and Richter, 2010; Hartline and Christie, 2010; Fritsch and Richter, 2010). Also in three taxa of Insecta, namely in Archaeognatha (Strausfeld, 2009), Zygentoma, and Coleoptera (Strausfeld et al., 2009), a single tract on each side of the brain – here called 'antennocerebral tract' – connects the antennal lobe in the deutocerebrum to the mushroom body (absent in Archaeognatha) and lateral horn. A derived condition shown by many other Insecta is three to five antennocerebral tracts (Schachtner et al., 2005; Strausfeld, 2009; Galizia and Rössler, 2009). Only in Eumalacostraca (e.g., Tsvileneva and Titova, 1985; Sandeman and Scholtz, 1995), and Remipedia (Fanenbruck et al., 2004), the olfactory globular tracts from both body sides were reported to form a decussation in the median protocerebrum, in which both ipsilateral and contralateral axons of olfactory interneurons converge. Recent data do not give a clear picture of the condition in Leptostraca: a decussation was found in *Nebalia* cf. *herbstii* (M. Kenning and S. Harzsch, personal communication), but not in *Nebalia pugettensis* (N.J. Strausfeld, personal communication). Whether a decussation was present in the ground pattern of Malacostraca thus remains open. In contrast, the respective tracts in *H. macracantha* (Elofsson and Hessler, 1990, this study) and Insecta (Strausfeld, 2009) are ipsilateral. The only comparable data in Myriapoda are given by Strausfeld et al. (1995), who depicted three ipsilateral antennocerebral tracts in *L. variegatus* (Chilopoda).

4.3.2. Evolutionary interpretations

The absence of a decussation in cephalocarids might support Harzsch's (2006: Fig. 6) hypothesis that Remipedia and Malacostraca are sister-groups with decussating olfactory globular tracts as a synapomorphy, although the apparently conflicting evidence in Leptostraca needs further study. The single ipsilateral olfactory globular tract in Cephalocarida and Insecta thus represents the plesiomorphic condition and might belong to the ground pattern of Tetraconata. Although the exact number of tracts in the mandibulate ground pattern cannot be resolved, facing the three ipsilateral tracts in Chilopoda, it is suggested that they were ipsilateral.

4.4. Olfactory lobes

4.4.1. Taxonomic distribution of olfactory glomeruli

An olfactory glomerulus *sensu stricto* is a small, spheroidal (*Latin* glomerulus – 'little ball') neuropil, where the axons of olfactory receptor neurons terminate and establish synapses with olfactory interneurons. Here we use the term in a wider sense to include also olfactory neuropils that are geometrically distinct from ball-shaped elements. Olfactory glomeruli can be comprised in centers called antennal or olfactory lobes but are not universal to those. Olfactory glomeruli show a wide taxonomic distribution in taxa as diverse as malacostracans, some orders of Insecta, some polychaetes (Heuer and Loesel, 2009), Mollusca (Wertz et al., 2006), or Craniata (Cajal, 1972). Strausfeld and Hildebrand (1999) suggested that olfactory glomeruli may have evolved several times independently within Bilateria. Here, the present comparison of olfactory glomeruli in *H. macracantha* and other species focuses on taxa whose olfactory lobes lie in the deutocerebrum; namely, Malacostraca (Schachtner et al., 2005), Remipedia (Fanenbruck et al., 2004), Hexapoda (Hanström, 1940; Schachtner et al., 2005), Chilopoda (Strausfeld et al., 1995; Sombke et al., 2010) and Diplopoda (Duy-Jacquemin and Arnold, 1991). Hanström's (e.g., 1928, 1931) descriptions of olfactory glomeruli in the deutocerebrum of Anostraca, Ostracoda, Copepoda, and Cirripedia have been questioned in more recent accounts (reviewed by Schachtner et al., 2005).

4.4.2. Shape and arrangement of olfactory glomeruli

Based on TEM and LM, Elofsson and Hessler (1990) found the vertical stacks of the olfactory lobe in *H. macracantha* compartmentalized into "horizontal layers" by glial cells, but they did not comment on the exact shape of single olfactory glomeruli within the stacks. Although the round shape of the vertical stacks in horizontal sections suggests that the comprised olfactory glomeruli are discoid, transverse sections and our data on RFLI rather indicate an elongate shape. Since none of the antibodies used here stained the olfactory glomeruli completely, our conclusions on their shape remain preliminary. In any case, they are certainly not spheroidal as the olfactory glomeruli described in non-decapod Malacostraca (Hanström, 1928, 1929, 1931, 1947; Derby et al., 2003; Johansson and Hallberg, 1992; Harzsch et al., 2011), Remipedia (Fanenbruck et al., 2004), Diplopoda (Duy-Jacquemin and Arnold, 1991), and several hexapod taxa including Diplura, Zygentoma (Hanström, 1940), some Orthoptera (Ignell et al., 2001), Dictyoptera, Hymenoptera (Schachtner et al., 2005), and Lepidoptera (Sadek et al., 2002). Neither do they resemble the elongate, wedge-like glomeruli in decapod olfactory lobes (Schmidt and Ache, 1992; Harzsch and Hansson, 2008) nor the elongate, sausage-like olfactory glomeruli in Chilopoda, which extend through the whole antennal lobe (Sombke et al., 2010: 'olfactory neuropils').

4.4.3. Immunoreactive interneurons in the olfactory lobe

Given the borders of the vertical stacks in *H. macracantha* by nuclear stains or autofluorescence, it was possible to determine whether immunoreactivity was shown in the inner or outer part of the olfactory glomeruli (with respect to the olfactory lobe). The immunoreactive patterns described in the Results, and in other crustaceans and insects, suggest that olfactory glomeruli of

H. macracantha, Malacostraca, Remipedia, and Insecta are innervated by corresponding interneurons.

In *H. macracantha*, SL-ir fibers that extend through the olfactory lobe belong to two local interneurons (s8), whose somata lie in the dorsal deutocerebrum on each side of the brain. These correspond well to the two SL-ir dorsal giant neurons in crayfish (Malacostraca Decapoda: *Orconectes virilis*, *Cherax destructor*), which occupy a similar position in the dorsal deutocerebrum and send ipsilateral neurites both into the olfactory lobe and accessory lobe (Sandeman and Sandeman, 1987; Sandeman et al., 1995a,b; see also Schachtner et al., 2005). Other Decapoda feature one SL-ir dorsal giant neuron on each side of the brain (Beltz et al., 1990; Benton and Beltz, 2001: lobsters; Schmidt and Ache, 1997: spiny lobsters). Also, the deutocerebrum in Remipedia features several SL-ir somata that send their neurites into the olfactory lobe (T. Stemme et al., personal communication). Only a single SL-ir neuron is present in the deutocerebrum of Insecta, whose soma is situated within the antennal lobe and sends fibers not only into the antennal lobe but, in contrast to the above-mentioned crustaceans, also into the protocerebrum (Kent et al., 1987; Ignell, 2001; Dacks et al., 2006). In contrast, SL-ir interneurons are absent in taxa without olfactory lobes (Fritsch and Richter, 2010: Branchiopoda, Hartline and Christie, 2010: Copepoda; Brenneis and Richter, 2010: Mystacocarida). Myriapoda have not been studied in this respect.

Similarly to *H. macracantha*, RFLI in the wedge-like olfactory glomeruli of the decapod olfactory lobe is absent in the peripheral 'cap', but concentrated in the inner 'base' and 'subcap' region (Schachtner et al., 2005; Harzsch and Hansson, 2008), the latter of which is innervated by local interneurons (Schmidt and Ache, 1997). Also, olfactory glomeruli in Insecta are innervated by RFL-ir local interneurons as well as by RFL-ir fibers originating from somata in other brain regions (Homberg, 2002; Schachtner et al., 2005). Although neurites from RFL-ir somata (r11) and (r12) in *H. macracantha* could not be traced, the location of some somata around the olfactory lobe suggests that they belong to local interneurons that innervate olfactory glomeruli. In contrast, the few RFL-ir fibers in the antennal lobe of Chilopoda rather surround the olfactory glomeruli diffusely, but do not appear to invade those (Sombke et al., 2010).

Their position suggests that also the deutocerebral HL-ir somata (h7) and (h8) in *H. macracantha* belong to HL-ir local interneurons like those innervating the olfactory glomeruli in Decapoda and some Insecta (Wachowiak and Ache, 1997, 1998; reviewed by Schachtner et al., 2005). In some Insecta, olfactory glomeruli also receive HL-ir processes from HL-ir somata outside of the deutocerebrum (Homberg and Müller, 1999).

4.4.4. Evolutionary interpretations

Although the shape and arrangement of olfactory glomeruli in Cephalocarida is unique, correspondences of their immunoreactive pattern to that in Insecta, Malacostraca, and Remipedia add support to Schachtner's et al. (2005) hypothesis that olfactory glomeruli are homologous across Tetraconata. Harzsch's (2006) proposal that the four taxa form a monophyletic clade with "local interneurons including serotonergic giant neurons" as an apomorphy would be supported by our finding of SL-ir local interneurons (s8) in *H. macracantha* and could well be extended to RFL-ir and HL-ir interneurons. However, Harzsch (2006) based his proposal on the hypothesis that the olfactory system is a synapomorphy of Cephalocarida, Remipedia, Malacostraca, and Hexapoda, a view that was recently questioned in the light of new data on the olfactory glomeruli in Chilopoda (Sombke et al., 2010). Given the debatable descriptions of olfactory glomeruli in several other Crustacea (Hanström, 1928, 1929, 1931) and Diplopoda (Duy-Jacquemin and Arnold, 1991), it seems more reasonable to assume that deutocerebral olfactory glomeruli were already present in the urmandibulate (see also Sombke et al., 2010). Whether this ground pattern includes SL-ir local interneurons cannot be reconstructed, because respective studies on Myriapoda are lacking. Also the original immunoreactive pattern in Crustacea that lost their olfactory lobes secondarily remains unclear.

4.5. Conclusion

The occurrence of corresponding components of the olfactory system (olfactory lobes linked by olfactory globular tracts to second order olfactory centers in the protocerebrum) amongst Hexapoda, Malacostraca, Remipedia, Cephalocarida as well as Chilopoda suggests that the olfactory system as a whole constitutes one functional unit that is part of the mandibulate ground pattern. The correspondences of the second order olfactory centers in Cephalocarida, Chilopoda and Insecta suggest that the multi-lobed complex widely conforms to this ground pattern. Differences, such as the number of multi-lobed complex neuropils, or the arrangement of olfactory glomeruli within the olfactory lobes, would be evolutionarily derived. As a consequence, the reported lack of a comparable olfactory system in many other Crustacea, and the disparate morphology of second order olfactory centers within Myriapoda, needs to be explained with secondary reduction or modification. This conclusion, however, complicates any argumentation on the phylogenetic position of Cephalocarida, because the complex olfactory system cannot count anymore as an argument for a closer relationship of hexapods, cephalocarids, malacostracans, and remipedes (as suggested by Harzsch, 2006), because the exact original conditions in those crustaceans that secondarily lost a complex olfactory system remain uncertain.

A central complex including a central body, a protocerebral bridge, and a pair of lateral accessory lobes has been suggested for the ground pattern of Tetraconata (Harzsch, 2006). Considering, however, the unknown relationships within Tetraconata (and the often suggested paraphyly of crustaceans), it might well be that a central complex consisting of all elements evolved only within Tetraconata, leaving the possibility open that in some crustacean taxa originally only a central body precursor was present. This might for example be true for *H. macracantha*, where the sickle-shaped SL-ir domain (sd1) might represent a central body rudiment, but no indications exist for the original presence of a protocerebral bridge and lateral accessory lobes.

Acknowledgements

We thank Georg Brenneis for his invaluable spadework in immunolabeling as well as for helpful comments on the manuscript. We are grateful to George Hampson, Steve Aubrey, Christian Wirkner, Günther Jirikowski, and all volunteers who helped collect *Hutchinsoniella macracantha* from the muddy bottom of Buzzards Bay, and to Simone Bourgeois and Arthur Dutra from Sea Lab, New Bedford, for kindly offering us their laboratory and help during our collection journeys from 2007 to 2010. We would like to thank Steffen Harzsch, Verena Rieger, and Jakob Krieger for their kind support in vibratome sectioning and fruitful discussions, and we thank Kerstin Schwandt for a series of semi-thin sections. We are also grateful to Rolf Elofsson and Robert Hessler for their advice on interpreting our results. We thank Nicholas Strausfeld and two anonymous reviewers for reading the manuscript and their many constructive remarks; Nicholas Strausfeld also improved the English. Finally, we thank the Deutsche Forschungsgemeinschaft (DFG) for funding (RI 837/9-1,2). This project is part of the DFG priority program "Deep Metazoan Phylogeny" (SPP 1174).

Appendix. Supplementary material

Supplementary data associated with this article can be found, in the online version, at: doi:10.1016/j.asd.2011.04.001.

References

Aramant, R., Elofsson, R., 1976. Monoaminergic neurons in the nervous system of crustaceans. Cell and Tissue Research 170, 231–251.

Ax, P., 1999. Das System der Metazoa II. Ein Lehrbuch der phylogenetischen Systematik. Gustav Fischer Verlag, Stuttgart, Jena, Lübeck, Ulm.

Babu, K.S., 1985. Patterns of Arrangement and Connectivity in the Central Nervous System of Arachnids. In: Barth, F.G. (Ed.), Neurobiology of Arachnids. Springer-Verlag, Berlin, Heidelberg, New York, Tokyo, pp. 3–19.

Beltz, B.S., Pontes, M., Helluy, S.M., Kravitz, E.A., 1990. Patterns of appearance of serotonin and proctolin immunoreactivities in the developing nervous system of the American lobster. Journal of Neurobiology 21, 521–542.

Bender, J.A., Pollack, A.J., Ritzmann, R.E., 2010. Neural activity in the central complex of the insect brain is linked to locomotor changes. Current Biology 20, 921–926.

Benton, J.L., Beltz, B.S., 2001. Effects of serotonin depletion on local interneurons in the developing olfactory pathway of lobsters. Journal of Neurobiology 46, 193–205.

Brenneis, G., Richter, S., 2010. Architecture of the nervous system in Mystacocarida (Arthropoda, Crustacea) - an immunohistochemical study and 3D-reconstruction. Journal of Morphology 271, 169–189.

Burnett, B.R., 1981. Compound eyes in the cephalocarid crustacean *Hutchinsoniella macracantha*. Journal of Crustacean Biology 1, 11–15.

Cajal, R.S., 1972. Histologie du système nerveux de l'homme et des vertébrés. Edition française (revue et mise à jour par l'auteur) (Textura del sistema nerviosa del hombre y vertebrados. Traduite par L. Azoulay). Consejo Superior de Investigaciones Cientificas. Instituto Ramon y Cajal, Madrid.

Carcupino, M., Floris, A., Addis, A., Castelli, A., Curini-Galletti, M., 2006. A new species of the genus *Lightiella*: the first record of Cephalocarida (Crustacea) in Europe. Zoological Journal of the Linnean Society 148, 209–220.

Dacks, A.M., Christensen, T.A., Hildebrand, J.G., 2006. Phylogeny of a serotonin-immunoreactive neuron in the primary olfactory center of the insect brain. Journal of Comparative Neurology 498, 727–746.

Derby, C.D., Fortier, J.K., Harrison, P.J.H., Cate, H.S., 2003. Peripheral and central antennular pathway of the Caribbean stomatopod crustacean *Neogonodactylus oerstedii*. Arthropod Structure and Development 32, 175–188.

Duy-Jacquemin, M.N., Arnold, G., 1991. Spatial organization of the antennal lobe in *Cylindroiulus puctatus* (Leach) (Myriapoda Diplopoda). International Journal of Insect Morphology and Embryology 20, 205–214.

Edgecombe, G.D., Wilson, G.D.F., Colgan, D.J., Gray, M.R., Cassis, G., 2000. Arthropod Cladistics: combined analysis of Histone H3 and U2 snRNA sequences and morphology. Cladistics 16, 155–203.

Elofsson, R., 1992. Monoaminergic and peptidergic neurons in the nervous system of *Hutchinsoniella macracantha* (Cephalocarida). Journal of Crustacean Biology 12, 531–536.

Elofsson, R., Hessler, R.R., 1990. Central nervous system of *Hutchinsoniella macracantha* (Cephalocarida). Journal of Crustacean Biology 10, 423–439.

Fahrenbach, W.H., 1977. The brain of the horseshoe crab (*Limulus polyphemus*). II. Architecture of the corpora pendunculata. Tissue and Cell 9, 157–166.

Fahrenbach, W.H., 1979. The brain of the horseshoe crab (*Limulus polyphemus*). III. Cellular and synaptic organization of the corpora pedunculata. Tissue and Cell 11, 163–199.

Fanenbruck, M., Harzsch, S., 2005. A brain atlas of *Godzilliognomus frondosus* Yager, 1989 (Remipedia, Godzilliidae) and comparison with the brain of *Speleonectes tulumensis* Yager, 1987 (Remipedia, Speleonectidae): implications for arthropod relationships. Arthropod Structure and Development 34, 343–378.

Fanenbruck, M., Harzsch, S., Wägele, J.W., 2004. The brain of the Remipedia (Crustacea) and an alternative hypothesis on their phylogenetic relationships. Proceedings of the National Academy of Sciences of the United States of America 101, 3868–3873.

Farris, S.M., 2005a. Developmental organization of the mushroom bodies of *Thermobia domestica* (Zygentoma, Lepismatidae): insights into mushroom body evolution from a basal insect. Evolution and Development 7, 150–159.

Farris, S.M., 2005b. Evolution of insect mushroom bodies: old clues, new insights. Arthropod Structure and Development 34, 211–234.

Farris, S.M., Sinakevitch, I., 2003. Development and evolution of the insect mushroom bodies: towards the understanding of conserved developmental mechanisms in a higher brain center. Arthropod Structure and Development 32, 79–101.

Fritsch, M., Richter, S., 2010. The formation of the nervous system during larval development in *Triops cancriformis* (Bosc) (Crustacea, Branchiopoda): an immunohistochemical survey. Journal of Morphology 271, 1457–1481.

Galizia, C.G., Rössler, W., 2009. Parallel olfactory systems in insects: anatomy and function. Annual Review of Entomology 55, 399–420.

Giribet, G., Richter, S., Edgecombe, G.D., Wheeler, W.C., 2005. The position of crustaceans within Arthropoda - Evidence from nine molecular loci and morphology. In: Koenemann, S., Jenner, R.A. (Eds.), Crustacea and Arthropod Relationships. Tailor Francis Group, Boca Raton, London, New York, Singapore.

Hanström, B., 1928. Vergleichende Anatomie des Nervensystems der wirbellosen Tiere unter Berücksichtigung seiner Funktion. Julias Springer, Berlin, Heidelberg, New York.

Hanström, B., 1929. Das Deutocerebrum der Crustaceen. Zoologische Jahrbücher Abteilung Anatomie und Ontogenie der Tiere 51, 535–548.

Hanström, B., 1931. Neue Untersuchungen über Sinnesorgane und Nervensystem der Crustaceen. I. Zeitschrift für Morphologie und Ökologie der Tiere 23, 80–236.

Hanström, B., 1940. Inkretorische Organe, Sinnesorgane und Nervensystem des Kopfes einiger niederer Insektenordnungen. In: Kungliga Svenska Vetenskapsakademiens Handlingar Tredje serien, 8. Almqvist & Wiksells Boktryckeri-A.-B, Stockholm, pp. 1–266.

Hanström, B., 1947. The brain, the sense organs, and the incretory organs of the head in the Crustacea Malacostraca. Lunds Universitets Årsskrift 43, 1–49.

Harley, C.M., Ritzmann, R.E., 2010. Electrolytic lesions within central complex neuropils of the cockroach brain affect negotiation of barriers. Journal of Experimental Biology 213, 2851–2864.

Hartline, D.K., Christie, A.E., 2010. Immunohistochemical mapping of histamine, dopamine, and serotonin in the central nervous system of the copepod *Calanus finmarchicus* (Crustacea; Maxillopoda; Copepoda). Cell and Tissue Research 341, 49–71.

Harzsch, S., 2006. Neurophylogeny: architecture of the nervous system and a fresh view on arthropod phyologeny. Integrative and Comparative Biology 46, 162–194.

Harzsch, S., 2007. The architecture of the nervous system provides important characters for phylogenetic reconstructions: Examples from the Arthropoda. Species, Phylogeny and Evolution 1, 33–57.

Harzsch, S., Glötzner, J., 2002. An immunohistochemical study of structure and development of the nervous system in the brine shrimp *Artemia salina* Linnaeus, 1758 (Branchiopoda, Anostraca) with remarks on the evolution of the arthropod brain. Arthropod Structure and Development 30, 251–270.

Harzsch, S., Hansson, B.S., 2008. Brain architecture in the terrestrial hermit crab *Coenobita clypeatus* (Anomura, Coenobitidae), a crustacean with a good aerial sense of smell. BMC Neuroscience 9.

Harzsch, S., Rieger, V., Krieger, J., Seefluth, F., Strausfeld, N.J., Hansson, B.S., 2011. Transition from marine to terrestrial ecologies: Changes in olfactory and-tritocerebral neuropils in land-living isopods. Arthropod Structure & Development 40, 244–257.

Harzsch, S., Waloszek, D., 2000. Serotonin-immunoreactive neurons in the ventral nerve cord of Crustacea: a character to study aspects of arthropod phylogeny. Arthropod Structure and Development 29, 307–322.

Hessler, R.R., 1964. The Cephalocarida – comparative skeletomusculature. Memoirs of the Connecticut Academy of Arts and Sciences XVI, 1–97.

Hessler, R.R., 1992. Reflections on the phylogenetic position of the Cephalocarida. Acta Zoologica 73, 315–316.

Hessler, R.R., Elofsson, R., 1992. Cephalocarida. In: Harrison, F.W. (Ed.), Microscopic Anatomy of Invertebrates. Wiley-Liss, New York, pp. 9–24.

Hessler, R.R., Elofsson, R., Hessler, A.Y., 1995. Reproductive system of *Hutchinsoniella macracantha* (Cephalocarida). Journal of Crustacean Biology 15, 493–522.

Heuer, C.M., Loesel, R., 2009. Three-dimensional reconstruction of mushroom body neuropils in the polychaete species *Nereis diversicolor* and *Harmothoe areolata* (Phyllodocida, Annelida). Zoomorphology 128, 219–226.

Heuer, C.M., Müller, C.H.G., Todt, C., Loesel, R., 2010. Comparative neuroanatomy suggests repeated reduction of neuroarchitectural complexity in Annelida. Frontiers in Zoology 7, 13.

Holmgren, N., 1916. Zur vergleichenden Anatomie des Gehirns von Polychaeten, Onychophoren, Xiphosuren, Arachniden, Crustaceen, Myriapoden und Insekten. Kungliga Svenska Vetenskapsakademiens Handlingar 56.

Homberg, U., 1991. Neuroarchitecture of the central complex in the brain of the locust *Schistocerca gregaria* and *S. americana* as revealed by serotonin immunocytochemistry. Journal of Comparative Neurology 303, 245–254.

Homberg, U., 2002. Neurotransmitters and neuropeptides in the brain of the locust. Microscopy Research and Technique 56, 189–209.

Homberg, U., 2008. Evolution of the central complex in the arthropod brain with respect to the visual system. Arthropod Structure and Development 37, 347–362.

Homberg, U., Müller, U., 1999. In: Hansson, B.S. (Ed.), Neuroactive Substances in the Antennal Lobe. Insect olfaction Springer-Verlag, Berlin, Heidelberg, New York, pp. 181–206.

Ignell, R., 2001. Monoamines and neuropeptides in antennal lobe interneurons of the desert locust, *Schistocerca gregaria*: an immunocytochemical study. Cell and Tissue Research 306, 143–156.

Ignell, R., Anton, S., Hansson, B.S., 2001. The antennal lobe of Orthoptera—anatomy and evolution. Brain, Behavior and Evolution 57, 1–17.

Johansson, K.U.I., Hallberg, E., 1992. The organization of the olfactory lobes in Euphausiacea and Mysidacea (Crustacea, Malacostraca). Zoomorphology 112, 81–89.

Kent, K.S., Hoskins, S.G., Hildebrand, J.G., 1987. A novel serotonin-immunoreactive neuron in the antennal lobe of the sphinx moth *Manduca sexta* persists throughout postembryonic life. Journal of Neurobiology 18, 451–465.

Kirsch, R., Richter, S., 2007. The nervous system of *Leptodora kindtii* (Branchiopoda, Cladocera) surveyed with confocal scanning microscopy (CLSM), including general remarks on the branchiopod neuromorphological ground pattern. Arthropod Structure and Development 36, 143–156.

Koenemann, S., Jenner, R.A., Hoenemann, M., Stemme, T., von Reumont, B.M., 2010. Arthropod phylogeny revisited, with a focus on crustacean relationships. Arthropod Structure and Development 39, 88–110.

Kollmann, M., Huetteroth, W., Schachtner, J., 2011. Brain organization in Collembola (springtails). Arthropod Structure & Development 40, 304–316.

Krieger, J., Sandeman, R.E., Sandeman, D.C., Hansson, B.S., Harzsch, S., 2010. Brain architecture of the largest living land arthropod, the giant robber crab *Birgus latro* (Crustacea, Anomura, Coenobitidae): evidence for a prominent central olfactory pathway? Frontiers in Zoology 7, 25.

Lauterbach, K.-E., 1974. Die Muskulatur der Pleurotergite im Grundplan der Euarthropoda. Zoologischer Anzeiger 193, 70–84.

Lauterbach, K.-E., 1983. Zum Problem der Monophylie der Crustacea. Verhandlungen des naturwissenschaftlichen Vereins Hamburg 26, 293–320.

Lauterbach, K.-E., 1986. Zum Grundplan der Crustacea. Verhandlungen des naturwissenschaftlichen Vereins Hamburg 28, 27–63.

Loesel, R., 2004. Comparative morphology of central neuropils in the brain of arthropods and its evolutionary and functional implications. Acta Biologica Hungarica 55, 39–51.

Loesel, R., Heuer, C.M., 2010. The mushroom bodies – prominent brain centres of arthropods and annelids with enigmatic evolutionary origin. Acta Zoologica 91, 29–34.

Loesel, R., Nässel, D.R., Strausfeld, N.J., 2002. Common design in a unique midline neuropil in the brains of arthropods. Arthropod Structure and Development 31, 77–91.

Mulisch, M., Welsch, U., 2010. Romeis. Mikroskopische Technik. 18. Auflage. Spektrum Akademischer Verlag, Heidelberg.

Paul, D.H., 1989. A neurophylogenist's view of decapod Crustacea. Bulletin of Marine Science 45, 487–504.

Pohl, L., 1958. Vergleichende anatomisch-histologische Untersuchungen an *Lepisma saccharina* Linné und der Myrmecophilen *Atelura formicaria* Heyden (Beitrag zur Myrmecophilie, zweiter Abschnitt). Insectes Sociaux 5, 67–76.

Regier, J.C., Shultz, J.W., Zwick, A., Hussey, A., Ball, B., Wetzer, R., Martin, J.W., Cunningham, C.W., 2010. Arthropod relationships revealed by phylogenomic analysis of nuclear protein-coding sequences. Nature 463, 1079–1083. U98.

Richter, S., 2002. The Tetraconata concept: hexapod-crustacean relationships and the phylogeny of Crustacea. Organisms Diversity and Evolution 2, 217–237.

Richter, S., Loesel, R., Purschke, G., Schmidt-Rhaesa, A., Scholtz, G., Stach, T., Vogt, L., Wanninger, A., Brenneis, G., Döring, C., Faller, S., Fritsch, M., Grobe, P., Heuer, C.M., Kaul, S., Møller, O.S., Müller, C.H.G., Rieger, V., Rothe, B.H., Stegner, M.E.J., Harzsch, S., 2010. Invertebrate neurophylogeny – suggested terms and definitions for a neuroanatomical glossary. Frontiers in Zoology 7, 29.

Sadek, M.M., Hansson, B.S., Rospars, J.P., Anton, S., 2002. Glomerular representation of plant volatiles and sex pheromone components in the antennal lobe of the female *Spodoptera littoralis*. Journal of Experimental Biology 205, 1363–1376.

Sandeman, D., Scholtz, G., 1995. Ground plans, evolutionary changes and homologies in decapod crustacean brains. In: Breidbach, O., Kutsch, W. (Eds.), The Nervous System of Invertebrates: An Evolutionary and Comparative Approach. Birkhäuser, Basel, Boston, Berlin.

Sandeman, D.C., Sandeman, R.E., Aitken, A.R., 1988. Atlas of serotonin-containing neurons in the optic lobes and brain of the crayfish, *Cherax destructor*. Journal of Comparative Neurology 269, 465–478.

Sandeman, D., Sandeman, R., Derby, C., Schmidt, M., 1992. Morphology of the brain of crayfish, crabs, and spiny lobsters - a common nomenclature for homologous structures. Biological Bulletin 183, 304–326.

Sandeman, D.C., Scholtz, G., Sandeman, R.E., 1993. Brain evolution in decapod Crustacea. Journal of Experimental Zoology 265, 112–133.

Sandeman, D., Beltz, B., Sandeman, R., 1995a. Crayfish brain interneurons that converge with serotonin giant cells in accessory lobe glomeruli. Journal of Comparative Neurology 352, 263–279.

Sandeman, R.E., Sandeman, D.C., 1987. Serotonin-like immunoreactivity of giant olfactory interneurons in the crayfish brain. Brain Research 403, 371–374.

Sandeman, R.E., Watson, A.H.D., Sandeman, D.C., 1995b. Ultrastructure of the synaptic terminals of the dorsal giant serotonin-ir neuron and deutocerebral commissure interneurons in the accessory and olfactory lobes of the crayfish. Journal of Comparative Neurology 361, 617–632.

Sanders, H.L., 1954. The Cephalocarida, a new subclass of Crustacea from long Island Sound. Proceedings of the National Academy of Sciences of the United States of America 41, 61–66.

Sanders, H.L., 1957. The Cephalocarida and crustacean phylogeny. Systematic Zoology 6, 112–148.

Sanders, H.L., 1963. The Cephalocarida. Memoirs of the Connecticut Academy of Arts and Sciences 15, 1–80.

Schachtner, J., Schmidt, M., Homberg, U., 2005. Organization and evolutionary trends of primary olfactory brain centers in Tetraconata (Crustacea plus Hexapoda). Arthropod Structure and Development 34, 257–299.

Schmidt, M., Ache, B.W., 1992. Antennular projections to the midbrain of the spiny lobster. 2. Sensory innervation of the olfactory lobe. Journal of Comparative Neurology 318, 291–303.

Schmidt, M., Ache, B.W., 1997. Immunocytochemical analysis of glomerular regionalization and neuronal diversity in the olfactory deutocerebrum of the spiny lobster. Cell and Tissue Research 287, 541–563.

Scholtz, G., Edgecombe, G.D., 2006. The evolution of arthropod heads: reconciling morphological, developmental and palaeontological evidence. Development Genes and Evolution 216, 395–415.

Schürmann, F.W., 1987. Histology and ultrastructure of the onychophoran brain. In: Gupta, A.P. (Ed.), Arthropod Brain: Its Evolution, Structure and Functions. John Wiley, New York, pp. 159–180.

Sombke, A., Harzsch, S., Hansson, B.S., 2010. Organization of deutocerebral neuropils and olfactory behavior in the centipede *Scutigera coleoptrata* (Linnaeus, 1758) (Myriapoda: Chilopoda). Chemical Senses 36, 43–61.

Spears, T., Abele, L.G., 1999. Phylogenetic relationships of the crustaceans with foliaceous limbs: an 18S rDNA study of Branchiopoda, Cephalocarida, and Phyllocarida. Journal of Crustacean Biology 19, 825–843.

Strausfeld, C.M., Buschbeck, E.K., Gomez, R.S., 1995. The arthropod mushroom body: its functional roles, evolutionary enigmas and mistaken identities. In: Breidbach, O., Kutsch, W. (Eds.), The Nervous System of Invertebrates: An Evolutionary and Comparative Approach. Birkhäuser, Basel, Boston, Berlin.

Strausfeld, N.J., 1976. Atlas of an Insect Brain. Springer, Berlin, Heidelberg, New York.

Strausfeld, N.J., 1998. Crustacean – insect relationships: the use of brain characters to derive phylogeny amongst segmented invertebrates. Brain Behavior and Evolution 52, 186–206.

Strausfeld, N.J., 2009. Brain organization and the origin of insects: an assessment. Proceedings of the Royal Society B-Biological Sciences 276, 1929–1937.

Strausfeld, N.J., Andrew, D.R., 2011. A new view of insect-crustacean relationships I. Inferences from neural cladistics and comparative neuroanatomy. Arthropod Structure & Development 40, 276–288.

Strausfeld, N.J., Barth, F.G., 1993. Two visual systems in one brain: neuropils serving the secondary eyes of the spider *Cupiennius salei*. Journal of Comparative Neurology 328, 43–62.

Strausfeld, N.J., Hildebrand, J.G., 1999. Olfactory systems: common design, uncommon origins? Current Opinion in Neurobiology 9, 634–639.

Strausfeld, N.J., Hansen, L., Li, Y.S., Gomez, R.S., Ito, K., 1998. Evolution, discovery, and interpretations of arthropod mushroom bodies. Learning and Memory 5, 11–37.

Strausfeld, N.J., Strausfeld, C.M., Loesel, R., Rowell, D., Stowe, S., 2006a. Arthropod phylogeny: onychophoran brain organization suggests an archaic relationship with a chelicerate stem lineage. Proceedings of the Royal Society B-Biological Sciences 273, 1857–1866.

Strausfeld, N.J., Strausfeld, C.M., Stowe, S., Rowell, D., Loesel, R., 2006b. The organization and evolutionary implications of neuropils and their neurons in the brain of the onychophoran *Euperipatoides rowelli*. Arthropod Structure and Development 35, 169–196.

Strausfeld, N.J., Sinakevitch, I., Brown, S.M., Farris, S.M., 2009. Ground plan of the insect mushroom body: functional and evolutionary implications. Journal of Comparative Neurology 513, 265–291.

Strauss, R., 2002. The central complex and the genetic dissection of locomotor behaviour. Current Opinion in Neurobiology 12, 633–638.

Sullivan, J.M., Beltz, B.S., 2001a. Neural pathways connecting the deutocerebrum and lateral protocerebrum in the brains of decapod crustaceans. Journal of Comparative Neurology 441, 9–22.

Sullivan, J.M., Beltz, B.S., 2001b. Development and connectivity of olfactory pathways in the brain of the lobster *Homarus americanus*. Journal of Comparative Neurology 441, 23–43.

Sullivan, J.M., Beltz, B.S., 2004. Evolutionary changes in the olfactory projection neuron pathways of eumalacostracan crustaceans. Journal of Comparative Neurology 470, 25–38.

Triphan, T., Poeck, B., Neuser, K., Strauss, R., 2010. Visual targeting of motor actions in climbing *Drosophila*. Current Biology 20, 663–668.

Tsvileneva, V.A., Titova, V.A., 1985. On the brain structures of decapods. Zoologische Jahrbücher Abteilung für Anatomie und Ontogenie der Tiere 113, 217–266.

Utting, M., Agricola, H.J., Sandeman, R., Sandeman, D., 2000. Central complex in the brain of crayfish and its possible homology with that of insects. Journal of Comparative Neurology 416, 245–261.

Wachowiak, M., Ache, B.W., 1997. Dual inhibitory pathways mediated by GABA- and histaminergic interneurons in the lobster olfactory lobe. Journal of Comparative Physiology A-Sensory Neural and Behavioral Physiology 180, 357–372.

Wachowiak, M., Ache, B.W., 1998. Multiple inhibitory pathways shape odor-evoked responses in lobster olfactory projection neurons. Journal of Comparative Physiology A-Sensory Neural and Behavioral Physiology 182, 425–434.

Walossek, D., 1993. The upper Cambrian *Rehbachiella* and the phylogeny of Branchiopoda and Crustacea. Fossils and Strata 32, 1–202.

Wertz, A., Rössler, W., Obermayer, M., Bickmeyer, U., 2006. Functional neuroanatomy of the rhinophore of *Aplysia punctata*. Frontiers in Zoology 3, 1–11.

Williams, J.L.D., 1975. Anatomical studies of the insect central nervous system: a ground-plan of the midbrain and an introduction to the central complex in the locust, *Schistocerca gregaria* (Orthoptera). Journal of Zoology 176, 67–86.

Williams, J.L., Boyan, G.S., 2008. Building the central complex of the grasshopper *Schistocerca gregaria*: axons pioneering the w, x, y, z tracts project onto the primary commissural fascicle of the brain. Arthropod Structure and Development 37, 129–140.

Zajac, J.M., Mollereau, C., 2006. Special issue: RFamide peptides - Introduction. Peptides 27, 941–942.

11. The central complex in Crustacea. Stegner MEJ, Fritsch M, Richter S. 2014a. In: Deep Metazoan Phylogeny: The backbone of the Tree of Life. Wägele JW, Bartolomaeus T (Hrsg). Berlin: de Gruyter. S. 361-384

Martin E.J. Stegner, Martin Fritsch, and Stefan Richter

14 The central complex in Crustacea

Abstract: The central complex is an intricate cluster of three interconnected neuropils (i.e. the unpaired central body and protocerebral bridge, and the paired lateral accessory lobes) situated in the brain of insects and crustaceans, which has been interpreted as a synapomorphy of all Tetraconata. However, the neuropils have been reported to be missing in several other crustacean taxa such as Cephalocarida and Mystacocarida, allowing for the alternative hypothesis that the central complex is a synapomorphy of only some tetraconate taxa. In order to better evaluate the disparity from a phylogenetic perspective, our contribution is to establish a well-founded comparison of the central complex across Crustacea, including its morphological structures as well as immunoreactive domains of neuro-active substances such as serotonin, RFamide, or histamine. In extension of the glossary of neuroanatomical terms developed within the Deep Metazoan Phylogeny framework, we define and clarify morphological terms related to the central complex. On the basis of improved comparability, we describe the central complex for all crustacean taxa, presenting selected data from our own immunohistochemical and histological investigations into Cephalocarida, Mystacocarida, Branchiopoda, Malacostraca, Copepoda, Ostracoda, and giving an updated review of the relevant literature. Our results and literature review add further support that the central complex is part of the tetraconate ground pattern. We discuss that in the light of all current phylogenetic hypotheses, the central complex would have been reduced several times independently during crustacean evolution. Central-body-like immunoreactive domains such as in Cephalocarida or Mystacocarida are here interpreted as plesiomorphic rudiments. Whether the central complex is indeed a tetraconate or rather a mandibulate apomorphy remains unclear, unless Myriapoda are studied in higher detail.

14.1 Introduction

One of the most interesting topics in arthropod neuroanatomy over the past decades has been the central complex, an intricate cluster of neuropils and tracts that occurs in the brain of various arthropods (reviewed by Harzsch, 2006; 2007; Homberg, 2008; Strausfeld, 2012). Following the definition proposed by Richter et al. (2010), the central complex consists of three interconnected neuropils: (1) the unpaired central body, (2) the unpaired protocerebral bridge, and (3) a pair of lateral accessory lobes. Although descriptions of these three neuropils date back to early neuroanatomists (e.g., Holmgren, 1916; Hanström, 1928; 1940; 1947), it was Williams (1975) who first recognized that, in the locust *Schistocerca gregaria*, the neuropils are interconnected by tracts, together forming one functional unit for which he then suggested the term 'central complex'.

The finding that the shape and arrangement of unpaired midline neuropils in Decapoda widely correspond to those in Hexapoda led Hanström (1928) to propose a sister-group relationship between Hexapoda and Crustacea – long before a monophyletic 'Tetraconata' composed of Hexapoda and Crustacea found support in molecular data. Detailed studies, especially of the hexapod (e.g., Boyan and Williams, 2011) and decapod central complex (e.g., Utting et al., 2000) have revealed further correspondences in the pattern of interconnecting tracts. A central complex has also been documented in three other crustacean taxa, namely anostracan Branchiopoda (Harzsch and Glötzner, 2002), Remipedia (Fanenbruck, Harzsch, and Wägele, 2004; Fanenbruck and Harzsch, 2005; Stemme et al., 2012) and Copepoda (Andrew, Brown, and Strausfeld, 2012). Although earlier investigators have described both a protocerebral bridge and a central body in the myriapod brain (Holmgren, 1916; Hanström, 1928; Joly and Descamps, 1987), this view has been questioned repeatedly by recent authors assuming that only one unpaired midline neuropil termed either 'central body' or 'central neuropil' occurs in Myriapoda (Lösel, Nässel, and Strausfeld, 2002; Loesel, 2004; Harzsch, 2006; Homberg, 2008; Sombke, Rosenberg, and Hilken, 2011). Unlike the central body, which is embedded within the protocerebrum, the single unpaired midline neuropil in Onychophora and Chelicerata is situated in the periphery of the brain and termed the 'arcuate body' (Strausfeld et al., 2006a; Loesel et al., 2011).

Besides these obvious differences between the major arthropod taxa, morphological disparity is also found within the taxa. Within Tetraconata, for example, the central body of Hexapoda is split into two distinct subunits, the ellipsoid body and the fan-shaped body (Strausfeld, 1976; Hanström, 1940; Kollmann, Huetteroth, and Schachtner, 2011), while the central body of Decapoda (e.g., Harzsch and Hanson, 2008; Krieger et al., 2010; 2012) appears as a horizontally layered but structurally coherent unit. Several other crustacean taxa, e.g. Mystacocarida (Brenneis and Richter, 2010) and Cephalocarida (Stegner and Richter, 2011) have even been reported to lack the neuropils of a central complex completely, or only to exhibit certain components of a central complex, e.g., phyllopod Branchiopoda (Fritsch and Richter, 2010).

Various studies have been carried out in an attempt to shed light on the morphological disparity in unpaired midline neuropils across Arthropoda and unravel their evolutionary origin. Approaches have taken in the innervation pattern, internal structure, development during ontogeny and functional aspects of these neuropils (reviewed by Homberg, 2008, see also Strausfeld, 2012). The association between both the arcuate body (e.g. Strausfeld, Weltzen, and Barth, 1993; Loesel, 2004) and the central complex (Liu et al., 2006) on the one hand and the optic pathway on the other initially led to the assumption that unpaired midline neuropils might constitute second order visual centers (reviewed by Homberg, 2008). However, a well-developed central body also occurs in blind taxa such as Symphyla (Joly and Descamps, 1987), Remipedia (Fanenbruck, Harzsch, and Wägele, 2004) and spelaeogriphacean and cumacean Malacostraca (this study). As convincingly demonstrated by Strauss (2002) and Bender, Pollack, and Ritzmann (2010), all the evidence points towards the

central complex playing a cardinal role in controlling motor activity, irrespective of whether in response to visual stimuli (Triphan et al., 2010) or tactile stimuli (Harley and Ritzmann, 2010).

Strausfeld et al. (2006a) suggested an evolutionary scenario in which the onychophoran/chelicerate arcuate body, the myriapod central neuropil and the tetraconate central complex all come from a hypothetical central neuropil in an ancestral urarthropod. Broadly in line with this hypothesis, Harzsch (2006) suggested that the central complex – consisting of a central body, a protocerebral bridge and lateral accessory lobes – constitutes an apomorphy of Tetraconata. The morphological correspondences between Decapoda, Hexapoda and Remipedia certainly suggest homology (Fanenbruck and Harzsch, 2005; Harzsch, 2006), but what about the "missing" central complex neuropils reported in other crustacean taxa? Since the phylogenetic relationships within Tetraconata are unclear (see for example Richter, Møller, and Wirkner, 2009; Jenner, 2010; Regier et al., 2010; von Reumont et al., 2012; Oakley et al., 2013), an explanation alternative to Harzsch (2006) would be that a central complex only evolved within Tetraconata as a synapomorphy of a limited group of tetraconate subtaxa (including Hexapoda, Malacostraca and Remipedia).

Methods of neuroanatomical investigation have advanced considerably over the past two decades thanks to progress in immunolabeling, confocal laser scanning microscopy and computerized 3D modeling. Given the improved morphological detail which present-day techniques make it possible to obtain, neuroanatomical structures such as the central complex can be used increasingly to address phylogenetic questions. This promising discipline has been coined 'neurophylogeny' (e.g., Harzsch, 2006), and the 'Invertebrate Neurophylogeny' section was a major constituent of the Deep Metazoan Phylogeny (DMP) program. Modern neurophylogenetic studies permit a reevaluation of earlier morphological descriptions and character definitions such as the presence of a central body. Using immunolabeling and confocal microscopy, immunoreactive neurons can be described individually right down to their neurites (e.g., Harzsch and Waloszek, 2000), bringing a wealth of new characters to phylogenetics. The serotonin-like immunoreactive pattern has proven especially useful in this respect (Harzsch, 2002b; 2003b; 2004; Harzsch, Müller, and Wolf, 2005; Brenneis and Richter, 2010; Stegner and Richter, 2011; Fritsch and Richter, 2012).

Since early neurophylogenetic studies focused on the long-debated relationships between the major arthropod taxa (Chelicerata, Myriapoda, Hexapoda, Crustacea), investigators of the central complex have tended to concentrate on hexapod or malacostracan representatives of Tetraconata – i.e. those species which are larger and more easily available – neglecting the less common non-malacostracan crustacean taxa.

One of our aims within the framework of DMP was to unravel phylogenetic relationships between the individual tetraconate subtaxa and, ultimately, to trace the evolution of the central complex within Tetraconata. Given the sparse data available on non-decapod Crustacea, it seemed the natural step to reinvestigate representa-

tives of those taxa for which neuroanatomical data was missing or incomplete. We are aware of the recent approach by Strausfeld and Hirth (2013) who identified potential "deep homology" between the hexapod central complex and the vertebrate basal ganglia based on common gene expression. However, we focus on structural correspondences existing between arthropods only.

In this DMP project, we studied Mystacocarida and Cephalocarida, two taxa whose nervous system had long been neglected and which it was finally possible to re-investigate using present-day methods. We revealed that the organization of the mystacocarid brain is comparatively simple, while the ventral nerve cord and peripheral nervous system broadly correspond to those in other crustaceans (Brenneis and Richter, 2010). In contrast, the cephalocarid nervous system contains several conspicuously complex features, including the olfactory system (Stegner and Richter, 2011), the thoracic commissures and the pattern of serotonin-like immunoreactive neurons (Stegner, Brenneis, and Richter, in press).

To establish a well-founded comparison of central complex components – and potentially homologous structures – across Crustacea, we present results from the DMP program pertaining to the mystacocarid and cephalocarid brain along with the results of independent investigations pertaining to Branchiopoda, Ostracoda, Copepoda and peracarid Malacostraca, complemented by data from the literature.

14.2 Definitions

In our view, morphological descriptions and terminology should be free of homology assumptions of any kind (see Vogt, Bartolomaeus, and Giribet, 2010). This is not to deny that homology exists, but simply to acknowledge the distinction between the various steps which need to be followed in (evolutionary) morphology, starting with pure description and only then going on to conceptualize evolutionary characters (Wirkner and Richter, 2010). In this context it is important to point out that not only must the terms used to denote concepts be free of homology assumptions, the concepts themselves should also be based on 'pure' description alone.

To establish a well-founded comparison of morphological structures and immunoreactive patterns across the different taxa, we use a standardized nomenclature based on the suggestions for a neuroanatomical glossary developed within the 'Invertebrate Neurophylogeny' section of the DMP program (Richter et al., 2010).

In continuation and elaboration of the glossary, our definitions are as follows:

14.2.1 Protocerebral bridge

The protocerebral bridge is an unpaired or paired midline neuropil which is situated in the anterior periphery of the protocerebrum, directly adjacent to the anteromedial

protocerebral somata. If the protocerebral bridge is paired, the neuropils are transversely connected via a tract.

14.2.2 Central body

The central body is an unpaired midline neuropil. It is situated within and surrounded by the protocerebral neuropil. The central body may be composed of columnar neurons and/or tangential neurons. The terms 'columnar neurons' and 'tangential neurons' refer to the orientation of their respective columnar or tangential neurite. If the central body occurs as a part of the central complex, it is connected to the lateral accessory lobes and the protocerebral bridge.

14.2.3 Lateral accessory lobes

The lateral accessory lobes are a pair of neuropils located laterally in the protocerebrum. The lateral accessory lobes are connected with the protocerebral bridge and the central body via tracts.

14.2.4 PB-CB tracts

A PB-CB tract is a tract which connects the protocerebral bridge to the central body. Where the specific arrangement of four PB-CB tracts per body side is present, the tracts are termed the W, X, Y, Z tracts.

14.2.5 Immunoreactive domains

An immunoreactive domain is a distinct cluster of immunoreactive neurites. It may overlap with all or part of a distinct neuropil.

Background: The term 'immunoreactive domain' refers to a category which needs to be specified by naming which neuro-active substance is labeled to become a structural term. A number of neurons have been found to synthesize neuro-active substances such as serotonin, tachykinin, RFamide and histamine. The immunoreactive neurites of these neurons extend into the protocerebral neuropil where they arborize to form chemical synapses with other neurons, thus contributing to immunoreactive domains. We have avoided calling these immunoreactive domains 'neuropils'. An immunoreactive domain may overlap with part but not all of a neuropil, and immunoreactive domains may even be present where distinct neuropils cannot be identified. Although they may correlate with each other, neuropils and domains and their

respective shape, position and innervation pattern should be described separately. While neuropils are recognizable in semithin sections and histological and immunohistochemical stains by their density and their spatial and structural separation from the surrounding brain neuropil, immunoreactive domains stand out from the surrounding neuropil solely because of their pattern of immunoreactivity.

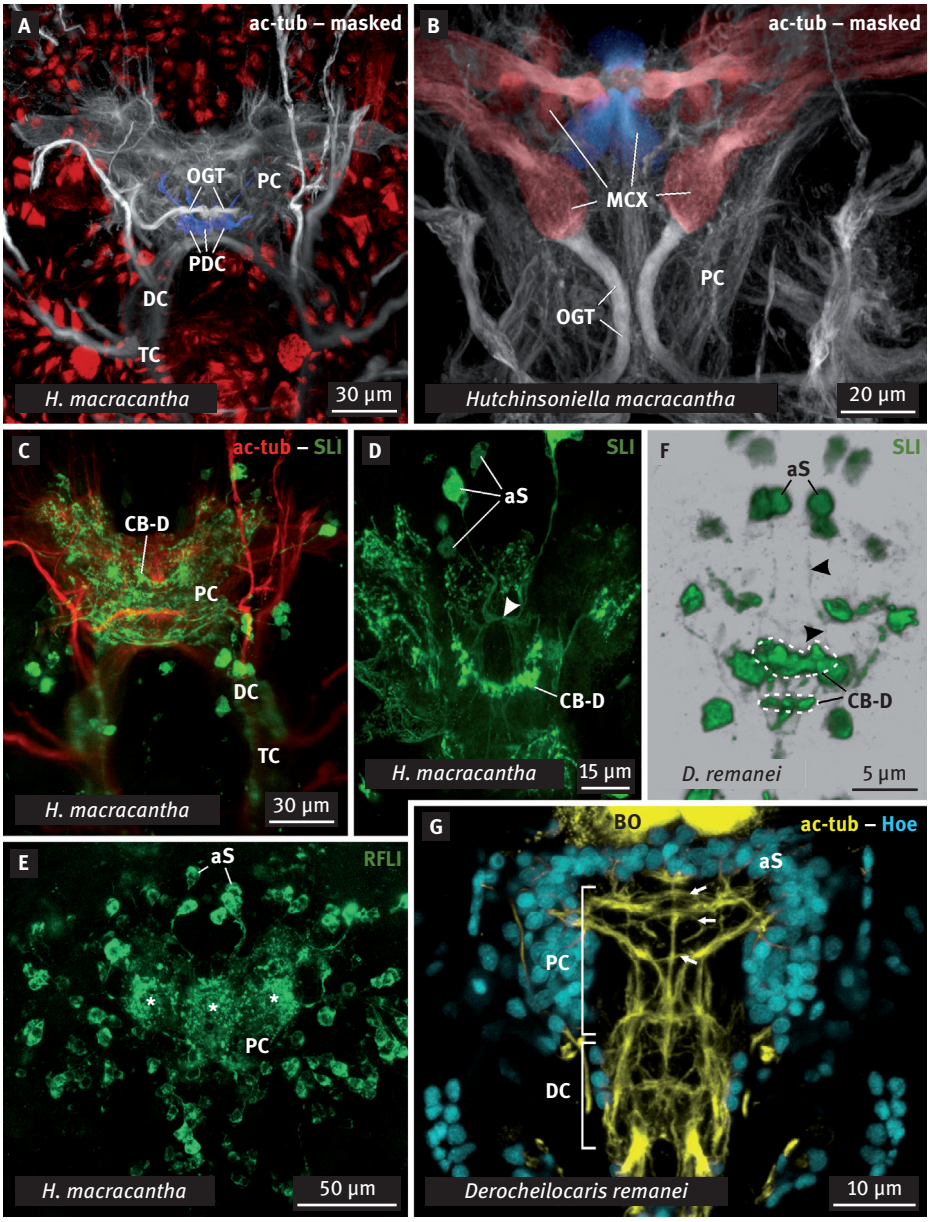

The brain may contain domains in different regions. For the purposes of this publication, three types are of special interest:

- the anterior immunoreactive domain, here termed the 'protocerebral bridge-like immunoreactive domain' (PB-like domain)
- the central immunoreactive domain, here termed the 'central body-like immunoreactive domain' (CB-like domain)
- a pair of lateral immunoreactive domains, here termed 'lateral accessory lobe-like immunoreactive domains' (LAL-like domain)

Those immunoreactive domains which are not associated with the central complex in any way are ignored in this publication.

We use the following abbreviations for the various types of immunoreactivity: serotonin-like immunoreactivity/immunoreactive (SLI/SL-ir); histamine-like immunoreactivity/immunoreactive (HLI/HL-ir); RFamide-like immunoreactivity/immunoreactive (RFLI/RFL-ir).

14.3 Results

14.3.1 Cephalocarida

The cephalocarid species *Hutchinsoniella macracantha* lacks distinct neuropils such as a central body, a protocerebral bridge or lateral accessory lobes (Elofsson and Hessler, 1990; Stegner and Richter, 2011). The only distinct unpaired midline neuropils described in the cephalocarid brain are the median neuropil of the posterodorsal neuropil cluster (Figure 14.1A) and three neuropils of the multi-lobed complex (Figure 14.1B), none of which correspond to the central complex neuropils

◂ **Figure 14.1:** Confocal horizontal micrographs of the protocerebrum in Cephalocarida **(A–D)** and Mystacocarida **(F,G)**. **A.** Dorsal view of a whole-mount. The 'posterodorsal neuropil cluster' (*blue*) includes an unpaired midline neuropil but cannot be related to the central complex of other arthropods. **B.** Transverse vibratome section. The multi-lobed complex includes both paired (*red*) and unpaired (*blue*) components which do not correspond to central complex neuropils. **C.** Dorsal view of a whole-mount. The unpaired sickle-shaped SL-ir domain (*CB-D*) lies within the protocerebrum. **D.** Horizontal vibratome section. The SL-ir domain receives decussating SL-ir axons (*arrowhead*) from anterior somata. **E.** Dorsal view of the brain. None of the cephalocarid RFL-ir domains (*asterisks*) can be related to the central complex neuropils of other crustaceans. **F.** Ventral view of the mystacocarid brain showing two CB-like SL-ir domains receiving ipsilateral neurites from anterior somata. **G.** Ventral view of a whole-mount. *Arrows* point at various commissures, but midline neuropils are not present. *ac-tub* acetylated α-tubulin, *aS* anterior somata, *BO* Bellonci organ, *CB-D* CB-like domain, *DC* deutocerebrum, *Hoe* Hoechst nuclear counterstain, *MCX* multi-lobed complex, *OGT* olfactory globular tract, *PC* protocerebrum, *PDC* posterodorsal neuropil cluster, *RFLI* RFamide-like immunoreactivity, *SLI* serotonin-like immunoreactivity, *TC* tritocerebrum. Originals by Stegner and Richter (A–E), Brenneis and Richter (F,G).

in other arthropods (see Stegner and Richter, 2011). There is a CB-like SL-ir domain (Figure 14.1C,D) in *Hutchinsoniella macracantha* which corresponds to the central body of other arthropods in four respects: (1) its elongated shape, (2) its central position within the protocerebral neuropil, (3) the fact that SL-ir neurites project into it from anteromedial somata, (4) the fact that these neurites cross the midline (Stegner and Richter, 2011). In contrast, none of the RFL-ir and HL-ir unpaired immunoreactive domains in *H. macracantha* (labeled rd1, hd2, hd3 by Stegner and Richter, 2011) correspond to neuropils of the central complex (see, for example, the middle asterisk in Figure 14.1E).

14.3.2 Mystacocarida

Mystacocarida do not exhibit any distinct neuropils in the protocerebrum, and also lack a central body, a protocerebral bridge and lateral accessory lobes (Baccari and Renaud-Mornant, 1974; Elofsson and Hessler, 2005; Brenneis and Richter, 2010). There are two SL-ir CB-like domains in the mystacocarid species *Derocheilocaris remanei* (Figure 14.1F) which correspond to the central body of other arthropods in three respects: (1) their elongated shape, (2) their central position within the protocerebral neuropil, (3) the fact that SL-ir neurites project into them from anteromedial somata (Brenneis and Richter, 2010). Unlike in Cephalocarida, these neurites do not cross the midline before entering the SL-ir CB-like domains (Brenneis and Richter, 2010). Although embedded centrally within the protocerebral neuropil, the two mystacocarid SL-ir CB-like domains lie more dorsally than the cephalocarid SL-ir CB-like domain. Protocerebral RFL-ir domains in Mystacocarida do not correspond to neuropils of the central complex (Brenneis and Richter, 2010).

Figure 14.2: Central complex neuropils in Isopoda **(A)**, Amphipoda (*Parhyale hawaiensis*, **B**), Cumacea **(C)**, Spelaeogriphacea **(D)**, Copepoda **(E)** and Ostracoda **(F)**. **A.** 3D reconstruction of the brain based on semithin sections in posterior view. Somata in light blue, neuropil semi-transparent. The W tract lies posterior to the decussating olfactory globular tracts, and the X, Y, Z tracts anterior to them. **B, C.** Vibratome section in posterior view. **D.** Transverse semithin section through the protocerebrum. The protocerebral bridge is split, and the Z and Y tracts cannot be distinguished. The W tract, which passes posterior to the olfactory globular tract, is situated in a more posterior section (not shown). **E.** Ventral view of a whole-mount. Within the protocerebrum no distinct central complex neuropils are identifiable. **F.** Ventral view of a whole-mount. Within the protocerebrum prominent tracts (arrows) but no distinct central complex neuropils are identifiable. *ac-tub* acetylated α-tubulin, *aS* anterior somata, *CB* central body, *DC* deutocerebrum, *LAL* lateral accessory lobes, *OGT* olfactory globular tract, *OL* olfactory lobe, *PC* protocerebrum, *Syt* Sytox nuclear counterstain, *W/X/Y/Z* PB-CB tracts. Originals by Stegner, Wirkner, Richter (A,D), C. Wittfoth (B,E), C. Döring (C), M. Dreiling (F). ▸

14.3.3 Malacostraca

All the major malacostracan taxa exhibit a well-developed central complex which includes a central body, a protocerebral bridge and lateral accessory lobes (Hanström, 1928; 1934; 1947; Sandeman et al., 1992; Sandeman, Scholtz, and Sandeman, 1993; Sandeman and Scholtz, 1995; Utting et al., 2000; Krieger et al., 2010; 2012; Strausfeld, 2012). This is also true for Leptostraca, which is the sister-group to all remaining Mala-

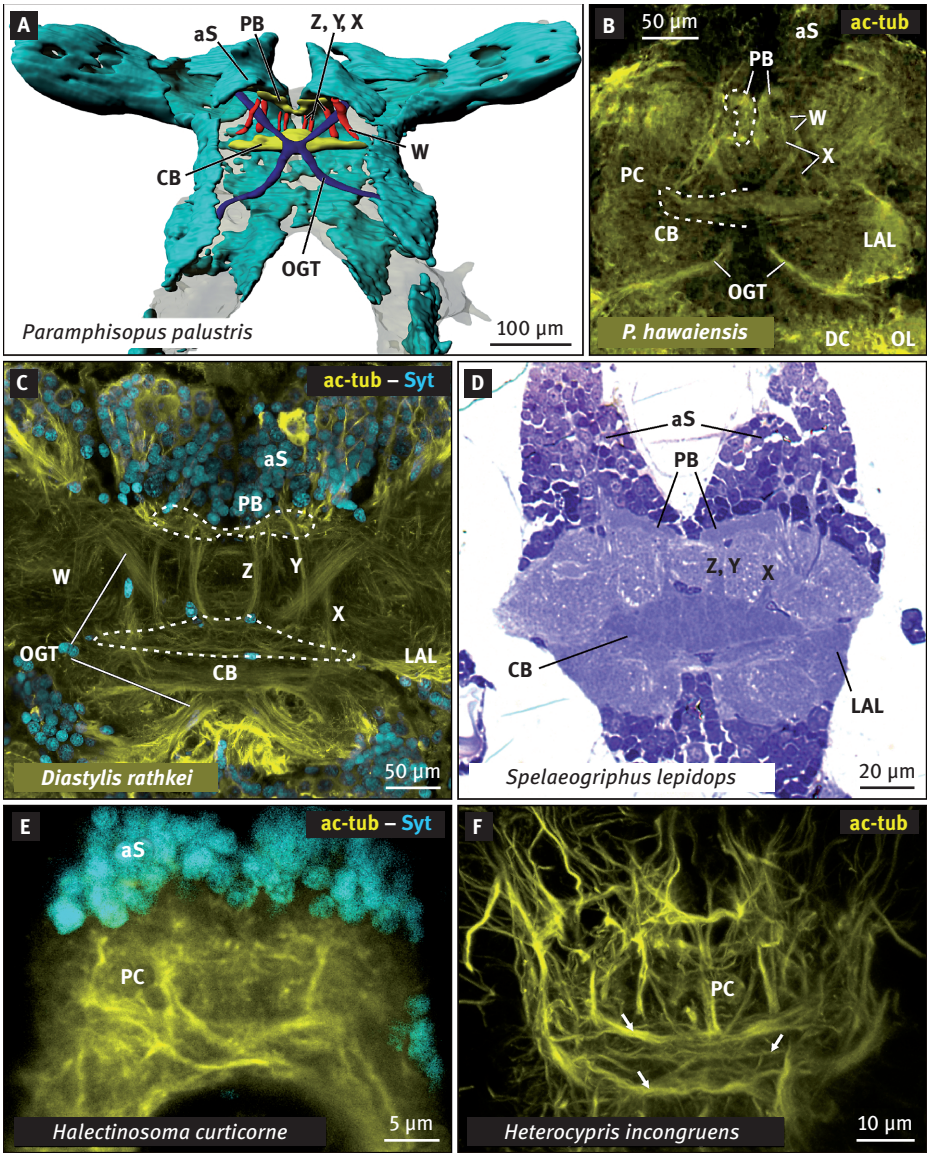

costraca (Kenning et al., 2013). Utting et al. (2000) studied the central complex of the lobster *Cherax destructor* in great detail, tracing the anatomy of individual neurons and showing that the lobster's PB-CB tracts occur in a specific arrangement of four major tracts on each side of the body: these are termed the W, X, Y and Z tracts. A corresponding pattern is found in the leptostracan *Nebalia herbstii* (Kenning et al., 2013), the isopod *Paramphisopus palustris* (Figure 14.2A), the amphipod *Parhyale hawaiensis* (Figure 14.2B), the cumacean *Diastylis rathkei* (Figure 14.2C), while the spelaeogriphacean *Spelaeogriphus lepidops* displays three tracts: W, X, Y/Z (Figure 14.2D). This implies that a central complex featuring W, X, Y and Z tracts can be assumed to be part of the ground pattern of Malacostraca (Kenning et al., 2013). No distinct W, X, Y and Z tracts have been described in Stomatopoda (Hanström, 1947; Sandeman and Scholtz, 1995; Strausfeld, 2012).

There are several SL-ir domains in Malacostraca: unpaired domains which overlap with the central body and the protocerebral bridge respectively, and paired domains which overlap with the lateral accessory lobes (Sandeman, Sandeman, and Aitken, 1988; Langworthy et al., 1997; Utting et al., 2000; Harzsch and Hansson, 2008). The central body and lateral accessory lobes comprise RFL-ir domains, while the protocerebral bridge is not RFL-ir (Harzsch and Hansson, 2008). Synapsin-like immunoreactive (SYNL-ir) domains have been shown to overlap with the protocerebral bridge and lateral accessory lobes, while the central body is only weakly SYNL-ir (Harzsch and Hansson, 2008). All the neuropils of the central complex in Decapoda exhibit HL-ir domains (Langworthy et al., 1997).

14.3.4 Branchiopoda

14.3.4.1 Anostraca

In the anostracan *Artemia salina* a well-developed central body is present. The unstratified and evenly-shaped mesh of the spindle-shaped central body is clearly identifiable via histological sectioning (Hanström, 1924; Benesch, 1969; Harzsch and Glötzner, 2002). Anterior to the central body, a slender protocerebral bridge is distinguishable (Hanström, 1924; Benesch, 1969; Harzsch and Glötzner, 2002). Posterolaterally on both sides of the central body, lateral accessory lobes have been described (Benesch, 1969; Harzsch and Glötzner, 2002).

An HL-ir and SL-ir domain which broadly overlaps with the central body is also present (Harzsch and Glötzner, 2002). Anterior to this domain, Harzsch and Glötzner (2002) discovered a tripartite HL-ir and SL-ir domain. In our view, only the median component of this HL-ir and SL-ir domain corresponds to the unpaired and slender protocerebral bridge identified histologically by Hanström (1924) and Benesch (1969). HL-ir and SL-ir domains overlap with the lateral accessory lobes (Harzsch and Glötzner, 2002).

Recent immunohistochemical investigations into the larvae of the anostracan *Branchinella* sp. have revealed a central body and a slender protocerebral bridge (Figure 14.3A), but lateral accessory lobes were not distinguished using nervous system markers (Frase and Richter, unpublished). Frase and Richter (unpublished) were also able to reveal two potential PB-CB tracts in the developing protocerebral architecture of *Branchinella* sp. larvae. Each tract emanates anterolaterally in the protocerebral superficial somata cluster, runs posteriorly, enters the central body anterolaterally and interconnects with the internal mesh. However, no true connection between these tracts and the protocerebral bridge was found.

14.3.4.2 Notostraca

Both a central body and a slender protocerebral bridge have been identified in the Notostraca (Hanström, 1924; Fritsch and Richter, 2010; Strausfeld, 2012). As in the anostracans, the central body in the Notostraca consists of a mesh of evenly distributed neurites. No lateral accessory lobes have yet been found. Two potential PB-CB tracts are discernible in the protocerebrum of *Triops cancriformis* larvae. Each tract emanates from the superficial anterolateral layer of protocerebral somata and enters the central body anterolaterally, but no true connection has been found between these tracts and the protocerebral bridge. Using neuro-active substance markers, both a CB-like domain (tachykinin: Loesel, 2004 in *Triops longicaudatus*, histamine and serotonin: Fritsch and Richter, 2010 in *Triops cancriformis*) and a PB-like weakly HL-ir domain (Fritsch and Richter, 2010) are detectable in the protocerebrum (Figure 14.3B). No reports of the presence of LAL-like domains exist.

14.3.4.3 Laevicaudata, Spinicaudata and Cyclestherida ("Conchostraca")

A central body and a slender protocerebral bridge are also identifiable in the protocerebrum of the Laevicaudata (Hanström, 1934), Spinicaudata (Hanström, 1934) and Cyclestherida (Figure 14.3C–E). The unstratified and even mesh of the central body is shaped like a spindle. The inner scaffold of the protocerebral bridge forms a horizontal network connecting the two lateral protocerebral hemispheres. Two pairs of potential PB-CB tracts are identifiable in the adult protocerebrum of *Lynceus brachyurus* (Laevicaudata) and *Leptestheria dahalacensis* (Spinicaudata) (arrows: Figure 14.3C,D). Both pairs of tracts emanate from the anterolateral protocerebral somata layer, run posteriorly to the anterolateral margins of the central body and interconnect with the internal mesh of the central body. No distinct connection to the protocerebral bridge has yet been found.

HL-ir and SL-ir domains overlapping with the protocerebral bridge and central body are present in the protocerebrum of the spinicaudatan *L. dahalacensis*, but neither histological sectioning nor neuro-active substance markers reveal the presence of lateral accessory lobes or LAL-like domains.

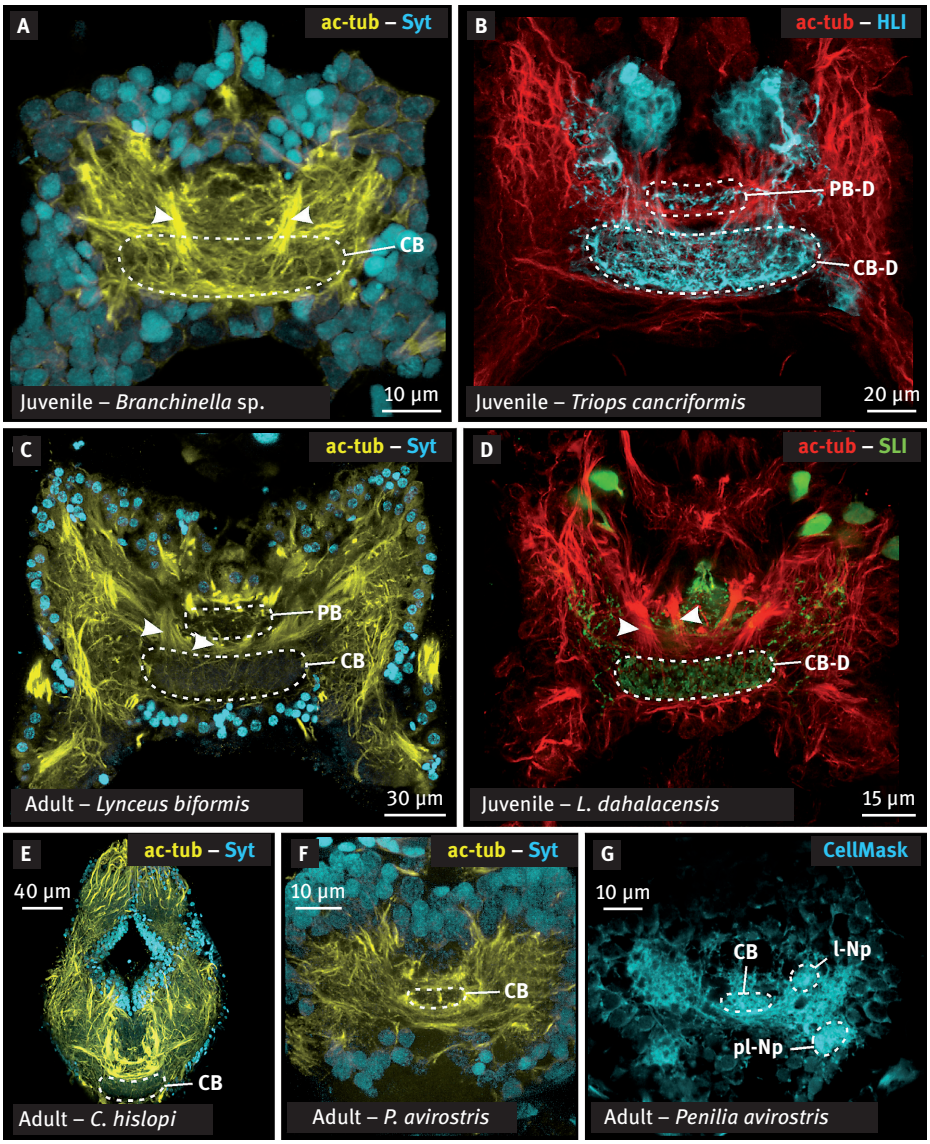

14.3.4.4 Cladocera

Within the protocerebrum of the cladocerans, a well-formed central body is present (Claus, 1876; Leder, 1915; Hanström, 1931; 1934; Bullock and Horridge, 1965; Kirsch and Richter, 2007; Strauß et al., 2011; Weiss et al., 2012; see also Fig. 14.3F,G). A protocerebral bridge has been documented in the haplopod *Leptodora kindtii* (Kirsch and Richter, 2007) and, less distinctive, in the ctenopod *Penilia avirostris* (this study, not depicted). Lateral accessory lobes have been described for the protocerebrum of *L.*

◂ **Figure 14.3:** Ventral view of the branchiopod protocerebrum. Anostraca **(A)**, Notostraca **(B)**, Laevicaudata **(C)**, Spinicaudata (*Leptestheria dahalacensis*, **D**), Cyclestherida (*Cyclestheria hislopi*, **E**) and Cladocera, Ctenopoda **(F, G)**. **A–F.** Immunohistochemical stainings. **A.** A well-developed central body spans the protocerebrum. Two PB-CB tracts (*arrowheads*) enter the central body anteriorly. **B.** The PB-like weakly HL-ir domain is situated anterior to the prominent central body-like HL-ir domain. **C.** Altogether four PB-CB tracts (*arrowheads*) enter the prominent central body at the anterior margin. **D.** Using serotonin markers only, a distinct CB-like SL-ir domain is identifiable. Four PB-CB tracts (*arrowheads*) are present altogether. **E.** Only a central body can clearly be identified. **F.** Using immunohistochemical markers only, the central body can be distinguished in the protocerebrum. **G.** In histological CellMask stainings additional anterior and lateral neuropils are visible next to the central body. *ac-tub* acetylated α-tubulin, *CB* central body, *CB-D* CB-like domain, *HLI* histamine-like immunoreactivity, *l-Np* lateral neuropil, *pl-Np* posterolateral neuropil, *PB* protocerebral bridge, *PB-D* PB-like domain, *PC* protocerebrum, *SLI* serotonin-like immunoreactivity, *Syt* Sytox nuclear counterstain. Originals by T. Frase (A), M. Fritsch (B–E), M. Becker (F,G).

kindtii (Kirsch and Richter, 2007), but while lateral neuropils are detectable anteriorly and posteriorly on each side of the central body in *Daphnia pulex* (Anomopoda) (Strauß et al., 2011; Weiss et al., 2012), and *P. avirostris* (Ctenopoda) (Fig. 14.3G), they do not necessarily correspond to the lateral accessory lobes. In fact we think that the posterolateral neuropils actually constitute the deutocerebral lobes in which the nerve of the antennula ends (see Figure 14.3G). Using neuro-active substance markers (monoaminergic amines: Aramont and Elofsson, 1976; pigment disperse hormone: Strauß et al., 2011), a CB-like domain is detectable in the protocerebrum of *D. pulex*.

14.3.4.5 Branchiopod central complex

A well-formed central body is present in all recent branchiopod taxa, as is, anteriorly, a slender protocerebral bridge. These neuropils are assumed to be part of the branchiopod ground pattern. Lateral accessory lobes are only described in the anostracan *Artemia salina* and the haplopod *Leptodora kindtii*, with none identifiable in the anostracan *Branchinella* sp. or the Notostraca, Laevicaudata, Spinicaudata and Cyclestherida. In Anomopoda, Ctenopoda and Onychopoda, paired lateral neuropils have been identified, but their homology to lateral accessory lobes is questionable. Thus, whether lateral accessory lobes are part of the branchiopod ground pattern remains unclear. We suggest that a single potential PB-CB tract in Anostraca and Notostraca represents the branchiopod ground pattern. The pattern of two tracts per side as found in “conchostracans” would have evolved within Branchiopoda.

14.3.5 Copepoda

The literature on the copepod brain does not paint a consistent picture of the central complex. As reviewed by Andrew, Brown, and Strausfeld (2012), a central body had been described in some calanoid (Lowe, 1935) and cyclopoid Copepoda (Aramant and Elofsson, 1976), while the absence of a central body and protocerebral bridge had been reported for many harpactoid Copepoda (Lang, 1948; Fahrenbach, 1962). Most of the studies concerned were based on traditional histological methods. In a detailed study combining immunolabeling with histological methods, Andrew, Brown, and Strausfeld (2012) described a central body in the protocerebrum of the harpacticoid species *Tigriopus californicus*, and the decussation of a pair of associated tracts which the authors interpreted as PB-CB tracts indicative of a protocerebral bridge. They did, however, mention the difficulties involved in identifying this neuropil on the basis of semithin sections. A lobed lateral protrusion on each side of the protocerebrum was suggested to correspond to the lateral accessory lobes (Andrew, Brown, and Strausfeld, 2012). Immunolabeling and methylene-staining of the harpactoid species *Halectinosoma curticorne* (Wittfoth and Richter unpublished, see Figure 14.2E) did not reveal distinct neuropils in the protocerebrum. Two SL-ir domains were found in both the protocerebrum of *T. californicus* (Andrew, Brown, and Strausfeld, 2012) and that of *H. curticorne* (Wittfoth and Richter unpublished), but were not related to neuropils of the central complex. Although domains of varying immunoreactivity have been found in calanoid Copepoda, none of them correlated with the neuropils of a central complex (Benzid, Morris, and Barthéléma, 2005; Barthélémy et al., 2006; Hartline and Christie, 2010: serotonin; Hartline and Christie, 2010: histamine, dopamine; Wilson and Christie, 2010: allatostatin; Sousa et al., 2008: tachykinin; but see Aramant and Elofsson, 1976 who noted a central body on the basis of an unspecified "monoamine").

14.3.6 Ostracoda

In Myodocopida the protocerebrum innervates a frontal filament organ, a nauplius eye and the compound eyes, while in Podocopida it only innervates a nauplius eye (see Hartmann, 1967). Within the protocerebrum, histological sectioning has revealed a well-defined central body and, anteriorly, a protocerebral bridge in the myodocopids and podocopids (Hanström, 1924; 1928; Cannon, 1931; see Hartmann, 1967). None of the studies mentioned report PB–CB tracts in Ostracoda. Aramant and Elofsson (1976: their Fig. 25a) suggested that a spheroidal domain of unspecified "monoaminergic" immunoreactivity may constitute the central body in a podocopid species. In a preliminary immunohistochemical study in podocopids, neither an unpaired immunoreactive domain nor an unpaired midline neuropil was found.

14.3.7 Branchiura

All the studies into the branchiuran brain which exist to date have been based on traditional histological methods (Leydig, 1889; Martin, 1932; Zaćwilichowski, 1935; Zaćwilichowska, 1948; Overstreet et al., 1992). Putative neuropils of a central complex have not been either described or depicted. Nothing is known about the immunoreactive pattern in the branchiuran brain.

14.3.8 Cirripedia

The reduced brain of adult Thoracica consists of two supraesophageal, transversely connected ganglia (Bullock and Horridge, 1965; Gwilliam and Cole, 1979; Walker, 1992; Webster, 1998; Callaway and Stuart, 1999; Harrison and Sandeman, 1999). Division into a proto-, deuto- and tritocerebrum is vague to non-existent in the adult brain but clearly distinguishable in thoracican cypris larvae (Semmler et al., 2008). In the protocerebrum of larval *Balanus improvisus* a CB-like SL-ir domain (labeled pcn) exists which corresponds to the central body of other arthropods in (1) its central position within the protocerebral architecture and (2) its reception of SL-ir neurites from lateral and posterolateral somata (Semmler et al., 2008). Neuro-active substances fail to reveal any other reactive domains associated with the central complex in the larval protocerebrum.

The nervous system of the Acrothoracica and the Rhizocephala is even more concentrated and reduced than that of the Thoracica (Bullock and Horridge, 1965). No detailed information is available on the protocerebral architecture of either the adult or the larval brain. In his general morphological description of the rhizocephalan cypris larva, Glenner (2001) described the nervous system but made no mention of an unpaired midline neuropil.

14.3.9 Remipedia

Remipedia are equipped with a central complex made up of a small central body, a large protocerebral bridge and lateral accessory lobes (Fanenbruck, Harzsch, and Wägele, 2004; Fanenbruck and Harzsch, 2005). In fact, Remipedia exhibit four main lateral protrusions from each side of the protocerebral neuropil which Fanenbruck and Harzsch (2005) termed ‘lateral protocerebral sublobes a–d’. The same authors demonstrated that only ‘sublobes d’ (which are further divided into the four subunits d1-d4) are associated with the central body, suggesting that only they correspond to the lateral accessory lobes in other arthropods.

In a detailed investigation of the remipede brain based on immunolabeling methods, Stemme et al. (2012) recently showed an unpaired SL-ir domain (labeled

sd2) overlapping with the central body and several paired SL-ir domains overlapping with the protocerebral bridge (sd4–6) and lateral accessory lobes (sd9). The SL-ir domains of the central body and protocerebral bridge were found to be connected by four well-separated SL-ir neurites on each side of the body, providing the first indication of W, X, Y and Z tracts in Remipedia. It remains unclear from which somata these neurites originate. Neither the SL-ir domains (sd4–6) of the protocerebral bridge nor that of the central body (sd2) are innervated directly by an "anterior" assemblage of protocerebral somata (Stemme et al., 2012, "anterior" here refers to the neuraxis, because the remipede brain bends posteriorly). However, a group of SL-ir "anterior" somata (sA1) projects SL-ir neurites passing the protocerebral bridge to a convergence point with other SL-ir neurites which extend medially and cross the midline to innervate the SL-ir domain (sd2) of the central body (Stemme et al., 2012, see especially their Figure 14.7). Another "anterior" group of SL-ir somata (sA2) projects SL-ir neurites across the midline of the protocerebral neuropil to supply the SL-ir domain (sd9) of the lateral accessory lobes (Stemme et al., 2012).

14.4 Discussion

The results of our investigation and short literature review are summarized in Table 14.1, based on the definitions given above. Neuropils and specific immunoreactive domains of the central complex are treated separately. It has long been known that the neuropils of the central complex are innervated by neurons containing stainable neuro-active substances (e.g., Aramant and Elofsson, 1976). In other words, the neuropils overlap, to some extent, with immunoreactive domains. Interestingly, our investigations into Mystacocarida (Brenneis and Richter, 2010) and Cephalocarida (Stegner and Richter, 2011) revealed immunoreactive domains in the protocerebrum even where complementary staining methods failed to detect correlated neuropils (i.e. condensed and distinct compartments of protocerebral neuropil). Vice versa, in taxa whose central body occurs as a distinct neuropil, those domains immunoreactive to a certain neuro-active substance were found to overlap with part but not all of the neuropil in question (e.g., Homberg and Hildebrand, 1991; Homberg, 2002; Loesel, 2004; Strausfeld, 2012).

14.4.1 Structural comparison

Given the correspondences in the overall shape and position of central complex neuropils in different crustaceans (Table 14.1), it would be interesting to know whether these correspondences extend to internal neuropil anatomy too. Moreover, how are immunoreactive domains in taxa without distinctive neuropils – e.g. Mystacocarida and Cephalocarida – related to immunoreactive domains and neuropils in other taxa?

The internal anatomy of central complex neuropils, especially in Hexapoda and Malacostraca, has been investigated in impressive detail, as recent reviews make clear (Homberg, 2008; Strausfeld, 2012). We concentrate here on five features of particular relevance for the interpretation of our new data.

14.4.1.1 Columnar neurons

The central body is generally supplied by neurites of 'columnar neurons' whose somata lie anteriorly in the brain. In taxa with a protocerebral bridge, columnar neurites may connect the bridge with the central body ('PB-CB-tracts'). In both Hexapoda (e.g. Kollmann, Huetteroth, and Schachtner, 2011; Boyan, Williams, and Herbert, 2008) and Malacostraca (Utting et al., 2000), the columnar neurites have been known to be arranged into four distinct bundles on each side, respectively termed the 'W, X, Y and Z tracts'. Serotonin-labeling recently revealed corresponding tracts in Remipedia (Stemme et al., 2012). The W, X, Y and Z tracts in decapod (Utting et al., 2000), various peracarid (this study) and leptostracan Malacostraca imply that the tracts are part of the ground pattern of Malacostraca (see Kenning et al., 2013). The central body of "conchostracan" Branchiopoda receives two PB-CB-tracts of columnar neurites per body side, and that of Copepoda (Andrew, Brown, and Strausfeld, 2012) and anostracan and notostracan Branchiopoda only receives one tract (Fritsch and Richter, 2010; 2012; this publication). In a conspicuous correspondence to those taxa, the SL-ir CB-like domain of Mystacocarida and Cephalocarida is also supplied by columnar neurites which project from anterior somata. In contrast, columnar neurites have never been found in Ostracoda, despite this taxon reportedly being equipped with a protocerebral bridge and central body (Hanström, 1924; 1928; Cannon, 1931; Hartmann, 1967).

14.4.1.2 Decussation of columnar neurites

After originating from anterior somata, columnar neurites may either remain ipsilateral or eventually traverse the midline in one of two ways. *Outside the midline neuropil:* Neurites from both sides of the body form a visible decussation before reaching the central body, as shown in Pterygota (Boayn, Williams, and Herbert, 2008; Boyan and Williams, 2011) and Copepoda (Andrew, Brown, and Strausfeld, 2012). The columnar neurites of Cephalocarida decussate in this way before reaching the CB-like domain. *Inside the midline neuropil:* Columnar neurites initially remain ipsilateral and only cross the midline within the central body itself. This pattern is clearly followed by the W, X, Y and Z tracts in Malacostraca (Utting et al., 2000; Kenning et al., 2013; this study) and Remipedia (Stemme et al., 2012), and by the columnar neurites in Branchiopoda (this study). Columnar neurites visibly decussate within the arcuate body of Onychophora and Chelicerata (e.g. Lösel, Nässel, and Strausfeld, 2002; Strausfeld et al., 2006a; Loesel et al., 2011), and within the central body of Chilopoda (Loesel, Nässel, and Strausfeld, 2002). Unlike in Cephalocarida, the CB-like SL-ir domains of

Table 14.1: Central complex in Mandibulata. The distinctive neuropils of the central complex (protocerebral bridge, central body, lateral accessory lobes) are here set against the co-localized immunoreactive domains with which they overlap, and against the arrangements of columnar and tangential neurites in the different taxa. As seen in Mystacocarida, Cephalocarida and Cirripedia, even taxa that lack the distinctive neuropils of a central complex may exhibit CB-like immunoreactive domains or columnar and tangential neurites. Abbreviations: absent – ; present +. CB, central body; …-D, immunoreactive domain; LAL, lateral accessory lobes; PB, protocerebral bridge; X, decussation of columnar neurites outside midline neuropil.

	Structures and patterns	distinctive neuropil			serotonin-like immunoreactive domains			histamine-like immunoreactive domains			columnar neurites	tangential neurites	Selected literature
Taxa		**PB**	**CB**	**LAL**	**PB-D**	**CB-D**	**LAL-D**	**PB-D**	**CB-D**	**LAL-D**	**decussation (X)**		
Cephalocarida		–	–	–	–	+	–	–	–	–	1 bundle (X)	–	Elofsson and Hessler, 1990; Stegner and Richter, 2011
Maxillopoda	Mystacocarida	–	–	–	–	++	–	?	?	?	1 bundle	–	Baccari and Renaud-Mornant, 1974; Elofsson and Hessler, 2005; Brenneis and Richter, 2010
	Ostracoda	(+)	(+)	–	?	?	?	?	?	?	–	–	Hanström, 1924; 1928; Cannon, 1931; Hartmann, 1967; Aramant and Elofsson, 1976
	Copepoda	+	+	(+)	–	–	–	–	–	–	1 PB-CB tract (X)	+	Lowe, 1935; Lang, 1948; Fahrenbach, 1962; Aramant and Elofsson, 1976; Hartline and Christie, 2010; Andrew, Brown, and Strausfeld, 2012
	Cirripedia	–	–	–	–	+	–	?	?	?	–	+	Bullock and Horridge, 1965; Callaway and Stuart, 1999; Harrison and Sandeman, 1999; Semmler et al., 2008
	Branchiura	–	–	–	?	?	?	?	?	?	?	?	Leydig, 1889; Martin, 1932; Zaćwilichowski, 1935; Zaćwilichowska, 1948; Overstreet et al., 1992

Branchiopoda	Anostraca	+	+	+	+	+	+	+	+	+	1 PB-CB tract	+	Hanström, 1924; Benesch, 1969; Harzsch and Glötzner, 2002; this study
	Notostraca	+	+	–	–	+	–	+	+	–	1 PB-CB tract	–	Hanström, 1924; Loesel, 2004; Fritsch and Richter, 2010; Strausfeld, 2012
	"Conchostraca"	+	+	–	–	+	–	+	+	–	2 PB-CB tracts	–	Hanström, 1934; this study
	Cladocera	+	+	(+)	?	?	?	?	?	?	?	?	Hanström, 1931; 1934; Bullock and Horridge, 1965; Aramont and Elofsson, 1976; Kirsch and Richter, 2007; Strauß et al. 2011; Weiss et al., 2012; this study
Malacostraca	Leptostraca	+	+	+	+	+	+	?	?	?	W, X, Y, Z tracts	+	Hanström 1928; Kenning et al. 2013
	Stomatopoda	+	+	+	?	?	?	?	?	?	?	?	Hanström, 1928; 1947; Sandeman and Scholtz, 1995; Strausfeld, 2012
	Caridoidea	+	+	+	+	+	+	+	+	+	W, X, Y, Z tracts	+	Hanström, 1928; 1934; Utting et al., 2000; Krieger et al., 2010; 2012; this study
Remipedia		+	+	+	+	+	+	?	?	?	W, X, Y, Z tracts	+	Fanenbruck, Harzsch, and Wägele, 2004; Fanenbruck and Harzsch, 2005; Stemme et al., 2012
Hexapoda		+	+	+	+	+	+	–	+	?	W, X, Y, Z tracts (X)	+	Williams, 1975; Strausfeld, 1976; Homberg, 2002; Boyan, Williams, and Herbert, 2008; Kollmann et al., 2011; Strausfeld, 2012
Chilopoda		?	+	?	?	?	?	?	?	?	several neurites	+	Loesel, Nässel, and Strausfeld, 2002; Loesel, 2004; Sombke, Harzsch, and Hansson, 2011

Mystacocarida receive non-decussating SL-ir 'columnar neurites' which may cross the midline within the domain (Brenneis and Richter, 2010).

14.4.1.3 Tangential neurons

Additionally to the columnar neurites, lateral somata may also send out 'tangential neurites' (Strausfeld et al., 2006a). Columnar and tangential neurites have been shown to form a more or less rectangular network in the arcuate body of onychophorans (e.g. Strausfeld et al., 2006) and chelicerates (Loesel et al., 2011). Although the neurite arrangement in the tetraconate central body was initially suggested to be fundamentally similar between all subtaxa (Strausfeld et al., 2006a), it appears to be less geometrical than in other arthropods (see, e.g., Harzsch and Hanson, 2008; Krieger et al., 2010; Strausfeld, 2012; and this study). Our study revealed that tangential neurites supply the central body in various peracarid Malacostraca but only some Branchiopoda (Harzsch and Glötzner, 2002; this study). The SL-ir domains in Cephalocarida and Mystacocarida do not receive SL-ir tangential neurites laterally, and in fact it is questionable whether tangential neurites exist at all in these two taxa since the lateral side of the protocerebrum is soma-free in both cases.

14.4.1.4 Innervation of SL-ir domains

In what is a conspicuous correspondence, unpaired SL-ir immunoreactive domains are found in Mystacocarida, Cephalocarida (e.g., this study) and Cirripedia (Semmler et al., 2008), but also in association with the unpaired neuropils in Hexapoda (Homberg, 2002), Malacostraca (Utting et al., 2000; Harzsch and Hansson, 2008), Branchiopoda (Harzsch and Glötzner, 2002; Fritsch and Richter, 2010; this study) and Remipedia (Stemme et al., 2012). Are there further correspondences in these domains with regard to their innervation by SL-ir neurons? In the three taxa mentioned which do not have a central complex, SL-ir neurites originate from different assemblages of somata, anteriorly in the protocerebrum of Mystacocarida and Cephalocarida and laterally in the protocerebrum of Cirripedia (Semmler et al., 2008). Both patterns are found in other Tetraconata (in taxa where the brain bends upwards, we translate the position of somata to an imagined "straight neuraxis"). *Innervation by anterior somata (columnar neurons):* The anterior SL-ir somata of Anostraca (Harzsch and Glötzner, 2002) and Malacostraca (Utting et al., 2000: their Fig. 9A; Harzsch and Hansson, 2008) only innervate the protocerebral bridge, with the result that the PB-CB tracts in these taxa are not SL-ir. The anterior SL-ir somata (labeled sA1) in Remipedia only connect indirectly to the central body (Stemme et al., 2012: sd2). (Remember that the W, X, Y and Z tracts in Remipedia are SL-ir but do not originate from anterior somata.) Only in Hexapoda do anterior SL-ir somata innervate not only the protocerebral bridge but also the fan-shaped body (Homberg and Hildebrand, 1991: somata S1, S2, S4, S5). This pattern is reminiscent of that of the CB-like domain found in Mystaco-

carida and Cephalocarida. *Innervation by lateral somata (tangential neurons):* Lateral SL-ir somata innervate the central body and lateral accessory lobes in Malacostraca (Utting et al., 2000) and Anostraca (Harzsch and Glötzner, 2002). In Hexapoda, lateral SL-ir somata (Homberg and Hildebrand, 1991: S3) innervate the fan-shaped body of the central body only. This lateral innervation pattern is reminiscent of that of the SL-ir domain in Cirripedia (Semmler et al., 2008). In contrast, lateral SL-ir somata in Remipedia only innervate the lateral accessory lobes (Stemme et al., 2012).

14.4.1.5 Horizontal layers of the central body

The clear differentiation of the central body into an 'ellipsoid body' and a 'fan-shaped body' is unique to Hexapoda (Williams, 1975; Strausfeld, 1976). Interestingly, however, both the hexapod ellipsoid body (Müller, Homberg, and Kühn, 1997; Loesel and Homberg, 1999; Homberg, 2002) and the malacostracan central body (Strausfeld, 2009; Krieger et al., 2012) display "horizontal layers" which are innervated by neurites from well-separated groups of somata that may differ in their immunoreactivity. Layers of varying immunoreactivity were not found in the central body of notostracan Branchiopoda (Fritsch and Richter, 2010). Nothing indicates that the CB-like SL-ir domains in Mystacocarida and Cephalocarida constitute layers of a larger neuropil. Domains of other immunoreactivity (RFLI, HLI) were not found to correlate to any putative central complex neuropil (Brenneis and Richter, 2010; Stegner and Richter, 2011).

14.4.1.6 Conclusion of structural comparison

Since we have seen that both the protocerebral bridge and the central body may be innervated by columnar neurons (anterior SL-ir somata) in other Tetraconata, a comparison of innervation patterns alone delivers no clear indication of how to classify the SL-ir domains in Mystacocarida and Cephalocarida. However, given their elongated overall appearance, their central position and their innervation by columnar neurites, we suggest that the SL-ir domains in Mystacocarida and Cephalocarida correspond to the SL-ir domain of the central body in other tetraconates, rather than to that of the protocerebral bridge.

14.4.2 'Neurophylogeny' of Tetraconata

What do the distribution of central complex neuropils in general and their internal anatomy in detail contribute to the phylogenetic debate? The 'Invertebrate Neurophylogeny' section of the Deep Metazoan Phylogeny program is currently developing a comprehensive morphology-based phylogenetic matrix into which neuroanatomical data including our own on the central complex and many other structures and patterns will be integrated. Since this work is still in progress, our data on the central

complex of Crustacea is discussed here on the basis of some of the phylogenetic hypotheses currently suggested in the literature. Our aim is to determine which of the evolutionary scenarios proposed is the most plausible (requiring the lowest number of transformational steps from one morphological pattern to the other).

Within Mandibulata, an overwhelming number of molecular studies and a growing number of morphological studies point towards a sister-group relationship between Myriapoda and Tetraconata, the latter of which comprise by definition all hexapods and crustaceans. The relationships between crustaceans have been the subject of numerous morphology- and molecular-based studies and under controversial phylogenetic debate for decades. This debate continues for Tetraconata (reviewed by Richter, Møller, and Wirkner, 2009; Jenner, 2010). While the monophyly of Hexapoda, Branchiopoda, Malacostraca, Cephalocarida, Remipedia and the maxillopod subtaxa is widely accepted, their interrelationships remain unclear.

While earlier hypotheses based on external morphology assigned Cephalocarida (Sanders, 1957), Remipedia (Schram et al., 1986) and Malacostraca (Walossek, 1993, without Remipedia) to the base of Crustacea, neuroanatomical data suggest alternative hypotheses. Correspondences in the optic neuropils (Strausfeld, 2005) support a close relationship between Hexapoda and Malacostraca, while some correspondences in the olfactory system (hemiellipsoid bodies, chiasma of olfactory globular tracts) and larval features (Koenemann et al., 2007; 2009) support a sister-group relationship between Remipedia and Malacostraca (Fanenbruck and Harzsch, 2005). Higher-level correspondences in the olfactory systems (olfactory lobes, olfactory globular tracts, second-order olfactory centers) of Cephalocarida, Remipedia, Hexapoda and Malacostraca were initially interpreted as synapomorphies (Fanenbruck, Harzsch, and Wägele, 2004; Fanenbruck and Harzsch, 2005; Harzsch, 2006). Today, however, in the light of a number of recent investigations into Cephalocarida (Stegner and Richter, 2011), Myriapoda (Sombke, Harzsch, and Hansson, 2011; Sombke, Rosenberg, and Hilken, 2011; Sombke et al., 2012), Hexapoda (Strausfeld, 2009; Loesel and Heuer, 2010) and Malacostraca (Wolff et al., 2012), they must be considered symplesiomorphies dating back to the mandibulate ground pattern. Our reinvestigation of the cephalocarid nervous system found neither brain (Stegner and Richter, 2011) nor ventral nerve cord features (Stegner, Brenneis, and Richter, in press) supportive of a close relationship, i.e. synapomorphies, between Cephalocarida and Hexapoda, Malacostraca or Remipedia (but see Stemme et al., 2013). Unlike the cephalocarid nervous system with its plesiomorphic complexity, the mystacocarid nervous system is considerably reduced (Brenneis and Richter, 2010), rendering potential synapomorphies with other tetraconate taxa elusive. The hypothesis that Mystacocarida and Cephalocarida occupy a "basal" position within Tetraconata is not contradicted by neuroanatomical data. A recent phylogenetic analysis considering neuroanatomical (Strausfeld and Andrew, 2011) and EST data (Andrew, 2011) did not include Mystacocarida and Cephalocarida.

Where do molecular hypotheses place the tetraconates lacking a central complex? Giribet et al. (2005: their Fig. 5), combining molecular with morphological data, suggested that Branchiura form the sister-group to all other tetraconates. Within the latter, taxa with a reportedly well-developed central complex (Malacostraca, Hexapoda, Remipedia, Branchiopoda, Copepoda) are not closely related. Regier et al. (2010: their Fig. 1) suggested that Tetraconata consist of two sister-groups, one termed 'Oligostraca', the other 'Altocrustacea'. Conspicuously, Oligostraca are mainly comprised of crustacean taxa which have been found to lack a distinct central complex – Mystacocarida, Branchiura and Pentastomida, which together form the monophyletic unit 'Ichthyostraca' – and Ostracoda, which do exhibit a protocerebral bridge and central body. The Ichthyostraca hypothesis was also supported by Koenemann et al. (2010). Altocrustacea (Regier et al., 2010) comprise all other tetraconates, including the groups mentioned which have a well-developed central complex and the remaining groups which do not possess distinctive neuropils, namely Cephalocarida and Cirripedia. Although the monophylum 'Xenocarida' composed of Cephalocarida and Remipedia found support in various studies (Regier et al., 2010; Spears and Abele, 1998; Giribet, Edgecombe, and Wheeler, 2001; Koenemann et al., 2010), it may be an artifact. Koenemann et al. (2010), for example, mentioned possible long-branch attraction between Remipedia and Cephalocarida, and von Reumont et al. (2012) demonstrated that the support for Xenocarida has, in fact, often been weak. According to a recent phylogenomic analysis (von Reumont et al., 2012), Ostracoda occupy a basal position within Tetraconata. Within the remaining tetraconates, Remipedia, Hexapoda and Branchiopoda together form one monophylum, and the remaining crustaceans form another (von Reumont et al., 2012). These authors did not include Cephalocarida.

On the basis of all the phylogenetic analyses mentioned, at least the protocerebral bridge and central body, potentially also the lateral accessory lobes, can be traced back to the tetraconate ground pattern, thus in line with Harzsch's (2006) hypothesis that the central complex is an autapomorphy of Tetraconata. As a consequence, in every evolutionary scenario that is strictly based on the mentioned current analyses (Giribet et al., 2005; Regier et al., 2010; Koenemann et al., 2010; von Reumont et al., 2012), the lack of all central complex neuropils in Cephalocarida, Mystacocarida, Cirripedia and Branchiura, and the lack of lateral accessory lobes in some phyllopod Branchiopoda, can only be explained if we accept that the respective neuropils underwent an independent reduction. The columnar neurons and CB-like SL-ir domains in the mystacocarid and cephalocarid brain may be rudiments of the columnar neurons and central body found in other tetraconates.

While our knowledge on the different tetraconate taxa is successively improving, data on their outgroup Myriapoda has remained sparse. The contemporary assumption of a single central neuropil in the myriapod ground pattern (Loesel, 2004; Harzsch, 2006; Homberg, 2008) is in fact based on representatives of only one genus (Loesel, Nässel, and Strausfeld, 2002: *Scolopendra*, but see Holmgren, 1916; Hanström, 1928;

Joly and Descamps, 1987). Sombke, Harzsch, and Hansson (2011: Fig. 2C) labeled a protocerebral bridge in the myriapod *Scutigera coleoptrata*, but did not comment on this interesting finding, because they focused on the deutocerebrum. A thorough re-investigation of the protocerebrum in different myriapod taxa is of great interest to reconstruct the ground pattern of Myriapoda and finally Mandibulata. The debate on the origin of the central complex will go on.

Acknowledgments

We thank Marlen Becker, Georg Brenneis, Clemens Döring, Maria Dreiling, Thomas Frase, Christian Wirkner and Christin Wittfoth for original images and valuable information on the brain in different crustaceans. We are grateful to Matthes Kenning for his expertise in leptostracan brain anatomy. We thank Steffen Harzsch, Rudi Loesel, Andy Sombke, and two anonymous reviewers for critical reading of our manuscript and constructive comments, and Lucy Cathrow for improving the English. Finally, we thank the Deutsche Forschungsgemeinschaft (DFG) for funding (RI 837/9-1,2 and RI 837/10-1,2). This project is part of the DFG priority program "Deep Metazoan Phylogeny" (SPP 1174).

References of chapter 14 – The central complex in Crustacea

Andrew, D.R. (2011). A new view of insect-crustacean relationships II. Inferences from expressed sequence tags and comparisons with neural cladistics. Arthr. Struct. Dev. 40, 289–302.

Andrew, D.R., Brown, S.M., and Strausfeld, N.J. (2012). The minute brain of the copepod *Tigriopus californicus* supports a complex ancestral ground pattern of the tetraconate cerebral nervous systems. J. Comp. Neurol. 520, 3446–70.

Aramant, R. and Elofsson, R. (1976). Distribution of monoaminergic neurons in the nervous system of non-malacostracan crustaceans. Cell Tiss. Res. 166, 1–24.

Baccari, S. and Renaud-Mornant, J. (1974). Etude du système nerveux de *Derocheilocaris remanei* Delamare et Chappuis 1951 (Crustacea, Mystacocarida). Cah. Biol. Mar. 15, 589–604.

Barthélémy, R.M., Jule, Y., Da Prato, J.-L., and Liberge, M. (2006). Expression of serotonin and enkephalins in calanoid copepods (Crustacea): An immunohistochemical study. J. Plankt. Res. 28, 1047–1053.

Bender, J.A., Pollack, A.J., and Ritzmann, R.E. (2010). Neural activity in the central complex of the insect brain is linked to locomotor changes. Curr. Biol. 20, 921–926.

Benesch, R. (1969). Zur Ontogenie und Morphologie von *Artemia salina* L. Zoologische Jahrbücher der Abteilung für Anatomie und Ontogenie der Tiere 86, 307–458.

Benzid, D., Morris, C., and Barthélémy, R.M. (2005). First detection of serotonin in the nervous system of the marine calanoid copepod *Centropages typicus*. J. Mar. Biol. Assoc. United Kingdom 85, 71–72.

Boyan, G.S. and Williams, J.L.D. (2011). Embryonic development of the insect central complex: Insights from lineages in the grasshopper and *Drosophila*. Arthr. Struct. Dev. 40, 334–48.

Boyan, G.S., Williams, J.L.D., and Herbert, Z. (2008). Fascicle switching generates a chiasmal neuroarchitecture in the embryonic central body of the grasshopper *Schistocerca gregaria*. Arthr. Struct. Dev. 37, 539–44.

Brenneis, G. and Richter, S. (2010). Architecture of the nervous system in Mystacocarida (Arthropoda, Crustacea): An immunohistochemical study and 3D reconstruction. J. Morph. 271, 169–89.

Bullock, T.H. and Horridge, G.A. (1965). Structure and function in the nervous system of invertebrates. (San Francisco, London: Freeman and Company).

Callaway, J.C. and Stuart, A.E. (1999). The distribution of histamine and serotonin in the barnacle's nervous system. Microsc. Res. Tech. 44, 94–104.

Cannon, H.G. (1931). On the anatomy of a marine ostracod, *Cypridina* (*Doloria*) *levis* Skogsberg, Discovery Reports, 2nd edition (London: Cambridge University Press), pp. 435–82.

Claus, C. (1876). Zur Kenntnis der Organisation und des feineren Baues der Daphniden und verwandter Cladoceren. Zeitschrift für wissenschaftliche Zoologie 17.

Elofsson, R. and Hessler, R.R. (2005). The tegumental sensory organ and nervous system of *Derocheilocaris typica* (Crustacea: Mystacocarida). Arthr. Struct. Dev. 34, 139–152.

Elofsson, R. and Hessler, R.R. (1990). Central nervous system of *Hutchinsoniella macracantha* (Cephalocarida). J. Crust. Biol. 10, 423–439.

Fanenbruck, M. and Harzsch, S. (2005). A brain atlas of *Godzilliognomus frondosus* Yager, 1989 (Remipedia, Godzilliidae) and comparison with the brain of *Speleonectes tulumensis* Yager, 1987 (Remipedia, Speleonectidae): Implications for arthropod relationships. Arthr. Struct. Dev. 34, 343–78.

Fanenbruck, M., Harzsch, S., and Wägele, J.W. (2004). The brain of the Remipedia (Crustacea) and an alternative hypothesis on their phylogenetic relationships. Proc. Nat. Acad. Sci. USA 101, 3868–3873.

Fritsch, M. and Richter, S. (2010). The formation of the nervous system during larval development in *Triops cancriformis* (Bosc) (Crustacea, Branchiopoda): An immunohistochemical survey. J. Morph. 271, 1457–81.

Fritsch, M. and Richter, S. (2012). Nervous system development in Spinicaudata and Cyclestherida (Crustacea, Branchiopoda)—Comparing two different modes of indirect development by using an event pairing approach. J. Morph. 273, 672–695.

Giribet, G., Edgecombe, G., and Wheeler, W.C. (2001). Arthropod phylogeny based on eight molecular loci and morphology. Nature 413, 157–161.

Giribet, G., Richter, S., Edgecombe, G.D., and Wheeler, W.C. (2005). The position of crustaceans within Arthropoda: Evidence from nine molecular loci and morphology. In: Crustacea and Arthropod Relationships, S. Koenemann, R.A. Jenner, eds. (Boca Raton, London, New York, Singapore: Tailor Francis Group).

Glenner, H. (2001). Cypris metamorphosis, injection and earliest internal development of the rhizocephalan *Loxothylacus panopaei* (Gissler). Crustacea: Cirripedia: Rhizocephala: Sacculinidae. J. Morph. 249, 43–75.

Gwilliam, G.F. and Cole, E.S. (1979). The morphology of the central nervous system of the barnacle, *Semibalanus cariosus* (Pallas). J. Morph. 159, 297–310.

Hanström, B. (1924). Untersuchungen über das Gehirn, insbesondere die Sehganglien der Crustaceen. Arkiv för Zoologi Stockholm 16, 1–119.

Hanström, B. (1928). Crustacea. Vergleichende Anatomie des Nervensystems der Wirbellosen Tiere (Berlin: Springer), pp. 430–497.

Hanström, B. (1931). Neue Untersuchungen der Sinnesorgane und Nervenzentren der Crustaceen. I. Zoologische Jahrbücher, Abteilung Anatomie und Ontogonie der Tiere 23, 81–236.

Hanström, B. (1934). Neue Untersuchungen der Sinnesorgane und Nervenzentren der Crustaceen. III. Zoologische Jahrbücher, Abteilung Anatomie und Ontogenie der Tiere 58, 101–144.

Hanström, B. (1940). Inkretorische Organe, Sinnesorgane und Nervensystem des Kopfes einiger niederer Insektenordnungen, Vol. 8, (Almqvist & Wiksells Boktryckeri).

Hanström, B. (1947). The brain, the sense organs, and the incretory organs of the head in the Crustacea Malacostraca. Lunds Universitets Årsskrift 43, 1–49

Harley, C.M. and Ritzmann, R.E. (2010). Electrolytic lesions within central complex neuropils of the cockroach brain affect negotiation of barriers. J. Exp. Biol. 231, 2851–2864.

Harrison, P.J.H. and Sandeman, D.C. (1999). Morphology of the nervous system of the barnacle larva (*Balanus amphritre* Darwin) revealed by light and electron microscopy. Biol. Bull. 197, 144–58.

Hartline, D.K. and Christie, A.E., (2010). Immunohistochemical mapping of histamine, dopamine, and serotonin in the central nervous system of the copepod *Calanus finmarchicus* (Crustacea; Maxillopoda; Copepoda). Cell Tiss. Res. 341, 49–71.

Hartmann, G. (1967). Klassen und Ordnungen des Tierreichs. In: Arthropoda, I. Abteilung: Crustacea, 2. Buch, IV. Teil, 2 Ostracoda, H.E. Gruner, ed. (Leipzig: Akademische Verlagsgesellschaft Geest & Portig K.-G.), pp. 217–408.

Harzsch, S. (2002). Neurobiologie und Evolutionsforschung: „Neurophylogenie“ und die Stammesgeschichte der Euarthropoda. Neuroforum 4, 267–273.

Harzsch, S. (2003). Evolution of identified arthropod neurons: The serotonergic system in relation to *engrailed*-expressing cells in the embryonic ventral nerve cord of the American lobster *Homarus americanus* Milne Edwards, 1873 (Malacostraca, Pleocyemata, Homarida). Dev. Biol. 258, 44–56.

Harzsch, S. (2004). Phylogenetic comparison of serotonin-immunoreactive neurons in representatives of the Chilopoda, Diplopoda, and Chelicerata: Implications for arthropod relationships. J. Morph. 259, 198–213.

Harzsch, S. (2006). Neurophylogeny: Architecture of the nervous system and a fresh view on arthropod phylogeny. Integr. Comp. Biol. 46, 162–194.

Harzsch, S. (2007). The architecture of the nervous system provides important characters for phylogenetic reconstructions: Examples from the Arthropoda. Spec. Phyl. Evol. 1, 33–57.

Harzsch, S. and Glötzner, J. (2002). An immunohistochemical study of structure and development of the nervous system in the brine shrimp *Artemia salina* Linnaeus, 1758 (Branchiopoda, Anostraca) with remarks on the evolution of the arthropod brain. Arthr. Struct. Dev. 30, 251–70.

Harzsch, S. and Hansson, B.S. (2008). Brain architecture in the terrestrial hermit crab *Coenobita clypeatus* (Anomura, Coenobitidae), a crustacean with a good aerial sense of smell. BMC Neurosci. 9, 58.

Harzsch, S., Müller, C.H.G., and Wolf, H. (2005). From variable to constant cell numbers: Cellular characteristics of the arthropod nervous system argue against a sister-group relationship of Chelicerata and "Myriapoda" but favour the Mandibulata concept. Dev. Gen. Evol. 215, 53–68.

Harzsch, S. and Waloszek, D. (2000). Serotonin-immunoreactive neurons in the ventral nerve cord of Crustacea: A character to study aspects of arthropod phylogeny. Arthr. Struct. Dev. 29, 307–322.

Holmgren, N. (1916). Zur Vergleichenden Anatomie des Gehirns. Kungl. Svenska Vetenskapsakademiens Handlingar 56, 1–303.

Homberg, U. (2002). Neurotransmitters and neuropeptides in the brain of the locust. Microsc. Res. Tech. 56, 189–209.

Homberg, U. (2008). Evolution of the central complex in the arthropod brain with respect to visual system. Arthr. Struct. Dev. 37, 347–362.

Homberg, U. and Hildebrand, J.G. (1991). Histamine-immunoreactive neurones in the midbrain and subesophageal ganglion of the sphinx moth *Manduca sexta*. J. Comp. Neurol. 307, 647–657.

Jenner, R.A. (2010). Higher-level crustacean phylogeny: Consensus and conflicting hypotheses. Arthr. Struct. Dev. 39(2–3), 143–53.

Joly, R. and Descamps, M. (1987). Histology and ultrastructure of the myriapod brain. In: Arthropod brain: Its evolution, development, structure and functions, A. Gupta, ed. (New York, Chirchester, Brisbane, Toronto, Singapore: John Wiley & Son), pp. 135–157.

Kenning, M., Müller, C., Wirkner, C.S., and Harzsch, S. (2013). The Malacostraca from a neurophylogenetic perspective: New insights from brain architecture in *Nebalia herbstii* Leach, 1814 (Leptostraca, Phyllocarida). Zoologischer Anzeiger 252, 319–336.

Kirsch, R. and Richter, S. (2007). The nervous system of *Leptodora kindtii* (Branchiopoda, Cladocera) surveyed with confocal scanning microscopy (cLSM), including general remarks on the branchiopod neuromorphological ground pattern. Arthr. Struct. Dev. 36, 143–56.

Koenemann, S., Schram, F.R., Bloechl, A., Iliffe, T., Hoenemann, M., and Held, C. (2007). Post-embryonic development of remipede crustaceans. Evol. Dev. 9(2), 117–121.

Koenemann, S., Jenner, R.A., Hoenemann, M., Stemme, T., and von Reumont, B.M. (2010). Arthropod phylogeny revisited, with a focus on crustacean relationships. Arthr. Struct. Dev. 39, 88–110.

Koenemann, S., Olesen, J., Alwes, F., Iliffe, T.M., Hoenemann, M., Ungerer, P., Wolff, C., and Scholtz, G. (2009). The post-embryonic development of Remipedia (Crustacea): Additional results and new insights. Dev. Gen. Evol. 219, 131–145.

Kollmann, M., Huetteroth, W., and Schachtner, J. (2011). Brain organization in Collembola (springtails). Arthr. Struct. Dev. 40, 304–316.

Krieger, J., Sandeman, R.E., Sandeman, D.C., Hansson, B.S., and Harzsch, S. (2010). Brain architecture of the largest living land arthropod, the giant robber crab *Birgus latro* (Crustacea, Anomura, Coenobitidae): Evidence for a prominent central olfactory pathway? Front. Zool. 7.

Krieger, J., Sombke, A., Seefluth, F., Kenning, M., Hansson, B.S., and Harzsch, S. (2012). Comparative brain architecture of the European shore crab *Carcinus maenas* (Brachyura) and the common hermit crab *Pagurus bernhardus* (Anomura) with notes on other marine hermit crabs. Cell Tiss. Res. 348, 47–69.

Lang, K. (1948). Monographie der Harpacticiden, 2 Vol. (Stockholm: Nordiska Bokhandeln).

Fahrenbach, W.H. (1962). The biology of a harpacticoid copepod. La Cellule 62, 303–376.

Langworthy, K., Helluy, S., Benton, J., and Beltz, B. (1997). Amines and peptides in the brain of the American lobster: Immunocytochemical localization patterns and implications for brain function. Cell Tiss. Res. 288, 191–206.

Leder, H. (1915). Untersuchungen über den feineren Bau des Nervensystems der Cladoceren. Arbeiten aus den Zoologischen Instituten der Universitaet Wien. 297–392.

Leydig, F. (1889). Ueber *Argulus foliaceus*. Archiv für mikroskopische Anatomie 23, 1–51.

Liu, G., Seiler, H., Wen, A., Zars, T., Ito, K., and Wolf, R. (2006). Distinct memory traces for two visual features in the *Drosophila* brain. Nature 439, 551–556.

Loesel, R. (2004). Comparative morphology of central neuropils in the brain of arthropods and its evolutionary and functional implications. Acta Biol. Hungar. 55, 39–51.

Loesel, R. and Heuer ,C.M. (2010). The mushroom bodies: Prominent brain centres of arthropods and annelids with enigmatic evolutionary origin. Acta Zool. 91, 29–34.

Loesel, R. and Homberg, U. (1999). Histamine-immunoreactive neurons in the brain of the cockroach *Leucaphaea maderae*. Brain Res. 842, 408–418.

Loesel, R., Nässel, D.R., and Strausfeld, N.J. (2002). Common design in a unique midline neuropil in the brains of arthropods. Arthr. Struct. Dev. 31, 77–91.

Loesel, R., Seyfarth, E.-A., Bräunig, and Agricola, R. (2011). Neuroarchitecture of the arcuate body in the brain of the spider *Cupiennius salei* (Araneae, Chelicerata) revealed by allatostatin-, proctolin-, and CCAP-immunocytochemistry and its evolutionary implications. Arthr. Struct. Dev. 40, 210–220.

Lowe, E. 1935. On the anatomy of a marine copepod, *Calanus finmarchicus* (Gunnerus). Trans. Roy. Soc. Edinburgh 58, 561–603.

Martin, M.F. (1932). On the morphology and classification of *Argulus* (Crustacea). Proc. Zool. Soc. London 103, 771–806.

Müller, M., Homberg, U., and Kühn, A. (1997). Neuroarchitecture of the lower division of the central body in the brain of the locust (*Schistocerca gregaria*). Cell Tiss. Res. 288, 159–176.

Oakley, T.H., Wolfe, J.M., Lindgren, A.R., and Zaharoff, A.K. (2013). Phylotranscriptomics to bring the understudied into the fold: monophyletic Ostracoda, fossil placement, and pancrustacean phylogeny. Mol. Biol. Evol. 30(1), 215–233.

Overstreet, R.M., Dyková, I., and Hawkins, W.E. (1992). Branchiura. In: Microscopic anatomy of invertebrates, Vol. 9, F.W. Harrison, A.G. Humes, eds. (New York: Wiley-Liss), pp. 385–413.

Regier, J.C., Shultz, J.W., Zwick, A., Hussey, A., Ball, B., Wetzer, R., Martin, J.W., and Cunningham, C.W. (2010). Arthropod relationships revealed by phylogenomic analysis of nuclear protein-coding sequences. Nature 463, 1079–1083.

Richter, S., Loesel, R., Purschke, G., Schmidt-Rhaesa, A., Scholtz, G., Stach, T., Vogt, L., Wanninger, A., Brenneis, G., Döring, C., Faller, S., Fritsch, M., Grobe, P., Heuer, C.M., Kaul, S., Møller, O.S., Müller, C.H.G.,

Rothe, B.H., Stegner, M.E.J., and Harzsch, S. (2010). Invertebrate neurophylogeny: Suggested terms and definitions for a neuroanatomical glossary. Front. Zool. 7, 29.

Richter, S., Møller, O.S., and Wirkner, C.S. (2009). Advances in crustacean phylogenetics. Arthr. Syst. Phyl. 67, 275–286.

Sandeman, D.C., Sandeman, R.E., and Aitken, A.R. (1988). Atlas of serotonin-containing neurons in the optic lobes and brain of the crayfish *Cherax destructor*. J. Comp. Neurol. 269, 465–478.

Sandeman, D.C., Sandeman, R.E., Derby, C., and Schmidt, M. (1992). Morphology of the brain of crayfish, crabs, and spiny lobsters: A common nomenclature for homologous structures. Biol. Bull. 183, 304–326.

Sandeman, D.C. and Scholtz, G. (1995). Ground plans, evolutionary changes and homologies in decapod crustacean brains. In: The nervous system in invertebrates: An evolutionary aspect, O. Breidbach, W. Kutsch, eds. (Basel: Birkenhäuser Verlag), pp. 329–347.

Sandeman, D.C., Scholtz, G., and Sandeman, R.E. (1993). Brain evolution in decapod Crustacea. J. Exp. Zool. 265, 112–133.

Sanders, H.L. (1957). The Cephalocarida and crustacean phylogeny. Syst. Zool. 6, 112–148.

Schram, F.R., Yager, J., and Emerson, M.J. (1986). Remipedia. Part I. Systematics. Memoirs of the San Diego Society of Natural History 15, 1–60.

Semmler, H., Wanninger, A., Høeg, J.T., and Scholtz, G. (2008). Immunocytochemical studies on the naupliar nervous system of *Balanus improvisus* (Crustacea, Cirripedia, Thecostraca). Arthr. Struct. Dev. 37, 383–395.

Sombke, A., Harzsch, S., and Hansson, B.S. (2011a). Organization of deutocerebral neuropils and olfactory behavior in the centipede *Scutigera coleoptrata* (Linnaeus, 1758) (Myriapoda: Chilopoda). Chem. Senses 36, 43–61.

Sombke, A., Rosenberg, J., and Hilken, G. (2011b). Chilopoda—nervous system. In: Treatise on Zoology. Anatomy, Taxonomy, Biology. The Myriapoda, Volume 1, A. Minelli, ed. (Leiden, Boston: Brill), pp. 217–234.

Sombke, A., Lipke, L., Kenning, M., Müller, C.H.G., Hansson, B.S., and Harzsch, S. (2012). Comparative analysis of deutocerebral neuropils in Chilopoda (Myriapoda): Implications for the evolution of the arthropod olfactory system and support for the Mandibulata concept. BMC Neurosci. 13, 1–17.

Sousa, G.L., Lenz, P.H., Hartline, D.K., and Christie, A.E. (2008). Distribution of pigment dispersing hormone- and tachykinin-related peptides in the central nervous system of the copepod crustacean *Calanus finmarchicus*. Gener. Comp. Endocrinol. 156, 454–459.

Spears, T. and Abele, L.G. (1998). Crustacean phylogeny inferred from 18S rDNA. In: Arthropods relationships, R.A. Fortey, R.H. Thomas, eds. (London: Chapman & Hall), pp. 169–187.

Stegner, M.E.J., Brenneis, G., and Richter, S. The ventral nerve cord of Cephalocarida (Crustacea)—New insights into the ground pattern of Tetraconata. J. Morph. in press.

Stegner, M.E.J. and Richter, S. (2011). Morphology of the brain in *Hutchinsoniella macracantha* (Cephalocarida, Crustacea). Arthr. Struct. Dev. 40, 221–243.

Stemme, T., Iliffe, T.M., Bicker, G., Harzsch, S., and Koenemann, S. (2012). Serotonin immunoreactive interneurons in the brain of the Remipedia: New insights into the phylogenetic affinities of an enigmatic crustacean taxon. BMC Evol. Biol. 12, 168.

Stemme, T., Iliffe, T.M., von Reumont, B.M., Koenemann, S., Harzsch, S., and Bicker, G. (2013). Serotonin-immunoreactive neurons in the ventral nerve cord of Remipedia (Crustacea"—Support for a sister group relationship of Remipedia and Hexapoda? BMC Evol. Biol. 13, 119.

Strauss, R. (2002). The central complex and the genetic dissection of locomotor behavior. Curr. Opin. Neurobiol. 6, 633–638.

Strausfeld, N.J. (2005). The evolution of crustacean and insect optic lobes and the origins of chiasmata. Arthr. Struct. Dev. 34(3), 235–256.

Strausfeld, N.J. (1976). Atlas of an Insect Brain (Berlin: Springer).

Strausfeld, N.J. (2009). Brain organization and the origin of insects: An assessment. Proc. Roy. Soc. B, Biol. Sci. 276, 1929–1937.

Strausfeld, N.J. (2012). Arthropod brains: Evolution, functional elegance, and historical significance (Cambridge MA, London: Belknap Press of Harvard University Press).

Strausfeld, N.J. and Andrew, D.R. (2011). A new view of insect crustacean relationships I. Inferences from neural cladistics and comparative neuroanatomy. Arthr. Struct. Dev. 40, 276–288.

Strausfeld, N.J. and Hirth, F. (2013). Deep homology of arthropod central complex and vertebrate basal ganglia. Science 340, 157.

Strausfeld, N.J., Strausfeld, C.M., Loesel, R., Rowell, D., and Stowe, S. (2006). Arthropod phylogeny: Onychophoren brain organization suggests an archaic relationship with a chelicerate stem lineage. Proc. Roy. Soc. B, Biol. Sci. 273, 1857–1866.

Strausfeld, N.J., Weltzen, P., and Barth, F.G. (1993). Two visual systems in one brain: Neuropils serving the principal eyes of the spider *Cupiennius salei*. J. Comp. Neurol. 328, 63–75.

Strauß, J., Zhang, Q., Verleyen, P., Huybrechts, J., Neupert, S., Predel, R., Pauwels, K., and Dircksen, H. (2011). Pigment-dispersing hormone in *Daphnia* interneurons, one type homologous to insect clock neurons displaying circadian rhythmicity. Cellul. Mol. Life Sci. 68, 3403–3423.

Triphan, T., Poeck, B., Neuser, K., and Strauss, R. (2010). Visual targeting of motor actions in climbing *Drosophila*. Curr. Biol. 20, 663–668.

Utting, M., Agricola, R., Sandeman, R.E., and Sandeman, D.C. (2000). Central complex in the brain of crayfish and its possible homology with that of insects. J. Comp. Neurol. 416, 245–261.

Vogt, L., Bartolomäus, T., and Giribet, G. (2010). The linguistic problem of morphology: structure versus homology and the standardization of morphological data. *Cladistics* 26(3), 301–325.

von Reumont, B.M., Jenner, R.A., Wills, M.A., Dell'Ampio, E., Pass, G., Ebersberger, I., Meyer, B., Koenemann, S., Iliffe, T.M., Stamatakis, A., Niehuis, O., Meusemann, K., and Misof, B. (2012). Pancrustacean phylogeny in the light of new phylogenomic data: Support for Remipedia as the possible sister group of Hexapoda. Mol. Biol. Evol. 29, 1031–1045.

Walker, G., Clare, A.S., Rittschof, D., and Mensching, D. (1992). Aspects of the life cycle of *Loxothylacus panopaei* (Gissler), a sacculinid parasite of the mud crab, *Rhithropanopeus harrisii* (Gould): A laboratory study. J. Exp. Mar. Biol. Ecol. 157, 181–193.

Walossek, D. (1993). The Upper Cambrian *Rehbachiella* and the phylogeny of Branchiopoda and Crustacea. Fossils and Strata 32, 1–202.

Webster, S.G. (1998). Peptidergic neurons in barnacles: An immunohistochemical study using antsera against crustacean neuropeptides. Biol. Bull. 195, 282–289.

Weiss, L.C., Tollrian, R., Herbert, Z., and Laforsch, C. (2012). Morphology of the *Daphnia* nervous system: A comparative study on *Daphnia pulex*, *Daphnia lumholtzi*, and *Daphnia longicephala*. J. Morph. 273(12), 1392–1305.

Williams, J.L.D. (1975). Anatomical studies of insect central nervous system: Ground plan of midbrain and an introduction to central complex in locust, *Schistocerca gregaria* (Orthoptera). J. Zool. 176, 67–86.

Wilson, C.H. and Christie, A.E. (2010). Distribution of C-type allatostatin (C-AST)-like immunoreactivity in the central nervous system of the copepod *Calanus finmarchicus*. Gener. Comp. Endocrinol. 2, 252–260.

Wirkner, C.S. and Richter, S. (2010). Evolutionary morphology of the circulatory system in Peracarida (Malacostraca; Crustacea). Cladistics 26, 143–167.

Wolff, G., Harzsch, S., Hansson, B.S., Brown, S., and Strausfeld, N.J. (2012). Neuronal organization of the hemiellipsoid body of the land hermit crab, *Coenobita clypeatus*: Correspondence with the mushroom body ground pattern. J. Comp. Neurol. 520, 2824–2846.

Zaćwilichowska, J. (1948). The nervous system of the carplouse *Argulus foliaceus* L. Bulletin International de l'Académie Polonaise des Sciences et des Lettres, Classe des Sciences Mathematiques et Naturelles, Série B: Sciences Naturelles (II) 1, 117–128.

Zaćwilichowski, J. (1935). Über die Innervation der Haftapparate der Karpfenlaus *Argulus foliaceus* L. (Branchiura). Bulletin International de l'Académie Polonaise des Sciences et des Lettres, Classe des Sciences Mathematiques et Naturelles, Série B: Sciences Naturelles (II) 2, 145–162.

12. The ventral nerve cord of Cephalocarida (Crustacea): New insights into the ground pattern of Tetraconata. Stegner MEJ, Brenneis G, Richter S (2014b). Journal of Morphology 275:269-294

JOURNAL OF MORPHOLOGY 275:269–294 (2014)

The Ventral Nerve Cord in Cephalocarida (Crustacea): New Insights into the Ground Pattern of Tetraconata

Martin E.J. Stegner,* Georg Brenneis,[#] and Stefan Richter

Universität Rostock, Institut für Biowissenschaften, Allgemeine und Spezielle Zoologie, Universitätsplatz 2, 18055 Rostock, Mecklenburg-Vorpommern, Germany

ABSTRACT Cephalocarida are Crustacea with many anatomical features that have been interpreted as plesiomorphic with respect to crustaceans or Tetraconata. While the ventral nerve cord (VNC) has been investigated in many other arthropods to address phylogenetic and evolutionary questions, the few studies that exist on the cephalocarid VNC date back 20 years, and data pertaining to neuroactive substances in particular are too sparse for comparison. We reinvestigated the VNC of adult *Hutchinsoniella macracantha* in detail, combining immunolabeling (tubulin, serotonin, RFamide, histamine) and nuclear stains with confocal laser microscopy, complemented by 3D-reconstructions based on serial semithin sections. The subesophageal ganglion in Cephalocarida comprises three segmental neuromeres (Md, Mx1, Mx2), while a separate ganglion occurs in all thoracic segments and abdominal segments 1–8. Abdominal segments 9 and 10 and the telson are free of ganglia. The maxillar neuromere and the thoracic ganglia correspond closely in their limb innervation pattern, their pattern of mostly four segmental commissures and in displaying up to six individually identified serotonin-like immunoreactive neurons per body side, which exceeds the number found in most other tetraconates. Only two commissures and two serotonin-like immunoreactive neurons per side are present in abdominal ganglia. The stomatogastric nervous system in *H. macracantha* corresponds to that in other crustaceans and includes, among other structures, a pair of lateral neurite bundles. These innervate the gut as well as various trunk muscles and are, uniquely, linked to the unpaired median neurite bundle. We propose that most features of the cephalocarid ventral nerve cord (VNC) are plesiomorphic with respect to the tetraconate ground pattern. Further, we suggest that this ground pattern includes more serotonin-like neurons than hitherto assumed, and argue that a sister-group relationship between Cephalocarida and Remipedia, as favored by recent molecular analyses, finds no neuroanatomical support. J. Morphol. 275:269–294, 2014.

KEY WORDS: entomostracan abdomen; mandible; maxillula; maxilla; Mandibulata; serotonergic neurons; stomatogastric nervous system; Xenocarida

INTRODUCTION

General Aspects

Most external anatomical features of Cephalocarida have been interpreted as being plesiomorphic with respect to the ground pattern of Crustacea, Mandibulata, or even Arthropoda (summarized by Olesen et al., 2011; for details, see, for example, Sanders, 1957, 1963; Hessler, 1964, 1992; Lauterbach, 1974, 1983, 1986; Walossek, 1993; Scholtz and Edgecombe, 2005). Our recent investigation into the cephalocarid brain showed that certain features in the cephalocarid olfactory system can also be traced back to the ur-mandibulate (Stegner and Richter, 2011). In contrast, other features suggested to belong to the tetraconate ground pattern (e.g., Harzsch, 2006) have been reduced in Cephalocarida. These include the optic lobes (Elofsson and Hessler, 1990; Stegner and Richter, 2011) and the central complex (Stegner and Richter, 2011; Stegner et al., in press). Since potential morphological synapomorphies between Cephalocarida and other tetraconates are scarce (see, e.g., Hessler, 1992; Jenner, 2010; Olesen et al., 2011), and molecular analyses reveal no definitive picture, the phylogenetic relationships between Cephalocarida and the rest of the Tetraconata remain a matter for debate (Koenemann et al., 2010; Regier et al., 2010; von Reumont et al., 2012; Oakley et al., 2013).

In the last decade, phylogenetic and evolutionary questions have started to be addressed by looking

This article was published online on 4 November 2013. An error was subsequently identified. This notice is included in the online and print versions to indicate that both have been corrected 18 November 2013.

Additional Supporting Information Figure S1 and Text S1 are found in the online version of this article.

Contract grant sponsor: German Science Foundation (DFG) (RI 837/10-1,2).

*Correspondence to: Martin E.J. Stegner; Institut für Biowissenschaften, Allgemeine und Spezielle Zoologie, Universitätsplatz 2, 18055 Rostock, Germany. E-mail: martin. stegner@uni-rostock.de; Georg Brenneis, E-mail: georg.brenneis@ gmx.de
[#]Present address: E-mail: georg.brenneis@gmx.de

Received 2 May 2013; Revised 28 August 2013; Accepted 6 September 2013.

Published online 4 November 2013 in Wiley Online Library (wileyonlinelibrary.com).
DOI 10.1002/jmor.20213

at the arthropod VNC, and in particular, its serotonin-like immunoreactive (SL-ir) pattern (e.g., Harzsch and Waloszek, 2000; Harzsch, 2004, 2007). Our current knowledge of the cephalocarid VNC dates back to three previous studies. Elofsson and Hessler (1990) studied the species *Hutchinsoniella macracantha* using light and transmission electron microscopy. Although they focussed mainly on the brain, they also provided the first description of the VNC, including the pattern of segmental ganglia, commissures, and nerve roots therein. Hessler and Elofsson (1992) presented the first lateral drawing of the complete VNC, but did not provide further anatomical details. The only study so far to apply immunohistochemical techniques documented a few SL-ir and RFamide-like immunoreactive (RFL-ir) neurons in the cephalocarid VNC (Elofsson, 1992), but lacked the necessary detail to be incorporated into later comparative analyses (e.g., Harzsch and Waloszek, 2000, see below).

Cephalocarid Abdomen

The trunk of Cephalocarida and of other entomostracan crustaceans (i.e., non-malacostracans except Remipedia, see Walossek, 1993) is divided into a limb-bearing thorax and a limbless abdomen. The evolutionary origin of the abdomen has been tackled from different angles in the past. Authors have included in their definition of an "abdomen" not only the absence of segmental limbs but also Hox gene expression patterns (e.g., Schram and Koenemann, 2004), the nervous system (e.g., Deutsch, 2001), and muscles (Huys, 1991, but see Brenneis and Richter, 2010). In the present study, we aim to investigate to what extent segmental structures and patterns of the cephalocarid VNC are tagma-specific, to compare them between different tetraconates, and to detect potential evolutionary interdependences (i.e., coherences).

Maxillar Appendage and Neuroanatomy

Another topic addressed here is the morphology and evolution of the mandibulate head (traditionally termed "cephalon" in Crustacea) and its segments (see e.g., Lauterbach, 1980; Budd, 2001; Waloszek et al., 2005; Scholtz and Edgecombe, 2005, 2006; Giribet and Edgecombe, 2012; Richter et al., 2013). Although the maxillar segment (Mx2) forms part of the cephalon in all recent mandibulates, the anatomy of maxillar appendages is morphologically disparate. The hypothesis that the maxilla specialized into a feeding appendage several times independently (e.g., Walossek and Müller, 1990) is supported by the thoracopod-like anatomy of the "maxilla" in Cephalocarida (Sanders, 1954, 1957). According to Scholtz and Edgecombe (2006, p. 409f.), the fusion of cephalic segments during mandibulate evolution, especially of cuticular tergites and pleurites, predated the specialization of limbs. We aim to investigate how the nervous system relates to this scenario, that is, to find out whether the cephalocarid maxillar neuromere shows any kind of "subesophageal" specialization or whether it is more thoracic-like.

Serotonin-Like Immunoreactivity and Phylogenetics

Harzsch and Waloszek (2000) first noted the phylogenetic relevance of segmental individually identified SL-ir neurons in the arthropod VNC. Thanks to a growing corpus of comparable data (e.g., see Harzsch, 2002, 2003, 2004; Harzsch et al., 2005), phylogenetic inferences could soon be drawn on a larger scale. Harzsch et al. (2005) suggested that the tetraconate ground pattern featured four individually identified SL-ir bipolar neurons per hemiganglion, from which they deduced the diverging (often more simple) patterns in recent hexapods and crustaceans. The evolutionary scenarios suggested by Harzsch et al. (2005) are reconsidered here in the light of new data on Remipedia (Stemme et al., 2010, 2013) and Cephalocarida (this study). The current hypothesis of a sister-group relationship between Remipedia and Cephalocarida (Koenemann et al., 2010; Regier et al., 2010) also calls for a more detailed understanding of the cephalocarid SL-ir pattern and a detailed comparison to other tetraconates and myriapods.

In order to address these phylogenetic and evolutionary problems, we reinvestigated the VNC of *H. macracantha* using present-day methods, namely a combination of fluorescent immunolabeling, confocal laser scanning microscopy and computer-aided 3D-reconstruction. As a first step in this study, we refine and add to earlier descriptions of the cephalocarid VNC (Elofsson and Hessler, 1990; Elofsson, 1992; Hessler and Elofsson, 1992) and better correlate nervous structures with the serotonin-like, RFamide-like, and histamine-like immunoreactive patterns. As a second step, our data are compared to that on other arthropods. Homology hypotheses are formulated and interpreted in a phylogenetic and evolutionary context.

MATERIAL AND METHODS

Collection, Fixation, and Storage

Adults of the cephalocarid species *Hutchinsoniella macracantha* were collected in the daytime during the summer months from 2007 to 2011 at different spots in Buzzards Bay, MA. Samples of benthic mud were collected by boat from depths of 10–25 m using a Van Veen grab or via scuba diving. The animals were separated from the sieved samples using fine forceps or pipettes.

Wildt et al. (2004) showed that the expression level of serotonin in lobsters underlies circadian rhythm, showing a peak before dusk and a trough before dawn. This phenomenon does not explain the intraspecific variability observed in the SL-ir pattern of *H. macracantha* (this study), however, as all the animals were fixed at the same time before dusk at the end of our collecting days.

Three different fixation methods were required for the procedures used in this study. 1) For semithin sectioning, one animal was fixed and stored in Bouin's fixative (Mulisch and Welsch,

2010), the salinity of which had been increased to 3% by adding NaCl. 2) For the immunolabeling of acetylated α-tubulin and serotonin-like and RFamide-like proteins, 18 animals were fixed with a 4% paraformaldehyde solution [16% PFA stem solution (Electron Microscopy Sciences, Hatfield, PA: № CAS #30525-89-4) diluted in phosphate buffered saline (PBS) solution which was produced by diluting 10 x PBS stock solution in filtered water from Buzzards Bay] for 30 min to 1 h. Fixed specimens were transferred to 100% methanol for storage at 4°C. Serotonin-like immunoreactivity was investigated in eleven animals, FMRFamide-like immunoreactivity was investigated in seven animals. 3) For the immunolabeling of histamine-like proteins, four animals were fixed in a 4% carbodiimid solution [400 mg of carbodiimid (Sigma-Aldrich, St. Louis, MO: № E1769) in 10 ml of filtered water from Buzzards Bay] for 24 h at 4°C. Afterward, specimens were postfixed with a 4% paraformaldehyde solution for 1 h and stored in PBS solution at 4°C (both solutions using filtered water from Buzzards Bay).

Pretreatment of Whole Mounts for Immunolabeling

After a series of dilutions from their storage medium into PBS, specimens were exposed to short pulses (<1 s at 35 kHz) in a bath-ultrasonicator (Elma, Singen, Germany: Elmasonic One). Between pulses, specimens were investigated with a stereomicroscope to check for any signs of external or internal damage due to the treatment. Though ultrasonication permeabilized the cuticle in PFA-fixed specimens, it destroyed carbodiimid/PFA-fixed specimens in one pulse. In some cases, specimens were cut transversely near the thorax/abdomen border with a razor blade. In some specimens, the maxilla and thoracopods were removed on one or both sides of the body using dissecting instruments such as forceps (Dumont 5) and tungsten needles. To facilitate the penetration of antibodies, thoracic (pleural) and abdominal (intersegmental) cuticle was perforated with forceps or a tungsten needle in some specimens. Pretreatment procedures were often combined.

Immunolabeling and Mounting

Irrespective of the primary antibodies/antisera applied, specimens underwent the same general immunolabeling procedure. Antibody incubation was conducted in PBT (PBS with 0.5% bovine serum albumin, 0.3% Triton X-100, 1.5% dimethylsulfoxide) containing 5% Normal Goat Serum (Calbiochem, Merck KGaA, Darmstadt, Germany: № NS02L). Labeling of the cytoskeletal protein acetylated α-tubulin was performed with a primary monoclonal mouse antibody [anti-ac-α-tub IgG 2b Isotype, clone 6-11 B-1, Sigma-Aldrich, St. Louis, MO: № T6793 (dilution 1:100)] and a Cy-3-coupled secondary goat antibody [antimouse IgG (H+L), Jackson/Dianova, Hamburg, Germany: № 115-001-003 (dilution 1:200)]. To label the neuropeptide FMRFamide and the biogenic amines serotonin and histamine, polyclonal rabbit antisera were used [Neuromics, Edina, MN: №: 20002 (dilution 1:1000); Immunostar, Hudson, WI: № 20080 (dilution 1:100); and Progen, Heidelberg, Germany: № 16043 (dilution 1:100), respectively]. An Alexa 488-coupled secondary goat antibody [antirabbit IgG (H+L), Invitrogen Molecular Probes, Darmstadt, Germany: № A11008 (dilution 1:500)] was applied for visualization. Nuclei were labeled using Hoechst (Invitrogen Molecular Probes, Darmstadt, Germany: № H33342, 1 μg/ml in PBS). Incubations were carried out overnight at 4°C, each followed by thorough washing in PBT on a horizontal shaker (neoLab, Heidelberg, Germany: DOS-20S) at 50 rpm. Stained whole mounts were mounted in Vectashield Mounting Medium (Vector Laboratories, Burlingame, CA), after placing tiny pieces of plasticine as spacers in the corners of the cover slips.

Confocal Laser Scanning Microscopy

Stained specimens were scanned using a DM IRE2 confocal laser scanning microscope (UV: 405 nm; Arg/Kr: 488 nm, HeNe: 543 nm) equipped with a TCS SP2 AOBS laser scanning unit (Leica Microsystems GmbH, Wetzlar, Germany) at step sizes of 0.4–1 μm between successive scanning planes. Alternatively, a DMI 6000 CS confocal laser scanning microscope (Arg/Kr: 488 nm, HeNe: 543 nm) equipped with a TCS SP5 II laser scanning unit (Leica Microsystems GmbH, Wetzlar, Germany) was used at the same step sizes.

Semithin Sectioning and Digitization

The specimen fixed in Bouin's fixative (see above) was dehydrated in a graded ethanol series and, after an intermediate step in epoxypropane, embedded in araldite epoxy resin under vacuum. Serial semithin sections (2160 × 1 μm) were made in the transverse plane with an RM 2165 microtome (Leica Microsystems GmbH, Wetzlar, Germany) using glass knives. Sections were stained with a mixture of 1% azure II blue and 1% methylene blue in aqueous 1% borax solution for approximately 20–35 s at 80–90°C and subsequently digitized using an AxioCam ICc 3 digital camera mounted on an Axio Scope Imager.M1 microscope (Carl Zeiss Jena GmbH, Jena, Germany). Every third section (Z-distance of 3 μm) was digitized at 20× magnification to yield an overall image of the central nervous system in relation to other organ systems. Digitized sections were aligned into a 3D-virtual stack using the software AutoAligner (Bitplane AG, Zurich, Switzerland).

Analysis and 3D-Reconstruction

The software Imaris (Bitplane AG, Zurich, Switzerland: versions 6.0.2, 6.4.0, and 7.0) was used for all analyses and 3D-reconstructions of the 3D-virtual stacks obtained through laser scanning microscopy and histological sectioning. Volumes are shown in the Imaris "maximum intensity projection" mode on all confocal laser micrographs if not stated otherwise in the legend. The "surpass view" of this program can be used to display the 3D-volume of the complete data set, while the "extended section mode" generates virtual sections of individually definable thickness, achieved by varying the number of images included. The "shadow projection" option renders scanned structures opaque and shaded, thus allowing their surface and external shape to be examined. In many cases, in particular to delineate SL-ir somata and nerves, the "contour surface" tool was used to artificially highlight specific structures or to mask structures that obscured the view of the nervous system. All figure plates were created and labeled using the software Corel Draw X3. Bitmap images were edited using the software Corel PhotoPaint X3, with the images subjected to global changes of contrast, brightness, and color only. Two sets of 3D-schematics of SL-ir neurons were designed and edited using the software Maya 2010 (Autodesk GmbH, Munich, Germany) and integrated into PDF files using the software Deep Exploration 5 (Right Hemisphere, San Ramon, CA).

Nomenclature and Presentation

We follow the neuroanatomical terminology proposed by Richter et al. (2010) wherever applicable. Crucially, the term "neurite" is used here for all neuronal processes, and the term "commissure" is used for neurite bundles that link the paired neuropils of one ganglion transversely. Morphological descriptions of nerves or neurites can require coordinates and phrases of direction such as "extend into" or "project anteriorly." Please note that no physiological or developmental inferences should be drawn from such phrases. Descriptions are preferably given from anterior to posterior and from central to peripheral, with all adjectives of position (such as "anterior" or "dorsal") refering to the body axis. If not stated otherwise, only one side of the body is described. Exceptions are mentioned explicitly. The term "pair" is used solely for bilaterally symmetrical pairs, not for ipsilateral duads.

In all figures showing the results of immunolabeling, the molecules presumed to be labeled are indicated (e.g., "tub" for

acetylated α-tubulin, "Hoe" for the DNA-marker Hoechst). Using polyclonal antisera against serotonin, FMRFamide, and histamine does not rule out the possibility of labeling related neuroactive substances, however. This holds in particular for the neuropeptide FMRFamide, which is a member of a large neuropeptide family characterized by a shared RFamide motif (see Zajac and Mollereau, 2006 for a short overview). In the light of this, we refer to serotonin-like, RFamide-like, and histamine-like immunoreactivity (SLI, RFLI, HLI) and to serotonin-like, RFamide-like, and histamine-like immunoreactive (SL-ir, RFL-ir, HL-ir) structures, respectively.

In order to describe the SL-ir pattern in the VNC in detail, most SL-ir neurons were characterized individually, taking into account the relative position of their soma within the ganglion, the course of their neurite (ipsilateral or contralateral), and the commissure or nerve to which the respective neurite contributes.

We use the term "individually identified neuron" only for those neurons whose neurites could be traced into distinct structures such as a specific commissure (these neurons are marked in different colors in Table 1, Figs. 5 and 6). SL-ir neurons for which a soma was found but whose neurites could not be traced are marked in gray (Table 1, Figs. 5 and 6). In these cases, either the neurite could not be detected at all due to weak staining, or it was found but could not be traced unambiguously because it interlaced too closely with other SL-ir neurites. Individually identified SL-ir neurons in the VNC are labeled from s14 to s20 (thorax) and from s27 to s28 (abdomen), continuing our recent numbering of neurons s1–s13 in the brain (Stegner and Richter, 2011). SL-ir neurons with unknown neurites are preliminarily numbered from s21? to s26?.

Segments are abbreviated as follows: mandibular (Md), maxillular (Mx1), maxillar (Mx2), thoracic 1–9 (Th1–Th9), abdominal 1–10 (Ab1–Ab10).

RESULTS

VNC—General Anatomy

As in most arthropods, the central nervous system of *H. macracantha* comprises the brain and the VNC. The VNC mainly consists of a number of segmental ganglia (sg, Th1–Th9, Ab1–Ab8) that are interconnected by connectives (Figs. 1A,C,D, 2A, and 4A). The VNC is confluent with the pair of post-tritocerebral connectives from the brain (br) and extends posteriorly through the nine-segmented thorax and the 10-segmented abdomen as far as the telson (not counted as a segment) with its furca (frc, Figs. 1A,B, 2A, and 4A). Throughout the VNC, the neuraxis lies parallel to the body axis (Fig. 1A).

The mandibular (Md), maxillular (Mx1), and maxillar segments (Mx2) share a continuous, segment border-crossing subesophageal ganglion (sg, Figs. 1 and 2A). In contrast, the thoracic segments (Th1–Th9, Figs. 1 and 2A) and the abdominal segments Ab1–Ab8 (Figs. 1 and 4A) are each equipped with a separate ganglion. The two posteriormost segments of the abdomen (Ab9 and Ab10) and the telson (tel, Figs. 1 and 4A) lack ganglia completely.

In each ganglion, the neuronal somata of the two body halves are fused into one continuous cortex that extends across the midline. On each side, the somata cortex envelops one segmental neuropil, forming a hemiganglion (see, e.g., Ab1, Fig. 4B). The neuropils are transversely connected to their contralateral counterpart by commissures (Fig. 3), which are likewise embedded in the midline-spanning somata cortex. Segmental neuropils of the same body side are longitudinally connected via soma-free connectives (marked as solid bars in Fig. 3A,C).

Though there are some differences (described below), all thoracic ganglia correspond to each other in their pattern of nerves, commissures, and SL-ir, RF-ir and HL-ir neurons (see, e.g., Th1 and Th2, Fig. 3C,D, Supporting Information Fig. S1C). A thoracic-like pattern is also found in the neuromeres of the subesophageal ganglion, especially in that of Mx2. In comparison, the organization of the abdominal ganglia is less complex (Fig. 4A–C,G, see below). On the basis of the correspondences between respective segments, the VNC can thus be subdivided into four regions: 1) the subesophageal ganglion (Md, Mx1, Mx2); 2) the thoracic ganglia (Th1–Th9); 3) the abdominal ganglia (Ab1–Ab8); and 4) the posterior region of the abdomen, which lacks ganglia (Ab9, Ab10, telson).

The thoracic ganglia are described before the subesophageal ganglion in the following so as to better illustrate the correspondences between thoracic and subesophageal structures and patterns.

Thoracic Ganglia

In contrast to the coherent cephalon of *H. macracantha*, all the thoracic segments are articulated separately. Each thoracic ganglion lies embedded in the bulging sternite of its segment (Supporting Information Fig. S1H).

The contiguous, midline-spanning somata cortex of each thoracic ganglion is mainly situated ventral and medial to the neuropil (Figs. 1C and 2A). The dorsal side of the neuropil, which lies directly below the gut, is only covered by a thin layer of somata and is partially soma-free (Fig. 1D).

Intersegmental nerve. The intersegmental nerve arises from a nerve root on the connective between two successive ganglia and extends in a lateral direction. Tubulin staining reveals that the nerve root is bipartite and that it lies closer to the next posterior than to the next anterior ganglion. Most of the nerve's neurites (black arrows, Fig. 3C) emerge in the medial region of the connective, from where they extend laterally to be joined by another thin bundle (gray arrows, Fig. 3C).

The intersegmental nerve splits distally into two main branches (isnv, Fig. 2C,D). The dorsal branch ascends (white arrows), passing the gut laterally, to innervate the medial region of the tergite. The lateral branch bifurcates. One of its two subbranches (yellow arrows) innervates the lateral region of the tergite. The other subbranch (blue arrows) innervates the pleurite (Fig. 2C,D), which is an articulated plate of the cuticle (see Sanders, 1957).

Thoracopod nerves. The exopodite nerve (exnv) and endopodite nerve (ennv) originate in a

TABLE 1. Serotonin-like immunoreactive (SL-ir) neurons in the subesophageal and thoracic ganglia. The rows of "individually identified neurons" comprise those SL-ir neurons whose neurites could be traced into a specific commissure or into the exopodite nerve. The rows of "other SL-ir neurons" comprise those neurons whose somata we were able to describe on the basis of position, but the course of whose neurites we were unable to follow. Where all studied specimens show the same pattern, that value is given (e.g., "1"). Where studied specimens differ from each other, the diverging patterns are separated by a dash (e.g., "1/0"). If numbers stand alone ("0," "1," or "2"), they represent a pair of SL-ir somata. Numbers with a "u" after them ("1u," "2u," "3u") represent unpaired somata which only occur on one side of the body. "1+1u" means there is one pair of somata and an additional unpaired soma, that is, three somata in total.

Individually identified neuron	Color index	Position of soma in segment	Neurite contra-/ ipsilateral	Course of neurite through	Md	Mxl	Mx2	Thl	Th2	Th3	Th4	Th5	Th6	Th7	Th8	Th9
s14	Dark blue	Antero-medial	Contra-lateral	avc	0	0	**1**	**1**	0	1u/1	0	0	0	0	0	0
s15a&b	Light blue	Postero-lateral	Contra-lateral	spc, (Md, Mxl) & spc (Mx2 to Th9)	2/1+1u/1	2	2/2/1+1u	2	2	2	2	2	2	1	0	0
s16	Red	Medial	Ipsilateral	exnv		0/1/?	1	1	1	1	1	1	1u	1	0	0
s17	Light green	Medial	Contra-lateral	adc_p (Mx2) & adc (others)	0	0	1/1/1u	1/1u	1u/1	1u/0	1/0	1u	1/0	1u/0	1/1u	0
s18	Purple	Ventral	Ipsilateral	neuropil (Th8) & ? (others)	0	0	0	0	0	1/0	1	1/0	1/0	0	0/1	0
s19	Pink	Medial	Contra-lateral	fpc	0	0	1	1	0/1	0	0	0	0	0/1	1	1
s20	Yellow	Antero-lateral	Ipsilateral	Connective	0	0	0	0	0	0	0	0	1	1	1	1
Other SL-ir neurons					Md	Mxl	Mx2	Thl	Th2	Th3	Th4	Th5	Th6	Th7	Th8	Th9
s21?	Grey	(Antero-) medial	?	?	3/3/2	1/2/?	1u/1/1	1u/1	1+1u/1	l/2u	1u/1+1u	2/2u	1+1u	1+1u/1	2/3u	1
s22?	Grey	Antero-latero-dorsal	?	?	0	0	0	1u/0	1u/0	1u/0	0	1u/0	0	0	0	0
s23?	Grey	Postero-medial	?	?	0	0	0	0	1u/0	1u/0	0	0	0	1/0	0	0
s24?	Grey	Antero-medio-ventral	?	?	0	0	0	0	0	0	0/1u	0	0	0	0	0
s25?	Grey	Dorso-lateral	?	?	1	0	0	0	0	0	0	0	0	0/1	0	0
s26?	Grey	Ventro-lateral	?	?	0	1u/0/?	0	0	1u/0	0	0	0	0	0	0	0

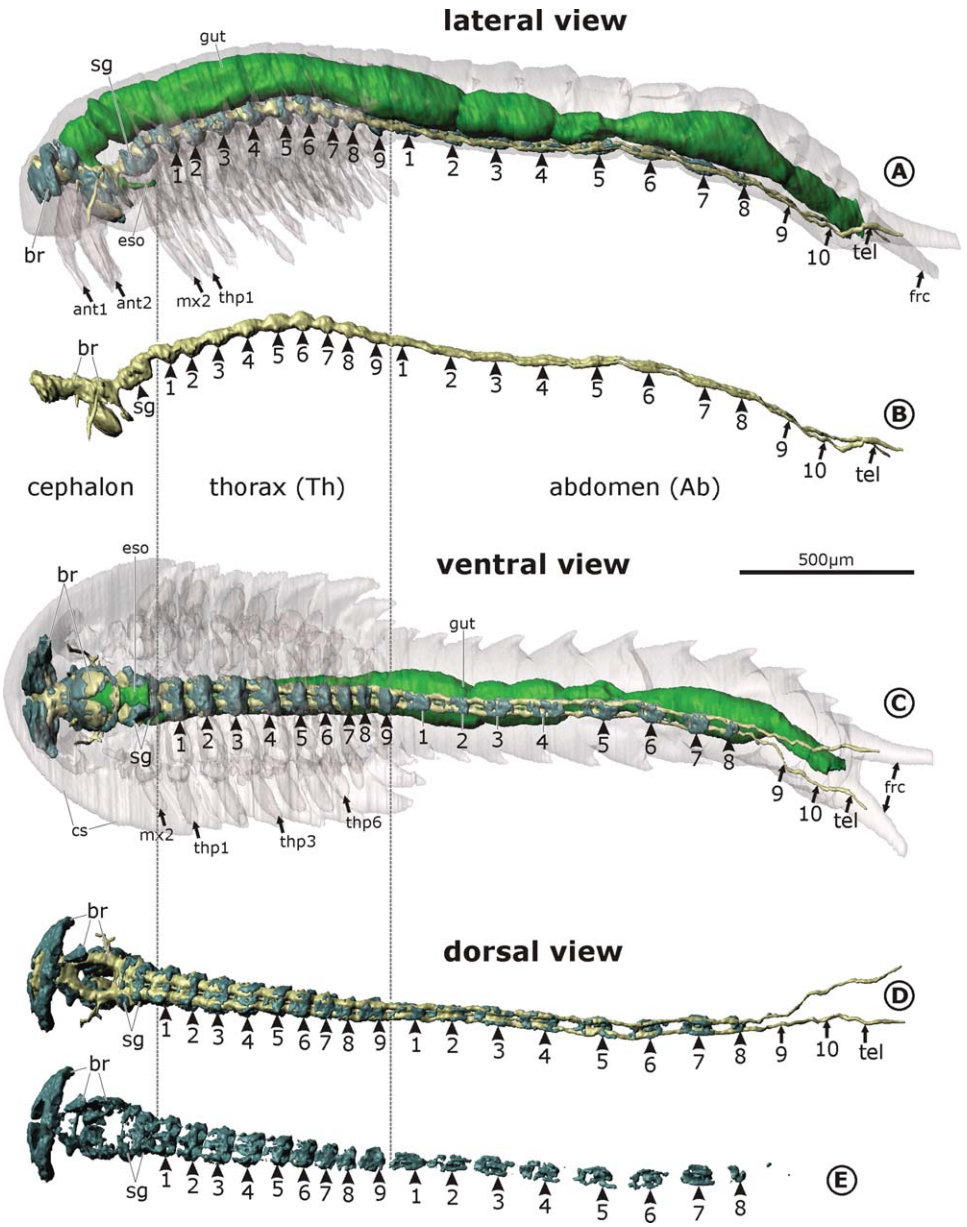

Fig. 1. *Hutchinsoniella macracantha*, overview of the VNC. 3D-reconstructions of cuticle (semitransparent), somata (light blue), neuropil and neurite bundles (yellow), and gut (green), based on serial semithin sections of a complete adult. Trunk nerves omitted. ant1: antennula, ant2: antenna, br: brain, cs: cephalic shield, eso: esophagus, frc: furca, gut: gut, mx2: maxilla, sg: subesophageal ganglion, tel: telson, thp1–6: thoracopods 1–6.

common root. The exopodite nerve forms a characteristic anterior arc before extending into the thoracopod (Fig. 3C,D). This arc bypasses a thick muscle bundle spanning the proximal portion of the protopodite.

In the distal portion of the protopodite, the exopodite nerve gives rise to the pseudepipodite nerve, which innervates the setae of the paddle-like pseudepipodite (penv, Fig. 2B). The exopodite nerve proceeds distally, innervating three single setae of the middle portion of the exopodite as well as a number of setae distributed over its paddle-like distal portion (Fig. 2B).

We assume that the thoracic (and the maxillar) endopodite consist of six podomeres (labels in our Fig. 2B based on Hessler, 1964, discussed critically by Olesen et al., 2011). Extending through the medial (i.e., gnathal) region of the protopodite, the endopodite nerve (Fig. 2B) sends off a number of medial side branches which innervate the densely grouped setae on the five gnathal endites and on the first podomere of the endopodite. In some thoracopods, these side branches branch off in endite-specific bundles; in others, they branch off in a less morphologically distinct, "bush-like" fashion.

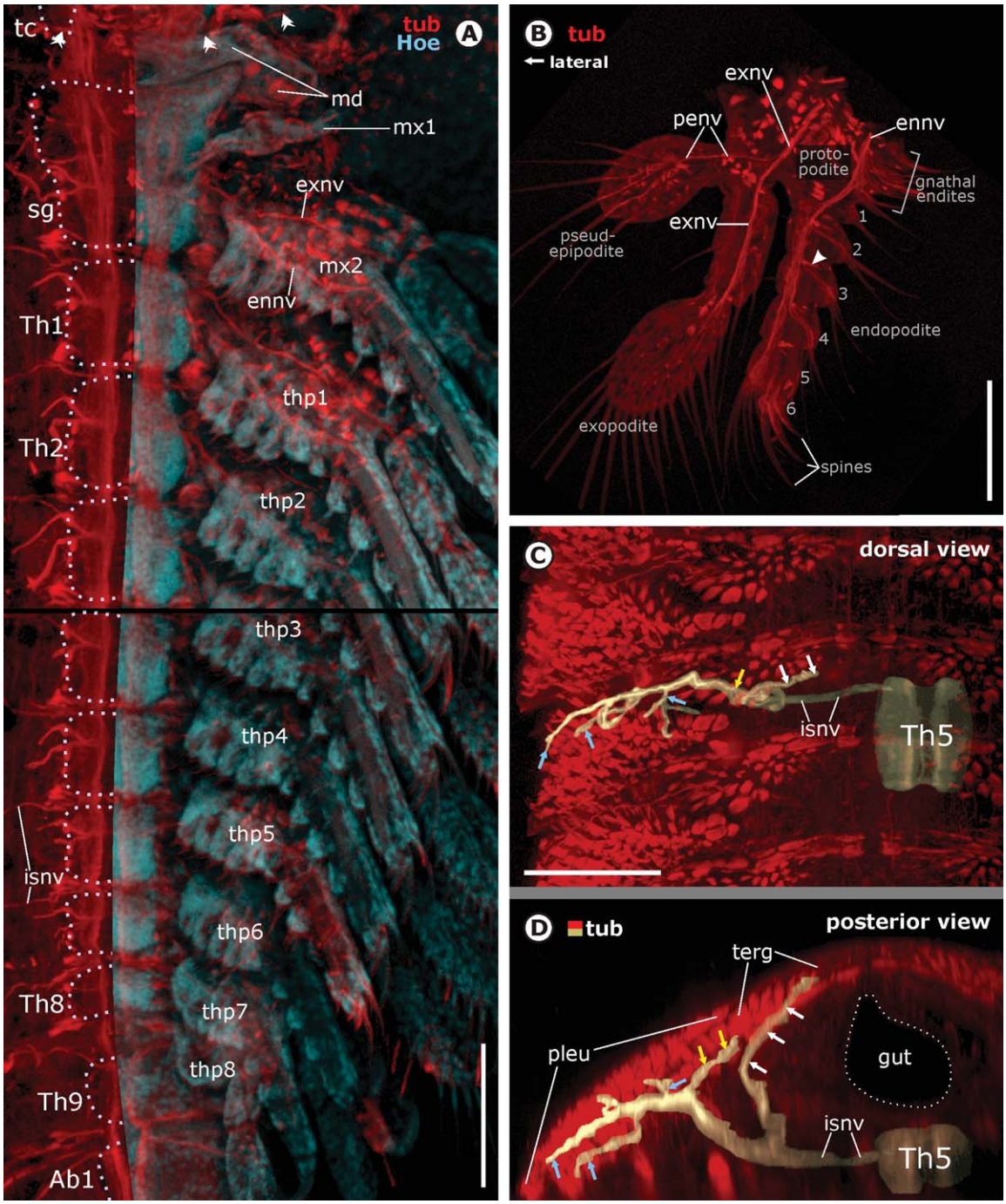

Fig. 2. *Hutchinsoniella macracantha*, VNC and major nerves in the subesophageal region and thorax. Confocal laser scans of whole mounts. (**A, B**) Imaris surpass view. (A) Thorax in ventral aspect. Dotted lines (left side of figure) and Hoechst staining (right) show somata assemblages of each ganglion. On the morphologically right body half, limbs were removed and Hoechst staining is not shown. An intersegmental nerve (double arrowheads) lies far anterior to the subesophageal ganglion. (B) Innervation of right trunk limb. Anterior aspect. Arrowhead indicates the insertion site of a podomere muscle. (**C, D**) Course of the intersegmental nerve in Th5. Imaris extended section view. Nerve and ganglion were artificially highlighted (yellow) using the Imaris contour surface tool. The dorsal branch (white arrows) innervates the tergite, while the lateral branch arborizes to innervate both the tergite (yellow arrows) and the pleurite (blue arrows). Ab1: abdominal segment 1, ennv: endopodite nerve, exnv: exopodite nerve, isnv: intersegmental nerve, md: mandible, mx1: maxillula, mx2: maxilla, penv: pseudepipodite nerve, pleu: pleurite, sg: subesophageal ganglion, tc: tritocerebrum, terg: tergite; Th1–9: thoracic segments 1–9, thp1–thp8: thoracopods 1–8. Scalebars: 100 μm.

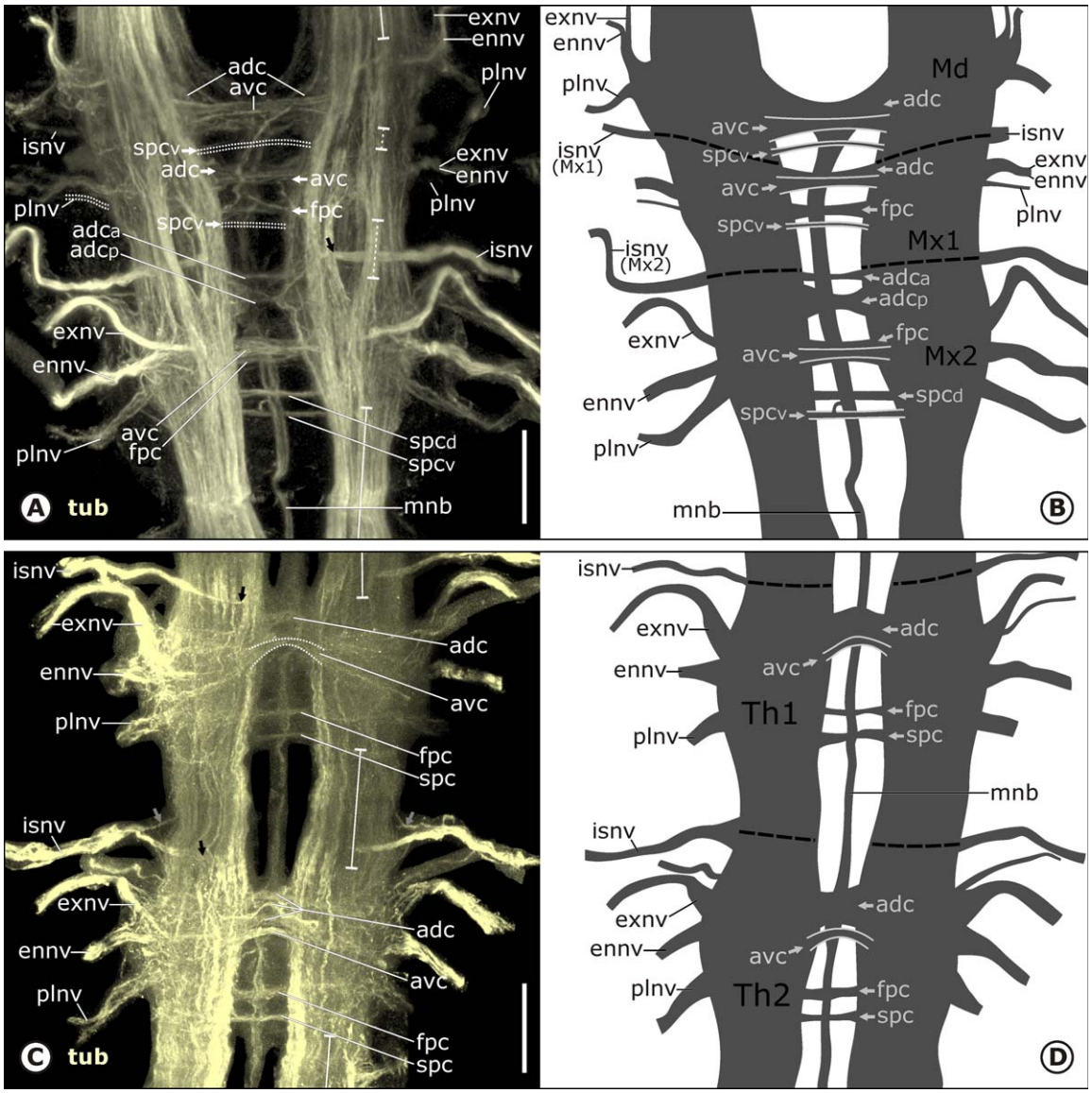

Fig. 3. *Hutchinsoniella macracantha*, subesophageal ganglion (**A, B**) and thoracic ganglia (**C, D**) of *H. macracantha*. Confocal laser scans in Imaris surpass view (A, C) and corresponding semischematic representation (B, D) in ventral aspect. (A) Within the contiguous subesophageal somata cortex (not shown), the neuropils of Md, Mx1, and Mx2 are longitudinally linked by connective-like bundles of parallel neurites (dashed white bars), which are comparable with the soma-free connectives marked by solid white bars in B. (A, B) The nerve roots and commissures of the three segmental components (Md, Mx1, Mx2) of the subesophageal ganglion correspond to a significant extent to the thoracic pattern. (A, C) Most neurites of the intersegmental nerve arise from the anteromedial region of the respective ganglion (black arrow). The nerve leaves the ganglion anterolaterally. (C) Thoracic ganglia are interlinked by soma-free connectives (continuous lines). adc: anterodorsal commissure, adc_a: anterior part of adc, adc_p: posterior part of adc, avc: anteroventral commissure, ennv: endopodite nerve, exnv: exopodite nerve, fpc: first posterior commissure, isnv: intersegmental nerve, Md: mandibular segment, mnb: median neurite bundle, Mx1 and Mx2: maxillular and maxillar regions, plnv: posterolateral nerve, spc: second posterior commissure, spc_d: dorsal part of spc, spc_v: ventral part of spc, Th1 and Th2: thoracic segments 1 and 2. Scalebars: 25 μm. [Color figure can be viewed in the online issue, which is available at wileyonlinelibrary.com.]

The posterolateral nerve (plnv, Fig. 3C) arises from each thoracic hemiganglion in a separate root posterior to the common root of the exo- and endopodite nerves. It extends posterolaterally toward the proximal region of the thoracopod. Considerable cuticular autofluorescence and the tubulin immunoreactivity of the protopodite muscles in this region made it impossible to trace the nerve any further.

Commissures. Four commissures are present in each thoracic ganglion. The anterodorsal and anteroventral commissure lie one on top of the other anteriorly in the ganglion (Figs. 3C,D and 6). The anterodorsal commissure (adc) is a

prominent bundle of a large number of neurites that may occur coherently (e.g., in Th1, Fig. 3C) or be loosely split into several bundles (e.g., in Th2, Fig. 3C). The anteroventral commissure is thinner and may either be straight or describe an anterior arc (see Fig. 3C,D). The first and second posterior commissures are situated one behind the other posteriorly in each thoracic ganglion (Figs. 3C,D and 6). The first posterior commissure (fpc) originates dorsally in the neuropil. The second posterior commissure (spc) has a dorsal and a ventral root and may be split into two separate neurite bundles. If the commissure occurs as one bundle, it may describe a dorsal arc, connecting at its dorsalmost point to the median neurite bundle (see spc, Fig. 5D–F). The anterodorsal and the first posterior commissure are also connected to the median neurite bundle.

Thoracic ganglia 8 and 9. In terms of their commissural pattern, Th8 and Th9 correspond to the rest of the thorax. However, the thoracopod nerves of Th8 and Th9 differ slightly from the rest. The endopodite nerve in Th8 is thinner than in the other segments, comprising only a few neurites. No endopodite nerve could be identified for Th9. The ganglia of Th8 and Th9 are compressed and spatially separated from each other by the cement gland (cg), which lies adjacently in the anteroventral region of Th9 (Fig. 5A; refer also to Hessler et al., 1995).

Subesophageal Ganglion

Position and general anatomy. The subesophageal ganglion (sg), which comprises the mandibular, maxillular, and maxillar neuromere, is situated in the posterior cephalon and constitutes the anteriormost part of the VNC (Figs. 1 and 2A, and 3A,B). Although connectives *sensu stricto* (which are by definition soma-free, see Richter et al., 2010) are absent within the subesophageal ganglion, it should be noted that the mandibular, maxillular, and maxillar neuropils on each side are separated from each other by bundles of parallel neurites (region indicated by dashed white bars in Fig. 3A) lying within the contiguous, midline-spanning subesophageal somata cortex. The dorsal side of the three neuropils, which lies close to the esophagus and gut, is partially covered by a thin layer of somata and is partially soma-free (Fig. 1D).

Nerves. Each of the three subesophageal neuromeres exhibits the three appendage nerves that are also found in the thoracic ganglia: one exopodite nerve (exnv), one endopodite nerve (ennv), and one posterolateral nerve (plnv, Fig. 3A,B). The three mandibular nerves emerge from a common root anterolaterally in the subesophageal ganglion (Md, Fig. 3B). The maxillular endopodite and exopodite nerves originate from a common root situated lateral to the anteroventral commissure (avc) of Mx1, separated from the delicate maxillular posterolateral nerve (Fig. 3A,B). The three maxillar nerves (Figs. 2A and 3A,B) correspond in detail to those in Th1–Th7. The pattern of innervation of the thoracopod-like cephalocarid maxilla by the exopodite, pseudepipodite, and endopodite nerves corresponds in detail to that in thoracopods 1–7 (see above).

The intersegmental nerve between the tritocerebrum and the mandibular neuromere (Fig. 2A, double arrowheads) originates clearly anterior to the subesophageal ganglion, its root lying directly lateral to the posterior postesophageal commissure (pec) of the tritocerebrum (see Stegner and Richter, 2011). The borders between subesophageal neuromeres (Md, Mx1, Mx2) are indicated by the respective intersegmental nerve (Fig. 3A,B), which is especially helpful in identifying the subesophageal commissures.

Commissures. What we denote as subesophageal commissures are visualized on the schematic drawing in Figure 3B. Despite the fact that they are higher in number and display some deviations in need of explanation, all 13 subesophageal commissures can be correlated with the four commissures that exist in each thoracic ganglion.

Maxillar commissures. Given that the intersegmental nerve (isnv) marks the border between Mx1 and Mx2, six commissures are counted in Mx2 (Fig. 3A,B). Two of the three studied specimens exhibited two well-separated anterodorsal commissures in Mx2 rather than one (adc_a, adc_p, Fig. 3A,B). As in the thorax, the anteroventral commissure (avc) of Mx2 constitutes the only commissure of the neuromere which is not connected with the median neurite bundle (Fig. 3B). The first posterior commissure (fpc) of Mx2 is situated directly dorsal to the anteroventral commissure (avc, Fig. 3A,B). All studied specimens exhibited two clearly separated "second posterior commissures" (spc_d, spc_v) in Mx2 rather than one. The relationship between the commissural and the SL-ir pattern in Mx2 corresponds in detail to that in Th1 (see section Serotonin-Like Immunoreactivity below).

Mandibular and maxillular neuromere. The anterodorsal commissures in Md and Mx1 (adc, Fig. 3A,B) are situated anteriorly in their respective neuromeres. They are relatively thick, and connected with the median neurite bundle (Fig. 3A,B). Distinctively, the anterodorsal commissure in Md (adc, Fig. 3A,B) gives rise to the median neurite bundle, and appears to be looser and broader than other commissures, receiving neurites both from the mandibular neuropil and from the connectives anterior to the subesophageal ganglion. The anteroventral commissures (avc) in Md and Mx1, respectively, lie directly ventral to the respective anterodorsal commissure and are not connected with the median neurite bundle (Fig. 3A,B). They are closely associated with the

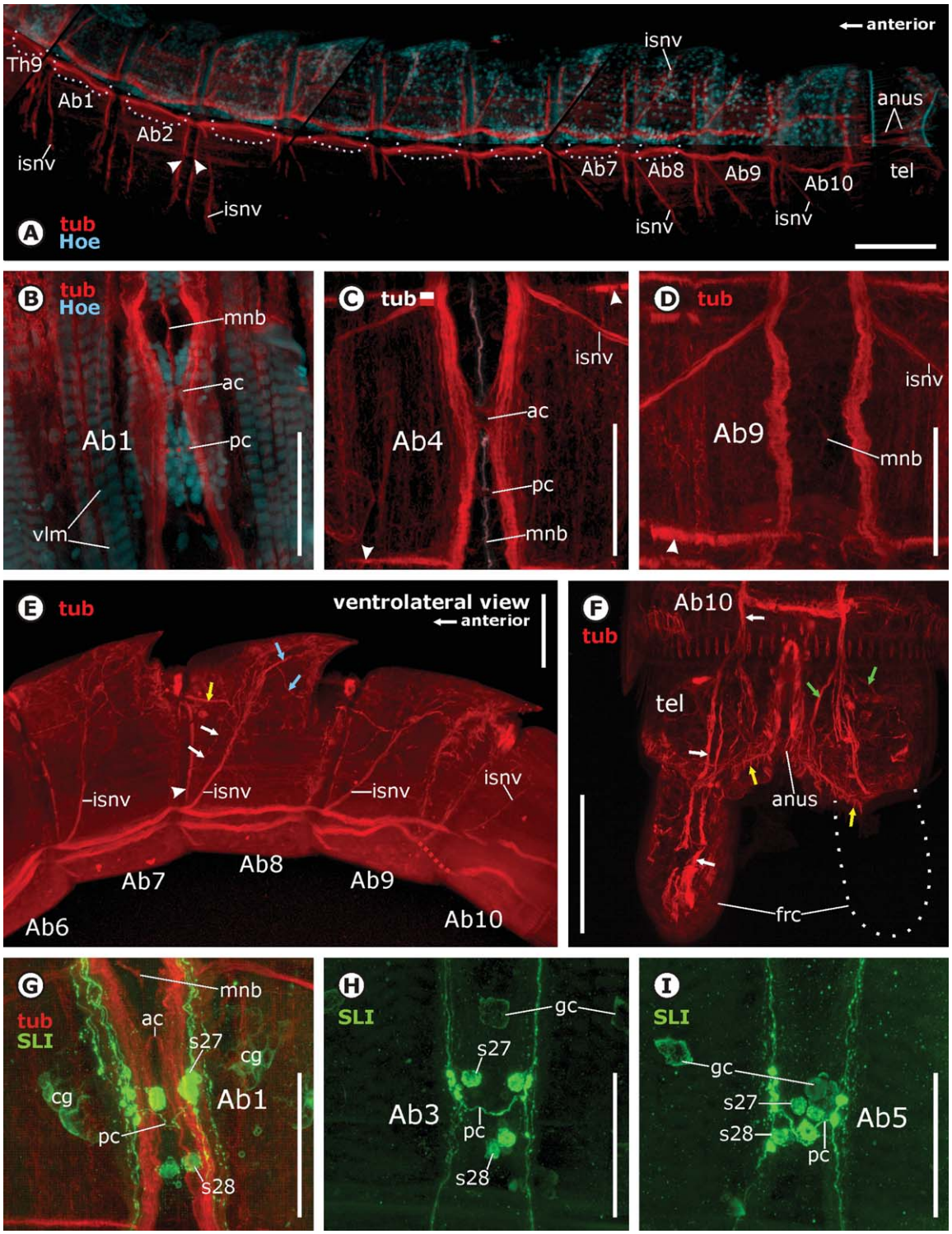

Fig. 4. Continued

root of the respective appendage nerves, as in the case of the maxillar and thoracic neuromeres.

While Md lacks a first posterior commissure (fpc) (Fig. 3A,B), the first posterior commissure in Mx1 lies posterior to the anterodorsal commissure and is connected with the median neurite bundle (Fig. 3A,B).

Both Md and Mx1 exhibit one slim commissure (here labeled spc_v) which seems to consist solely of neurites from the respective SL-ir neurons s15a

and s15b (Fig. 3A,B, see section Serotonin-Like Immunoreactivity). SL-ir neurons s15a and s15b in the neuromeres of Mx2 to Th7 contribute their neurites to the respective second posterior commissure, which is connected with the median neurite bundle. Since the slim commissure in Md and Mx1 is not connected with the median neurite bundle, we interpret it as the ventral part of a "second posterior commissure." The dorsal part of this second posterior commissure is missing in Md and Mx1.

Median neurite bundle. Emerging from the anterodorsal commissure (adc) of Md, the median neurite bundle extends posteriorly in a straight line (Figs. 3 and 4B–D). We traced it as far as Ab9 (Fig. 4D), but it may proceed to the anus (which lies in the telson, see Elofsson et al., 1992). The median neurite bundle is connected to all subesophageal, thoracic, and abdominal commissures except to the respective anteroventral commissure (avc) and, in Md and Mx1, except to the ventral part of the second posterior commissure (spc_v; e.g., Fig. 3B,D).

Abdominal Ganglia From Ab1 to Ab8

In each of the abdominal ganglia from Ab1 to Ab8, the somata are arranged in one continuous cortex around the bilateral neuropil (Fig. 1). They are mainly situated ventrally (Ab1–Ab8, Figs. 1C–E and 4A) and medially within the ganglion (see, e.g., Ab1, Fig. 4B). In dorsal or ventral aspect, the middle region of each cortex appears to be soma-free. Ab1–Ab8 show a broadly corresponding pattern of nerves and commissures. An intersegmental nerve (isnv, Fig. 4A,C,E) arises slightly anterior to each abdominal hemiganglion from the lateral region of the connective. It initially extends posterolaterally before splitting into two main branches (Fig. 4E). One main branch turns anteriorly, innervating the lateral (yellow arrow) and—via a thinner branch—medial rim of the segmental border (white arrows, Fig. 4E). The other main branch proceeds laterally (blue arrows, Fig. 4E), innervating the unarticulated, spine-like lateral extrusion of the tegument ("pleura" *sensu* Sanders, 1963). Each abdominal ganglion exhibits a thicker anterior commissure (ac) and a more delicate posterior commissure (pc, most conspicuous in Fig. 4C, see also Fig. 4B,G). Both are connected to the median neurite bundle (mnb, Fig. 4B,C).

Posterior Abdominal Region (Ab9–Ab10 and Telson)

Ab9, Ab10 and the telson completely lack ganglia and commissures. The paired longitudinal neurite bundles of the VNC extend through this region, diverging slightly (Figs. 1A–C and 4A,D–F). In the telson, each longitudinal neurite bundle splits into several smaller branches. Only a few of these branches (green arrows) innervate the tegument of the telson; most (white arrows) proceed posteriorly to innervate the furca (frc, Fig. 4F). The intersegmental nerves (isnv) between Ab8, Ab9 and Ab10 correspond to those between other abdominal segments (Fig. 4A,D,E).

Serotonin-Like Immunoreactivity

General pattern. The VNC comprises a high number of SL-ir neurons that contribute their neurites to SL-ir neuropil domains (*sensu* Stegner et al. in press), some commissures, and the connectives (Figs. 4G–I and 5). Most SL-ir neurons occur in bilaterally symmetrical pairs and could be identified individually (labeled "s14–s20, s27, s28," see Table 1; detailed description below). Notably, even where the course taken by the respective neurites of the same pair of neurons corresponded (e.g., passing through the same commissure), the exact position of their somata was often found to differ. This implies that individual SL-ir neurons identified on the basis of soma position alone (labeled "s21?–s26?" in Table 1) may have to be revised when the course of the corresponding neurites is clarified in the future.

All SL-ir neurons in the VNC are unipolar. The cement gland (see Hessler et al., 1995) in Th9 and

Fig. 4. *Hutchinsoniella macracantha*, VNC and serotonin-like immunoreactivity in the abdomen. Confocal laser scans. Imaris surpass view from ventral, if not stated otherwise. (**A, C–E)** Arrowheads point at insertion sites of longitudinal muscles. A. Overview of the abdomen. Dotted lines (lower side of figure) and Hoechst staining (upper side) show somata assemblages for abdominal ganglia in Ab1–Ab8, but not in Ab9 and Ab10. Hoechst staining not shown on lower, morphologically right side. (**B**) Imaris extended section view. Abdominal ganglion 1 lies embedded between the pair of ventral longitudinal muscles, which show autofluorescence under UV excitation (cyan stripes). (C) The two commissures of Ab4 are connected with the faint median neurite bundle, which was masked and assigned to a white channel here. (D) In Ab9, the longitudinal neurite bundles are not linked by commissures. (E) Posterior region of abdomen. Insertion sites of longitudinal muscles (arrowhead) are innervated by a branch (white arrows) of the intersegmental nerve. Other branches innervate the intersegmental joint region (yellow arrow) and the lateral extrusions of the tegument (blue arrows). (**F)** Anterior to where the longitudinal neurite bundles proceed into the furca (white arrows), they give rise to several side branches (green arrows) which innervate various setae (yellow arrows) of the telson. (**G–I)** Abdominal ganglia generally feature two pairs of strongly SL-ir somata. Only the posterior commissure is SL-ir, encompassing the axons of s28 neurons. (H, I) Additionally, a pair of lateral and a median group of weakly SL-ir gland-like cells (gc) were found in most abdominal segments. Ab1–Ab10: abdominal segments 1–10, ac: anterior commissure, anus: anus, cg: cement gland, frc: furca, gc: gland-like cells, isnv: intersegmental nerve, mnb: median neurite bundle, pc: posterior commissure, s27 and s28: serotonin-like immunoreactive somata 27 and 28, tel: telson, Th9: thoracic segment 9, vlm: ventral longitudinal muscle. Scalebars: A: 100 μm. B–I: 50 μm.

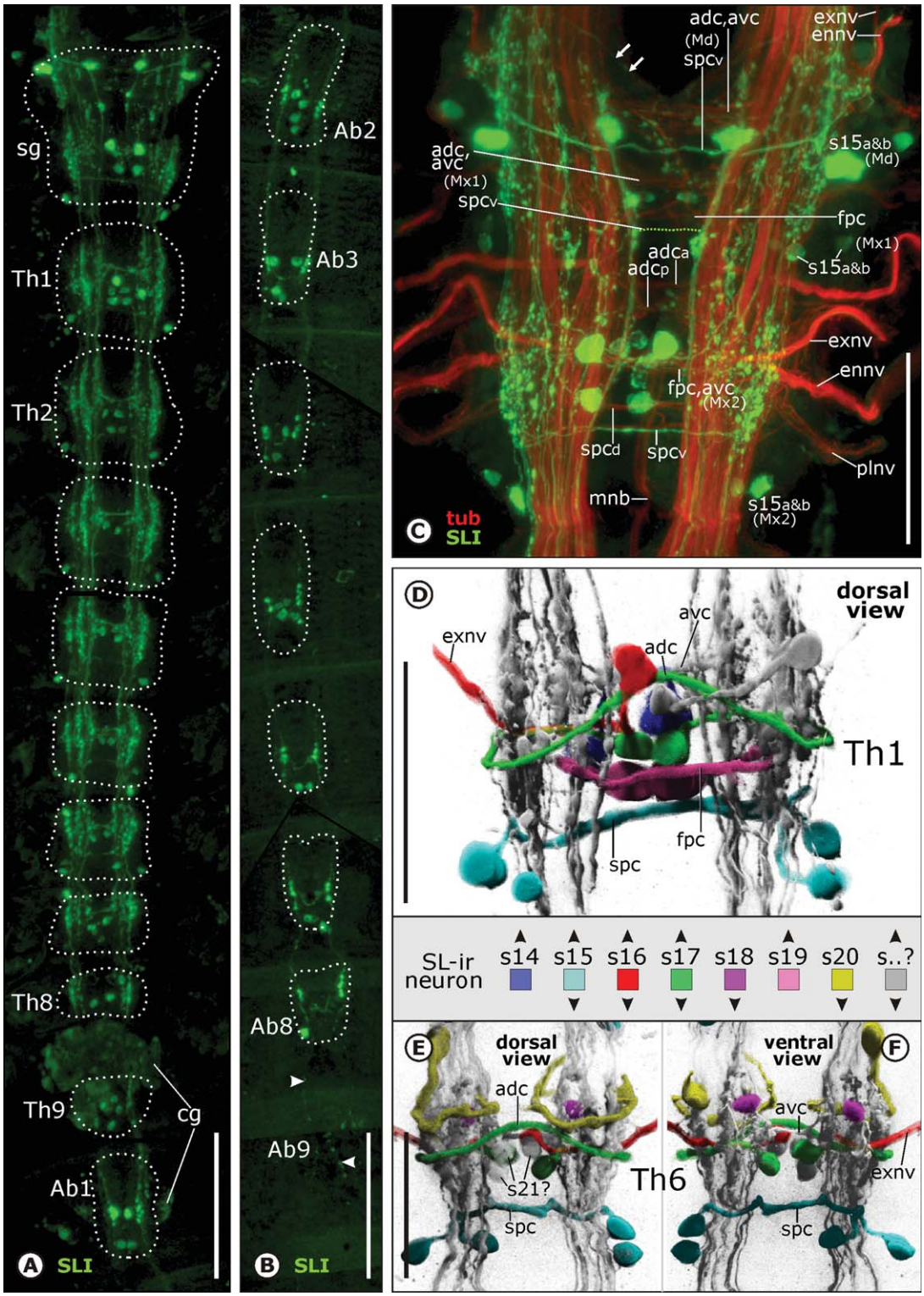

Fig. 5. Continued

Ab1 (cg, Figs. 4G and 5A) and gland-like cells in the abdomen (gc, Fig. 4H,I) are also weakly SL-ir.

Longitudinal neurites. Each side of the VNC features several single longitudinal SL-ir neurites (Fig. 5A,B) which extend through all the neuropils and connectives. Because they interlace with other SL-ir neurites in the SL-ir domains of the ganglionic neuropils, it is not easy to trace them back to

their respective soma. Soma s20 gives rise to a longitudinal neurite in segments Th6–Th9 (e.g., Fig. 5E, and see below). A distinct decrease in the number of longitudinal SL-ir neurites is observable along the anteroposterior axis. Only a single SL-ir neurite on each side proceeds posteriorly from Ab8 as far as the furca.

Thoracic ganglia. Mx2 and all the thoracic ganglia exhibit a complex pattern of SL-ir neurons with many intersegmental correspondences. Since there are also intersegmental differences as one proceeds from Mx2 to Th9, however, the segmental SL-ir pattern cannot be considered entirely homonomous. Moreover, differences between the specimens studied indicate a certain degree of intraspecific variability.

Th1. Th1 exhibits six individually identified SL-ir somata on each body side, here labeled s14, s15a, s15b, s16, s17, and s19 (see Table 1, Figs. 5D and 6B). The two somata s15a and s15b (light blue in Figs. 5D and 6B) occupy a posterolateral position, sending their respective neurite into the ipsilateral neuropil and from there a contralateral axon through the second posterior commissure (spc) into the neuropil of the opposite body side. Although s15a and s15b are indistinguishable within their duad, we count them as "individually identified" as they differ considerably from all other SL-ir neurons.

All other individually identified somata in Th1 are positioned anteromedially in the hemiganglion, often close to each other. Soma s14 (dark blue in Figs. 5D and 6B) sends its neurite into the anteroventral commissure (avc), where the neurite splits into an ipsilateral and a contralateral neurite which extend into the opposite neuropils of the ganglion. Soma s16 (red in Figs. 5D and 6B) sends its neurite ipsilaterally through the neuropil into the exopodite nerve. Neuron s17 (green) has the most conspicuous anatomy. Its neurite extends ipsilaterally from the soma into the neuropil, where it interlaces with other neurites. The axon bends upward in a dorsal arc, bypassing the neuropil before turning contralaterally to contribute to the anterodorsal commissure (adc). Soma s19 (pink) sends its neurite ipsilaterally into the

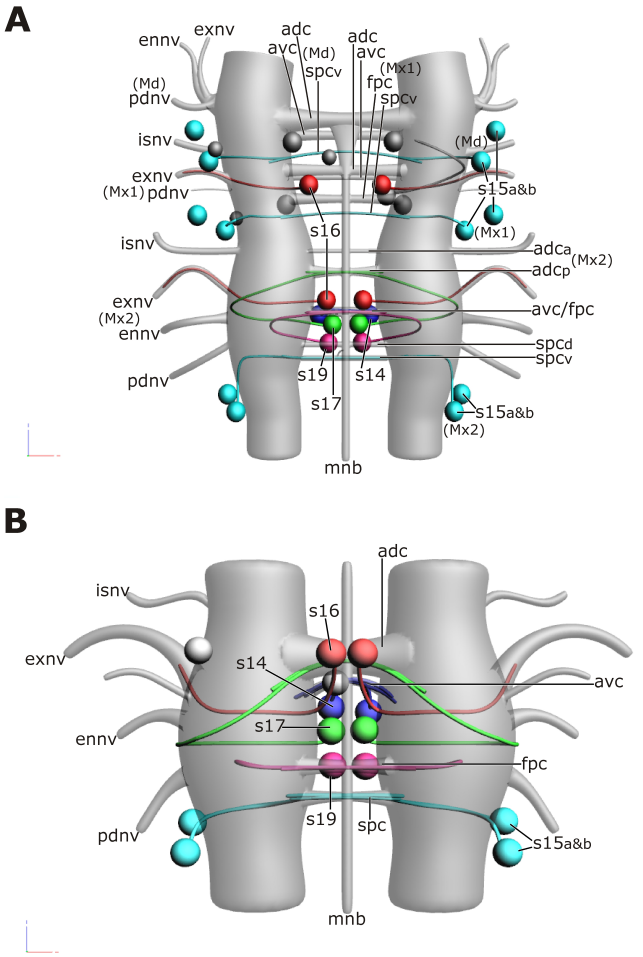

Fig. 6. *Hutchinsoniella macracantha*, interactive 3D-schematics of the SL-ir neurons in the VNC of *H. macracantha*. Ganglionic neuropil, nerves, commissures, and median neurite bundle are shown in semitransparent. Denotations of individually identified neurons (colored, see also Table 1) are given in the interactive PDF. Neurons with untraceable neurites are shown in gray. Dorsal aspect. Please use other preset aspects to turn the 3D-models. (**A**) Subesophageal ganglion. (**B**) Thoracic ganglion 1. adc: anterodorsal commissure, adc_a: anterior part of adc, adc_p: posterior part of adc, avc: anteroventral commissure, ennv: endopodite nerve, exnv: exopodite nerve, fpc: first posterior commissure, isnv: intersegmental nerve, Md/Mx1/Mx2: attributed to mandibular/maxillular/maxillar segment, mnb: median neurite bundle, plnv: posterolateral nerve, s14–s20: serotonin-like immunoreactive somata 14–20, spc: second posterior commissure, spc_d: dorsal part of spc, spc_v: ventral part of spc.

Fig. 5. *Hutchinsoniella macracantha*, serotonin-like immunoreactivity (SLI) in the VNC. (**A–C**) Confocal laser scans. Imaris surpass view. (**D–F**) Imaris shadow projection. (A, B) Ventral overview of SLI in thorax and abdomen. Dotted lines indicate the position of ganglia. On each side, the VNC encompasses a number of longitudinal SL-ir neurites, a few of which (arrowheads) also proceed through abdominal segments 9 and 10, which lack ganglia. (C) Dorsal aspect of the subesophageal ganglion. SL-ir neurites from the posttritocerebral connectives (white arrows) enter the anterodorsal commissure in Md. The neurites from SL-ir somata s15a and s15b form the ventral part of the second posterior commissure. (D–F) Individually identified neurons were masked and assigned to different color channels (see legend and Table 1) using the Imaris contour surface tool. There are both correspondences (compare, e.g., s15a, s15b, s16, s17 in D and E, F) and differences (e.g., s14, s18, s20) in the SL-ir pattern of the various thoracic ganglia. Ab1–Ab9: abdominal segments 1–9, adc: anterodorsal commissure, adc_a: anterior part of adc, adc_p: posterior part of adc, avc: anteroventral commissure, cg: cement gland, ennv: endopodite nerve, exnv: exopodite nerve, fpc: first posterior commissure, Md/Mx1/Mx2: attributed to mandibular/maxillular/maxillar segment, mnb: median neurite bundle, plnv: posterolateral nerve, s14–s20, s21?: serotonin-like immunoreactive somata 14–20 and s21?, sg: subesophageal ganglion, spc: second posterior commissure, spc_d: dorsal part of spc, spc_v: ventral part of spc, Th1–9: thoracic segments 1–9. Scalebars: A, B: 100 μm. C–F: 50 μm.

neuropil, from where the axon turns back contralaterally to contribute to the first posterior commissure (fpc). Th1 contains two additional somata whose neurites could not be traced. Soma s21? lies medially and soma s22? anterolaterally/dorsally in the hemiganglion. Comparing two specimens of *H. macracantha*, we found soma s21? to be either unpaired or paired, and s22? to be either unpaired or absent (see Table 1).

Th6. Th6 contains six individually identified SL-ir neurons, some of which differ in their neurite morphology from those in Th1. Th6 lacks neurons s14 and s19 but exhibits neurons s18 and s20 (Fig. 5E,F, Table 1). Soma s18 (purple in Fig. 5F) is situated ventrally and soma s20 (yellow in Fig. 5E,F) anterolaterally in the hemiganglion. The neurite from soma s18 extends directly into the neuropil and could not be traced further on. The neurite from soma s20 extends in a medial arc around the ipsilateral neuropil before entering the latter to continue anteriorly into the connective, toward the next hemiganglion. Altogether three additional medial somata s21? (Fig. 5E), here interpreted as one unpaired soma and two occuring in a pair (Table 1), were also identified in Th6. Their neurites could not be identified.

Intraspecific variability. To address potential intraspecific variability in the SL-ir pattern of *H. macracantha*, we compared three specimens in detail with respect to the subesophageal ganglion and two specimens with respect to the thoracic ganglia. Intraspecific variability is displayed by neurons s14–s19 (see all cells with a dash [/] in Table 1), which were present in one and missing in the other specimen(s) (e.g., s18 in Th3), or paired in one specimen and unpaired in the other(s) (e.g., s17 in Th2). Only neuron s20 occurred consistently in a pair from segment Th6 to Th9 in both compared specimens (Table 1).

If an anteromedial or medial soma with an untraceable neurite could not be identified individually (as either s14, s16, s17, s19, or something else), it was labeled as "s21?." Table 1 shows that unspecified somata s21? were found in all studied segments of three individuals. The degree of intraspecific variability might thus be lower than suggested by Table 1, with somata s21? possibly belonging to the "missing" anteromedial neurons s14, s16, s17, s19.

In some cases, the anteroventral, anterodorsal, and first posterior commissure are SL-ir without seeming to be contributed to by soma s14, s17, or s19, suggesting that these commissures may comprise additional SL-ir neurites.

Distribution of individually identified neurons across the thorax. A comparison of individually identified neurons across the successive segments of the thorax reveals a number of intersegmental differences. While Figure 5D (Th1) and Figure 5E (Th6) permit a direct comparison of the morphology of SL-ir neurons in two different ganglia, the color-coded rows s14–s20 in Table 1 show precisely which SL-ir neurons are found in which thoracic ganglion. Four general facts become clear: 1) There is no simple anteroposterior increase or decrease in the distribution of SL-ir neurons across the thoracic segments. Though the three neurons s14, s18, and s19 each occur in both anterior and posterior thoracic segments, they are not present in intermediate ones. 2) No single thoracic ganglion exhibits all the individually identified SL-ir neurons (s14–s20). 3) No SL-ir neuron occurs in all thoracic ganglia. 4) Neurons s14–s20 are present in at least one thoracic ganglion in all the specimens studied, though the exact ganglion may differ. Neurons s14–s20 can thus be considered a constant feature of *H. macracantha*.

Subesophageal ganglion. The pattern of SL-ir neurons in Mx2 is nearly identical to that in Th1 and features neurons s14, s15a, s15b, s16, s17, and s19 (Table 1, compare Fig. 6A with 6B). In specimens whose anterodorsal commissure is split into two parts, neurite s17 contributes to the more posterior part (adc_p). Neurites s15a and s15b in Mx2 consistently contribute to the ventral part (spc_v) of the split "second posterior commissure." Although the relative position of the first posterior commissure is different in Mx2 than in thoracic ganglia, it also receives neurite s19. One additional medial soma with an unknown neurite is present in Mx2.

Only some (s15a, s15b [Md], s15a, s15b, s16 [Mx1]) of the 11 SL-ir neurons per body side in Md and Mx1 could be identified individually (Table 1, Fig. 6A; compare with Fig. 6B). In most other cases, the neurites could not be traced. The anteroventral and anterodorsal commissures of Md include SL-ir neurites which could not be traced to their somata.

Abdominal ganglia (Ab1–Ab8). From Ab1 to Ab8, the abdominal ganglia correspond closely to each other in their pattern of SLI (Figs. 4G,I and 5A,B). From Ab1 to Ab7, one anteromedial soma s27 sends its neurite ipsilaterally into the neuropil and a posteromedial soma s28 sends its neurite contralaterally through the posterior commissure (Fig. 4G,H,I). Ab8 exhibits the posteromedial soma but lacks the anteromedial one. The anterior commissure lacks SLI in all abdominal ganglia.

Posterior abdominal region (Ab9, Ab10, telson). The posterior abdominal region is devoid of either SL-ir somata or SL-ir neuropil domains (see Ab9, Fig. 5B). Only a single SL-ir neurite extends posteriorly through each of the paired longitudinal neurite bundles. Around the anus, this SL-ir neurite forms a network with the SL-ir lateral bundle (see the section Stomatogastric Nervous System below) and other neurites.

RFamide-Like and Histamine-Like Immunoreactivity

Please refer to Supporting Information Text S1 and Supporting Information Figure S1.

Stomatogastric Nervous System

The stomatogastric nervous system in *H. macracantha* includes the labral commissure and the unpaired labral neuropil, an unpaired dorsomedian neurite bundle and a pair of dorsolateral neurite bundles (see also Stegner and Richter, 2011), as well as a pair of lateral neurite bundles (Fig. 8).

Dorsomedian neurite bundle. An unpaired dorsomedian neurite bundle (dbs) originates anteriorly from the labral neuropil which lies at the vertex of the labral commissure (Fig. 8, see Stegner and Richter, 2011), bending dorsally and extending posteriorly adjacent to the gut. On the basis of its tubulin immunoreactivity and SLI, this neurite bundle could be traced as far as the maxillar segment. Between the tritocerebrum and the subesophageal ganglion, a weakly SL-ir dorsolateral neurite bundle branches off from each side of the dorsomedian neurite bundle (Fig. 7E), proceeding posterolaterally adjacent to the gut toward the peri-esophageal network to which the lateral neurite bundle also contributes (see below).

Longitudinal lateral bundle. A lateral neurite bundle (latb) comprising both SL-ir (Fig. 7A–D,G,H) and RFL-ir neurites (Fig. 7I) extends longitudinally from the brain along each side of the gut as far as the telson region. In some regions, single neurites trail away from each other (follow arrows in Th1–Th3, Fig. 7A,C) and later reassemble to form one neurite bundle (Th8, Fig. 7C).

In the subesophageal region, the lateral neurite bundle contributes to a loose peri-esophageal network of SL-ir neurites (rocket arrowheads in Figs. 7A,B and 8) situated in close proximity to esophageal and gut muscles (esom, gutm in Fig. 7G). Near the anterior border of each thoracic segment, each lateral neurite bundle sends off an SL-ir side-nerve laterally (arrowheads, Figs. 7A,C,H and 8) which meanders around the longitudinal (lm) and various dorsoventral muscles (dva, dvp, dvv, Fig. 7H; compare with Hessler, 1964: his Fig. 2). Furthermore, the lateral neurite bundle (latb) in each thoracic segment is indirectly connected with the median neurite bundle (mnb) of the VNC via an anterior (atb) and a posterior transverse neurite bundle (ptb, Fig. 7F). Medially, the lateral neurite bundle is associated with a loose plexus of SL-ir and RFL-ir neurites that extends along the ventral side of the whole gut (e.g., double arrowheads in Fig. 7I). In the telson, the lateral neurite bundle of each body side meets the main longitudinal neurite bundle of the VNC to form a loose, midline-spanning, peri-anal network of SL-ir and RFL-ir neurites (Fig. 8).

DISCUSSION

Earlier Studies into the Cephalocarid Nervous System

General anatomy. Our results broadly confirm earlier descriptions of the distribution of ganglia and commissures throughout the VNC of *Hutchinsoniella macracantha* (Elofsson and Hessler, 1990; Hessler and Elofsson, 1992). A major exception is segment Ab9, in which Elofsson and Hessler (1990: their p. 433) reported a ganglion with "at least one commissure." Based on our data, the existence of this ganglion can be unequivocally refuted. Moreover, we identified three hitherto undescribed commissures in the subesophageal ganglion (spc_v in Md and Mx1, fpc in Mx1), and provided new insights into the peripheral nervous system of Cephalocarida.

Serotonin- and RFamide-like immunoreactive pattern. We were able to refine the results of Elofsson's (1992) investigation into the SL-ir and RFL-ir pattern considerably. That study was carried out using immunolabeled 2 μm semithin sections, but using confocal microscopy, we found a number of additional, hitherto undescribed SL-ir and RFL-ir neurons whose neurites could be traced into various different commissures and nerves. While Elofsson reported a homonomous SL-ir and RFL-ir pattern for the thorax, our comparison revealed a number of intersegmental differences. Interestingly, Elofsson (1992) described four SL-ir somata in each abdominal hemiganglion, whereas we generally only found two. The supernumerary somata he described may correspond to the groups of slightly larger, moderately SL-ir gland-like cells that we detected dorsomedially and dorsolaterally in several abdominal segments.

Subesophageal Region and the Evolution of the Maxillar Segment

No intermediate segment. The hypothesis put forward by Tiegs and Manton (1958) of an additional, intermediate segment in the subesophageal region was fairly quickly refuted by Sanders (1963). Since the separation in the anterodorsal (adc_a, adc_p) and second posterior commissures (spc_d, spc_v) in Mx2 is comparable to the split in these commissures found across the thoracic ganglia, the comparatively high number of six commissures in Mx2 is not a convincing argument for an intermediate segment.

Different numbers of segments contribute to the subesophageal ganglion across Mandibulata. The mandibulate cephalon is a coherent unit comprising six cephalic regions (ocular, antennular, antennal, mandibular, maxillular, maxillar). In some cases, thoracic segments may be fused to the cephalon to form a cephalothorax. A clear-cut cephalon/thorax boundary directly posterior to Mx2 is found in many recent mandibulates

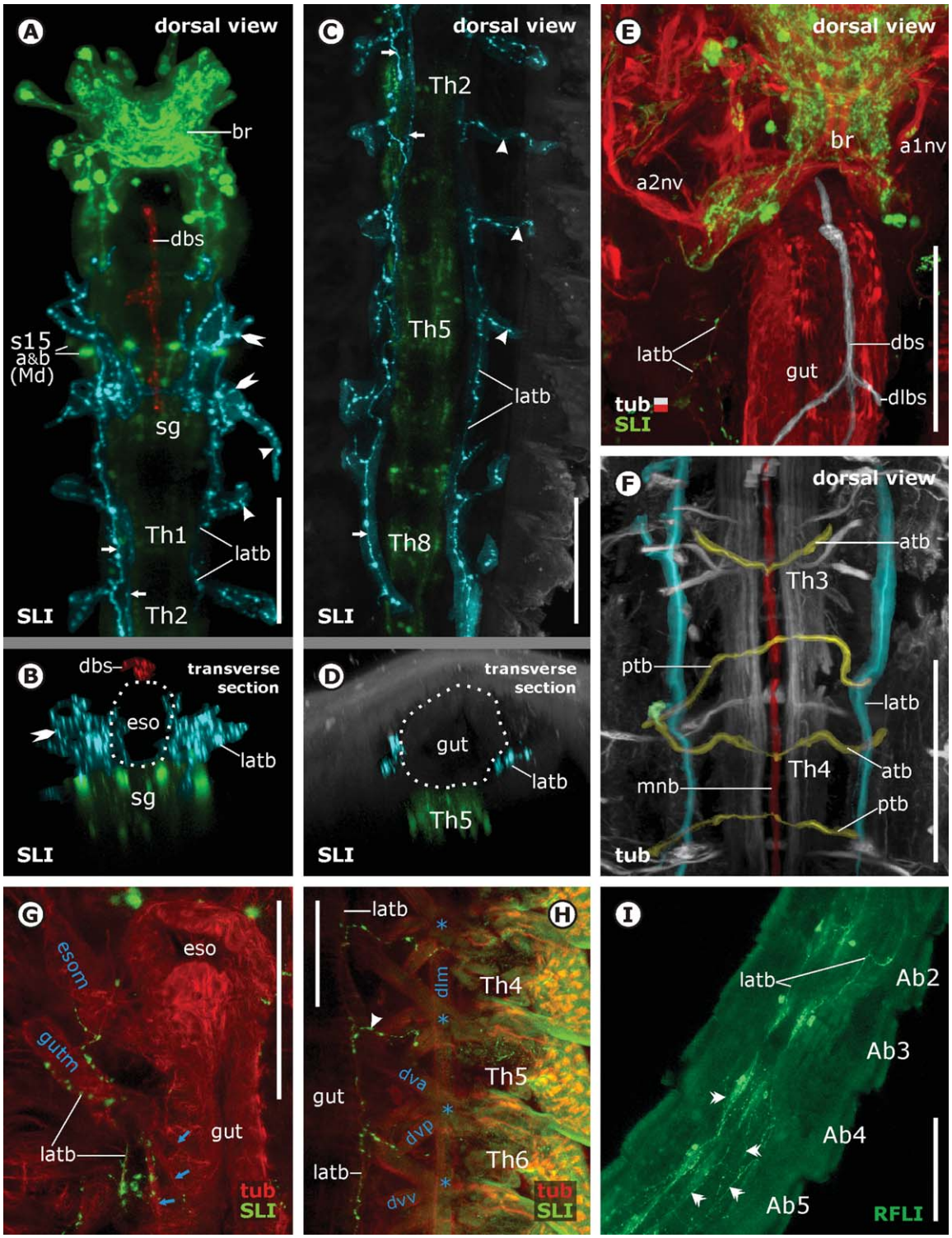

Fig. 7. Continued

such as Cephalocarida, Branchiopoda, Hexapoda, and Myriapoda. This condition is likely to be representative of the mandibulate ground pattern (Scholtz and Edgecombe, 2006).

The three anterior cephalic neuromeres (proto-, deuto-, tritocerebrum) mainly innervate receptor organs (visual, olfactory, and tactile) and together form the brain.

Subesophageal ganglion three-segmental (Md, Mx1, Mx2). The three posterior cephalic segments (Md, Mx1, Mx2) generally serve the coordination of mouthparts. It has long been known that the neuromeres of Md, Mx1, and Mx2 are fused into a three-segmental subesophageal ganglion in Hexapoda (e.g., Hanström, 1928; Bullock and Horridge, 1965; Strausfeld, 1976) including the apterygote taxa (Niven et al., 2008: see their Fig. 1), as well as in some Myriapoda (Fahlander, 1938: Geophilomorpha; Harzsch, 2004; Sombke et al., 2011: *Lithobius forficatus*). This situation corresponds to that in Cephalocarida (Elofsson and Hessler, 1990; Hessler and Elofsson, 1992; this study). Although their subesophageal ganglion is also "three-segmental," a different situation is found in some Ostracoda in that the three subesophageal neuromeres are not only fused with each other but also with the brain, thus forming a compact circumesophageal ring which is set apart from the thoracic ganglia (Cannon, 1940).

Subesophageal ganglion includes more than three neuromeres. Across Crustacea, the subesophageal ganglion may include additional neuromeres of the thorax. This is the case in Cirripedia (Harrison and Sandeman, 1999), some Ostracoda (Hartmann, 1967), Copepoda (Andrew et al., 2012), Remipedia (Fanenbruck and Harzsch, 2005), and various malacostracan taxa such as Stomatopoda (Ando and Kuwasawa, 2004), Decapoda (e.g., Schneider et al., 1993), and Isopoda (Schmitz, 1989). The fusion of one (Fahlander, 1938: Lithobiomorpha, Scolopendromorpha) or more additional thoracic neuromeres (Fahlander, 1938: Scutigeromorpha; Szucsich and Scheller, 2011: Symphyla) to the subesophageal ganglion is also reported in some Myriapoda.

Subesophageal ganglion two-segmental (Md, Mx1). In several crustacean taxa, however, the subesophageal ganglion comprises only the two neuromeres of Md and Mx1 and is separated from the ganglion of Mx2 by a pair of soma-free connectives. This is the case in Euphausiacea (Hanström, 1928: his Fig. 448IV) and Branchiura (e.g., Leydig, 1889; Zaćwilichowski, 1935).

No fused subesophageal ganglion (separate ganglion of Md). In Branchiopoda (Henry, 1948; Fritsch and Richter, 2010), and the malacostracan taxon Leptostraca (Claus, 1888; Hanström, 1928: his Fig. 448VI; Kenning et al., 2013) no fusion whatsoever is reported between neuromeres. The ganglia of Md, Mx1, and Mx2 are segmental and as well separated by soma-free connectives as the thoracic ganglia (see previous citations). Although the somata of the neuromeres of Md and Mx1 do not form a contiguous cortex in Mystacocarida (Brenneis and Richter, 2010), the authors report a "high degree of fusion in the joint neuropil of Md and Mx1," while the ganglion of Mx2 is separate.

Evolutionary interpretation. The clear-cut cephalon/thorax boundary coincides with a three-segmental subesophageal ganglion (Md, Mx1, Mx2) in Cephalocarida, Hexapoda, and some Myriapoda. Assigning a three-segmental subesophageal ganglion to the mandibulate ground pattern is problematic, however, considering the taxa in which only the anterior two neuromeres, if any, are fused. The condition in Branchiopoda and Leptostraca, which combine a clear-cut cephalon/thorax boundary with well-separated ganglia, would have to be interpreted as derived.

A possible alternative hypothesis is that well-separated ganglia in the subesophageal region represent the mandibulate ground pattern. In this case, the three-segmental subesophageal ganglion in Hexapoda, Cephalocarida, and Myriapoda would have evolved independently. The fusion of subesophageal neuromeres across several malacostracan taxa would also have to be interpreted as a derived feature that evolved in parallel to other specializations within Eumalacostraca (maxillipedes, cephalothorax, see Richter and Scholtz, 2001), while Leptostraca would represent the malacostracan ground pattern.

Neuroanatomy and appendages in Mx2. In all recent mandibulates except Cephalocarida, the

Fig. 7. *Hutchinsoniella macracantha*, peripheral nervous structures. Confocal laser scans. **(A, C, E, F)** Imaris surpass view. (**B, D, G–I**) Imaris extended section view. Extended horizontal sections. (A–F) The Imaris contour surface tool was used to mask and assign structures with the same staining to different color channels. (A, B) The lateral neurite bundle comprises several parallel neurites (white arrows) and contributes anteriorly to an SL-ir network of neurites (rocket arrowheads) in the subesophageal region. Simple arrowheads show side-nerves branching off the lateral neurite bundle. (B) Extended transverse section including the subesophageal region only. (C) Arrowheads and arrows as in A. (D) Extended transverse section including thoracic segment 5 only. (E) The dorsomedian neurite bundle of the stomatogastric nervous system proceeds along the dorsal side of the gut and gives rise to the dorsolateral neurite bundles. (F) Thoracic ganglia 3 and 4. The lateral neurite bundle is connected to the median neurite bundle via two pairs of transverse neurite bundles (atb, ptb) per segment. (G) The network of SL-ir neurites in the subesophageal region embraces the large esophageal and gut muscles both in the region of their insertion (blue arrows) and more distally. (H) In the thorax, the side-nerves (arrowheads) of the lateral neurite bundle are associated with dorsoventral muscles attached to the anterodorsal tendon (asterisk). (I) Abdomen in ventral view. RFLI shows the lateral neurite bundle and a number of other neurites (double arrowheads) closely associated with the gut. a1nv: antennula nerve, a2nv: antenna nerve, Ab2–Ab5: abdominal segments 2–5, atb: anterior transverse neurite bundle, br: brain, dbs: dorsomedian neurite bundle of the stomatogastric nervous system, dlbs: dorsolateral neurite bundle, dlm: dorsal longitudinal muscle, dva/dvp/dvv: dorsoventral anterior/posterior/ventral muscle, eso: esophagus, esom: esophageal muscle, gut: gut, gutm: gut muscle, latb: longitudinal lateral neurite bundle, mnb: median neurite bundle, ptb: posterior transverse neurite bundle, s15a and s15b: SL-ir neurons 15a and 15b in Md, sg: subesophageal ganglion, Th1–Th8: thoracic segments 1–8. Scalebars: 100 μm.

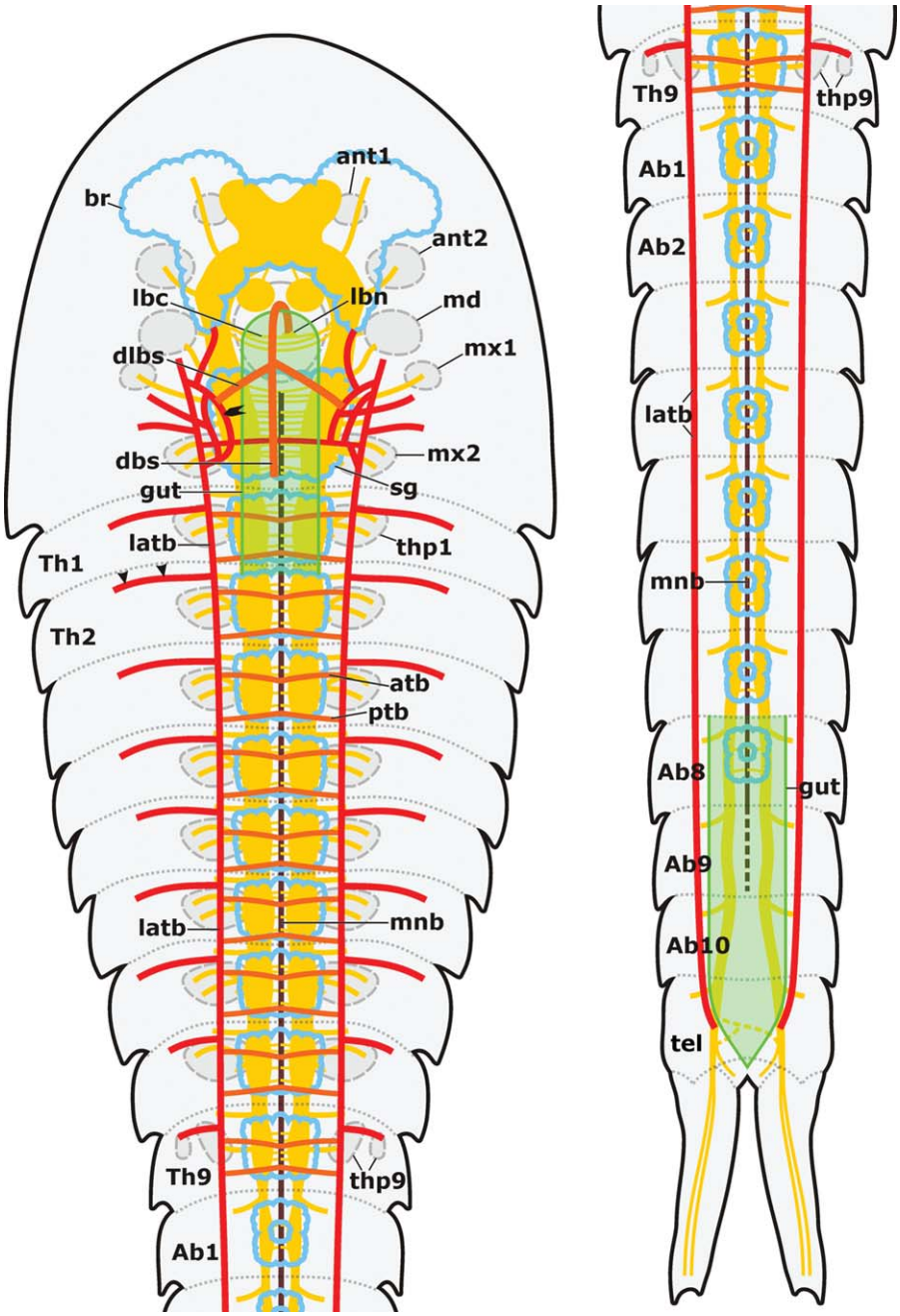

Fig. 8. *Hutchinsoniella macracantha*, schematic representation of ventral nerve cord and stomatogastric nervous system. Dorsal view. Intersegmental and appendage nerves omitted. Neuropils, commissures, connectives depicted in yellow, somata cortexes in blue, gut in semitransparent green omitted from Th2 to Ab7. The labral commissure (lbc) and labral neuropil (lbn), the median (mnb, brown), anterior transverse (atb), and posterior transverse neurite bundle (ptb) lie below the gut, the lateral neurite bundle lateral to the gut, the dorsomedian (dbs) and dorsolateral neurite bundle (dlbs) of the stomatogastric nervous system dorsal to the gut. Arrowheads denote a side-nerve of the lateral neurite bundle. The rocket arrowhead denotes the peri-esophageal network of neurites. ant1: antennula, ant2: antenna, Ab1–Ab10: abdominal segments 1–10, atb: anterior transverse neurite bundle, br: brain, dbs: dorsomedian neurite bundle, dlbs: dorsolateral neurite bundle, gut: gut, latb: lateral neurite bundle, lbc: labral commissure, lbn: labral neuropil, md: mandible, mx1: maxillula, mx2: maxilla, ptb: posterior transverse neurite bundle, sg: subesophageal ganglion, tel: telson, Th1–Th9: thoracic segments 1–9, thp1, thp9: thoracopods 1 and 9.

postmaxillular limb is either specialized into a feeding appendage or is largely reduced. Although it exhibits considerable morphological disparity across the different taxa, it is generally called the "maxilla" within Crustacea (Boxshall, 2004). The unique thoracopod-like anatomy of the cephalocarid maxilla has commonly been interpreted as being plesiomorphic with respect to the mandibulate ground pattern (see Sanders, 1957; Hessler, 1964; Lauterbach, 1980; Walossek, 1993; Scholtz,

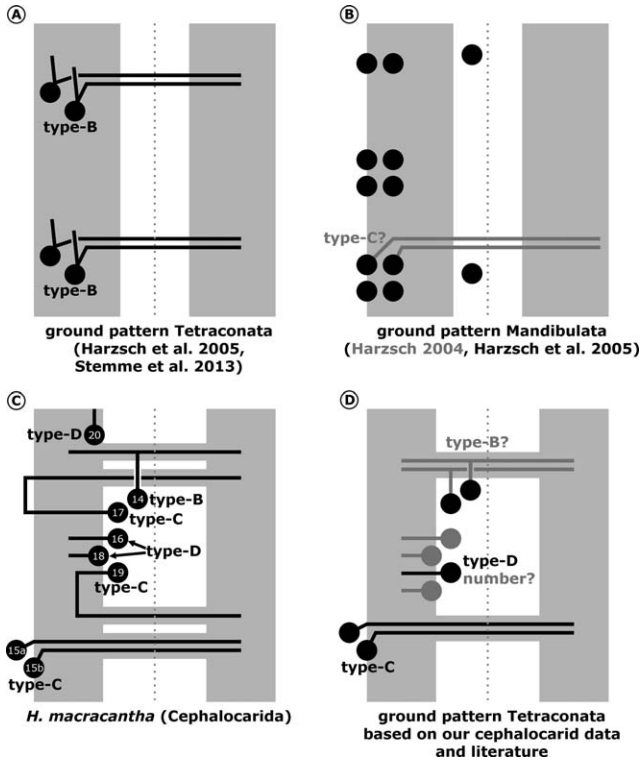

Fig. 9. Evolutionary interpretation of SL-ir neurons in the mandibulate VNC. Schematic representation does not imply that all neurons naturally co-occur in a specific segment. Structures in gray cannot be resolved unambiguously. (**A, B)** Ground pattern hypotheses from the literature. (**C)** Schematic representation of all SL-ir neurons in the thorax of *H. macracantha*. Numbers 14–20 indicate neurons labeled s14–s20 in this study. (**D)** Ground pattern of Tetraconata based on a comparison of the cephalocarid SL-ir pattern (this study) with literature data on other mandibulates (see discussion).

1997). We investigated the possibility of there also being neuroanatomical correspondences between Mx2 and the thoracic segments in Cephalocarida and can confirm that the pattern of commissures and nerve roots in Mx2 is identical to that in the thoracic segments (see also Elofsson and Hessler, 1990; Hessler and Elofsson, 1992). Moreover, our data reveal that the innervation pattern of the maxillar appendage corresponds to that in the thoracopods but differs from that in the mandibular and maxillular appendage. We were able to show with regard to the SL-ir pattern, too, that Mx2 corresponds in detail to the thoracic segments but deviates in several respects from Md and Mx1.

A correlation between neuroanatomy and appendage morphology also exists in crustaceans whose maxilla is a specialized limb. In Mystacocarida (Brenneis and Richter, 2010), Isopoda (Thompson et al., 1994), and Decapoda (Harzsch, 2003), there are close correspondences in the neuroanatomy of the maxillar and maxillipedal thoracic segments, which in turn differs from that of the more posterior, non-maxillipedal thoracic segments.

We found no differences between the maxillar and thoracic neuromeres in Cephalocarida which could point toward an ancestral specialization of the maxillar appendage. The neuroanatomy of Mx2 corresponds to that in thoracic ganglia and is here interpreted as plesiomorphic, in line with the hypothesis cited above that the thoracopod-like cephalocarid "maxilla" is plesiomorphic with respect to the mandibulate ground pattern.

Assuming that the phylogenetic position of Cephalocarida is deep within Tetraconata, as suggested by all recent analyses (e.g., Regier et al., 2010; Koenemann et al., 2010; von Reumont et al., 2012; Oakley et al., 2013), the maxilla in other crustaceans would have to have specialized into a feeding appendage several times independently.

Our comparison confirms Scholtz and Edgecombe's (2006) hypothesis that the fusion of tergites to the head shield, the fusion of neuromeres, and the transformation of limbs were all independent processes (see also Richter et al., 2013). In contrast, there seems to be evolutionary coherence between the shape of a segmental appendage and the anatomy of its associated neuromere (i.e., the pattern of commissures, nerves, SL-ir neurons).

Serotonin-Like Immunoreactive Neurons in the Thorax

Comparing serotonin-like immunoreactive neurons—Theoretical aspects. When comparing and homologizing the SL-ir pattern across Tetraconata, previous authors have, on the basis of the relative position of the neuronal soma, distinguished "anterior," "central," and "posterior" neurons (Harzsch and Waloszek, 2000; Harzsch, 2002, 2003, 2004; Stemme et al., 2010). This classification can only partially be applied to Cephalocarida (for an overview, see Fig. 9C). Neuron s20 in *H. macracantha* is clearly comparable to "anterior" neurons, and neurons s15a and s15b to "posterior" neurons. Since the ventral soma of cephalocarid neuron s18 lies neither anteriorly nor posteriorly in the hemiganglion, it is here compared to "central" neurons. In contrast, somata s14, s16, s17, and s19 lie in such close proximity anteromedially or medially in the ganglion that it is impossible to distinguish between "anterior" and "central" neurons as Harzsch (2002) and Stemme et al. (2010) managed to do in Zygentoma and Remipedia. Moreover, we found that the exact position of somata was subject to a certain degree of variability. Taking this ambiguity into account, we compare the critical cephalocarid neurons to both "anterior" and "central" neurons in other tetraconates. Certain myriapod neurons that were given their own classification (Harzsch, 2004) are also taken into account. Chelicerata differ significantly in their SL-ir pattern (Harzsch, 2004) and are not considered here.

In addition to identifying neurons based on the position of the soma, Harzsch and Waloszek (2000)

distinguished four different neuron types on the basis of neurite morphology. Their classification is established in the literature and may easily be applied to SL-ir neurons in the cephalocarid VNC. Their Type A includes bi- or multipolar neurons whose ipsi- and contralateral neurites exit the soma at separate locations (neurons of this type are absent in the VNC of *H. macracantha*). Type B includes monopolar neurons with a single primary neurite that splits into one ipsi- and one contralateral branch shortly after exiting the soma (neuron s14 in *H. macracantha*). Type C includes monopolar neurons with a single contralateral neurite (neurons s15a, s15b, s17, s19). Finally, Type D includes monopolar neurons with a single ipsilateral neurite (neurons s16, s18, s20).

The intersegmental differences in the SL-ir neuron pattern of *H. macracantha* complicates the straightforward generalization applied in other taxa (Harzsch and Waloszek, 2000; Harzsch, 2002, 2003, 2004). The most appropriate way to compare and homologize cephalocarid neurons s14–s20 with those in other taxa is to compare individual neurons, regardless of the segment in which they occur (this is based on the assumption that there is serial homology between the segments of one specimen). Two neurons can reasonably be concluded to be homologous if they correspond 1) in the position of their soma within the segment and 2) in their neurite type (for more theoretical aspects of homology, see Kutsch and Breidbach, 1994).

Anteromedial neurons s14 and s17. Although anterior neurons across Tetraconata are highly variable, typewise, two anterior SL-ir neurons comparable to s14 (Type B) and s17 (Type C) in *H. macracantha* occur also in Branchiopoda (Harzsch and Waloszek, 2000; Fritsch and Richter, 2010), Anaspidacea (Harrison et al., 1995), and Zygentoma (Harzsch, 2002). Only one SL-ir anterior neuron exists in leptostracan, decapod (Harzsch and Waloszek, 2000), and isopod Malacostraca (Thompson et al., 1994) and in Remipedia (Stemme et al., 2013). The anterior neurons in almost all of these taxa send their neurites through the (single) anterior commissure. Although Cephalocarida exhibit two "anterior" commissures (adc, avc) in the thorax through which the neurites s14 and s17 pass, the pattern is comparable. We, therefore, suggest homology between the cephalocarid s14 and s17 and the anterior neurons in other tetraconates, despite variations in type.

Type A or Type C occurs in notostracan Phyllopoda (Harzsch and Waloszek, 2000; Fritsch and Richter, 2010); Type B in Anostraca (Harzsch and Waloszek, 2000); Type C in spinicaudatan Phyllopoda (Harzsch and Waloszek, 2000), Anaspidacea (Harrison et al., 1995), and Isopoda (Thompson et al., 1994), and in Remipedia (Stemme et al., 2013) and Zygentoma (Harzsch, 2002). Leptostraca (Harzsch and Waloszek, 2000) and Decapoda (Antonsen and Paul, 2001; Harzsch, 2003) are exceptional in exhibiting Type D neurons whose neurites remain ipsilateral and do not contribute to the anterior commissure.

Anterior neurons are absent in Pterygota (Griss, 1989; Radwan et al., 1989; Breidbach, 1991; van Haeften and Schooneveld, 1992; Harzsch, 2002). Harzsch et al. (2005) also described SL-ir anteromedial neurons (which they labeled "c") in Myriapoda, but found no contralateral SL-ir neurites (implying that the neurites remain ipsilateral as in Type D).

Anterior neuron s20. Within Tetraconata, only Cephalocarida possess a third SL-ir anterior Type D neuron s20. In contrast to s14 and s17, this neuron cannot be related to the two anterior SL-ir neurons in the taxa previously mentioned. Interestingly, Myriapoda also feature two anterolateral SL-ir somata (labeled "a" by the author), whose lack of contralateral SL-ir neurites (Harzsch, 2004) may imply that they are Type D.

Anteromedial neuron s16 and ventral neuron s18. Given the either medial or basically central position of their somata, the Type D cephalocarid neurons s16 and s18 correspond to the three SL-ir central neurons that occur per hemineuromere in Remipedia (Stemme et al., 2013), and to the single central neuron in Zygentoma (Harzsch, 2002: see right neurite in his Fig. 5B). The one to four central neurons which Harzsch labeled "b" that occur across Myriapoda are also Type D (Harzsch, 2002: his Fig. 5C,D; Harzsch, 2004). We, therefore, suggest homology between s16 and s18 in Cephalocarida and two of the central neurons in Remipedia and Myriapoda.

Anteromedial neuron s19. Although the cephalocarid neuron s19 features a soma that corresponds in position to the Type D central neurons in Zygentoma (Harzsch, 2002) and Remipedia (Stemme et al., 2013), s19 is Type C, and its homology remains unclear.

Posterior neurons s15a and s15b. Corresponding to the two posterior Type C neurons s15a and s15b in Cephalocarida, two posterior Type C neurons occur in taxa as diverse as Remipedia (Stemme et al., 2013), Cirripedia (Callaway and Stuart, 1999), Zygentoma (Harzsch, 2002), many Pterygota (Harzsch, 2002, reviewed by Harzsch, 2003), Leptostraca (Harzsch and Waloszek, 2000), and Anaspidacea (Harrison et al., 1995). In all these taxa, these neurons contribute their neurites to the (single) posterior commissure. Posterior neurons "e" in Chilopoda (see Harzsch, 2004) display a corresponding pattern, and we suggest homology between all these posterior Type C neurons and the cephalocarid neurons s15a and s15b.

Two posterior Type A or Type B neurons occur across Branchiopoda (Harzsch and Waloszek, 2000; Fritsch and Richter, 2010), in each case

contributing a contralateral neurite to the posterior commissure. Two posterior Type D neurons occur in Decapoda (Harrison et al., 1995; Harzsch, 2003) and Isopoda (Thompson et al., 1994).

Evolutionary implications. Earlier hypotheses on the ground pattern of Tetraconata (Fig. 9A) and Mandibulata (Fig. 9B) based on Harzsch (2004) and Harzsch et al. (2005) have to be reconsidered in the light of our new data on Cephalocarida.

Harzsch et al. (2005) suggested two Type B anterior neurons to be representative of the tetraconate ground pattern. The fact that a corresponding Type B neuron (s14) also exists in Cephalocarida is in line with this hypothesis. In our view (Fig. 9D), however, all hypotheses regarding the type of anterior neurons in the tetraconate or mandibular ground pattern can only be viewed as preliminary in the light of the disparity of types across other taxa.

The two anterolateral neurons "a" in Myriapoda (Harzsch et al., 2005) have been suggested to be representative of the mandibulate ground pattern (Harzsch et al., 2005, Fig. 9B). In the absence of comparable neurons in all other tetraconates, and in line with Harzsch (2004), we consider it unlikely that a single anterior Type D neuron such as s20 in *H. macracantha* (Fig. 9C) is part of the tetraconate ground pattern (Fig. 9D).

Harzsch et al. (2005) suggested four (myriapod-like) central neurons to be part of the mandibulate ground pattern (Fig. 9B). The presence of the two central Type D neurons in Cephalocarida (this study), the three in Remipedia (Stemme et al., 2013), and the one in Zygentoma (Harzsch, 2002) renders it likely that a number (as yet uncertain) of these neurons is part of the tetraconate and mandibulate ground pattern (Fig. 9D). Although neuron s19 in Cephalocarida is unique in being Type C and having a central soma, a condition here suggested to be autapomorphic, it may have derived from an ancestral central Type D neuron (Fig. 9D).

It has been suggested that two posterior Type B neurons represent the tetraconate ground pattern (Fig. 9A; e.g., Harzsch et al., 2005). In the light of our new data on *H. macracantha*, and in the light of the presence of corresponding posterior Type C neurons across mandibulate taxa as diverse as Cephalocarida, Cirripedia, Remipedia, Hexapoda, and Chilopoda, we suggest that the two posterior neurons in both the tetraconate and the mandibulate ground pattern were actually Type C (Fig. 9D). Consequently, different types of posterior neurons as they occur in Branchiopoda would be derived.

Ganglia in the Abdominal Segments

The "abdomen" of entomostracan crustaceans (i.e., non-malacostracans) is traditionally defined as the limbless region of the trunk (Gruner and Scholtz, 2004). On the basis, mainly, of differences in Hox gene expression patterns, Schram and Koenemann (2004) suggested that the entomostracan abdomen (Averof and Akam, 1995), the hexapod abdomen (Angelini and Kaufman, 2004), and the malacostracan pleon (Abzhanov and Kaufman, 2000) are different structures. According to the authors' definition, the entomostracan abdomen is the region of the body which lies posterior to the expression of Hox gene *Abdominal-B* and which shows no Hox gene expression itself. A more rigorous definition which makes reference to the nervous system was suggested by Deutsch and Mouchel-Vielh (2003; based on Deutsch, 2001), who characterized the entomostracan abdomen additionally by its absence of segmental ganglia and commissures.

Indeed, the VNC of some entomostracan taxa features ganglia in the thorax but lacks ganglia in the limbless abdomen. Examples are Anostraca (Harzsch and Glötzner, 2002), Cirripedia (Hanström, 1928: pp. 430–433; Allison, 1981; Walker, 1992), Copepoda (Scott, 1901; Park, 1966; see Boxshall, 1992), and Branchiura (Leydig, 1889; Zaćwilichowski, 1935; Zaćwilichowska, 1948). The last ganglion in Branchiura has, erroneously, repeatedly been taken for abdominal by investigators who took into account its position but did not trace the nerves distally (Hanström, 1928; Martin, 1932; Overstreet et al., 1992).

In contrast to this, in the homonomous trunk of Remipedia (Fanenbruck and Harzsch, 2005) and Myriapoda (Hanström, 1928; Harzsch et al., 2005) and in the tagmatized trunk (composed of an eight-segmental thorax and a six-segmental pleon) of Eumalacostraca (Hanström, 1928; Chaudonneret, 1978a), every segment bears limbs and is equipped with a pair of ganglia which give rise to appendage nerves. Ganglia may be fused in the midline or anteroposteriorly. Leptostraca differ from their sister-group Eumalacostraca in exhibiting an additional limbless seventh pleonal segment that apparently lacks a ganglion (Claus, 1888; Cannon, 1960). Manton (1934), however, found the sixth and seventh pleonal ganglia to have fused within the sixth pleonal segment of Leptostraca.

Abdominal ganglia in Mystacocarida and Cephalocarida. Any notion of coherence between segmental appendages and the presence of corresponding ganglia and commissures in the VNC (see Deutsch and Mouchel-Vielh, 2003) is contradicted by our finding of ganglia and commissures in some abdominal segments of Mystacocarida (Brenneis and Richter, 2010) and Cephalocarida (this study). Though it is the last two abdominal segments that lack ganglia in both Mystacocarida and Cephalocarida, there are various neuroanatomical differences between the taxa. In Cephalocarida, the abdominal ganglia differ considerably from the thoracic ganglia in shape, size, commissural pattern, and SL-ir pattern (this study), while abdominal ganglia 1–3 in Mystacocarida correspond in many respects to

thoracic ganglia 2–5 (Brenneis and Richter, 2010). While two segmental SL-ir neurons are present in each abdominal hemiganglion of Cephalocarida, they are completely absent in the abdominal (and thoracic) hemiganglia of Mystacocarida (Brenneis and Richter, 2010). Conversely, only Mystacocarida feature a pair of tegumentary sensory nerves in each abdominal segment, arising either from the ganglia themselves (Ab1–Ab3) or, where those are absent, directly from the paired longitudinal neurite bundles (Ab4 and Ab5; Brenneis and Richter, 2010).

Neither Mystacocarida nor Cephalocarida exhibit any specific indications of ancestral limbs in their ganglionic abdominal segments (see also Brenneis and Richter, 2010). All the segments of the mystacocarid abdomen, irrespective of the presence of ganglia, correspond in their pattern of muscles (Hessler, 1964; Brenneis and Richter, 2010) and sensory pegs (Elofsson and Hessler, 2005). In Cephalocarida, the dorsal and ventral longitudinal muscles extend straight through from Th1 to Ab10 with no difference between ganglionic segments and segments without ganglia (Hessler, 1964: his Fig. 1b). Both Cephalocarida (Elofsson and Hessler, 1998: their Fig. 12) and Mystacocarida (Baccari and Renaud-Mornant, 1974: their Fig. 2) feature specific glands that only occur in the two ganglia-free abdominal segments.

Evolutionary interpretation. The fact that four mandibulate taxa (Myriapoda, Malacostraca, Remipedia, and Hexapoda in their ground pattern) have a trunk with an almost full compliment of segmental appendages and ganglia suggests that the same pattern was present in the ancestor of all Mandibulata. Walossek (1993) suggested a limbless abdomen to be an apomorphy of Entomostraca, but recent phylogenetic analyses have cast doubt on the monophyly of Entomostraca (e.g., Regier et al., 2010; Koenemann et al., 2010; von Reumont et al., 2012; Oakley et al., 2013). All recent cladograms imply that taxa with a thorax bearing limbs and ganglia but an abdomen free of ganglia on the one hand, and taxa with a trunk bearing limbs and ganglia on the other have a diffuse taxonomic distribution, and also that Cephalocarida and Mystacocarida—, i.e., the only crustaceans featuring abdominal ganglia—, are phylogenetically distant within Tetraconata. Under these circumstances, and in the light of the structural differences mentioned above in the abdominal nervous system across taxa, a limbless abdomen seems to have evolved several times independently within Tetraconata.

Nomenclature. Neuroanatomical differences in the mystacocarid and cephalocarid abdomen raise the problem of whether the abdomen in these taxa constitutes one tagma or two. If the presence or absence of ganglia is used as a defining criterion for thorax or abdomen, respectively (as suggested by Deutsch, 2001), the ganglion-bearing anterior part of the "abdomen" suddenly becomes problematic and would have to be viewed as a separate intermediate tagma situated between the thorax and the posterior "true abdomen," which lacks ganglia. If the definition is based purely on the presence/absence of limbs, the cephalocarid and mystacocarid abdomen constitutes one tagma, like the abdomen in other entomostracan taxa. The evolutionary significance of this nomenclatural problem will only be revealed when the function of abdominal ganglia and the Hox gene expression pattern in Cephalocarida and Mystacocarida are investigated.

Stomatogastric Nervous System

Labral commissure, labral neuropil, dorsomedian neurite bundle. A labral neuropil is situated at the vertex of the labral commissure that arises from the tritocerebrum in Cephalocarida (Stegner and Richter, 2011), Anostraca (Harzsch and Glötzner, 2002), and Mystacocarida (Brenneis and Richter, 2010). The labral neuropil in Anostraca and Mystacocarida is embedded in a coherent cortex of somata, thus forming a true "labral ganglion" (Harzsch and Glötzner, 2002; Brenneis and Richter, 2010), while the cephalocarid neuropil is only associated with a few diffuse somata (Stegner and Richter, 2011). Malacostraca exhibit a comparable but more complex pattern, featuring two or more commissures that are connected to an unpaired longitudinal "stomatogastric nerve" bearing two or more median ganglia rather than one (Chaudonneret, 1978b; Tierney et al., 1999; Böhm et al., 2001; Vilpoux et al., 2006). The malacostracan stomatogastric nerve (labeled "dvn" in Tierney et al., 1999: their Fig. 1) extends dorsally along the gut and innervates the stomach via medial ("mvn") and lateral ("lvn") branches. The labral ganglia in other crustaceans are connected to the brain by an unpaired inferior ventricular nerve (see citations above) which is not present in *H. macracantha*. Also the "frontal ganglion" which lies anterior to the gut in Hexapoda is associated with the tritocerebrum via a commissure and gives rise to an unpaired "recurrent nerve" extending posteriorly along the dorsal side of the gut (e.g., Chapman, 1985; Rand and Ayali, 2010). Corresponding to the stomatogastric nerve in Malacostraca (Tierney et al., 1999), the recurrent nerve in Hexapoda is connected with an additional "hypocerebral ganglion" posteriorly, from where each side of the esophagus is innervated via one inner and one outer esophageal nerve, respectively (Rand and Ayali, 2010). Although a hypocerebral ganglion is absent in Cephalocarida, we suggest that the pattern of innervation of the pyloric region of the gut (see Elofsson et al., 1992 for the digestive system in *H. macracantha*) by an unpaired dorsomedian neurite bundle and a pair of offbranching dorsolateral neurite bundles in Cephalocarida corresponds to the pattern in Malacostraca and Hexapoda.

Lateral neurite bundle. A lateral neurite bundle exists also in various other crustaceans such as Branchiopoda (Kirsch and Richter, 2007; Fritsch and Richter, 2012), Malacostraca (Chaudonneret, 1978b; Weiss et al., 2003), and Mystacocarida (Brenneis and Richter, 2010). The association between the lateral neurite bundle and the dorsoventral musculature found in Cephalocarida (this study) has not been shown in other taxa but is assumed to exist in the telson of Cladocera (Kirsch and Richter, 2007). Weiss et al. (2003) showed one of the two lateral neurite bundles per body side in Isopoda to comprise RFL-ir neurites that innervate the longitudinal musculature in the thorax and pleon.

Median neurite bundle. An unpaired median neurite bundle also exists in Malacostraca (Chaudonneret, 1978b; Harzsch et al., 1997; Gerberding and Scholtz, 2001; Vilpoux et al., 2006) and Mystacocarida (Brenneis and Richter, 2010), but is absent in Branchiopoda (Harzsch and Glötzner, 2002; Kirsch and Richter, 2007; Fritsch and Richter, 2010). Brenneis and Richter (2010) suggested it to be an autapomorphy of Tetraconata. As in Cephalocarida, the median neurite bundle in other taxa is connected to the pair of (main) longitudinal neurite bundles of the VNC by segmental commissures (Chaudonneret, 1978a; Brenneis and Richter, 2010). The additional connection between the median neurite bundle and the lateral neurite bundle formed by transverse neurite bundles is unique for cephalocarids.

Phylogenetic Implications

Many features which we discovered in the VNC of *H. macracantha* are interpreted here as plesiomorphic with respect to the tetraconate ground pattern. These include the dorsomedian and dorsolateral neurite bundle of the stomatogastric nervous system, the lateral neurite bundle, the median neurite bundle, the presence of abdominal ganglia, the posterior SL-ir neurons s15a and s15b, and the SL-ir neurons s16 and s18. Certain components of the olfactory system have also recently been traced back to the ur-tetraconate (and ur-mandibulate; see Stegner and Richter, 2011). Due to their diffuse taxonomic distribution across Tetraconata, however, the phylogenetic value of other features such as the three-segmental subesophageal ganglion, the anterior SL-ir neurons s14, s17, s20, and the central neuron s19 remains doubtful. Potential synapomorphies with other tetraconates which could contribute to the debate on internal tetraconate phylogeny (reviewed by Jenner, 2010; see also von Reumont et al., 2012; Oakley et al., 2013) continue, then, to be elusive.

Though a close relationship between Cephalocarida, Remipedia, and Hexapoda is implied by several molecular analyses, morphological evidence is still lacking. Harzsch (e.g., 2006) pointed out the phylogenetic significance of the segmental SL-ir pattern in Arthropoda, which was one emphasis of our study. In the light of our new data on Cephalocarida and a recent study on Remipedia (Stemme et al., 2013), several SL-ir neurons do indeed appear to be potentially homologous between the two taxa (one anterior Type C neuron, two central Type D neurons, two posterior Type C neurons). We interpret these neurons as being symplesiomorphic with respect to the ground pattern of Tetraconata, for the reason that every single one of them has a potentially homologous counterpart in the myriapod outgroup (Harzsch, 2002, 2004). Harzsch (2004) mentioned difficulties in tracing neurites from anterior and central neurons in Myriapoda, and a more detailed description of SL-ir neurons in the myriapod VNC could make a valuable contribution toward testing our hypothesis of symplesiomorphy. We suggest that the tetraconate ground pattern is more complex than hitherto assumed (Fig. 9D). If this is the case, the homologies identified between Remipedia and Cephalocarida would be uninformative with regard to inner-tetraconate phylogeny.

Finally, some features of the cephalocarid VNC are unique in Tetraconata and may be interpreted as autapomorphic. These include the thoracic commissural pattern, the connection between the median and lateral neurite bundles, the fact that SL-ir neuron s19 is Type C, and the presence of the SL-ir neuron s20. Although, in this light, the adult nervous system of Cephalocarida is certainly not that of a "living fossil," it has still retained many structures and patterns from the tetraconate ground pattern that were lost in other taxa.

ACKNOWLEDGMENTS

We thank George Hampson, Steve Aubrey, Christian Wirkner, Günther Jirikowski, Jonas Keiler, Bastian-Jesper Klußmann-Fricke, Martin Fritsch, and all the volunteers who helped to collect cephalocarids. Thanks to Simone Bourgeois and the late Arthur Dutra from SeaLab, New Bedford, for kindly offering laboratory space and help during our collecting trips. We are grateful to Kerstin Schwandt for a series of semithin sections. Special thanks to Christin Wittfoth, who created two elaborate 3D-schematics in Maya and helped refine 3D-reconstructions in Imaris. We are grateful to Steffen Harzsch (SLI in the VNC), Ole Møller (Branchiura), Andy Sombke (Myriapoda), Torben Stemme (Remipedia), Torben Göpel and Katarina Huckstorf (Maya and Deep Exploration software) for their expertise and the fruitful discussions that made such a valuable contribution to this manuscript. We thank Lucy Cathrow who improved the English.

LITERATURE CITED

Abzhanov A, Kaufman TC. 2000. Crustacean (malacostracan) Hox genes and the evolution of the arthropod trunk. Development 127(11):2239–2249.

Allison P. 1981. Aspects of the Neurobiology of *Balanus hameri* [dissertation]. Bangor: University of Wales.

Ando H, Kuwasawa K. 2004. Neuronal and neurohormonal control of the heart in the stomatopod crustacean, *Squilla oratotia*. J Exp Biol 207(26):4663–4677.

Andrew DR, Brown SM, Strausfeld NJ. 2012. The minute brain of the copepod *Tigriopus californicus* supports a complex ancestral ground pattern of the tetraconate cerebral nervous systems. J Comp Neurol 520(15):3446–3470.

Angelini DR, Kaufman TC. 2004. Functional analyses in the hemipteran *Oncopeltus fasciatus* reveal conserved and derived aspects of appendage patterning in insects. Dev Biol 271(2):306–321.

Antonsen BL, Paul DH. 2001. Serotonergic and octopaminergic systems in the squat lobster *Munida quadrispina* (Anomura, Galatheidae). J Comp Neurol 439(4):450–468.

Averof M, Akam M. 1995. Insect-crustacean relationships: Insights from comparative developmental and molecular studies. Philos Trans R Soc London Ser B 347(1321):293–303.

Baccari S, Renaud-Mornant J. 1974. Etude du système nerveux de *Derocheilocaris remanei* Delamare et Chappuis 1951 (Crustacea Mystacocarida). Cah Biol Mar 15:589–604.

Böhm H, Dybek E, Heinzel HG. 2001. Anatomy and in vivo activity of neurons connecting the crustacean stomatogastric nervous system to the brain. J Comp Physiol A 187(5):393–403.

Boxshall GA. 1992. Copepoda. In: Harrison FW, Humes AG, editors. Microscopic Anatomy of Invertebrates. New York, Chichester, Brisbane, Toronto, Singapore: Wiley-Liss. pp 347–384.

Boxshall GA. 2004. The evolution of arthropod limbs. Biol Rev 79(2):253–300.

Breidbach O. 1991. Constancies in the neuronal architecture of the subesophageal ganglion at metamorphosis in the beetle *Tenebrio molitor* L. Cell Tissue Res 266(1):173–190.

Brenneis G, Richter S. 2010. Architecture of the nervous system in Mystacocarida (Arthropoda, Crustacea)—An immunohistochemical study and 3D-reconstruction. J Morphol 271(2): 169–189.

Budd GE. 2001. Why are arthropods segmented? Evol Dev 3(5): 332–342.

Bullock TH, Horridge GA. 1965. Structure and Function in the Nervous Systems of Invertebrates. San Francisco: D.H. Freeman.

Callaway JC, Stuart AE. 1999. The distribution of histamine and serotonin in the barnacle's nervous system. Microsc Res Tech 44(2–3):94–104.

Cannon HG. 1940. On the anatomy of *Gigantocypris mülleri*. Discov Rep 19:185–244.

Cannon HG. 1960. Leptostraca. In: Gruner H-E, editor. Dr. H.G. Bronns Klassen und Ordnungen des Tierreichs, Band 5, Abteilung 1, Buch 4, Teil 1. Band ed. Leipzig: Geest & Portig. pp 1–81.

Chapman RF. 1985. Structure of the digestive system. In: Kerekut GA, editor. Comprehensive Insect Physiology Biochemistry and Pharmacology. Oxford: Pergamon Press. pp 165–212.

Chaudonneret J. 1978a. Évolution de la chaine nerveuse latérale chez quelques malacostracés. Arch Zool Exp Gén 119: 163–184.

Chaudonneret J. 1978b. La phylogenèse du système nerveux annélido-arthropodien. Bull Soc Zool Fr 103:69–95.

Claus C. 1888. Über den Organismus der Nebaliden und die systematische Stellung der Leptostraken. Arbeiten aus dem zoologischen Institute der Universität Wien und der zoologischen Station Triest 8(1):1–148.

Deutsch JS. 2001. Are Hexapoda members of the Crustacea? Evidence from comparative developmental genetics. Ann Soc Entomol Fr 37(1–2):41–49.

Deutsch JS, Mouchel-Vielh E. 2003. Hox genes and the crustacean body plan. Bioessays 25(9):878–887.

Elofsson R. 1992. Monoaminergic and peptidergic neurons in the nervous system of *Hutchinsoniella macracantha* (Cephalocarida). J Crustacean Biol 12(4):531–536.

Elofsson R, Hessler RR. 1990. Central nervous system of *Hutchinsoniella macracantha* (Cephalocarida). J Crustacean Biol 10(3):423–439.

Elofsson R, Hessler RR. 1998. Tegumental glands of *Hutchinsoniella macracantha* (Cephalocarida). J Crustacean Biol 18(1):42–56.

Elofsson R, Hessler RR. 2005. The tegumental sensory organ and nervous system of *Derocheilocaris typica* (Crustacea: Mystacocarida). Arthropod Struct Dev 34(2):139–152.

Elofsson R, Hessler RR, Hessler AY. 1992. Digestive system of the cephalocarid *Hutchinsoniella macracantha*. J Crustacean Biol 12:4–571.

Fahlander K. 1938. Beiträge zur Anatomie und systematischen Einteilung der Chilopoden. Zoologiska Didraf från Uppsala 17:1–148.

Fanenbruck M, Harzsch S. 2005. A brain atlas of *Godzilliognomus frondosus* Yager, 1989 (Remipedia, Godzilliidae) and comparison with the brain of *Speleonectes tulumensis* Yager, 1987 (Remipedia, Speleonectidae): Implications for arthropod relationships. Arthropod Struct Dev 34(3):343–378.

Fritsch M, Richter S. 2010. The formation of the nervous system during larval development in *Triops cancriformis* (Bosc) (Crustacea, Branchiopoda): An immunohistochemical survey. J Morphol 271(12):1457–1481.

Fritsch M, Richter S. 2012. Nervous system development in Spinicaudata and Cyclestherida (Crustacea, Branchiopoda): Comparing two different modes of indirect development by using an event pairing approach. J Morphol 273(7):672–695.

Gerberding M, Scholtz G. 2001. Neurons and glia in the midline of the higher crustacean *Orchestia cavimana* are generated via an invariant cell lineage that comprises a median neuroblast and glial progenitors. Dev Biol 235(2):397–409.

Giribet G, Edgecombe GD. 2012. Reevaluating the arthropod tree of life. Annu Rev Entomol 57:167–186.

Griss C. 1989. Serotonin-immunoreactive neurons in the subesophageal ganglion of the caterpillar of the hawk moth *Manduca sexta*. Cell Tissue Res 258(1):101–109.

Gruner H-E, Scholtz G. 2004. Segmentation, tagmata, and appendages. In: Forest J, von Vaupel-Klein JC, Schram FR, editors. Treatise on Zoology—Anatomy, Taxonomy, Biology. The Crustacea Revised and Updated from the Traité de Zoologie. Leiden: Koninklijke Brill. pp 13–57.

Hanström B. 1928. Vergleichende Anatomie des Nervensystems der wirbellosen Tiere unter Berücksichtigung seiner Funktion. Berlin, Heidelberg, New York: Julias Springer.

Harrison PJ, Macmillan DL, Young HM. 1995. Serotonin immunoreactivity in the ventral nerve cord of the primitive crustacean *Anaspides tasmaniae* closely resembles that of crayfish. J Exp Biol 198(2):531–535.

Harrison PJH, Sandeman DC. 1999. Morphology of the nervous system of the barnacle cypris larva (*Balanus amphitrite* Darwin) revealed by light and electron microscopy. Biol Bull 197(2):144–158.

Hartmann G. 1967. Ostracoda. In: Gruner H-E, editor. Dr. H. G. Bronns Klassen und Ordnungen des Tierreichs, Band 5, Abteilung 1, Buch 2, Teil 4. Leipzig: Akademische Verlagsgesellschaft Geest & Portig K.-G. pp 275–311.

Harzsch S. 2002. Neurobiologie und Evolutionsforschung: „Neurophylogenie" und die Stammesgeschichte der Euarthropoda. Neuroforum 4(02):267–273.

Harzsch S. 2003. Evolution of identified arthropod neurons: The serotonergic system in relation to engrailed-expressing cells in the embryonic ventral nerve cord of the American lobster *Homarus americanus* Milne Edwards, 1873 (Malacostraca, Pleocyemata, Homarida). Dev Biol 258(1):44–56.

Harzsch S. 2004. Phylogenetic comparison of serotonin-immunoreactive neurons in representatives of the Chilopoda, Diplopoda, and Chelicerata: Implications for arthropod relationships. J Morphol 259(2):198–213.

Harzsch S. 2006. Neurophylogeny: Architecture of the nervous system and a fresh view on arthropod phyologeny. Integr Comp Biol 46(2):162–194.

Harzsch S. 2007. The architecture of the nervous system provides important characters for phylogenetic reconstructions: Examples from the Arthropoda. Species Phylogeny Evol 1:33–57.

Harzsch S, Glötzner J. 2002. An immunohistochemical study of structure and development of the nervous system in the brine shrimp *Artemia salina* Linnaeus, 1758 (Branchiopoda, Anostraca) with remarks on the evolution of the arthropod brain. Arthropod Struct Dev 30(4):251–270.

Harzsch S, Waloszek D. 2000. Serotonin-immunoreactive neurons in the ventral nerve cord of Crustacea: A character to study aspects of arthropod phylogeny. Arthropod Struct Dev 29:307–322.

Harzsch S, Anger K, Dawirs RR. 1997. Immunocytochemical detection of acetylated alpha-tubulin and *Drosophila* synapsin in the embryonic crustacean nervous system. Int J Dev Biol 41(3):477–484.

Harzsch S, Müller CHG, Wolf H. 2005. From variable to constant cell numbers: Cellular characteristics of the arthropod nervous system argue against a sister-group relationship of Chelicerata and "Myriapoda" but favour the Mandibulata concept. Dev Genes Evol 215(2):53–68.

Henry L. 1948. The nervous system and the segmentation of the head in the Annulata. Section IV Arthropoda. Microentomol 13:1–26.

Hessler RR. 1964. The Cephalocarida—Comparative skeletomusculature. Mem Conn Acad Arts Sci 16:1–97.

Hessler RR. 1992. Reflections on the phylogenetic position of the Cephalocarida. Acta Zool 73:315–316.

Hessler RR, Elofsson R. 1992. Cephalocarida. In: Harrison FW, editor. Microscopic Anatomy of Invertebrates. New York: Wiley-Liss. pp 9–24.

Hessler RR, Elofsson R, Hessler AY. 1995. Reproductive system of *Hutchinsoniella macracantha* (Cephalocarida). J Crustacean Biol 15(3):493–522.

Huys R. 1991. Tantulocarida (Crustacea, Maxillopoda)—A new taxon from the temporary meiobenthos. Mar Ecol—Pubblicazioni Della Stazione Zoologica di Napoli I 12(1):1–34.

Jenner RA. 2010. Higher-level crustacean phylogeny: Consensus and conflicting hypotheses. Arthropod Struct Dev 39(2–3): 143–153.

Kenning M, Müller C, Wirkner CS, Harzsch S. 2013. The Malacostraca (Crustacea) from a neurophylogenetic perspective: New insights from brain architecture in *Nebalia herbstii* Leach, 1814 (Leptostraca, Phyllocarida). Zool Anz 252:319–336.

Kirsch R, Richter S. 2007. The nervous system of *Leptodora kindtii* (Branchiopoda, Cladocera) surveyed with confocal scanning microscopy (CLSM), including general remarks on the branchiopod neuromorphological ground pattern. Arthropod Struct Dev 36(2):143–156.

Koenemann S, Jenner RA, Hoenemann M, Stemme T, von Reumont BM. 2010. Arthropod phylogeny revisited, with a focus on crustacean relationships. Arthropod Struct Dev 39(2–3):88–110.

Kutsch W, Breidbach O. 1994. Homologous structures in the nervous systems of Arthropoda. Adv Insect Physiol 24:1–114.

Lauterbach K-E. 1974. Die Muskulatur der Pleurotergite im Grundplan der Euarthropoda. Zool Anz 193(1/2):70–84.

Lauterbach K-E. 1980. Schlüsselereignisse in der Evolution des Grundplans der Mandibulata (Arthropoda). Abhandlungen aus dem Gebiete der Naturwissenschaften, Naturwissenschaftlicher Verein Hamburg 23:105–161.

Lauterbach K-E. 1983. Zum Problem der Monophylie der Crustacea. Verhandlungen des naturwissenschaftlichen Vereins Hamburg 26:293–320.

Lauterbach K-E. 1986. Zum Grundplan der Crustacea. Verhandlungen des naturwissenschaftlichen Vereins Hamburg 28:27–63.

Leydig F. 1889. Ueber *Argulus foliaceus*. Archiv für mikroskopische Anatomie 23:1–51.

Manton SM. 1934. On the embryology of the crustacean *Nebalia bipes*. Philos Trans R Soc 223:163–238.

Martin MF. 1932. On the morphology and classification of *Argulus* (Crustacea). Proc Zool Soc London 103:771–806.

Mulisch M, Welsch U. 2010. Romeis. Mikroskopische Technik. 18. Auflage. Heidelberg: Spektrum Akademischer Verlag.

Niven JE, Graham CM, Burrows M. 2008. Diversity and evolution of the insect ventral nerve cord. Annu Rev Entomol 53: 253–271.

Oakley TH, Wolfe JM, Lindgren AR, Zaharoff AK. 2013. Phylotranscriptomics to bring the understudied into the fold: Monophyletic Ostracoda, fossil placement, and pancrustacean phylogeny. Mol Biol Evol 30(1):215–233.

Olesen J, Haug JT, Maas A, Waloszek D. 2011. External morphology of *Lightiella monniotae* (Crustacea, Cephalocarida) in the light of Cambrian "Orsten" crustaceans. Arthropod Struct Dev 40(5):449–478.

Overstreet RM, Dyková I, Hawkins WE. 1992. Branchiura. In: Harrison FW, Humes AG, editors. Microscopic Anatomy of the Invertebrates, Vol. 9: Crustacea. New York: Wiley-Liss. pp 385–413.

Park TS. 1966. The biology of a calanoid copepod, *Epilabidocera amphitrites* McMurrich. Cellule 66:129–251.

Radwan WA, Lauder JM, Granger NA. 1989. Development and distribution of serotonin in the central nervouss system of *Manduca sexta* during embryogenesis. 2. The ventral ganglia. Int J Dev Neurosci 7(1):43–53.

Rand D, Ayali A. 2010. Neuroanatomy and neurophysiology of the locust hypocerebral ganglion. J Insect Physiol 56:884–892.

Regier JC, Shultz JW, Zwick A, Hussey A, Ball B, Wetzer R, Martin JW, Cunningham CW. 2010. Arthropod relationships revealed by phylogenomic analysis of nuclear protein-coding sequences. Nature 463(7284):1079–1098.

Richter S, Scholtz G. 2001. Phylogenetic analysis of the Malacostraca (Crustacea). J Zool Syst Evol Res 39(3):113–136.

Richter S, Loesel R, Purschke G, Schmidt-Rhaesa A, Scholtz G, Stach T, Vogt L, Wanninger A, Brenneis G, Döring C, Faller S, Fritsch M, Grobe P, Heuer CM, Kaul S, Møller OS, Müller CHG, Rieger V, Rothe BH, Stegner MEJ, Harzsch S. 2010. Invertebrate neurophylogeny: Suggested terms and definitions for a neuroanatomical glossary. Front Zool 7:29.

Richter S, Stein M, Frase T, Szucsich NU. 2013. The arthropod head. In: Minelli A, Boxshall GA, Fusco G, editors. Arthropod Biology and Evolution. Berlin, Heidelberg: Springer-Verlag. pp 223–240.

Sanders HL. 1954. The Cephalocarida, a new subclass of Crustacea from Long Island Sound. PNAS 41:61–66.

Sanders HL. 1957. The Cephalocarida and crustacean phylogeny. Syst Zool 6(3):112–148.

Sanders HL. 1963. The Cephalocarida. Mem Conn Acad Arts Sci 15:1–80.

Schmitz EH. 1989. Anatomy of the central nervous system of *Armadillidium vulgare* (Latreille) (Isopoda). J Crustacean Biol 9(2):217–227.

Schneider H, Trimmer BA, Rapus J, Eckert M, Valentine DE, Kravitz EA. 1993. Mapping of octopamine-immunoreactive neurons in the central nervous system of the lobster. J Comp Neurol 329:129–142.

Scholtz G. 1997. Cleavage, germ band formation and head segmentation: The ground pattern of the Euarthropoda. In: Fortney RA, Thomas RH, editors. Arthropod Relationships. London: Chapman & Hall. pp 317–332.

Scholtz G, Edgecombe GD. 2005. Heads, Hox and the phylogenetic position of trilobites. In: Koenemann S, Jenner RA, editors. Crustacea and Arthropod Relationships. Boca Raton, London, New York, Singapore: Tailor Francis Group. pp 139–165.

Scholtz G, Edgecombe GD. 2006. The evolution of arthropod heads: Reconciling morphological, developmental and palaeontological evidence. Dev Genes Evol 216(7–8):395–415.

Schram FR, Koenemann S. 2004. Developmental genetics and arthropod evolution: On body regions of Crustacea. Lisse: Balkema. pp 75–92.

Scott A. 1901. *Lepeophtheirus* and *Lernea*. L.M.B.C. Mem Typical Br Mar Plants Anim 6:1–54.

Sombke A, Rosenberg J, Hilken G. 2011. Chilopoda—Nervous system. In: Minelli A, editor. Treatise on Zoology—Anatomy, Taxonomy, Biology. The Myriapoda, Vol. 1. Leiden, Boston: Brill. pp 217–234.

Stegner MEJ, Richter S. 2011. Morphology of the brain in *Hutchinsoniella macracantha* (Cephalocarida, Crustacea). Arthropod Struct Dev 40:221–243.

Stegner MEJ, Fritsch M, Richter S. The central complex in Crustacea. In: Wägele JW, Bartholomäus T Misof B, Vogt L, editors. Deep Metazoan Phylogeny: The backbone of the Tree of Life. Berlin: De Gruyter, in press.

Stemme T, Bicker G, Harzsch S, Koenemann S. 2010. Die rätselhaften Grottenkrebse der Blue Holes. Naturhistorica—Berichte der Naturhistorischen Gesellschaft Hannover 152: 7–28.

Stemme T, Iliffe TM, von Reumont BM, Koenemann S, Harzsch S, Bicker G. 2013. Serotonin-immunoreactive neurons in the ventral nerve cord of Remipedia (Crustacea): Support for a sister group relationship of Remipedia and Hexapoda? BMC Evol Biol 13:119.

Strausfeld NJ. 1976. Atlas of an Insect Brain. Berlin, Heidelberg, New York: Springer.

Szucsich NU, Scheller U. 2011. Symphyla. In: Minelli A, editor. Treatise on Zoology—Anatomy, Taxonomy, Biology. The Myriapoda, Vol. 1. Leiden: Brill. pp 445–466.

Thompson KSJ, Zeidler MP, Bacon JP. 1994. Comparative anatomy of serotonin-like immunoreactive neurons in isopods—Putative homologs in several species. J Comp Neurol 347(4): 553–569.

Tiegs OW, Manton SM. 1958. The evolution of the Arthropoda. Biol Rev Camb Philos Soc 33:255–337.

Tierney AJ, Godleski MS, Rattananont P. 1999. Serotonin-like immunoreactivity in the stomatogastric nervous systems of crayfishes from four genera. Cell Tissue Res 295(3):537–551.

van Haeften T, Schooneveld H. 1992. Serotonin-like immunoreactivity in the ventral nerve cord of the Colorado potato beetle, *Leptinotarsa decemlineata*: identification of five different neuron classes. Cell Tissue Res 270:405–413.

Vilpoux K, Sandeman R, Harzsch S. 2006. Early embryonic development of the central nervous system in the Australian crayfish and the Marbled crayfish (Marmorkrebs). Dev Genes Evol 216(4):209–223.

von Reumont BM, Jenner RA, Wills MA, Dell'Ampio E, Pass G, Ebersberger I, Meyer B, Koenemann S, Iliffe TM, Stamatakis A, Niehuis O, Meusemann K, Misof B. 2012. Pancrustacean phylogeny in the light of new phylogenomic data: Support for Remipedia as the possible sister group of Hexapoda. Mol Biol Evol 29(3):1031–1045.

Walker G. 1992. Cirripedia. In: Harrison FW, Humes AG, editors. Microscopic Anatomy of Invertebrates, Vol. 9: Crustacea. New York, Chichester, Brisbane, Toronto, Singapore: Wiley-Liss, Inc. pp 249–311.

Walossek D. 1993. The upper Cambrian *Rehbachiella kinnekullensis* and the phylogeny of Branchiopoda and Crustacea. Fossils Strata 32:1–202.

Walossek D, Müller KJ. 1990. Upper Cambrian stem-lineage crustaceans and their bearing upon the position of *Agnostus*. Lethaia 23:409–427.

Waloszek D, Chen J-Y, Maas A, Wang X. 2005. Early Cambrian arthropods—New insights into arthropod head and structural evolution. Arthropod Struct Dev 34(2):189–205.

Weiss T, Kreissl S, Rathmayer W. 2003. Localization of a FMRFamide-related peptide in efferent neurons and analysis of neuromuscular effects of DRNFLRFamide (DF2) in the crustacean *Idotea emarginata*. Eur J Neurosci 17(2):239–248.

Wildt M, Goergen EM, Benton JL, Sandeman DC, Beltz BS. 2004. Regulation of serotonin levels by multiple light-entrainable endogenous rhythms. J Exp Biol 207(21):3765–3774.

Zaćwilichowska K. 1948. The nervous system of the carplouse *Argulus foliaceus* L. Bulletin International de l'Académie Polonaise des Sciences et des Lettres, Classe des Sciences Mathematiques et Naturelles, Série B: Sciences Naturelles II 1: 117–128.

Zaćwilichowski J. 1935. Über die Innervation der Haftapparate der Karpfenlaus *Argulus foliaceus* L. (Branchiura). Bulletin International de l'Académie Polonaise des Sciences et des Lettres, Classe des Sciences Mathematiques et Naturelles, Série B: Sciences Naturelles II 2:145–162.

Zajac JM, Mollereau C. 2006. Special issue: RFamide peptides—Introduction. Peptides 27(5):941–942.

13. Development of the nervous system in Cephalocarida. Stegner MEJ, Richter S (2015). Zoomorphology 134:183-209.

Zoomorphology (2015) 134:183–209
DOI 10.1007/s00435-014-0248-1

ORIGINAL PAPER

Development of the nervous system in Cephalocarida (Crustacea): early neuronal differentiation and successive patterning

Martin E. J. Stegner · Stefan Richter

Received: 22 May 2014 / Revised: 31 October 2014 / Accepted: 10 November 2014 / Published online: 13 January 2015

Abstract The development of the nervous system in the cephalocarid *Hutchinsoniella macracantha* is investigated here for the first time using a combination of immunolabeling (tubulin, serotonin), nuclear counterstaining, confocal laser scanning microscopy, and computer-aided 3D reconstruction in order to compare cephalocarids to the growing number of other arthropods into which neurodevelopmental studies have been carried out. The existing description of external larval development in *H. macracantha* is complemented by a description of hitherto unknown embryonic and larval stages. The early embryo exhibits the three naupliar appendage anlagen (antennula, antenna, and mandible) and a short maxillular bud, all equipped with a segmental appendage nerve. As in other crustaceans, neurites of the proto-, deuto-, and tritocerebrum form a circumesophageal ring. In the late embryo, several telsonic neurons send their neurites anteriorly into the ventral nerve cord in a manner reminiscent of posterior pioneer neurons. The hatching metanauplius already comprises a well-developed brain, a subesophageal ganglion made up of three fused neuromeres, and four distinctive neuromeres containing segmental commissures in the yet limbless prospective thorax. Most postnaupliar segments arise from a distinct growth zone situated anterior to the telson that proliferates cells anteriorly. Neuronal differentiation begins before new segments are externally separated from the trunk ending and, in the thorax, before the formation of limb anlagen, i.e., earlier than in all other crustaceans studied so far. In the growth zone of one hatchling, we found a pair of large apical cells adjacent to an inward-pointing row of three smaller cells, an arrangement reminiscent of the neuroblasts and ganglion mother cells in other crustaceans. In the trunk, segmental nerves, commissures, and serotonin-like immunoreactive neurons differentiate successively from anterior to posterior. The sequence in which serially homologous neural features develop is basically the same throughout all segments of the trunk and correlated with the differentiation of limbs. It appears that the neuroanatomical differences between the adult thorax and the abdomen result from this developmental sequence stopping earlier in the abdomen than in the thorax.

Keywords Anameric/anamorphic development · Axogenesis · Heterochrony · Mandibulata · Metanauplius · Nauplius · Neurogenesis · Tetraconata

Communicated by Andreas Schmidt-Rhaesa.

Electronic supplementary material The online version of this article (doi:10.1007/s00435-014-0248-1) contains supplementary material, which is available to authorized users.

M. E. J. Stegner (✉) · S. Richter
Allgemeine und Spezielle Zoologie, Universität Rostock, Universitätsplatz 2, 18055 Rostock, Germany
e-mail: feuerschwade@yahoo.com

Introduction

We recently conducted a series of investigations into the adult nervous system of the cephalocarid crustacean *Hutchinsoniella macracantha* (Stegner and Richter 2011; Stegner et al. 2014a, b), complementing earlier studies (Elofsson and Hessler 1990; Elofsson 1992; Hessler and Elofsson 1992). As in other Mandibulata, the central nervous system can be distinguished into a tripartite brain (proto-, deuto-, tritocerebrum) and a ventral nerve cord, which extends through the subesophageal region and the trunk. The brain comprises a pronounced olfactory system

featuring large olfactory lobes and a unique multi-lobed complex, a small tripartite posterodorsal neuropil cluster (Stegner and Richter 2011), and a central body-like serotonin-like immunoreactive domain (see also Stegner et al. 2014b). The cephalocarid ventral nerve cord is formed by a pair of longitudinal nerve strands and features a fused subesophageal ganglion comprising the mandibular, maxillular, and maxillar neuromeres; nine segmental thoracic ganglia; and eight segmental abdominal ganglia, while the abdominal segments 9 and 10 lack ganglia (Stegner et al. 2014a). The maxillar neuromere and the thoracic ganglia all exhibit five to eight individually identified serotonin-like immunoreactive neurons on each side and four segmental commissures. In contrast, the abdominal ganglia exhibit only one or two serotonin-like immunoreactive neurons on each side and two commissures (Stegner et al. 2014a). In the light of the various neuroanatomical studies into other arthropod taxa that have been carried out over the past 20 years (reviews by Harzsch 2006, 2007; Strausfeld 2012; Loesel et al. 2013; Loesel and Richter 2014), we suggest that many adult neural features in Cephalocarida are likely to date back to the stem species of Tetraconata (see Stegner and Richter 2011; Stegner et al. 2014a, b).

This paper analyzes the development of the cephalocarid nervous system for the first time. Our main focus lies on the sequence (i.e., the temporal order) in which major neural features such as soma cortexes, neuropils, commissures, connectives, and serotonin-like immunoreactive neurons develop in each segment of the body, and how the development of neural features correlates with external morphological development, i.e., the posterior addition of trunk segments and limb development.

In *H. macracantha,* a free-swimming metanauplius with five cephalic appendages and two limbless trunk segments (Sanders 1963) hatches from a large egg carried on the transformed ninth thoracopods of the adult hermaphrodite (Hessler et al. 1995). Sanders (1963) described the larval development of *H. macracantha* in detail, mentioning a total of 18 larval stages but leaving open the question of whether this number was exhaustive. Our investigation led to the discovery of five additional larval stages. From a proliferation zone anterior to the telson, two segments per molt initially and then one segment per molt are added to the developing trunk until the adult number of 19 trunk segments is reached (Sanders 1963; this study). After this anameric phase, further molts are required to differentiate all the thoracopods (Sanders 1963; this study).

Most studies into crustacean neurodevelopment so far have been undertaken in representatives of Branchiopoda and Malacostraca. Some have concentrated on specific aspects of development such as neurogenesis and the neuronal precursor cells involved, i.e., neuroblasts and ganglion mother cells (Malacostraca: Dohle and Scholtz 1988; Harzsch et al. 1998; Ungerer and Scholtz 2008; Branchiopoda: Gerberding 1997; Ungerer et al. 2011a), and axogenesis and the pioneer neurons involved (e.g., Branchiopoda: Blanchard 1986; Malacostraca: Harzsch et al. 1998; Ungerer and Scholtz 2008; Ungerer et al. 2011b). These form the basis for a comparison with our first data on cephalocarid neurogenesis.

Other studies have looked at the sequence (i.e., temporal order) of development of neural features throughout the embryonic and larval phases and correlated these data with changes in external morphology (e.g., Malacostraca: Vilpoux et al. 2006; Fischer and Scholtz 2010; Ungerer et al. 2011a; Branchiopoda: Fritsch and Richter 2010, 2012; Fritsch et al. 2013). The present comprehensive analysis of development in *H. macracantha* serves as a basis for two different undertakings, the first being a comparison of the respective developmental sequence of neural and external features in different species. Crustaceans exhibit a broad variety of developmental modes (e.g., Minelli and Fusco 2013), and two recent series of comparative studies into Branchiopoda (Fritsch and Richter 2012; Fritsch et al. 2013) and Malacostraca (Jirikowski et al. 2013) have shown that different developmental modes (as defined by external morphology) are correlated with differences in the developmental sequence of internal and external features. The authors concluded that heterochronic shifts must have occurred during the evolution of developmental sequences within Branchiopoda (Fritsch et al. 2013) and within Malacostraca (unpublished data by G. Jirikowski, C. Wolff, S. Richter). Comparing neural and external development in *H. macracantha* to that in Branchiopoda and Malacostraca is an important step toward understanding the evolution of developmental sequences within Tetraconata. At present, our understanding is hindered by the fragmentary nature of the developmental data available on other crustacean taxa (e.g., Copepoda: Lacalli 2009; Cirripedia: Walley 1969; Semmler et al. 2008).

The second major undertaking tackled here is a comparison of the different trunk segments in *H. macracantha* with regard to the developmental sequence of their respective neural and external features in order to reveal potential serial homologies in the spatiotemporal pattern between the thorax and the abdomen. This comparison is especially interesting in light of the fact that Cephalocarida and Mystacocarida (Brenneis and Richter 2010) are the only crustaceans to exhibit segmental ganglia not only in their limb-bearing thoracic segments but in most of their limbless abdominal segments too (summarized by Stegner et al. 2014a).

Two embryonic (E1, E2) and nine larval stages (L1–L6, L8, L14, L18) are investigated with respect to their neuroanatomy using a combination of immunolabeling (acetylated α-tubulin, serotonin), nuclear counterstaining,

confocal laser scanning microscopy, and computer-aided 3D reconstruction. Although the number of specimens available was restricted, these stages provide a broad insight into the major developmental patterns.

Materials and methods

Collection, fixation, and storage

Different stages of *Hutchinsoniella macracantha* (numbers listed in Table 1) were collected in the daytime during the summer months from 2007 to 2012 at different spots in Buzzards Bay, Massachusetts (USA). Samples of benthic mud were collected by boat from depths of 10–25 m using a Van Veen grab or by SCUBA diving. The animals were separated from the sieved samples using fine forceps or pipettes. In order to avoid potential circadian effects on the expression level of serotonin (see Wildt et al. 2004), all animals were fixed at the same time before dusk at the end of our collecting days.

Animals were fixed with a 4 % paraformaldehyde solution (16 % PFA stem solution [Electron Microscopy Sciences, Hatfield, PA, USA: No. CAS #30525-89-4] diluted in PBS solution which was produced by diluting 10 × PBS stock solution in filtered water from Buzzards Bay) for 30 min to 1 h. Fixed specimens were transferred to 100 % methanol for storage at 4 °C.

Pretreatment of whole mounts for immunolabeling

After a series of dilutions from methanol into PBS, specimens were exposed to short pulses (<1 s at 35 kHz) in a bath ultrasonicator (Elma, Singen, Germany: Elmasonic One), permeabilizing the cuticle. Between pulses, specimens were investigated with a stereomicroscope to check for any signs of external or internal damage due to the treatment. In some specimens, appendages were removed on one or both sides of the body using dissecting instruments such as forceps (Dumont 5) and tungsten needles. To facilitate the penetration of antibodies, the cuticle was further perforated with forceps or a tungsten needle in some specimens. Pretreatment procedures were often combined.

Immunolabeling and mounting

All specimens underwent the same general immunolabeling procedure. Antibody incubation was conducted in PBT (PBS with 0.5 % bovine serum albumin, 0.3 % Triton X-100, 1.5 % dimethylsulfoxide) containing 5 % normal goat serum (Calbiochem, Merck KGaA, Darmstadt, Germany: No. NS02L). Labeling of the cytoskeletal protein acetylated α-tubulin was performed using a primary monoclonal mouse antibody [anti-ac-α-tub IgG 2b isotype, clone 6-11 B-1, Sigma-Aldrich, St. Louis, MO, USA: No. T6793 (dilution 1:100)] and a Cy-3-coupled secondary goat antibody [anti-mouse IgG (H + L), Jackson/Dianova, Hamburg, Germany: No. 115-001-003 (dilution 1:200)]. To label the biogenic amine serotonin, a polyclonal rabbit antiserum was used [Immunostar, Hudson, WI, USA: No. 20080 (dilution 1:100)]. Visualization of serotonin-like immunoreactivity was carried out using one of two secondary antibodies depending on the combined nuclear marker later to be used. If nuclei were later to be labeled using Hoechst (Invitrogen Molecular Probes, Darmstadt, Germany: No. H33342, 1 µg/ml in PBS), an AlexaFluor 488-coupled secondary goat antibody [anti-rabbit IgG (H + L), Invitrogen Molecular Probes, Darmstadt, Germany: No. A11008 (dilution 1:500)] was applied. If nuclei were later to be labeled using Sytox Green [Invitrogen Molecular Probes, Darmstadt, Germany: No. S34860 (dilution 1:600)], an AlexaFluor 633-coupled secondary goat antibody [anti-rabbit IgG (H + L), Invitrogen Molecular Probes, Darmstadt, Germany: No. A21070 (dilution 1:500)] was applied. In one specimen, the neuropeptide FMRFamide was labeled using a polyclonal rabbit antiserum [Neuromics, Edina, MN: @: 20002 (dilution 1:1,000)], coupled for visualization to the AlexaFluor 488-coupled secondary goat antibody described above. Incubations were carried out overnight at 4 °C, each followed by thorough washing in PBT on a horizontal shaker (neoLab, Heidelberg, Germany: DOS-20S) at 50 rpm. Stained whole mounts were mounted in Vectashield Mounting Medium (Vector Laboratories Inc., Burlingame, CA, USA), after tiny pieces of plasticine had been placed as spacers in the corners of the cover slips.

Confocal laser scanning microscopy

Stained specimens were scanned using a DM IRE2 confocal laser scanning microscope (UV: 405 nm; Arg/Kr: 488 nm, HeNe: 543 nm) equipped with a TCS SP2 AOBS laser scanning unit (Leica Microsystems GmbH, Wetzlar, Germany) at step sizes of 0.4–1 µm between successive scanning planes. Alternatively, a DMI 6000 CS confocal laser scanning microscope (Arg/Kr: 488 nm, HeNe: 543 nm, DPSS: 633 nm) equipped with a TCS SP5 II laser scanning unit (Leica Microsystems GmbH, Wetzlar, Germany) was used at the same step sizes.

Analysis and 3D reconstruction

The software Imaris (Bitplane AG, Zurich, Switzerland: version 6.0.2) was used for all analyses of the 3D virtual

Table 1 Developmental stages in *H. macracantha* and their external trunk morphology

Developmental stage			No. of articulated trunk segments	No. of limb-bearing trunk segments (limb bud—bifurcate limb anlage-complete limb)		No. of limbless trunk segments	
This study	Specimens studied here	Sanders's (1963) stage		This study	Sanders (1963: his text)	This study	Sanders (1963: his text)
E1	2	–	0	0 [0-0-0]	–	0	–
E2	2	–	2	0 [0-0-0]	–	2	–
L1	4	Nauplius 1	2	0 [0-0-0]	0 [0-0-0]	2	2
L2	7	Nauplius 2	4	1 [1-0-0]	0 [0-0-0]	3	4
L3	4	Nauplius 3	6	2 [1-1-0]	1 [0-1-0]	4	5
L4	6	Nauplius 4	8	2 [1-1-0]	2 [1-1-0]	6	6
L5	5	Nauplius 5	10	2 [0-1-1]	2 [1-0-1]	8	8
L6	1	–	11	3 [1-1-1]	–	8	–
L7	1	–	12	3 [1-1-1]	–	9	–
L8	2	Nauplius 6	13	3 [1-0-2]	2 [0-1-1]	10	11
L9	–	Nauplius 7	14	–	3 [0-1-2]	–	11
L10	1	Nauplius 8	15	4 [1-1-2]	3 [0-1-2]	11	12
L11	–	Nauplius 9	16	–	3 [0-0-3]	–	13
L12	1	–	17	4 [1-0-3]	–	13	–
L13	1	–	18	4 [1-0-3]	–	14	–
L14	1	Nauplius 10	18	4 [0-1-3]	4 [0-1-3]	14	14
L15	–	Nauplius 11	19	–	4 [0-1-3]	–	15
L16	1	Nauplius 12	19	5 [1-1-3]	4 [0-0-4]	14	15
L17	–	Nauplius 13	19	–	5 [1-0-4]	–	14
L18	1	–	19	6 [1-1-4]	–	13	–
L19	–	Juvenile 14	19	–	6 [1-0-5]	–	13
L20	–	Juvenile 15	19	–	6 [0-1-5]	–	13
L21	–	Juvenile 16	19	–	7 [1-1-5]	–	12
L22	–	Juvenile 17	19	–	7 [0-1-6]	–	12
L23	–	Juvenile 18	19	–	8 [1-1-6]	–	11
Adult	23 (Stegner et al. 2014a)	Adult	19	9 [1-0-8]*	8 [0-0-8]*	10*	11*

Revision of Sanders' (1963) staging system, here including the newly discovered stages E1, E2, L6, L7, L12, L13, and L18. The Sanders data provided are based on his text of 1963, not his Fig. 27, which deviates from his description. In general, subesophageal segments (Md, Mx1, Mx2) and the telson are not counted as trunk segments. (*) Note that unlike Sanders (1963), we count the egg-carrier of the adult thoracic segment Th9 as a limb

E1, early embryo; E2, late embryo before hatching; L1–L23, larval stages 1–23

stacks obtained through laser scanning microscopy. If not stated otherwise in the legend, volumes on all confocal laser micrographs are shown in the Imaris "maximum intensity projection" and "surpass view" mode, displaying the 3D volume of the complete data set. The "shadow projection" and "normal shading" options render scanned structures opaque and shaded, thus allowing their surface and external shape to be examined. In many cases, the "contour surface" tool was used to artificially highlight specific structures or to mask structures that obscured the view of the nervous system. All figure plates were created and labeled using the software Corel Draw X3.

Nomenclature and presentation

Our nomenclature follows previous descriptions of the adult brain (Stegner and Richter 2011) and ventral nerve cord (Stegner et al. 2014a; based on Richter et al. 2010). Morphological descriptions of nerves or neurites can require coordinates and phrases of direction such as "extend into" or "project anteriorly." Please note that no physiological or developmental inferences should be drawn from such phrases. All adjectives of position (such as "anterior" or "dorsal") refer to the body axis. If not stated otherwise, only one side of the body is described.

Exceptions are mentioned explicitly. The term "pair" is used solely for bilaterally symmetrical pairs, not for ipsilateral duads. We term the protocerebrum a neuromere, aware that the segmental identity of the pre-antennular region is unclear. Before the new trunk segments are separated from the telson by a transverse infolding of the postsegmental cuticle, the externally confluent trunk segments and telson are summarized as the "unsegmented trunk ending." Homonymy between segmental structures does not necessarily imply serial homology (though serial homology may often be the case). This applies in particular to the structures of the three-segmental subesophageal ganglion.

In all figures showing the results of immunolabeling and nuclear staining, the molecules labeled and stains used are indicated (e.g., "tub" for acetylated α-tubulin, "Hoe" for Hoechst, "Syt" for Sytox). Using polyclonal antisera against serotonin does not rule out the possibility that related neuroactive substances could also be labeled. As a result, we refer to serotonin-like immunoreactivity (SLI) and to serotonin-like immunoreactive (SL-ir) structures. The SL-ir neurons labeled s1–s13 (Stegner and Richter 2011: brain), s14–s20, s27, and s28 (Stegner et al. 2014a: ventral nerve cord) were identified individually on the basis of the target of their neurites. SL-ir neurons s21?–s26? are labeled on the basis of the location of their soma within the segment (the question mark indicates that course of their neurite is unknown; see Stegner et al. 2014a). A phenotypic division of the trunk into a thorax with limb-bearing segments and an abdomen with limbless segments applies only to the adult, yet also the developing segments are abbreviated as follows: mandibular (Md), maxillular (Mx1), maxillar (Mx2), thoracic 1–9 (Th1–Th9), and abdominal 1–10 (Ab1–Ab10).

In the only representative of larval stage L18, we found a significantly lower number of SL-ir neurons than in earlier and later stages. Although this aberration in the SL-ir pattern is included in our study (Table 3 and S1 and Fig. 9), it may be due to intraspecific variability (as has been described to a certain degree in the adult; Stegner et al. 2014a) and/or incomplete staining rather than to natural developmental change.

Results

External morphology

Sanders' (1963) description of external development in *H. macracantha* is here complemented by two embryonic stages (E1, E2; Fig. 3a, d) and five hitherto unknown intermediate larval stages (here labeled L6, L7, L12, L13, L18; Fig. 2; summarized in Table 1; Fig. 1).

Early embryo (E1)

The antennula is monofurcate, the antenna is bifurcate with a longer anterior branch, the mandible is bifurcate with even-sized branches, and the maxillula (i.e., the first maxilla) is a short monolobate bud (Fig. 3a). Both antenna and mandible exhibit a proximomedial protrusion (the prospective "naupliar process" of the antenna sensu Sanders 1963, compare with our Fig. 3a). The furca bears two short terminal setae on each branch (Fig. 3a, b). The telson is folded forward so that the furca points anteriorly toward the large labrum (Fig. 3a). The cephalic shield is subdivided into three portions (one median, one lateral on each side; Fig. 3a).

Late embryo (E2)

The four anteriormost appendage anlagen (antennula, antenna, mandible, and maxillula, Fig. 3d) correspond to those of the first larval stage described by Sanders (1963), suggesting that the three late embryos in our study were fixed shortly before hatching. One difference is found in the maxilla (i.e., the second maxilla), which is still monolobate rather than bilobate as in the hatchling. Th1 and Th2 are separated by intersegmental furrows (Fig. 3g, arrowheads in Fig. 4c, d). The trunk ending is still folded around (Fig. 3g) so that the furca points anteriorly (artificially unfolded in other figures).

Larval development

In extension of Sanders (1963), our revised staging system for *H. macracantha* now includes 23 larval stages (Fig. 1; Table 1). The first larva L1 in *H. macracantha* (Fig. 5a) hatches as a metanauplius. Larval stages L1–L12 were distinguished here on the basis of their unique number of separated trunk segments. As a cephalocarid peculiarity among crustaceans, two trunk segments are added per molt between L1 and L5, while only one is added between L5 and L13 and between L14 and L15. Development from L1 to L13 could, then, be considered anameric in the classical sense. No segments are added between L13 and L14 or after L15, which already features the adult number of 19 trunk segments (Fig. 1; Table 1).

We found in several stages that the degree of development of the thoracopods (Table 1) differed from that noted in the original description by Sanders (1963). While our system for distinguishing the early stages L1–L12 is straightforward, it is rendered problematic when it comes to distinguishing stages L13–L23, i.e., those stages that are *not* unique in their respective number of trunk segments but distinguished by the degree of development of their limbs. Here, we made the following distinctions: absent → limb

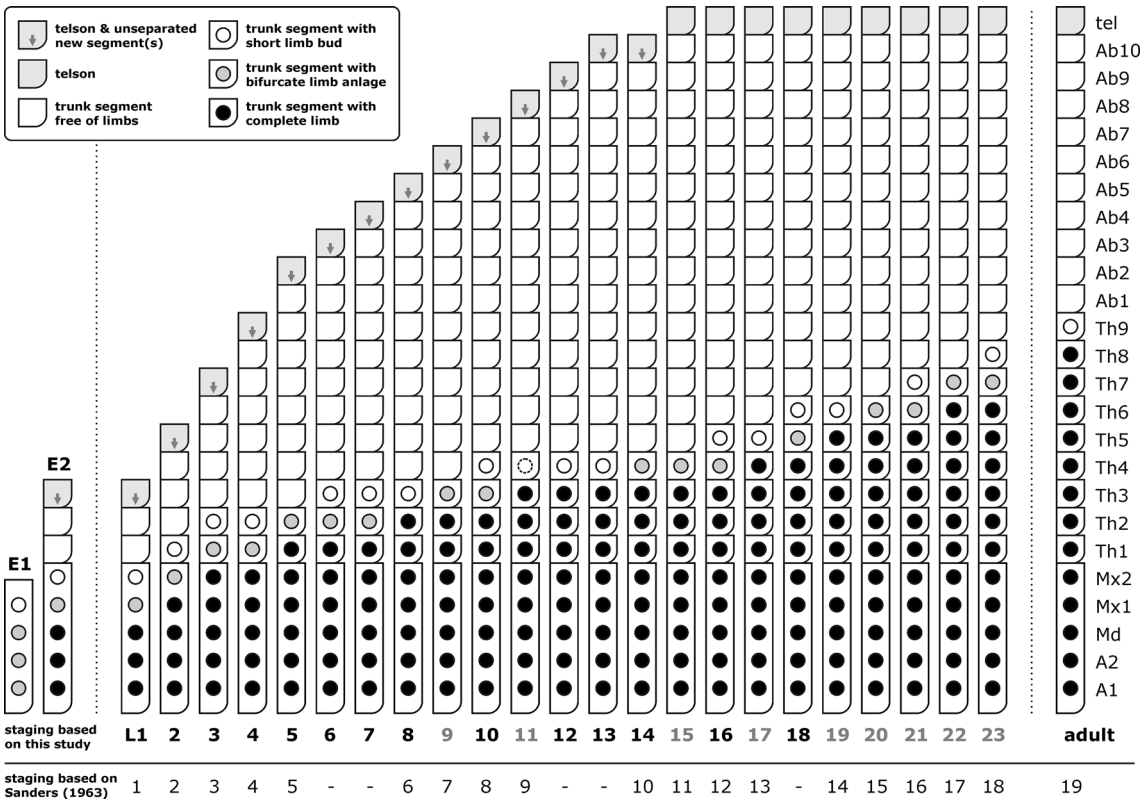

Fig. 1 Development of *H. macracantha* with respect to external morphology. Revision of Sanders' (1963) staging system to include the two embryonic and five larval stages discovered here. Revised data on the number of trunk segments and limb morphology are provided for all available stages (labeled in *black*). Data are based on Sanders' (1963) text only with regard to stages that were unavailable here (labeled in *gray*). Refer also to Table 1

bud (shorter than thoracomer) → bifurcate limb anlage (longer than thoracomer) → completely developed limb (Table 1; Fig. 1). Two specimens exhibiting hitherto unknown combinations of limbs and limb anlagen were thus assigned to the new stages L13 and L18. Stage L18 (Fig. 2i) is the first to lack the proximomedial naupliar process on the antenna (see Fig. 2b, h where this process is still present). We found no representatives of the larval stages L9, L11, L15, L17, or L19–L23.

Note on segment addition

In L1, thoracic segments 1 and 2 are separate and laterally lobate (Fig. 5a). Although the trunk ending posterior to Th2 appears externally to be smooth, autofluorescence reveals the intersegmental border between Th3/Th4 and between Th4/Th5 as faint infolds in the ventral cuticle (positions marked by arrowheads in Fig. 5e), and tubulin staining shows the associated muscle insertion sites (not depicted for L1, but see arrowheads in Fig. 7a, e, f). In contrast, in L1, no cuticular features point to a delineation between the developing segment Th5 and the telson. In L2, the separated segments Th1 to Th4 exhibit pleural spines (Fig. 6a), while the trunk ending posterior to Th4 appears externally to be smooth and unsegmented (Fig. 6a, d, finger). The prospective intersegmental articulations between Th5/Th6 and between Th6/Th7 are indicated by faint infolds in the ventral cuticle (dashed lines in Fig. 6e, finger). From stage L5 onwards, only one additional segment is visibly indicated by a ventral infold in the cuticle until the full number of segments has been reached (e.g., yellow arrowheads in Fig. 8c).

Fig. 2 External morphology in chosen larval stages of *H. macracantha*. Confocal micrographs in Imaris surpass view showing cuticular autofluorescence. As a pretreatment for immunolabeling (not shown), thoracopods have been partly or completely removed. **a–f** Larval stages L1–L12 are distinguished unambiguously by their differing number of trunk segments. **g–i** Larval stages L13, L14 (18 trunk segments), and L15–L23 (19 trunk segments) are distinguished by differences in the degree of development of the thoracopods. **i** The naupliar process observed in earlier stages is lost in L18. *Abbreviations* a1, antennula; a2, antenna; cs, cephalic shield; lb, labrum; md, mandible; mx1, mx2, maxillula and maxilla; npro, naupliar process on antenna; pleu, pleurite; sp, pleural spine; tel, telson; thp1-thp6, thoracopod (anlagen) 1–6. *Scale bars* 100 μm

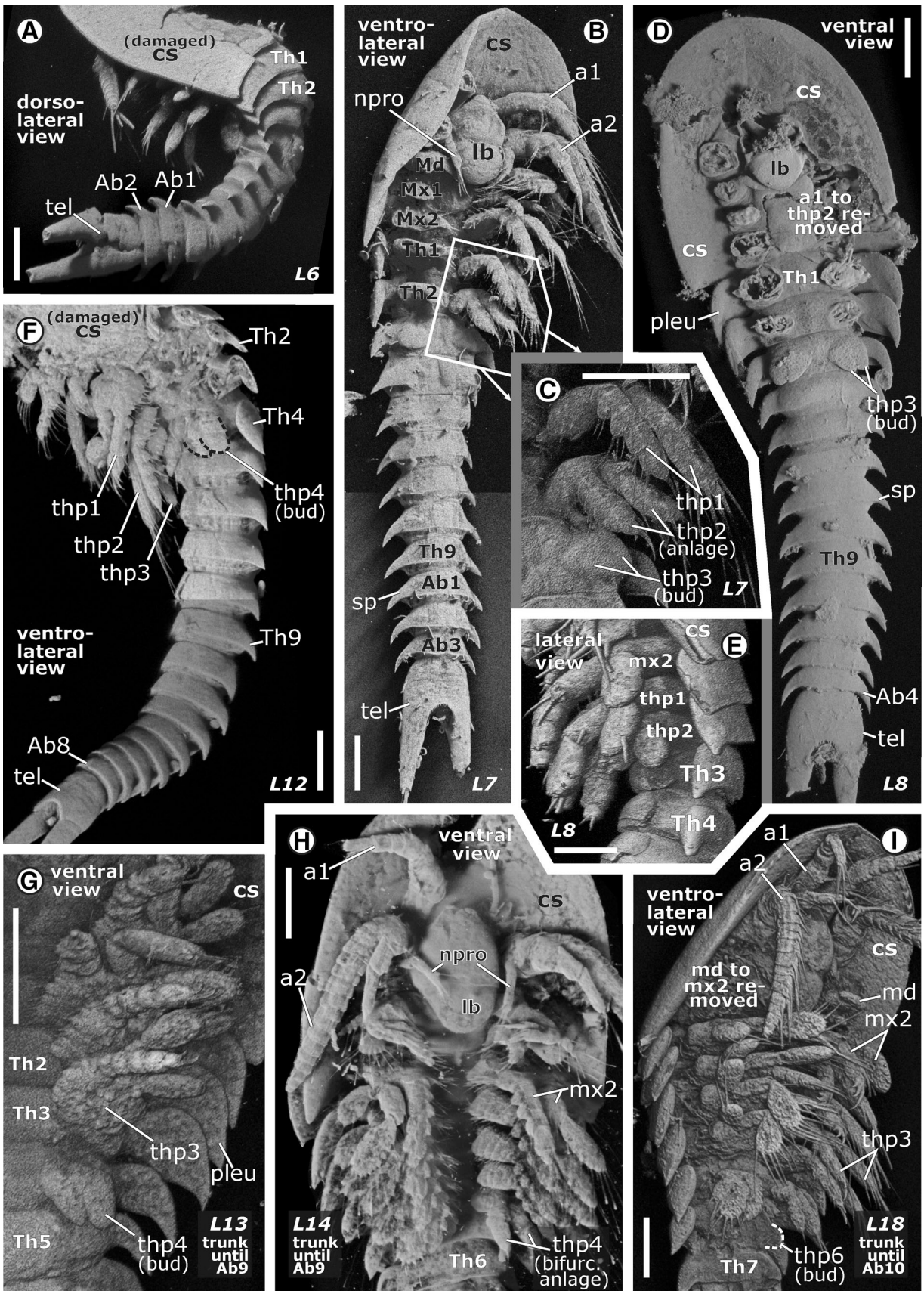
A
(damaged) CS
Th1
Th2
dorso-lateral view
Ab2
Ab1
tel
L6
B
ventro-lateral view
CS
a1
npro
a2
lb
Md
Mx1
Mx2
Th1
Th2
Th9
Ab1
sp
Ab3
tel
L7
C
thp1
thp2 (anlage)
thp3 (bud)
L7
D
ventral view
CS
lb
a1 to thp2 re-moved
CS
Th1
pleu
thp3 (bud)
sp
Th9
Ab4
tel
L8
E
lateral view
CS
mx2
thp1
thp2
Th3
Th4
L8
F
(damaged) CS
Th2
Th4
thp1
thp2
thp3
thp4 (bud)
ventro-lateral view
Th9
Ab8
tel
L12
G
ventral view
CS
Th2
Th3
thp3
pleu
Th5
thp4 (bud)
L13 trunk until Ab9
H
ventral view
a1
CS
a2
npro
lb
mx2
L14 trunk until Ab9
Th6
thp4 (bifurc. anlage)
I
a1
a2
ventro-lateral view
CS
md to mx2 re-moved
md
mx2
thp3
Th7
thp6 (bud)
L18 trunk until Ab10

Nervous system

Early embryo (E1)

The early embryo features anlagen of the three subunits of the brain: proto-, deuto-, and tritocerebrum (Fig. 3c). The ventral nerve cord consists of a pair of longitudinal neurite bundles that we were able to trace past the maxillular neuromere. The protocerebral neuropil is still a loose assembly of neurites on each side of the brain. Two pre-esophageal commissures in the protocerebral region, two post-esophageal tritocerebral commissures (Fig. 3c), and the connective-like interjacent neurite bundles on each side together form a visible circumesophageal ring (Fig. 3b). In one specimen, a developing (as yet unclosed) labral commissure was found connected with the tritocerebral neuropil (Fig. 3c). The anterodorsal commissure of the mandibular neuromere is connected to the median neurite bundle (Fig. 3c), which we were able to trace posteriorly as far as the maxillular neuromere. No other commissures are yet present. One segmental appendage nerve arises laterally from the deutocerebral, tritocerebral, mandibular, and maxillular neuromeres, respectively, each nerve extending into the associated appendage (Fig. 3c). Segmental neuropils are only faintly differentiated. A maxillular neuropil is not discernible at this stage. The putative deutocerebral and tritocerebral tegumentary nerves arise behind their respective neuromere, each from an intersegmental root (Fig. 3c) that lies more anteriorly than in the adult (compare Stegner and Richter 2011). Two intersegmental nerves on each side originate from the connectives between the tritocerebral, mandibular, and maxillular neuromeres (Fig. 3c), the more anterior nerve extending toward the dorsolateral region of the embryo. Pioneer neurons could not be distinguished within the telson. SLI is absent.

Late embryo (E2)

Brain The late embryonic brain corresponds to the adult brain in overall appearance and relative size with respect to the cephalon (Fig. 4a, b). All somata assemblages are present (Table 2; e.g., Fig. 3e, g). The protocerebral somata assemblage is contiguous across the midline and partitioned into several divisions by penetrating cephalic shield muscles (Fig. 3g). The median region of the protocerebral neuropil has grown particularly significantly with respect to the previous stage and now includes the tracts of the multi-lobed complex. The olfactory globular tract and the lateral tract appear as one continuous tract as neuropils 7 and 8, which separate them from stage L1 onwards, are still not yet present (Fig. 4b). A thin pedunculus (Fig. 4b) extends transversely from the lateral region of the protocerebral somata assemblage toward the medial tract. In the deutocerebrum, a lower root of the antennula nerve enters the large olfactory lobe ventrally (Fig. 3h), adding to the upper root already present in E1. Each olfactory lobe is organized into about seven vertical stacks composed of olfactory glomeruli (not shown) and gives rise to a faint olfactory globular tract that extends ipsilaterally into the protocerebral neuropil (Fig. 4b). The labral commissure is closed and is, at its vertex, connected with the faint dorsomedian bundle of the stomatogastric nervous system (Fig. 3h).

Most SL-ir neurons known from the adult brain (Stegner and Richter 2011; Stegner et al. 2014b) are already present in the late embryonic brain, namely somata s1–s3, s5, s6 (Fig. 4a), s9, s11 (Fig. 3h), s10, and s12 (Table 2). The faintly SL-ir neurons s4 described in the adult are not considered in this study. In E2, the SL-ir domain sd1 in the protocerebrum (Fig. 4a) and, faintly, sd4 in the tritocerebrum are also visible (Fig. 3h). The deutocerebral tegumentary nerve was traceable to one of the cephalic glands underneath the cuticle, which are the only RFL-ir structures present at this stage (Fig. 3f).

Ventral nerve cord We appear to have missed the critical moment between stages E1 and E2 when the first continuous neurites of the ventral nerve cord are pioneered between the maxillular neuromere and the telson. However, it was possible in E2 to trace some longitudinal

Fig. 3 Embryonic nervous system in *H. macracantha*. Confocal micrographs in Imaris surpass view showing immunolabeling. **a–c** Ventrolateral view of the early metanauplius. **a** External morphology showing the limb anlagen and furca, which is still folded forward. **b** Position of the circumesophageal ring of neurites. **c** In addition to the naupliar neuromeres with their various nerves and commissures, a maxillular nerve root is present. **d–h** Metanauplius shortly before hatching. **d**, **e** External morphology and cephalic appendages in ventral view. Furca artificially unfolded. **e** Brain, subesophageal ganglion of three fused neuromeres, and broadly differentiated thoracic ganglia 1–4 are visible anterior to the growth zone. **f**, **g** Dorsal view. **f** Neuropil (*yellow*) and tegumentary glands (*blue*) artificially highlighted. **h** Ventral view. The olfactory lobe in E2 corresponds to that in the adult, as do several nerves, commissures, and SL-ir neurons. *Abbreviations* a1, a2, antennula and antenna; a1nv, a2nv, antennula and antenna nerve; adc, anterodorsal commissure; cg, cephalic gland; cs, cephalic shield; dbs, dorsomedian neurite bundle; dc, deutocerebrum; dtnv, deutocerebral tegumntary nerve; ennv, exnv, endopodite and exopodite nerve; fpc, first posterior commissure; frc, furca; Hoe, Hoechst nuclear staining; isnv, intersegmental nerve; lb, labrum; lbc, labral commissure; md, mandible; mdn, mandibular neuropil anlage; mdnv mandible nerve; mnb, median neurite bundle; mx1, mx2, maxillula and maxilla; mx1nv, mx2nv, maxillula and maxilla nerve; ol, olfactory lobe; pec, post-esophageal commissures; plnv, posterolateral nerve; prec, pre-esophageal commissures; prs, protocerebral somata; ptc, protocerebrum; RFLI, RFamide-like immunoreactivity; ring, circumesophageal ring; s9, s11, SL-ir neurons 9 and 11; sd4, SL-ir domain 4; sg, subesophageal ganglion; sh, sheath in furca; SLI, serotonin-like immunoreactivity; tc, tritocerebrum; ttnv, tritocerebral tegumentary nerve; tub, tubulin staining; vnc, ventral nerve cord; zone, growth zone. *Scale bars* **a–g** 100 μm, h 50 μm

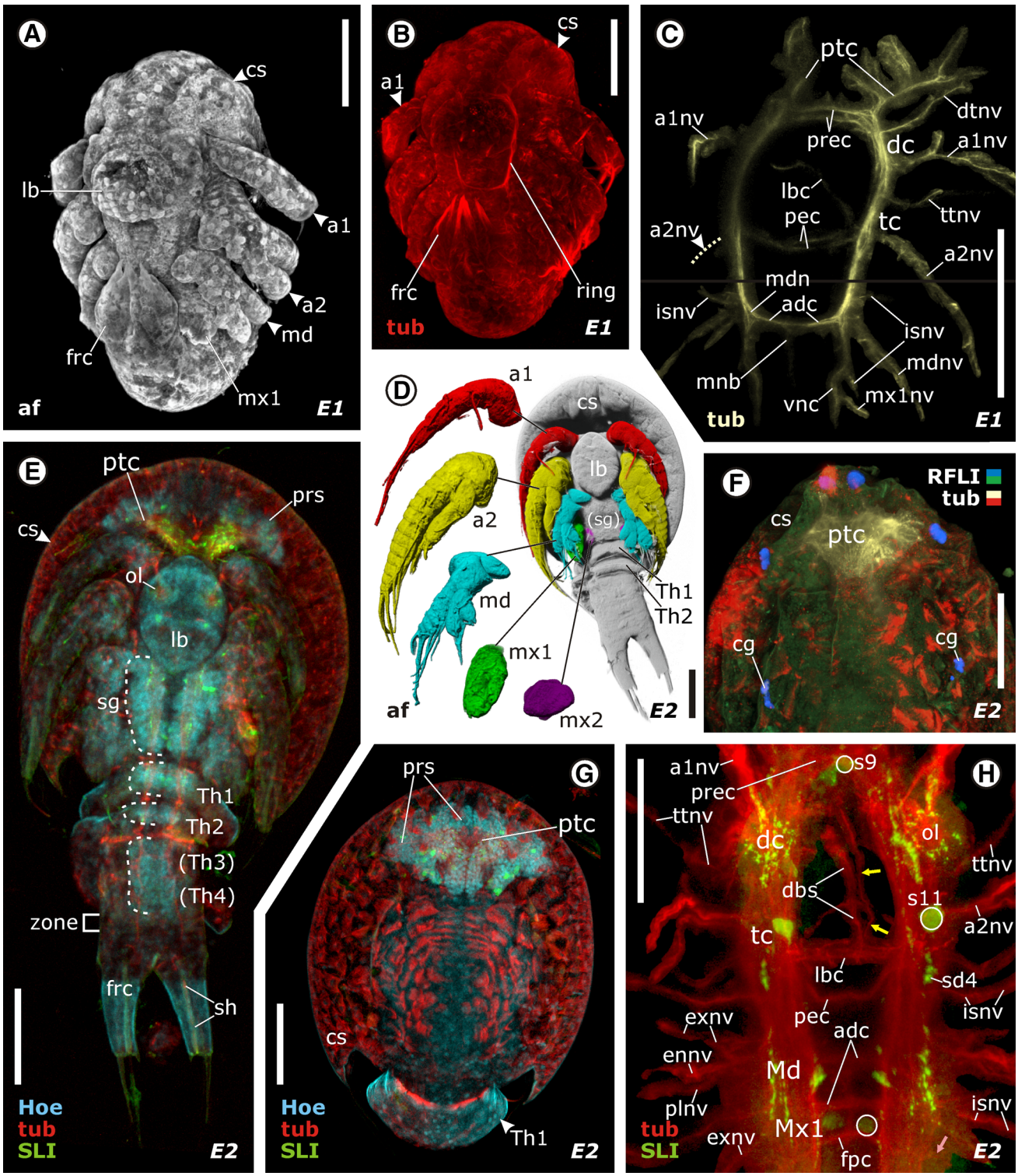

neurites of the ventral nerve cord back to the somata in which they originated (color-masked in Fig. 4e), which turned out to be located posterior to the growth zone in the telson, therein corresponding to the posterior pioneer neurons described in Branchiopoda (e.g., Blanchard 1986) and Malacostraca (e.g., Fischer and Scholtz 2010). Other longitudinal neurites of the ventral nerve cord seem to arise from the continuous somata assemblage of Th3 and Th4 (position indicated by double arrows in Fig. 4e), i.e., anterior to the growth zone.

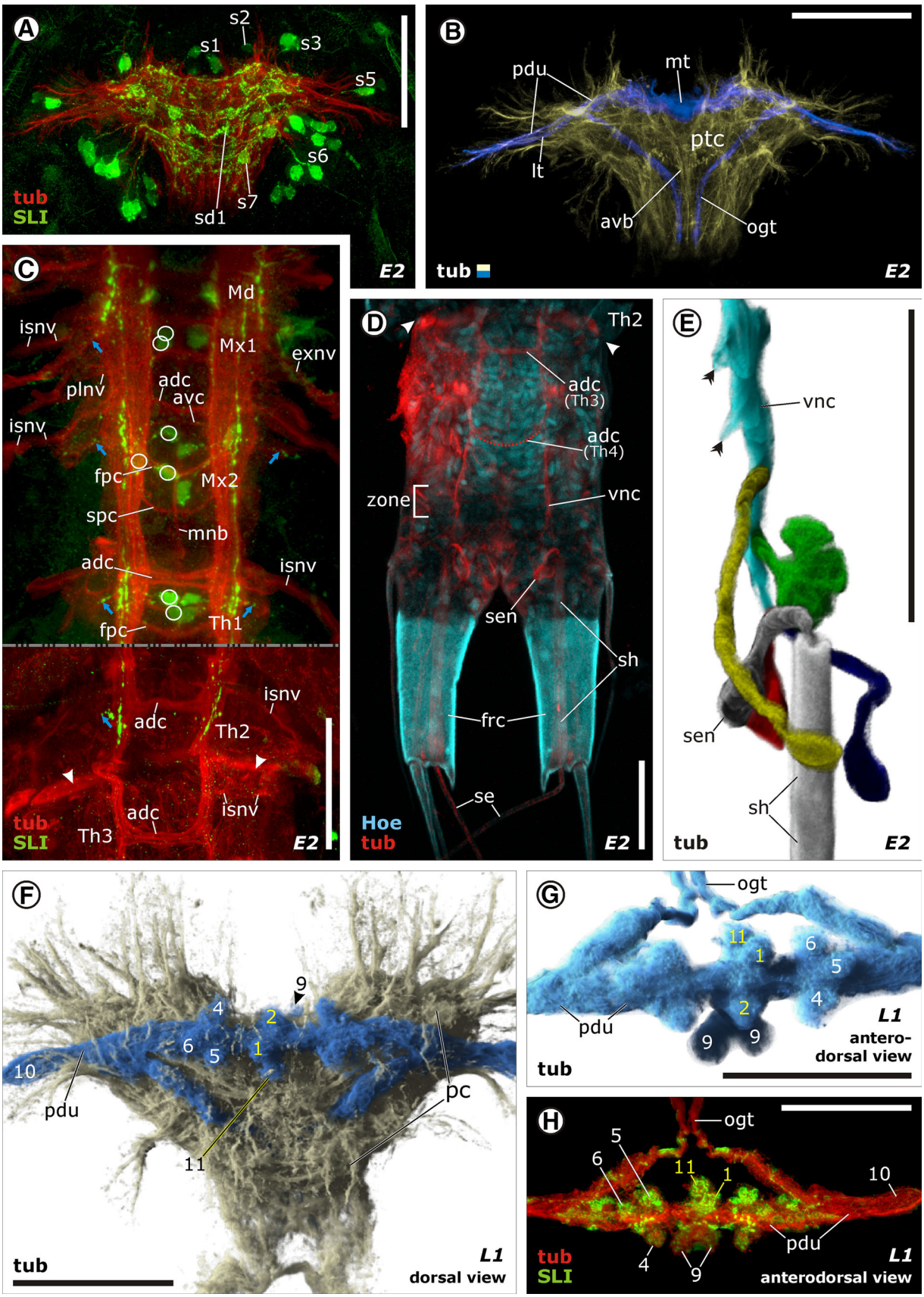
A
s2
s1
s3
s5
s6
s7
sd1
tub
SLI
E2
B
pdu
mt
ptc
lt
avb
ogt
tub
E2
C
Md
isnv
Mx1
exnv
plnv
adc
avc
isnv
fpc
Mx2
spc
mnb
adc
isnv
fpc
Th1
isnv
adc
Th2
tub
SLI
adc
isnv
Th3
E2
D
Th2
adc
(Th3)
adc
(Th4)
zone
vnc
sen
sh
frc
se
Hoe
tub
E2
E
vnc
sen
sh
tub
E2
F
9
4
2
6
5
1
10
pdu
pc
11
tub
L1
dorsal view
G
ogt
11
1
6
5
4
2
pdu
9
9
tub
L1
antero-
dorsal view
H
ogt
5
6
11
1
10
pdu
tub
SLI
4
9
L1
anterodorsal view

◀**Fig. 4** Late embryo (E2) and hatchling (L1). Confocal micrographs in Imaris surpass view showing immunolabeling. **a, b, f** Protocerebrum in dorsal view. **a** The SL-ir pattern in the brain corresponds broadly to that in the adult. **b** Before hatching, the multi-lobed complex (artificially highlighted in *blue*) comprises only tracts. **c, d** Ventral view of the ventral nerve cord, furca artificially unfolded. Exopodite nerve roots (*blue arrows*) and SLI occur as far posteriorly as Th2. *Arrowheads* indicate intersegmental furrows. **d** Although Th3, Th4, and the telson are not yet separated by intersegmental furrows, somata assemblages and anterodorsal commissures occur as far posteriorly as Th4. **e** Magnification of artificially masked neurons in the telson posterior to the growth zone. A setal neuron (*gray*) contributes its neurite to a tubulin-rich sheath in the furca. Other telsonic neurons (*red*, *yellow*, *green*, *blue*) contribute neurites to the ventral nerve cord, potentially constituting pioneer neurons. **f, g** Several neuropils are added to the multi-lobed complex (artificially highlighted in blue) after hatching. **h** Artificial masking of the multi-lobed complex reveals SL-ir neuropils 1, 5, and 11 as early as in L1. *Abbreviations* 1–11, neuropil 1–11 of the multi-lobed complex; adc, anterodorsal commissure; avb, anteroventral neurite bundle; avc, anteroventral commissure; ennv, exnv, endopodite and exopodite nerve; fpc, first posterior commissure; frc, furca; Hoe, Hoechst nuclear staining; isnv, intersegmental nerve; lt, lateral tract; mnb, median neurite bundle; mt, medial tract; ogt, olfactory globular tract; pdu, pedunculus; plnv, posterolateral nerve; ptc, protocerebral neuropil; s1-s7, SL-ir neurons 1–7; sd1, SL-ir domain 1; se, medial furcal seta; sen, setal neuron; sh, sheath in furca; SLI, serotonin-like immunoreactivity; spc, second posterior commissure; tub, tubulin staining; zone, growth zone. *Scale bars* 50 μm

In E2, the three neuromeres of Md, Mx1, and Mx2 form a subesophageal ganglion with one contiguous soma cortex, while the thoracic ganglia of Th1 and Th2 each exhibit separate soma cortexes (Fig. 3e). Somata of the developing segments Th3 and Th4 are present, but still lie condensed in one somata assemblage within the unsegmented trunk ending (Figs. 3e, 4d). The posterior margin of this somata assemblage is directly adjacent to the growth zone, which lies anterior to the telson (see Figs. 3e, 4d; zone described in detail below).

Intersegmental nerves exist between adjacent neuromeres from the tritocerebrum to Th4 (e.g., Fig. 4c; Tables 2, 3). In Md, all three appendage nerves (exnv, ennv, plnv) extend from one root toward the mandible (Fig. 3h). In Mx1, we were only able to identify the exopodite nerve and the posterolateral nerve, which arise from separate roots (Fig. 4c). In Mx2, Th1, and Th2, respectively, only the short root of an exopodite nerve is present (blue arrows in Fig. 4c). The four major segmental commissures known from the adult ventral nerve cord (Stegner et al. 2014a) are unevenly distributed over the subesophageal and trunk segments (Figs. 3h, 4c, d; Table 2).

One to a few SL-ir longitudinal neurites on each side extend between the brain and Th2, contributing to one SL-ir domain in the Md/Mx1 region (Figs. 3h, 4c) and to segmental domains in Mx2, Th1, and Th2, respectively (Fig. 4c). SLI is absent posterior to Th2. Md still lacks SL-ir neurons at this stage (Fig. 3h; Table 2). Mx1 features two, Mx2 three, and Th1 two SL-ir neurons (Fig. 4c), which we were able to identify individually as s16 and s19 (from Mx1 to Th1) and s14 (in Mx2 only; Tables 2, 3). The short root of the exopodite nerve present from Mx1 to Th2 is SL-ir (blue arrows in Fig. 4c), although Th2 lacks a contributing SL-ir soma s16.

Near the ventral nerve cord, the base of each furcal branch contains the large soma of one setal neuron (sen, Fig. 4e), which projects its neurite into a conspicuous tubular sheath (sh, Figs. 3e, 4d, e). This sheath traverses the furcal branch and is terminally associated with the more medial of two long setae (Fig. 4d).

Posterior growth zone

From E2 onwards, we found evidence of a distinctive growth zone situated anterior to the telson, which persists throughout the anameric larval phase. Sytox nuclear staining in the trunk ending revealed a visible difference between various large weakly stained cells on the one hand and numerous smaller cells on the other (see, e.g., Fig. 5b, c). Several of the large weakly stained cells were found to be irregularly arranged in one distinct transverse band spanning the ventrolateral and ventral region of the trunk (masked in yellow in Fig. 5e–g; see also Fig. 7b, f). Since the band's restriction to the anterior margin of the telson and its distinctive cell morphology persist throughout the anameric larval phase (e.g., Figs. 3e, 4d, 6a, 7b, c, f; not studied in L14), we suggest that it constitutes (or is part of) a posterior growth zone. In contrast, many of the smaller, more strongly stained cells in the trunk ending were assignable to the developing ganglion anlage anterior to the growth zone (e.g., Th5 in Fig. 5c–g; Ab1 in Fig. 7f). The growth zone is posteriorly confluent with a few longitudinal rows of what are presumed to be ectodermal cells (Fig. 5e, best visible in Fig. 5f).

In one specimen of L1, we found on each side of the growth zone one large apical cell (asterisks in Fig. 5b, e), which was situated adjacent to an inward-pointing row of three smaller cells (arrows in Fig. 5b). This conspicuous arrangement is reminiscent of the asymmetric cell division pattern of neuroblasts and ganglion mother cells in other crustaceans (see "Discussion"), but was only observed in this one L1 individual, despite attempts to locate it in numerous specimens of this and other stages.

Most Sytox-stained cells (or somata) in the trunk ending display considerable internal heterogeneity, containing minute areas of stronger and weaker fluorescence (see Fig. 6b). A few cells, however, exhibit uniformly strong fluorescence (marked in yellow in Fig. 6a, b). In the trunk ending of many stages, here exemplified in L2, Sytox fluorescence implies that some cells are in the metaphase of mitosis (marked in yellow in Fig. 6b). Mitotic cells are not

Table 2 Developing structures and patterns in the brain and the mandibular and maxillular neuromeres

region	structure or pattern	component	E1	E2	L1	L2	L3	L4	L5	L6	L14	A
brain	nerves & neurite bundles	a1nv (upper root), dtnv, a2nv, ttnv, prec, pec										
		a1nv (lower root), dbs										
		lbc	anlage									
	major neuropils	lateral ptc, dc, tc										
		median ptc, ol, lbn										
	multi-lobed complex	pedunculus										
		lt, ogt		continous	...	separate						
		neuropils 1, 2, 4-6, 9-11										
		neuropil 3										
		neuropil 7, 8										
		globuli cells specialized										
	pdc	mn, ln										
	SL-ir domains	sd1, sd4										
		sd2, sd3										
	SL-ir neurons	s1-3, s5-7, s8, s10, s11										
		s12, s13										
Md	nerves & neurites	isnv, exnv, ennv, mnb										
		plnv										
	commis-sures	adc										
		avc										
		spc_v										
	SL-ir neurons	s15a									?	
		s15b									?	
		s25?					2				?	
Mx1	nerves & neurites	isnv										
		exnv	anlage									
		plnv										
		ennv										
	commis-sures	adc, fpc										
		avc										
		spc_v			?							
	SL-ir neurons	s15a						?				
		s15b						?				
		s16						?		*		
		s18				*	*	?	*	*	*	*
		s19			*	*		?		*	*	*
		s21?			*	*	*	?	*	3 *	*	*
		s26?						?				

By the hatching stage (L1, *dark gray column*), the brain and the mandibular and maxillular neuromeres broadly correspond already to those in the adult. Fields containing numbers (2, 3) indicate that the respective SL-ir neurons were found more than once per hemineuromere. Two or three medial SL-ir neurons (s16 to s21?) per body side are found in Mx1 from the late embryonic phase onwards. All anteromedial neurons whose neurites could not be traced were labeled s21? (white asterisks). They might, however, be neurons s16, s18, or s19 (marked by a black asterisk if absent), so that apparent changes in the SLI of these neurons may be artifactual

a1nv, a2nv, antennula and antenna nerve; adc, avc, anterodorsal and anteroventral commissure; dbs, dorsomedian neurite bundle; dc, deutocerebral neuropil; dtnv, deutocerebral tegumentary nerve; ennv, exnv, endopodite and exopodite nerve; fpc, first posterior commissure; isnv, intersegmental nerve; lbc, labral commissure; lbn, labral neuropil; ln, lateral neuropil; lt, lateral tract; mn, median neuropil; mnb, median neurite bundle; ogt, olfactory globular tract; ol, olfactory lobe; pdc, posterodorsal neuropil cluster; pec, post-esophageal commissures; prec, pre-esophageal commissures; plnv, posterolateral nerve; ptc, protocerebral neuropil; s1–13, SL-ir neurons 1–13; sd1–4, SL-ir domain 1–4; spc, second posterior commissure; spcv, ventral part of spc; tc, tritocerebral neuropil; ttnv, tritocerebral tegumentary nerve

Table 3 Structures and patterns appearing in the maxillar and thoracic neuromeres

neuro-mere	structures and patterns	E2	L1	L2	L3	L4	L5	L6	L8	L14	L18	Adult
Mx2	nerves	isnv, exnv, plnv	…	+ ennv	…	…	…	…	…	…	…	…
	commissures	adc, avc, fpc, spc	…	…	…	…	...	…	…	…	…	…
	SL-ir neurons	s14, s16, s19	…	…	+ s15a, s21?	?	– s15a, s21?	+ s15a, s21?	?	+ s15b	– s16, s19 + s21?	– s21? + s16, s19
	segm. / *limb*	*bud*		*bifurcate*	*complete*	...	...	...	...	...	...	...
Th1	nerves	isnv, exnv	?	+ plnv	+ ennv	…	…	…	…	…	…	…
	commissures	adc, fpc	?	+ avc, spc	…	…	…	…	…	…	…	…
	SL-ir neurons	s16, s19	?	+ s14	…	…	…	…	…	+ s15a,b, s17, s18	– s16 to s19 + two s21?	– s21? + s16, s18, s19
	segm. / *limb*			*bud*	*bifurcate*	...	*complete*	...	...	...	...	...
Th2	nerves	isnv, exnv	?	+ plnv	…	…	+ ennv	…	…	…	…	…
	commissures	adc	+ fpc	+ avc, spc	…	…	…	…	…	…	…	…
	SL-ir neurons		?	s16, s19	…	…	…	…	…	+ s14, s15a,b, s21?	– s16, s19 + s21?	– s14 + s16, s17, s19
	segm. / *limb*				*bud*		*bifurcate*	...	*complete*	...	...	...
Th3	nerves	isnv	?	+ exnv	…	…	+ plnv	…	…	+ ennv	…	…
	commissures	adc	+ fpc	+ avc, spc	…	…	…	…	…	…	…	…
	SL-ir neurons		?	s16, s19	…	?	… + s20	…	– s19, s20	+ s15a, s19, s21?	– s16, s19 + s14, s15b, s21?	– s21? + s16 to s18, s22?, s23?
	segm. / *limb*							*bud*		*complete*	...	...
Th4	nerves	isnv	?	+ exnv	…	…	+ plnv	…	…	+ ennv	…	…
	commissures	adc	…	+ fpc	+ avc, spc	…	…	…	…	…	…	…
	SL-ir neurons		?	s16, s19	…	…	+ s20	…	…	…	+ s15a	– s19, s20 + s15b, s21?, s24?
	segm. / *limb*									*bifurcate*	*complete*	...
Th5	nerves		?	+ isnv	…	…	…	+ exnv	+ plnv	…	+ ennv	…
	commissures		adc	…	+ fpc, spc	…	…	+ avc	…	…	…	…
	SL-ir neurons			s16	+ s19	…	+ s20	…	…	…	…	– s19, s20 + s15a,b, two s21?, s22?
	segm. / *limb*										*bifurcate*	*complete*
Th6	nerves			isnv	…	…	…	…	+ exnv	+ plnv	…	+ ennv
	commissures			adc	+ fpc	+ spc	…	+ avc	…	…	…	…
	SL-ir neurons						s16, s19	+ s20	…	– s20	…	+ s15a,b, s17, s18, s20, two s21?
	segm. / *limb*										*bud*	*complete*
Th7	nerves			isnv	…	…	…	…	+ exnv	+ plnv	…	+ ennv
	commissures			adc	…	+ fpc	+ spc	…	+ avc	…	…	…
	SL-ir neurons						s16, s20	…	+ s19	– s20	- s19	+ s15a, s17, s19, s20, two s21?, s23?, s25?
	segm. / *limb*											*complete*
Th8	nerves				isnv	…	…	…	…	…	+ exnv	+ plnv, ennv
	commissures				adc	+ fpc	…	+ spc	+ avc	…	…	…
	SL-ir neurons						s16	+ s19	+ s20	…	– s20	– s16 + s17, s18, s20, two s21?
	segm. / *limb*											*complete*
Th9	nerves					isnv	…	…	…	…	…	+ exnv, ennv, plnv
	commissures				adc	…	+ fpc	+ spc	…	-spc	+ spc	+ avc
	SL-ir neurons							s16, s19	– s19	+ s19	– s19	– s16 + s19, s20, s21?
	segm. / *limb*											*bud-like lobe*

This table is based on Suppl. Tab. S1 but only lists the changes between stages. Dark gray cells in the row "segm., limb" indicate that the segment is completely distinct from the trunk ending. The degree of development of the limbs is divided into bud → bifurcate anlage → complete limb. Medium gray cells indicate that the respective nerval or commissural pattern is complete. Nerves are mentioned as soon as their root is visible. No change from the previous stage is indicated by "…." Changes are indicated by "+" and "–." Most developing thoracic segments pass through a distinct initial phase in which only one intersegmental nerve, two commissures, and two SL-ir neurons (cells marked in light gray, see text) are present. The transiently SL-ir neuron s20 in Th3 to Th5 does not remain SL-ir in the adult. s20 only retains SLI in Th6 to Th9. If a structure or pattern was present in one specimen of a stage, it is depicted; interspecific variability is not visualized. Aberrations in the SL-ir pattern of L18 may be due to incomplete staining (see "Materials and methods")

ac, adc, avc, anterior, anterodorsal, and anteroventral commissure; bud, appendage bud; ennv, exnv, endopodite and exopodite nerve; fpc, first posterior commissure; isnv, intersegmental nerve; pc, posterior commissure; plnv, posterolateral nerve; s14–s28, SL-ir neurons 14–28; spc, second posterior commissure

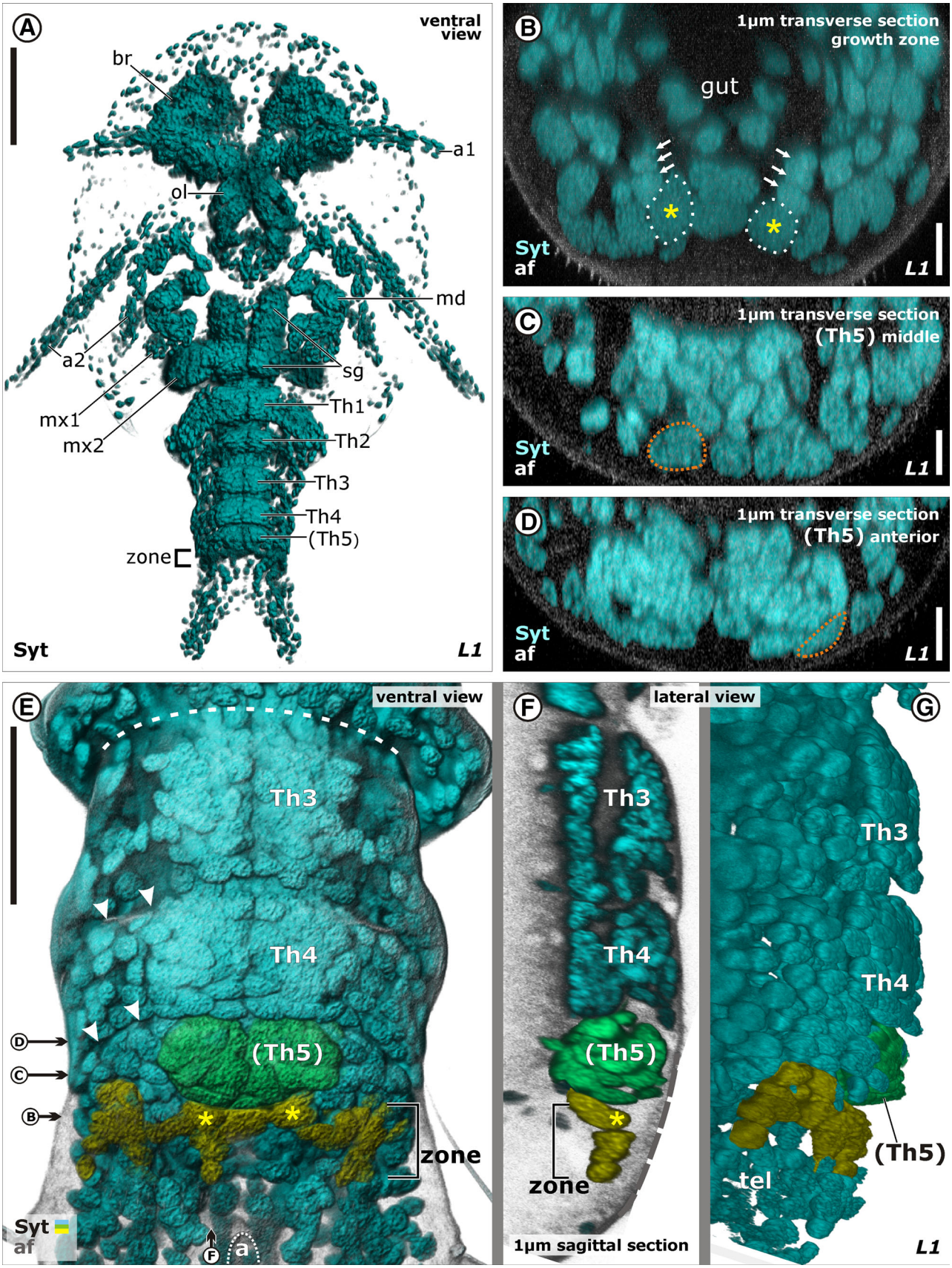
A
ventral view
br
a1
ol
md
a2
sg
mx1
Th1
mx2
Th2
Th3
Th4
(Th5)
zone
Syt
L1
B
1µm transverse section
growth zone
gut
Syt
af
L1
C
1µm transverse section
(Th5) middle
Syt
af
L1
D
1µm transverse section
(Th5) anterior
Syt
af
L1
E
ventral view
Th3
Th4
(Th5)
zone
Syt
af
F
lateral view
Th3
Th4
(Th5)
zone
1µm sagittal section
G
Th3
Th4
(Th5)
tel
L1

◀**Fig. 5** Neuronal differentiation in the trunk of one specimen of larval stage L1. Confocal micrographs in Imaris surpass view (**a**, **e**, **g**) or Imaris extended section view (**b–d**, **f**), showing Sytox nuclear staining. **a** Overview of the hatchling shows the separated, developing ganglia of the limbless thoracic segments 1–4. **b–d** Virtual transverse sections through the as yet unsegmented trunk ending. **b** A large apical cell (*asterisks*) on each side of the growth zone is adjacent to an inward-pointing row of three smaller cells (*arrows*), reminiscent of a neuroblast and three ganglion mother cells. **c**, **d** Large spheroidal or flattened apical cells (marked in *red*) also occur anterior to the growth zone. **e–g** A transverse band of irregularly, comparatively loosely arranged cells were assigned to the growth zone (artificially highlighted in *yellow*) on the basis of their weaker fluorescence. **e** *Arrowheads* mark prospective segment borders, which appear as infolds in the cuticle yet are externally invisible. *Abbreviations* a, anus; a1, a2, antennula and antenna; af, autofluorescence; br, brain; gut, gut; md, mx1, mx2, mandible, maxillula, and maxilla; ol, olfactory lobe; sg, subesophageal ganglion; Syt, Sytox nuclear staining; tel, telson; zone, growth zone. *Scale bars* **a** 100 µm, **b–d** 10 µm, **e–g** 50 µm

restricted to the growth zone but also occur in the more anterior, separated developing ganglia in the trunk (Fig. 6a, b). The axis of cell division does not appear to have a preferred orientation.

In all studied stages of the anameric larval phase, the posteriormost developing ganglion anlage is situated directly adjacent to the growth zone and already includes its first segmental neural structures, namely a distinct soma cortex and an anterodorsal/anterior commissure (e.g., Figs. 4d, 6b, d, 7a, b, f). Although we were not able to observe cell divisions directly, the direct proximity of the growth zone and newly formed ganglion anlagen implies a uniquely early neuronal differentiation in the trunk ending of *H. macracantha*.

Larval stage L1

Brain In terms of the brain, the only changes between E2 and L1 take place in the multi-lobed complex (summarized in Table 2). The pedunculus of the hatching stage (L1) now comprises more neurite bundles than in the previous stage and bears the bulbous neuropils 4, 5, and 6 (Fig. 4f–h). Neuropil 10 appears as a faint lateral swelling of each pedunculus (Fig. 4f, h). Moreover, the three unpaired neuropils 1, 2, and 11 connect the pedunculi in the midline, while neuropil 3 is still absent (Fig. 4f, g). Neuropils 1, 5, 6, and 11 are SL-ir (Fig. 4h).

Ventral nerve cord Although only Th1 and Th2 are externally separate in L1 (Fig. 1), thoracic ganglia 1–5 are distinctly separate from each other, the latter three being situated in the unsegmented trunk ending (Fig. 5a). Thoracic ganglion 5 is comparatively short. L1 features three new commissures: the first posterior commissures in Th2 and Th3, respectively, and the anterodorsal commissure in Th5 (Table 3). Due to the fragmentary nature of our data on acetylated α-tubulin and serotonin in the ventral nerve cord in stage L1, other changes which take place from E2 to L2 cannot be unambiguously assigned to either L1 or L2 (Tables 2, 3).

Larval stage L2

Brain In the multi-lobed complex, the anlagen of neuropils 7 and 8 have developed as swellings of the olfactory globular tract, separating the latter from the lateral tract (not depicted, but see Table 2) on each side. The pedunculus comprises more neurites than in L1. The globuli cell somata in division iv of the protocerebral somata assemblage are more densely packed and smaller in diameter than the surrounding somata (not depicted). The brain of L2 exhibits the four SL-ir domains sd1–sd4 found in the adult.

Ventral nerve cord Th1 to Th4 are externally separate in L2 (Figs. 1, 6e). The soma cortexes of thoracic ganglia 1–7 are separate from each other (e.g., Fig. 6a). The still developing thoracic ganglion 7 is directly adjacent to the growth zone (Fig. 6a).

Across the different specimens of L2 available for this study, we observed differences in the degree of development of the commissural and SL-ir patterns. In the trunk of early L2, only Th1 and Th2 exhibit the complete tetracommissural pattern, while Th3 and Th4 only feature an anterodorsal and first posterior commissure. Anterodorsal commissures also occur in the still confluent segments Th5–Th7 (Fig. 6c, d). Th1 features three SL-ir neurons (s14, s16, s19), Th2 and Th3 feature two (s16, s19), and Th4 just one (s16) per hemiganglion (Fig. 6c, d). In contrast, in the trunk of late L2, Th3 exhibits a faint second posterior and an anteroventral commissure (not depicted, but scored in Table 3). Th4 now exhibits two somata (s16, s19) and Th5 one per hemiganglion (s16, Fig. 6e, Table 3).

Larval stage L3

Brain The anlagen of one unpaired median neuropil and a pair of lateral neuropils of the posterodorsal neuropil cluster have developed between the olfactory globular tracts (Fig. 7d). Most components of the multi-lobed complex in L3 have grown to the same relative size as in the adult—including the thick pedunculus (Fig. 7d). The only exception is the still absent neuropil 3.

Ventral nerve cord As in the previous stage, thoracic ganglia 1–6 are separate from each other (Fig. 7b). Neural structures within the unsegmented trunk ending can be assigned to prospective segments Th7–Th9 by

autofluorescent ventral infolds in the cuticle (not depicted) and by tubulin-rich muscle insertion sites (arrowheads in Fig. 7a). Most somata of Th7 and some somata of Th8 and Th9 are present, but they still lie within one continuous assemblage posteriorly adjacent to the growth zone (Fig. 7b). As summarized in Table 3, new nerves and commissures are present in the trunk of L3. For instance, anterodorsal commissures now occur as far posteriorly as Th9 (Fig. 7a), and second posterior commissures, which may only comprise a few neurites, are identifiable as far posteriorly as Th5 (positions indicated by red dotted lines in Fig. 7a). Only one SL-ir neuron has appeared since the previous stage (s19 in Th5, Table 3; Fig. 7a).

Larval stage L4

Brain Neuropil 3 completes the multi-lobed complex in L4 (not depicted). Thus, as summarized in Table 2, all neural features in the brain have completely developed by this stage.

Ventral nerve cord Thoracic ganglia 1–8 are separate from each other. Ganglia anlagen of the prospective segments Th9 and Ab1 are discernible within one widely confluent assemblage adjacent to the growth zone (Fig. 7f). One specimen of L4 permitted a comparison between the intersegmental nerves of different segments, with the limbs exhibiting differences in their degree of development (Table 3). The main branch of the intersegmental nerve between the less-developed segments Th2 and Th1 innervates the pleural spine of Th2 (Fig. 7e), corresponding to the pattern in the adult abdomen (Stegner et al. 2014a). Additionally, we found an anterior side branch of this intersegmental nerve, which connected with the lateral neurite bundle in L4 (Fig. 7e). A similar but not identical innervation pattern is exhibited by the intersegmental nerve between the segments Th1 and Mx2, which are more developed. Proximally, the intersegmental nerve splits into a dorsal branch (white arrow in Fig. 7e), which innervates the tergite of Th1, and a lateral branch (yellow arrow), which bifurcates distally (blue arrows) to innervate the flattened pleural spine of Th1. The latter already anticipates the wing-shaped pleurite plate of the adult (Fig. 7d). The intersegmental nerve between Th1 and Th2 intersects the lateral neurite bundle proximally, but we were not able to trace any of its neurites actually into the bundle.

Although no abdominal segments are separated from the trunk ending as yet, L4 is the first stage to display neural structures of the prospective abdomen, including the intersegmental nerves between Th9/Ab1 and Ab1/Ab2 and the anterior commissure of Ab1 (Suppl. Table S1).

Larval stages L5, L6, L8

Although not depicted in the figures, our data on L5, L6, and L8 are summarized in Table 3. Several exopodite and posterolateral nerves are added to the ventral nerve cord during these stages, but only one additional endopodite nerve develops (Th2/L5 in Table 3). All thoracic segments except Th9 have completed their adult-like tetracommissural pattern by L8. By L6, all thoracic segments exhibit at least the SL-ir neurons s16 and s19. In addition, between L5 and L8, the SL-ir anterolateral neuron s20 appears from Th3 to Th8 (Table 3, depicted and described in more detail for L14).

The abdominal segments that develop from L5 to L8 correspond in external morphology to the limbless thoracic segments (e.g., Fig. 2a, b, d, f). In L8, intersegmental nerves occur as far posteriorly as between Ab5/Ab6, anterior commissures as far posteriorly as Ab4, and posterior commissures as far posteriorly as Ab3 (all structures listed in Suppl. Table S1). No data exist on the SL-ir pattern in L8.

Larval stage L14

In the thorax, the anteroventral commissure of Th9 is still absent, as in L8 (Table 3). However, additional nerves have developed. Th3 and Th4 now exhibit an endopodite nerve (masked in yellow in Fig. 8a, b). New short posterolateral nerve roots are recognizable in Th5 and Th6, respectively (masked in red in Fig. 8a, b; red arrows in Fig. 8e), but there have been no developments in exopodite nerves since L8 (Table 3).

Changes in the SL-ir pattern in comparison with L8 have taken place most noticeably in Mx2 and the anterior thoracic segments Th1–Th3, which now feature the additional SL-ir neurons s14, s15a, s15b, s17, s18, s21? (Fig. 8d; Table 3). In this respect, Mx2 and Th1 now correspond broadly to the adult pattern. Note that the anteroventral commissure in Th3 and Th4 is SL-ir, although a SL-ir soma s14 could not be confirmed to contribute to it (Fig. 8d). Unlike in L8, the SL-ir neuron s20 was not identifiable in Th3 (Fig. 8d). The more posterior segments Th4 (Fig. 8d) to Th9 (Table 3; Fig. 8d, e) exhibit the same pattern as in L8.

Except for the intersegmental nerve between Ab9/Ab10 and the SL-ir neurons in Ab7 and Ab8, all the neural features of the adult abdominal nervous system have developed by stage L14 (Fig. 8c, f, Suppl. Table S1). These comprise the respective intersegmental nerves, the anterior and posterior commissures, and SL-ir neurons s27 and s28 (Stegner et al. 2014a). Continuous longitudinal neurites that extend from the ventral nerve cord into the furcal branches (as present in the adult; Stegner et al. 2014a) do

not exist at any point between E1 and L14 (no data available on later larval stages).

Larval stage L18 to adult

In comparison with L14, three new structures are found in the L18 trunk: the endopodite nerve of Th5, the exopodite nerve of Th8, and the second posterior commissure of Th9 (not depicted, summarized in Table 3). As listed in Table 3, the additional SL-ir neurons s14, s15b (Th3), and s15a (Th4) were individually identifiable in the thorax of L18. Some additional anteromedial SL-ir somata were also found from Mx2 to Th3, here labeled s21? (Table 3). Since the SL-ir neurons in the only available specimen of L18 were only weakly stained, we cannot rule out the presence of further SL-ir neurons than listed in Table 3 in the thorax of L18.

The investigated abdominal structures in L18 correspond to those in stage L14. Unfortunately, however, the ventral nerve cord in the studied specimen of L18 was broken in Ab3 and between Ab8 and Ab10. The only new SL-ir neuron found was s28 in Ab1 (Suppl. Table S1). Apart from in the broken segments, for which data are missing, it appears that all SL-ir neurons in the abdomen are complete (compare to adult in Suppl. Table S1).

Discussion

Comparing neurodevelopment against the background of different developmental modes

Crustaceans exhibit a broad variety of developmental modes (e.g., Martin et al. 2014; Malacostraca: Scholtz 2000; Branchiopoda: Fritsch et al. 2013), with the hatching stages varying between species even within Cephalocarida (e.g., Addis et al. 2007). Many crustaceans hatch as a short free-swimming larva which differentiates most posterior segments and appendages during an anameric larval phase (e.g., Dahms 2000; Minelli and Fusco 2013). Examples of short hatching stages are the taxonomically widespread orthonauplius, whose only appendages are the antennula, antenna, and mandible, but also the L1 metanauplius in the cephalocarid *H. macracantha*, which has in addition a maxillula and maxilla. In other taxa, on the other hand, most development takes place in an embryonic phase under maternal protection, meaning that the released stage is a directly developed juvenile equipped with all trunk segments and appendages (e.g., Gruner 1993). Even though the orthonauplius of some malacostracans is likely to have evolved secondarily (e.g., Scholtz 2000), it is generally assumed that an orthonauplius hatching stage dates back to the last common ancestor of all crustaceans (e.g., Walossek and Müller 1990; Lauterbach 1983, 1986; Scholtz 2000), which implies that the metanauplius hatching stage of Cephalocarida is derived. Within an evolutionary framework, many differences in developmental mode can be explained by heterochronic shifts in the temporal order of comparable developmental events (Smith 2001; Minelli et al. 2006), a phenomenon which applies to both external and internal morphology (see, e.g., Haug et al. 2010; Fritsch et al. 2013). In order to understand the evolution of the different developmental modes across crustaceans, a broad comparison of developmental sequences incorporating comparable external and internal developmental events is needed. The present study into Cephalocarida contributes a key taxon to this comparison. The only other detailed crustacean neurodevelopmental data available are restricted to Malacostraca (Fischer and Scholtz 2010: Stomatopoda; Harzsch 2003, Vilpoux et al. 2006: Decapoda; Ungerer et al. 2011b: Amphipoda) and Branchiopoda (Harzsch and Glötzner 2002: Anostraca; Fritsch and Richter 2010, 2012, Fritsch et al. 2013: Phyllopoda). In other crustacean taxa, neurodevelopmental data are only available for specific stages (Lacalli 2009: Copepoda; Walley 1969, Semmler et al. 2008: Cirripedia). Two comparative studies into Branchiopoda (Fritsch et al. 2013) and Malacostraca (unpublished data by G. Jirikowski, C. Wolff, S. Richter) recently defined a number of external and internal developmental events, many of which are easily transferable to *H. macracantha* (listed in Suppl. Table S2). In the present study, they serve as a basis for an initial comparison between developmental sequences in Cephalocarida, Branchiopoda, and Malacostraca with respect to external and neural anatomy (Suppl. Table S3). Other neurodevelopmental studies into Branchiopoda, Malacostraca, Copepoda, and Cirripedia are included for their insights into particular questions.

Development of the nervous system in the naupliar region

H. macracantha corresponds to other crustaceans in that the first neuromeres to develop are those of the brain (proto-, deuto-, tritocerebrum) and the mandibular neuromere, summarized as the "naupliar neuromeres" (Suppl. Table 3; Fritsch and Richter 2010, 2012: Branchiopoda; Vilpoux et al. 2006, Fischer and Scholtz 2010, Ungerer et al. 2011b: Malacostraca; Lacalli 2009: Copepoda; Walley 1969, Semmler et al. 2008: Cirripedia). Correspondingly, during the embryonic development of *H. macracantha* and all other crustaceans studied, irrespective of hatching stage, the neuromeres of the brain form a conspicuous circumoral ring consisting of pre- and post-esophageal commissures and par-esophageal longitudinal neurites well before any postnaupliar commissure is visible in Mx1, Mx2, or more posteriorly (Fritsch and Richter

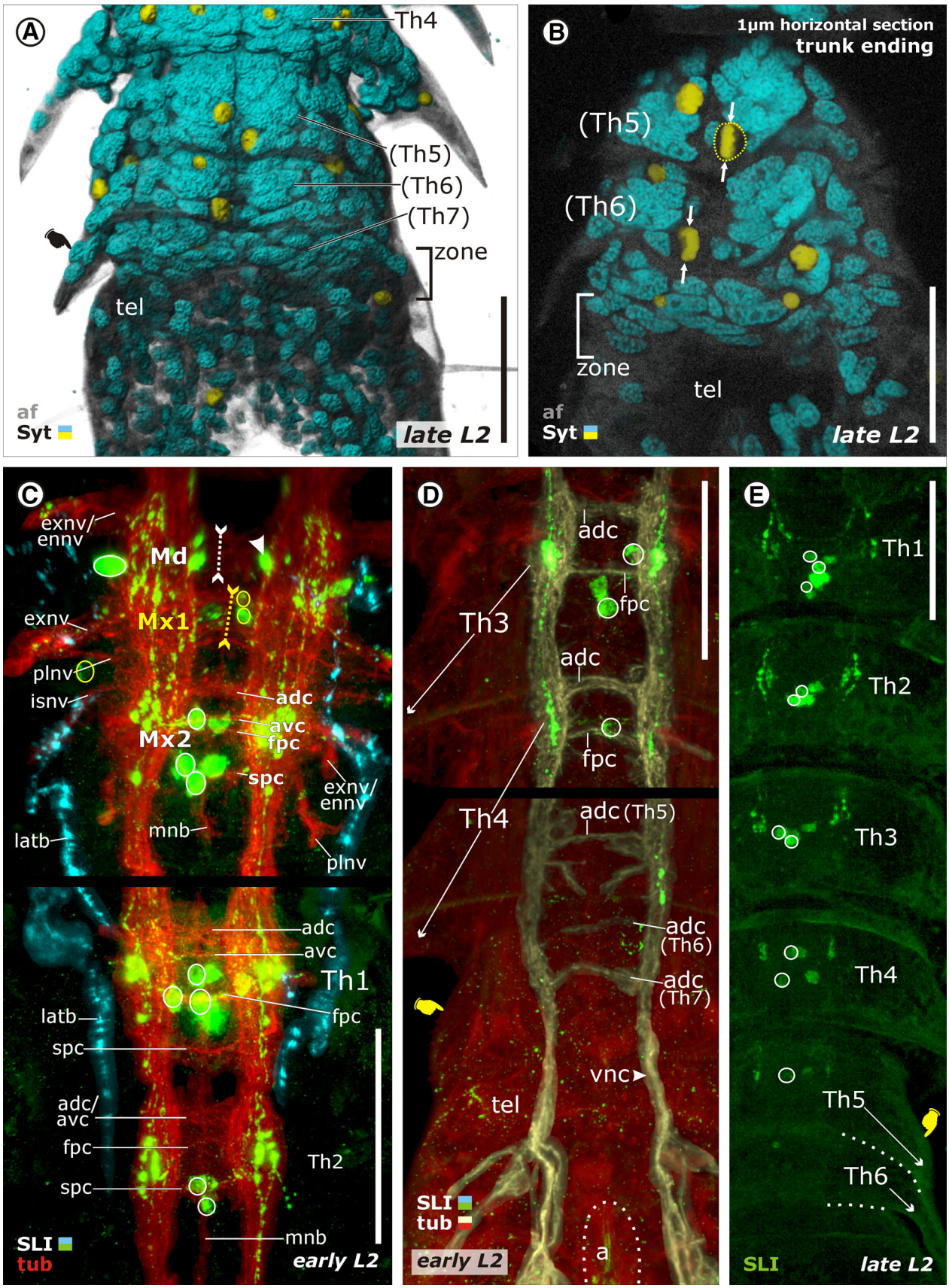
A
Th4
(Th5)
(Th6)
(Th7)
zone
tel
af
Syt
late L2
B
1µm horizontal section
trunk ending
(Th5)
(Th6)
zone
tel
af
Syt
late L2
C
exnv/
ennv
Md
Mx1
exnv
plnv
isnv
adc
avc
fpc
Mx2
spc
exnv/
ennv
latb
mnb
plnv
adc
avc
Th1
latb
fpc
spc
adc/
avc
fpc
Th2
spc
mnb
SLI
tub
early L2
D
adc
fpc
Th3
adc
fpc
Th4
adc (Th5)
adc
(Th6)
adc
(Th7)
vnc
tel
SLI
tub
early L2
a
E
Th1
Th2
Th3
Th4
Th5
Th6
SLI
late L2

◀**Fig. 6** Neurodevelopment throughout larval stage L2. Confocal micrographs in Imaris surpass view showing immunolabeling. **a**, **b** Mitotic cells (marked in *yellow*) in the trunk ending, recognizable by the concentration of chromosomes in the cell center (*arrows* in **b**). **a**, **e**. The pleural spines of prospective Th5 and Th6 start emerging from the trunk ending (finger). **c**–**e** SL-ir neurons of one body side marked. **c**, **d** Early representative of L2. **c** Neuropil and neurite bundles artificially masked (*red*), SL-ir lateral neurite bundle (*blue*) artificially highlighted. Commissures (positions marked for Md and Mx1) and nerves of the subesophageal ganglion correspond completely to those in the adult. **d** Neuropil and neurite bundles (*yellow*) artificially highlighted. Pleural spines of Th5 and Th6 still absent (finger). SL-ir neurons occur only as far posteriorly as Th4, anterodorsal commissures already as far posteriorly as Th7. **e** Segmental SL-ir neurons and domains occur as far posteriorly as Th5. *Abbreviations* a, anus; adc, anterodorsal commissure; af, autofluorescence; avc, anteroventral commissure; ennv, exnv, endopodite and exopodite nerve; fpc, first posterior commissure; isnv, intersegmental nerve; latb, lateral neurite bundle; mnb, median neurite bundle; plnv, posterolateral nerve; prs, protocerebral somata; SLI, serotonin-like immunoreactivity; spc, second posterior commissure; Syt, Sytox nuclear staining; tel, telson; zone, growth zone; tub, tubulin staining; zone, growth zone; vnc, ventral nerve cord. *Scale bars* 50 µm

2010, 2012: Branchiopoda; Vilpoux et al. 2006, Fischer and Scholtz 2010, Ungerer et al. 2011b: Malacostraca; Lacalli 2009: Copepoda). The early external morphological development of naupliar prior to postnaupliar segments, as has been described during the embryonic or larval phase for almost all crustaceans (except some peracarid malacostracans, see Scholtz 2000), is thus reflected in the early development of naupliar prior to distinctive postnaupliar neuromeres. The naupliar neuromeres and the maxillular nerve root in *H. macracantha* are evidently cephalic in origin as they develop before the posterior growth zone. Where exactly the neuromeres of Mx1 to Th4 originate is a question which remains open, as we missed the critical embryonic stages between E1 and E2. Dohle and Scholtz (1988) have demonstrated in Malacostraca that in addition to the naupliar segments, cells in some postnaupliar segments (Mx1, Mx2, Th1) also originate from cephalic precursors.

Aside from these general correspondences, it is noted that the naupliar neuromeres of the hatching metanauplius of *H. macracantha* exhibit a significantly higher degree of development than that observed in the hatching orthonauplius of other crustaceans. While the brain in *H. macracantha* is in possession of all its nerves, commissures, somata assemblages, tracts, serotonin-like immunoreactive neurons, and most of its neuropils before hatching (the last few neuropils develop by L3), the brain in the hatching orthonauplius of Branchiopoda (Harzsch and Glötzner 2002; Fritsch and Richter 2010, 2012), dendrobranchiate Malacostraca (unpublished data by G. Jirikowski, C. Wolff, S. Richter), and Cirripedia (Harrison and Sandeman 1999) only exhibits a faintly developed neuropil and (as far as studied) a few serotonin-like immunoreactive neurons (Fritsch and Richter 2010, 2012: Branchiopoda).

Development of the nervous system in the postnaupliar region

With some exceptions in the cephalic and near-cephalic region (e.g., Dohle and Scholtz 1988), all crustaceans including *H. macracantha* correspond in that their "postnaupliar neuromeres" differentiate from ectodermal cells that originated in a growth zone anterior to the telson (e.g., Malacostraca: Dohle and Scholtz 1997; Vilpoux et al. 2006; Fischer and Scholtz 2010; Branchiopoda: Harzsch and Glötzner 2002; Ungerer et al. 2011a; Remipedia: Koenemann et al. 2009). However, *H. macracantha* is the only known crustacean in which the differentiation of thoracic ganglia precedes the differentiation of limbs. Before their respective limb bud is visible, the thoracic segments develop a separate ganglion with a soma cortex, an exopodite and a posterolateral nerve root, and at least two commissures. In all other studied crustaceans, a neuromere comprising comparable neural features only develops after the thoracic limb bud (Branchiopoda: Fritsch and Richter 2010, 2012; Malacostraca: Harzsch 2003; Fischer and Scholtz 2010; Ungerer et al. 2011b; Suppl. Table S3). The extent of this difference becomes most obvious when the hatching free-swimming naupliuses of non-cladoceromorphan Branchiopoda (Harzsch and Glötzner 2002, Fritsch and Richter 2010, 2012), dendrobranchiate Malacostraca (unpublished data by G. Jirikowski, C. Wolff, S. Richter), or Cirripedia (Semmler et al. 2008)—all of which lack any postnaupliar appendages or neuromeres—are compared with the hatching metanauplius of *H. macracantha*, which only exhibits an additional two postnaupliar appendage anlagen (maxillula, maxilla) but an additional six postnaupliar ganglion anlagen (see also Suppl. Table S3).

Fritsch and Richter (2010) have suggested a correlation between limb functionality and the expression of serotonin in the developing trunk segments of Branchiopoda. Indeed, in all branchiopod taxa, two anterior and two posterior neurons per hemisegment become SL-ir after the formation of the limb (Harzsch and Glötzner 2002; Fritsch and Richter 2010, 2012; Fritsch et al. 2013). In certain Malacostraca too, two anterior SL-ir and two posterior SL-ir neurons per hemisegment have been found to be individually identifiable after the development of the limb (Harzsch and Dawirs 1995; Harzsch 2003). The homologous counterparts of the two anterior and two posterior neurons in *H. macracantha*—s14, s17 (anterior), s15a, and s15b (posterior)—also develop throughout the thorax after the limb. This correspondence to Branchiopoda and Malacostraca is especially interesting in light of the fact that other cephalocarid neural features (soma cortex, nerves, commissures) develop much

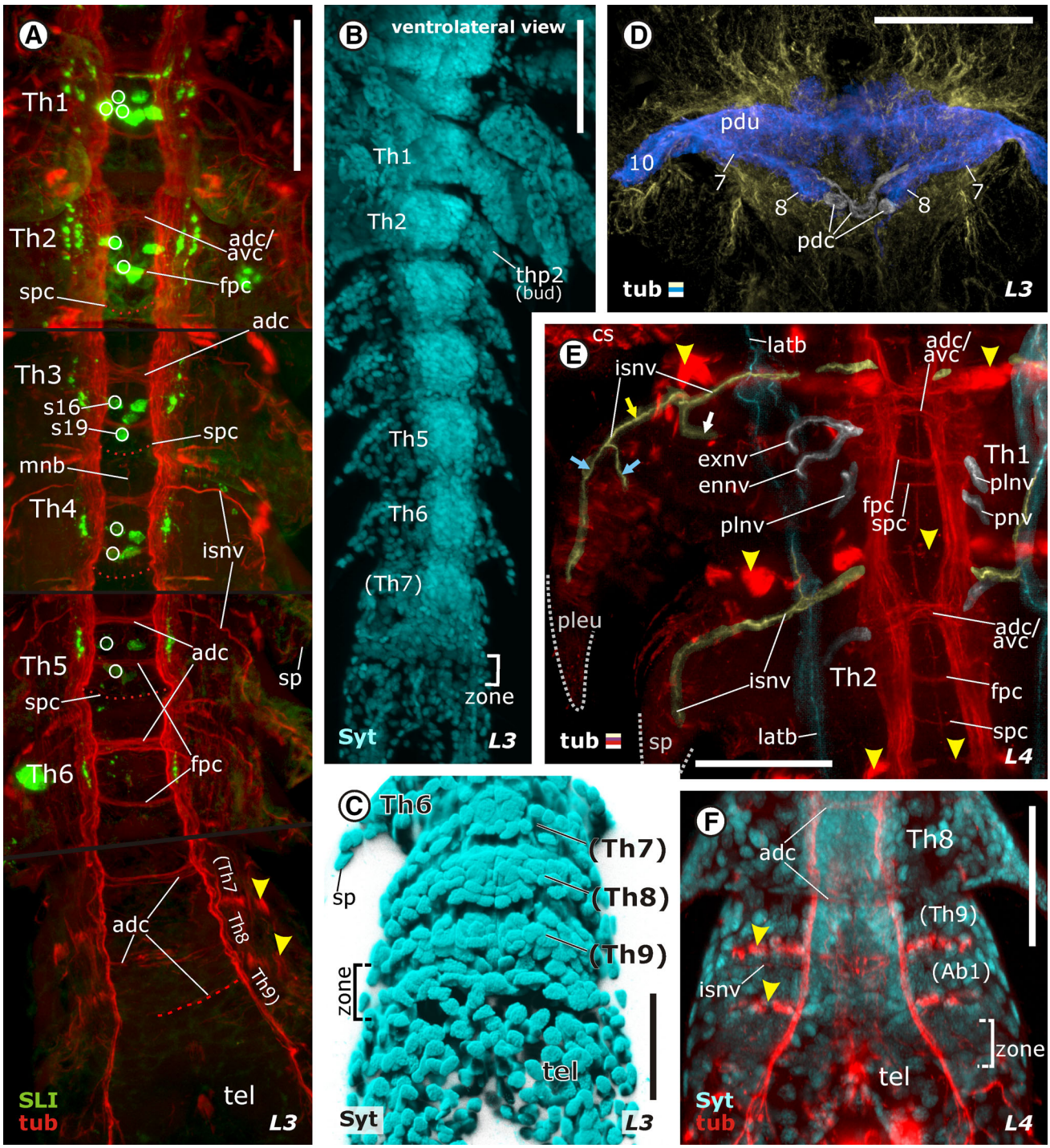

earlier in comparison, well before the limb. The two *H. macracantha* neurons s16 and s19, which become SL-ir before the development of the limb, are absent in Malacostraca and Branchiopoda (discussed by Stegner et al. 2014a). Putative homologous counterparts of s16 and s19 have been described as SL-ir "central neurons" in adult Remipedia (Stemme et al. 2013), but neurodevelopmental data on Remipedia are still lacking.

H. macracantha corresponds to other studied crustaceans in that its postnaupliar neuromeres differentiate their serially homologous neural features from anterior to posterior (e.g., Malacostraca: Harzsch 2003; Vilpoux et al.

◀**Fig. 7** Larval stages L3 and L4. Confocal micrographs in Imaris surpass view showing immunolabeling. *Yellow arrowheads* indicate muscular insertion sites at prospective (**a**, **f**) or distinct (**e**) intersegmental borders. **a**, **c**, **e**, **f** Ventral view. **a** The first two SL-ir neurons in Th2 to Th5 are s16 and s19, the first two segmental commissures in Th6 the anterodorsal and first posterior commissure. **b** At low magnification, the growth zone appears as a transverse row of loosely packed, weakly fluorescent cells. **c** While the neuromeres of Th7 and Th8 are separated in this specimen, it is difficult to distinguish between the growth zone and the developing neuromere of Th9. **D.** Dorsal view of the protocerebral neuropil. The multi-lobed complex, now comprising neuropils 7 and 8 (*blue*), and the posterodorsal neuropil cluster (*white*) are artificially highlighted. **e** As the pleural spine of young thoracic segments (see Th2) grows into an adult-like pleurite plate (see Th1), the intersegmental nerve exhibits several subbranches (*arrows*). More medially, each intersegmental nerve is connected with the lateral neurite bundle. **f** The as yet unseparated trunk ending of L4 also comprises ganglion anlagen of prospective segments. The intersegmental nerve and anterior commissure are the first distinct neurite bundles to develop. *Abbreviations* 7, 8, 10, neuropils 7, 8, and 10 of the multi-lobed complex; adc, avc, anterodosal and anteroventral commissure; ennv, exnv, endopodite and exopodite nerve; fpc, first posterior commissure; isnv, intersegmental nerve; latb, lateral neurite bundle; pdc, posterodorsal neuropil cluster; pdu, pedunculus; pleu, pleurite; plnv, posterolateral nerve; pnv, posterior nerve (unknown); s16, s19, SL-ir neurons 16 and 19; SLI, serotonin-like immunoreactivity; sp, pleural spine; spc, second posterior commissure; Syt, Sytox nuclear staining; tel, telson; thp2, thoracopod 2; tub, tubulin staining; zone, growth zone. S*cale bars* **a**, **d**–**f** 50 μm, **b** 100 μm

2006; Fischer and Scholtz 2010; Ungerer et al. 2011b; Branchiopoda: Harzsch and Glötzner 2002; Fritsch and Richter 2010, 2012). In this process, the developmental peculiarity of Cephalocarida—that two segments are added to the trunk from posterior during early molts (see also Sanders 1963; Walossek 1993; Addis et al. 2007)—is not reflected in the successive development of the nervous system.

Cephalocarid thorax and abdomen in neurodevelopmental comparison

The adult trunk in most Branchiopoda, in Cephalocarida, and in "maxillopodan" crustaceans (i.e., in all entomostracan crustaceans without Remipedia) is divided into a limb-bearing thorax and a limbless abdomen (Gruner 1993). As the terms "thorax" and "abdomen" refer to adult morphology, they have no morphological significance when applied to developmental stages. Most entomostracan crustaceans exhibit ganglia in their thoracic but not in their abdominal segments (reviewed by Stegner et al. 2014a), yet to distinguish between the two tagmata on this basis alone (Deutsch 2001) would be inappropriate for Cephalocarida (Elofsson and Hessler 1990; Stegner et al. 2014a) and Mystacocarida (Brenneis and Richter 2010), which both exhibit ganglia in the thoracic and most abdominal segments too, only the two posteriormost abdominal segments being ganglia-free.

The adult trunk ganglia in *H. macracantha* exhibit several intersegmental differences, some of which reflect the thorax/abdomen boundary (Stegner et al. 2014a). Three segmental appendage nerves, four commissures, and five to eight SL-ir neurons accompany each thoracic ganglion, but only two commissures and one or two SL-ir commissures accompany each abdominal ganglion, with segmental appendage nerves absent altogether (Stegner et al. 2014b). On the basis of the correspondence in their overall position within the segment and their direct connection with the median neurite bundle, it seems reasonable to homologize the anterodorsal commissure and the first posterior commissure in the thorax with, respectively, the anterior and posterior commissure in the abdomen (tagma-specific labels by Stegner et al. 2014a). Moreover, it also appears reasonable to homologize the SL-ir neurons s16 and s19 in the thorax with the SL-ir neurons s27 and s28 in the abdomen, as the position of their neuronal somata is correspondingly anteromedial (s16, s27) and medial (s19, s28). In further support of serial homology between the thoracic neuron s19 and the abdominal neuron s28, both neurons contribute their neurite to the (first) posterior commissure.

Given this serial homologization and the developmental data we collected, we are now able to compare the individual developmental sequences of the different trunk segments of *H. macracantha* (Fig. 9). We include in our comparison (1) the pattern of nerves, (2) the pattern of commissures, (3) the pattern of SL-ir neurons, and (4) limb differentiation. With respect to the latter, we distinguish between absent → limb bud → bifurcate limb anlage → completely developed limb (see "Results"). This permits us to consider neural developmental events in conjunction with events of limb differentiation throughout the trunk (Fig. 9). In many cases, we were unable to resolve the temporal order of events. Two events observed synchronously in one segment were not counted as contradicting the temporal order of the same two events where we succeeded in observing this order in another segment. Leaving aside all events whose temporal order differed between segments (these are treated below), one common developmental sequence was obtained, which is valid for all the segments of the trunk (with a minor exception in Th5). This sequence proceeds as follows (in both the thorax and the abdomen): (1) anterodorsal commissure/anterior commissure; (2) first posterior commissure/posterior commissure; (3) s16/s27; (4) s19/s28; (5) anteroventral commissure; (6) posterolateral nerve; (7) limb bud; (8) bifurcate limb anlage; (9) endopodite nerve; (10) bifurcate limb complete; (11) s15a, (12) s15b, (13) s17, and s18 (see Fig. 9). Though not all the external and neural events of this common sequence occur in every segment, what the sequence clearly demonstrates is that of 16 nervous

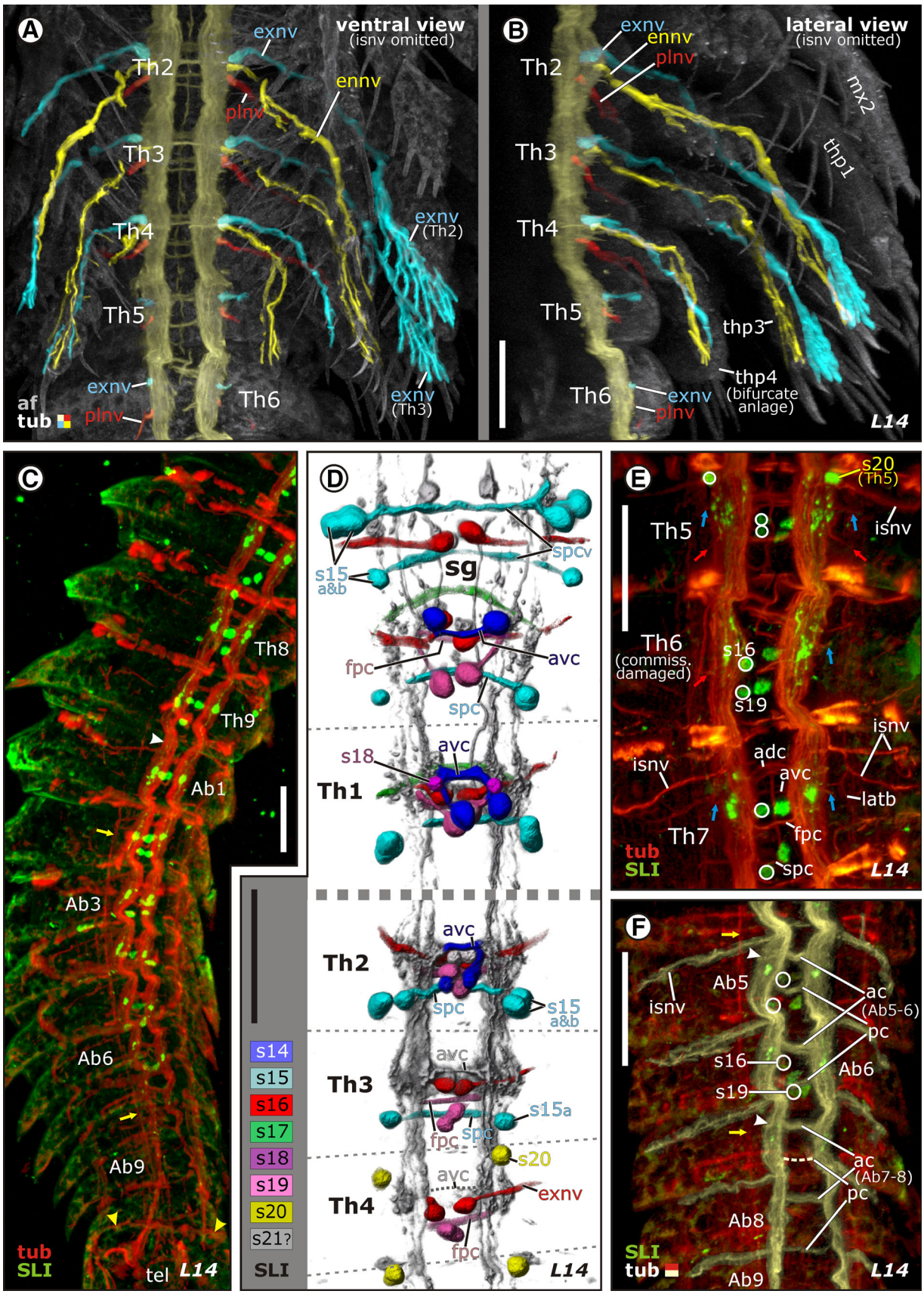
A
ventral view
(isnv omitted)
exnv
ennv
plnv
Th2
Th3
Th4
Th5
Th6
exnv (Th2)
exnv (Th3)
af tub
B
lateral view
(isnv omitted)
mx2
thp1
thp3
thp4 (bifurcate anlage)
L14
C
Th8
Th9
Ab1
Ab3
Ab6
Ab9
tub SLI
tel
L14
D
sg
spcv
s15 a&b
fpc
avc
spc
s18
Th1
Th2
Th3
Th4
s15a
s20
s14
s15
s16
s17
s18
s19
s20
s21?
SLI
L14
E
s20 (Th5)
isnv
Th5
Th6 (commiss. damaged)
s16
s19
adc
latb
Th7
tub SLI
L14
F
Ab5
ac (Ab5-6)
pc
Ab6
ac (Ab7-8)
Ab8
Ab9
SLI tub
L14

◀**Fig. 8** Larval stage L14 focusing on appendage innervation and SLI. Confocal micrographs in Imaris surpass view. **a**, **b** Ventral nerve cord (*bright yellow*), and segmental nerves (*blue*, *yellow*, *red*) artificially masked. The exopodite and posterolateral nerve roots develop before the thoracopod appendage (Th5, Th6), while the endopodite nerve develops alongside it. **c**, **f** *Yellow arrows* indicate longitudinal muscles extending straight through the trunk, while each segmental neuropil displays an anteroventral bulge (*white arrowheads*). **c** Continuity in the external morphology and SL-ir pattern from the prospective thoracic through the abdominal segments. The posterior trunk segments are significantly shorter. *Arrowheads* indicate the last prospective segment border. **d** Individually identified SL-ir neurons artificially highlighted. s20 of Th4 and Th5 is transiently SL-ir in L14, but not in the adult. SL-ir neurons s15a and s15b appear only when the segmental limb is fully developed. **e** *Blue* and *red arrows* indicate exopodite and posterolateral nerve roots, respectively. **f** In the prospective abdomen, the adult-like pattern of two commissures and two SL-ir neurons occurs as far posteriorly as Ab6. *Abbreviations* ac, anterior commissure; adc, avc, anterodorsal and anteroventral commissure; af, autofluorescence; ennv, exnv, endopodite and exopodite nerve; isnv, intersegmental nerve; latb, lateral neurite bundle; pc, posterior commissure; plnv, posterolateral nerve; s14-s21?, SL-ir neuron 14 to 21?; SLI, serotonin-like immunoreactivity; tel, telson; thp1-thp4, thoracopod 1 to 4; tub, tubulin staining. *Scale bars* 50 µm

system-related developmental events (nerves, commissures, SL-ir neurons), eleven are consistently temporally correlated with each other *and* with the development of the limbs, throughout the segments of the trunk. In contrast, none of the 16 nervous system-related events studied is correlated with the timing of molts (indicated by gaps between gray boxes in Fig. 9).

In the thorax, only four of the 16 neural events studied deviate significantly from the uniform intersegmental developmental sequence. These are the development of the exopodite nerve root, the development of the second posterior commissure, and the appearance of SL-ir neurons s14 and s20 (intersegmental differences indicated by black stars in Fig. 9). Only one inconsistency in the sequence may be related to the thorax/abdomen boundary, and that is the temporal order of development of the intersegmental nerve and anterodorsal/anterior commissure (see Fig. 9). However, as these structures were observed synchronously in most segments, this inconsistency could also be related to the Ab1/Ab2 boundary. In essence, then, it can be stated that the cephalocarid thorax and abdomen are not distinguished by tagma-specific developmental patterns.

Olesen et al. (2011) noted with respect to external morphology that all the cephalocarid trunk segments develop in more or less the same way. After formation, each trunk segment is ring-shaped and bears a pair of lateral spines. The authors termed this initial external morphology "abdominal" as it is retained by all abdominal

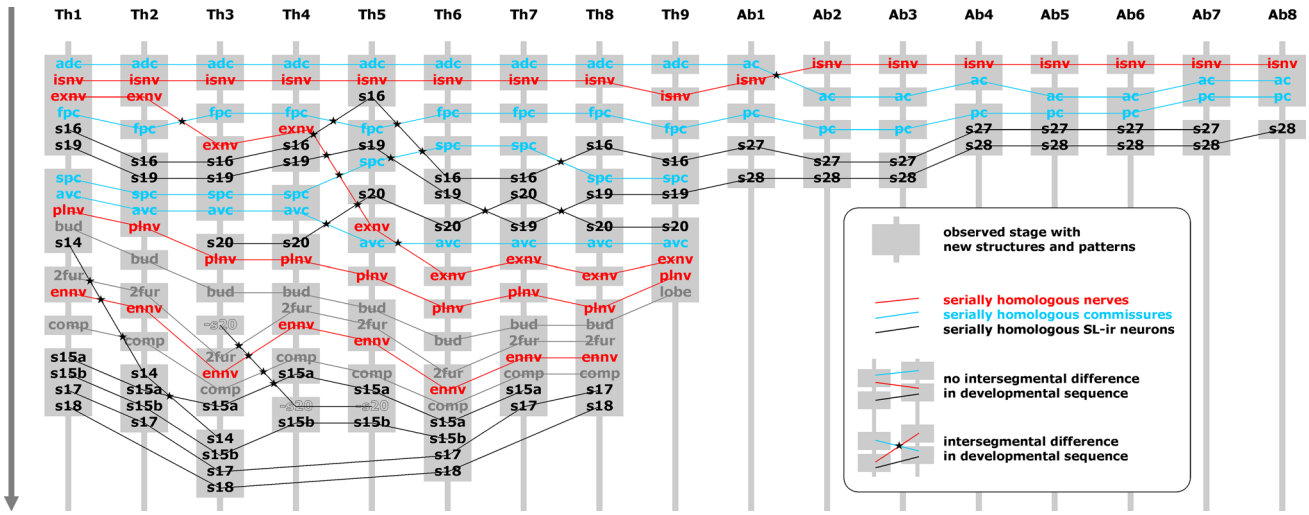

Fig. 9 Comparison of developmental sequence of each trunk segment. The two posteriormost abdominal segments Ab9 and Ab10 are not depicted, because their only serially homologous neural features are the respective intersegmental nerves. Based on Table 3, this schematic diagram illustrates the developmental sequence observed in each trunk segment, irrespective of larval stages and molts, until the adult pattern is complete. *Each gray box* represents a stage in which new nerves, commissures, or SL-ir neurons develop or in which the degree of development of the thoracopod changes. In other words, *each gray box* comprises a set of developmental events. The order of many developmental events observed in this study could not be resolved. Events observed synchronously are arranged here in the way that corresponds most closely to the developmental sequence of neighboring segments. Assuming serial homology across the trunk (indicated by *red*, *blue*, *black*, and *gray lines*), differences in the developmental sequences of neighboring segments are indicated by a *black star*. Our data imply that the developmental sequences of all trunk segments are broadly the same. *Abbreviations* 2fur, bifurcate appendage anlage; ac, adc, avc, anterior, anterodorsal, and anteroventral commissure; bud, appendage bud; comp, appendage complete; ennv, exnv, endopodite and exopodite nerve; fpc, first posterior commissure; isnv, intersegmental nerve; lobe, bud-like thoracopod 9; pc, posterior commissure; plnv, posterolateral nerve; s14 to s28, SL-ir neurons 14–28 ("-s20" means SLI is lost); spc, second posterior commissure

segments until the adult stage (see Sanders 1963; Addis et al. 2007; Olesen et al. 2011). In contrast, the thoracic segments pass through this morphology and continue to develop further, flattening dorsoventrally, growing their lateral spines into wing-shaped pleurae, and differentiating their limbs until they reach the adult stage (Sanders 1963; Addis et al. 2007; Olesen et al. 2011). The degree of this transformation is smaller in the posterior segments of the developing thorax and differs between species (Carcupino et al. 2006).

Where the nervous system is concerned, the situation appears more complex. The developmental sequence of all three neural patterns investigated here (nerves, commissures, and SL-ir neurons) is consistent throughout the trunk, e.g., the first nerve to develop is always the intersegmental nerve, and the first two commissures and the first two SL-ir neurons to develop are the same across the thorax and the abdomen (see Fig. 9; minor exception in Th5). These neural features are the only ones present in the adult abdomen, while in the developing thorax additional neural features keep appearing until the adult stage is reached. Differentiation of the developing abdominal segments appears to stop at a certain stage, which ultimately results in the adult trunk region-specific external (e.g., Carcupino et al. 2006; Olesen et al. 2011) and neuroanatomical patterns (Stegner et al. 2014a) that have been described for Cephalocarida. Interestingly, those neural features which are exclusive to the abdomen never occur at the same stage in the developing thorax, which shows that no thoracic segment passes through a truly "abdominal"-like stage during its development, contradicting what has been suggested on the basis of external morphology (Olesen et al. 2011).

Olesen et al. (2011) interpreted the formation of separate abdominal segments *before* the development of limbs in all thoracic segments as an autapomorphy of Cephalocarida, assuming that in all other entomostracan taxa, abdominal segments are formed only "after thorax segmentation has been completed and all thoracomeres bear appendages" (Olesen et al. 2011: their p. 476). This is certainly the case in the anostracan branchiopod *Artemia* (e.g., Schrehardt 1987) and the cyclopoid copepod *Apocyclops dengizicus* (Anandan et al. 2013). However, there are entomostracans apart from Cephalocarida in which separate abdominal segments develop before the thoracic limbs—these include the mystacocarid *Derocheilocaris remanei* (Haug et al. 2011) but also some calanoid (Golez et al. 2004) and harpacticoid copepods (Carter and Bradford 1972; Carotenuto 1999). In these taxa, differences in the external development of the thorax and abdomen are smaller than might be expected on the basis of Olesen et al. (2011). Given that Mystacocarida is the only comparable entomostracan taxon apart from Cephalocarida to exhibit both thoracic and abdominal ganglia in the adult (Brenneis and Richter 2010), a neurodevelopmental study into Mystacocarida could illuminate whether morphological consistencies between the thorax and abdomen also extend to neural development.

Neurogenesis in Cephalocarida

Growth zone

Scholtz and Wolff (2013) defined the growth zone in Malacostraca (Dohle 1972; Scholtz 1992), anostracan Branchiopoda (Williams et al. 2012), and other arthropods, as "the embryonic region from which the cells originate (encompassing some growth) that are subsequently involved in elongation and segment formation." This definition clearly applies to the growth zone of Cephalocarida. In the developing arthropod trunk, the *proliferation* of new cells from posterior to anterior on the one hand and the *differentiation* of these cells within metameric (parasegmental and segmental) units from anterior to posterior on the other are two independent developmental processes (Williams et al. 2012; Scholtz and Wolff 2013). However, cell proliferation and pattern differentiation also occur, and sometimes even predominantly, in more anterior segments than the growth zone (Mayer et al. 2010). In Cephalocarida, mitotic cell divisions are prevalent in but not restricted to the growth zone. *H. macracantha* appears to differ from all other studied arthropods in that the processes of proliferation and differentiation occur in extremely close physical and temporal proximity when the trunk neuromeres begin developing. We suggest that in *H. macracantha*, the differentiation of the first cells into neurons begins immediately after proliferation, directly anterior to the growth zone. This explains the unique phenomenon whereby each new ganglion anlage that is formed in the trunk ending in the course of the anameric larval phase exhibits a distinct soma cortex, an anterodorsal/anterior commissure, and an anteriorly adjacent intersegmental nerve *before* it is displaced from the growth zone by a more posterior, younger ganglion anlage. Other segmental neural features such as segmental nerves, additional commissures, and SL-ir neurons emerge later on as neuronal differentiation and patterning continue from anterior to posterior, as is the case in other crustaceans with anameric development (e.g., Branchiopoda: Fritsch et al. 2013; Malacostraca: Vilpoux et al. 2006; Ungerer et al. 2011b). The mitotic cells in the developing trunk of *H. macracantha* are arranged irregularly and divide with no preferred orientation either in the growth zone or in the ganglion anlagen. This is in clear contrast to Malacostraca, where the growth zone consists of a distinct row of posterior ectoteloblasts that give rise to well-distinguished

generations of ectodermal cells that are arranged, before segmentation and neuronal differentiation take place, in a regular geometrical pattern (e.g., Dohle 1976; Scholtz 1992; Dohle and Scholtz 1997; Dohle et al. 2004).

Neuroblasts and ganglion mother cells

The apical large cell and adjacent row of three smaller inward-pointing cells here observed in a stage L1 specimen of *H. macracantha* on each side of the growth zone (see Fig. 5b) is an arrangement reminiscent of that of the neuroblasts and ganglion mother cells in Malacostraca (Dohle and Scholtz 1988; Harzsch et al. 1998; Ungerer and Scholtz 2008) and Branchiopoda (Gerberding 1997; Ungerer et al. 2011a). In both latter taxa, ectodermal stem cells divide equally and tangentially to give rise to new stem cells or neuroblasts, all of which remain in the apical cell layer and remain about the same size as other apical cells (summarized in Brenneis et al. 2013). Conforming to this pattern, the apical cells in the growth zone of *H. macracantha* are also evenly sized. In contrast, individual neuroblasts in Hexapoda immigrate from the apical, neuroectodermal stem cell layer and soon grow significantly larger than the apical cells (Hartenstein et al. 1994; Bossing et al. 1996; Wheeler et al. 2003). In all studied tetraconates, each neuroblast divides unequally to give rise to a number of smaller ganglion mother cells that are initially arranged in a row oriented orthogonally to the apical cell layer (Hartenstein et al. 1994; Ungerer and Scholtz 2008; Ungerer et al. 2011a). A comparable arrangement is formed by the three inward-pointing cells here observed on each side of the growth zone in *H. macracantha.* In other tetraconates, the ganglion mother cells later divide equally into the first ganglion cells (e.g., Hartenstein et al. 1994; Ungerer and Scholtz 2008; Ungerer et al. 2011a). Since the ultimate fate of the large apical and three smaller inward-pointing cells in *H. macracantha* could not be traced, it is not possible to identify them definitively as neuroblasts and ganglion mother cells. The proximity between the distinctly arranged cells in the cephalocarid growth zone and the directly adjacent developing ganglion anlage would support the hypothesis that they are neuronal precursors. The lack of comparable cell arrangements in other studied specimens of *H. macracantha* may imply that these arrangements persist only for a short time—and that the differentiation of ectodermal cells via neuroblasts and ganglion mother cells into ganglion cells may happen extremely rapidly.

Acknowledgments We are grateful to Georg Brenneis for his valuable spadework in immunolabeling some specimens. Thanks to George Hampson, Steve Aubrey, Christian Wirkner, Günther Jirikowski, Jonas Keiler, Bastian-Jesper Klußmann-Fricke, Martin Fritsch, and all the volunteers who helped collect cephalocarids. We thank Simone Bourgeois and the late Arthur Dutra from SeaLab, New Bedford, who kindly offered their laboratory and help during our collecting trips. We are grateful to Caterina Biffis, Steffen Harzsch, Joachim Haug, Günther Jirikowski, Carsten Wolff, and Gerhard Scholtz for their expert opinions. We appreciate the suggestions and comments of two anonymous reviewers and thank Lucy Cathrow for improving the English. Finally, we thank the German Science Foundation (DFG) for funding this project (RI 837/10-1,2) as part of the DFG priority program Deep Metazoan Phylogeny.

References

Addis A, Biagi F, Floris A, Puddu E, Carcupino M (2007) Larval development of *Lightiella magdalenina* (Crustacea, Cephalocarida). Mar Biol 152(3):733–744

Anandan P, Krishnamurthy R, Altaff K (2013) Studies on different stages of post-embryonic development of cyclopoid copepod *Apocyclops dengizicus*. Int J Curr Microbiol Appl Sci 2(2):20–27

Blanchard CE (1986) Early development of the thorax and the nervous system of the brine shrimp *Artemia*. Dissertation, University of Leicester

Bossing T, Udolph G, Doe CQ, Technau GM (1996) The embryonic central nervous system lineages of *Drosophila melanogaster*. 1. Neuroblast lineages derived from the ventral half of the neuroectoderm. Dev Biol 179(1):41–64

Brenneis G, Richter S (2010) Architecture of the nervous system in Mystacocarida (Arthropoda, Crustacea): an immunohistochemical study and 3D-reconstruction. J Morphol 271(2):169–189

Brenneis G, Stollewerk A, Scholtz G (2013) Embryonic neurogenesis in *Pseudopallene* sp. (Arthropoda, Pycnogonida) includes two subsequent phases with similarities to different arthropod groups. EvoDevo 4(32):1–36

Carcupino M, Floris A, Addis A, Castelli A, Curini-Galletti M (2006) A new species of the genus *Lightiella*: the first record of Cephalocarida (Crustacea) in Europe. Zool J Linn Soc 148(2):209–220

Carotenuto Y (1999) Morphological analysis of larval stages of *Temora stylifera* (Copepoda, Calanoida) from the Mediterranean Sea. J Plankton Res 21(9):1613–1632

Carter ME, Bradford JM (1972) Postembryonic development of three species of freshwater harpacticoid Copepoda. Smithson Contrib Zool 119:1–26

Dahms HU (2000) Phylogenetic implications of the crustacean nauplius. Hydrobiology 417:91–99

Deutsch JS (2001) Are Hexapoda members of the Crustacea? Evidence from comparative developmental genetics. Ann Soc Entomol Fr 37(1–2):41–49

Dohle W (1972) Über die Bildung und Differenzierung des postnauplialen Keimstreifs von *Leptochelia* spec. (Crustacea, Tanadaicea). Zool Jahrb Abt Anat Ontog Tiere 89:503–566

Dohle W (1976) Die Bildung und Differenzierung des postnauplialen Keimstreifs von *Diastylis rathkei* (Crustacea, Cumacea). II. Die Differenzierung und Musterbildung des Ektoderms. Zoomorph 84(3):235–277

Dohle W, Scholtz G (1988) Clonal analysis of the crustacean segment: the discordance between genealogical and segmental borders. Development 104:147–160

Dohle W, Scholtz G (1997) How far does cell lineage influence cell fate specification in crustacean embryos? Semin Cell Dev Biol 8:379–390

Dohle W, Gerberding M, Hejnol A, Scholtz G (2004) Cell lineage, segment differentiation, and gene expression in crustaceans. In: Scholtz G (ed) Evolutionary developmental biology of

Crustacea. A.A. Balkema, Lisse, Abingdon, Exton (PA), Tokyo, pp 95–134
Elofsson R (1992) Monoaminergic and peptidergic neurons in the nervous system of *Hutchinsoniella macracantha* (Cephalocarida). J Crust Biol 12(4):531–536
Elofsson R, Hessler RR (1990) Central nervous system of *Hutchinsoniella macracantha* (Cephalocarida). J Crust Biol 10(3):423–439
Fischer AHL, Scholtz G (2010) Axogenesis in the stomatopod crustacean *Gonodactylaceus falcatus* (Malacostraca). Invertebr Biol 129(1):59–76
Fritsch M, Richter S (2010) The formation of the nervous system during larval development in *Triops cancriformis* (Bosc) (Crustacea, Branchiopoda): an immunohistochemical survey. J Morphol 271(12):1457–1481
Fritsch M, Richter S (2012) Nervous system development in Spinicaudata and Cyclestherida (Crustacea, Branchiopoda): comparing two different modes of indirect development by using an event pairing approach. J Morphol 273(7):672–695
Fritsch M, Bininda-Emonds ORP, Richter S (2013) Unraveling the origin of Cladocera by identifying heterochrony in the developmental sequences of Branchiopoda. Front Zool 10:35
Gerberding M (1997) Germ band formation and early neurogenesis of *Leptodora kindti* (Cladocera): first evidence for neuroblasts in the entomostracan crustaceans. Invertebr Reprod Dev 31(1):63–73
Golez SN, Takahashi T, Ishimaru T, Ohno A (2004) Post-embryonic development and reproduction of *Pseudodiaptomus annandalei* (Copepoda: Calanoida). Plankton Biol Ecol 51(1):15–25
Gruner H-E (1993) 1. Klasse Crustacea. In: Gruner H-E, Moritz M, Dunger W (eds) Lehrbuch der Speziellen Zoologie. Begründet von Alfred Kästner. 4. Teil: Arthropoda (ohne Insecta). Gustav Fischer Verlag, Jena, Stuttgart, New York, pp 448–1030
Harrison PJH, Sandeman DC (1999) Morphology of the nervous system of the barnacle cypris larva (*Balanus amphitrite* Darwin) revealed by light and electron microscopy. Biol Bull Woods Hole 197:144–158
Hartenstein V, Younossi-Hartenstein A, Lekven A (1994) Delamination and division in the *Drosophila* neurectoderm: spatiotemporal pattern, cytoskeletal dynamics, and common control by neurogenic and segment polarity genes. Dev Biol 165(2):480–499
Harzsch S (2003) Evolution of identified arthropod neurons: the serotonergic system in relation to engrailed-expressing cells in the embryonic ventral nerve cord of the American lobster *Homarus americanus* Milne Edwards, 1873 (Malacostraca, Pleocyemata, Homarida). Dev Biol 258(1):44–56
Harzsch S (2006) Neurophylogeny: architecture of the nervous system and a fresh view on arthropod phylogeny. Integr Comp Biol 46(2):162–194
Harzsch S (2007) The architecture of the nervous system provides important characters for phylogenetic reconstructions: examples from the Arthropoda. Species, Phylogeny and Evolution 1:33–57
Harzsch S, Dawirs RR (1995) A developmental study of serotonin-immunoreactive neurons in the larval central nervous system of the spider crab *Hyas araneus* (Decapoda, Brachyura). Invertebr Neurosci 1:53–65
Harzsch S, Glötzner J (2002) An immunohistochemical study of structure and development of the nervous system in the brine shrimp *Artemia salina* Linnaeus, 1758 (Branchiopoda, Anostraca) with remarks on the evolution of the arthropod brain. Arthropod Struct Dev 30(4):251–270
Harzsch S, Miller J, Benton J, Dawirs RR, Beltz B (1998) Neurogenesis in the thoracic neuromeres of two crustaceans with different types of metamorphic development. J Exp Biol 201(17):2465–2479
Haug JT, Waloszek D, Haug C, Maas A (2010) High-level phylogenetic analysis using developmental sequences: the Cambrian dagger *Martinssonia elongata*, dagger *Musacaris gerdgeyeri* gen. et sp. nov. and their position in early crustacean evolution. Arthropod Struct Dev 39(2–3):154–173
Haug JT, Olesen J, Maas A, Waloszek D (2011) External morphology and post-embryonic development of *Derocheilocaris remanei* (Mystacocarida) revisited, with a comparison to the Cambrian taxon *Skara*. J Crust Biol 31(4):668–692
Hessler RR, Elofsson R (1992) Cephalocarida. In: Harrison FW (ed) Microscopic anatomy of invertebrates. Wiley-Liss, New York, pp 9–24
Hessler RR, Elofsson R, Hessler AY (1995) Reproductive system of *Hutchinsoniella macracantha* (Cephalocarida). J Crust Biol 15(3):493–522
Jirikowski GJ, Richter S, Wolff C (2013) Myogenesis of Malacostraca: the "egg-nauplius" concept revisited. Front Zool 10:76
Koenemann S, Olesen J, Alwes F, Iliffe TM, Hoenemann M, Ungerer P, Wolff C, Scholtz G (2009) The post-embryonic development of Remipedia (Crustacea): additional results and new insights. Dev Genes Evol 219(3):131–145
Lacalli TC (2009) Serial EM analysis of a copepod larval nervous system: naupliar eye, optic circuitry, and prospects for full CNS reconstruction. Arthropod Struct Dev 38(5):361–375
Lauterbach K-E (1983) Zum Problem der Monophylie der Crustacea. Verh Naturwiss Vereins Hamburg 26:293–320
Lauterbach K-E (1986) Zum Grundplan der Crustacea. Verh Naturwiss Vereins Hamburg 28:27–63
Loesel R, Richter S (2014) Neurophylogeny: from description to character analysis. In: Wägele JW, Bartolomaeus T (eds) Deep metazoan phylogeny: the backbone of the tree of life. De Gruyter, Berlin, pp 505–514
Loesel R, Wolf H, Kenning M, Harzsch S, Sombke A (2013) Architectural principles and evolution of the arthropod central nervous system. In: Minelli A, Boxshall GA, Fusco G (eds) Arthropod biology and evolution: molecules, development, morphology. Springer, Heidelberg, pp 299–342
Martin JW, Olesen J, Hoeg JT (2014) Atlas of crustacean larvae. John Hopkins University Press, Baltimore
Mayer G, Kato C, Quast B, Chisholm RH, Landman KA, Quinn LM (2010) Growth patterns in Onychophora (velvet worms): lack of a localised posterior proliferation zone. BMC Evol Biol 10:339
Minelli A, Fusco G (2013) Arthropod post-embryonic development. In: Minelli A, Boxshall GA, Fusco G (eds) Arthropod biology and evolution: molecules, development, morphology. Springer, Heidelberg, pp 91–122
Minelli A, Brena C, Deflorian G, Maruzzo D, Fusco G (2006) From embryo to adult. Beyond the conventional periodization of arthropod development. Dev Genes Evol 216:373–383
Olesen J, Haug JT, Maas A, Waloszek D (2011) External morphology of *Lightiella monniotae* (Crustacea, Cephalocarida) in the light of Cambrian 'Orsten' crustaceans. Arthropod Struct Dev 40(5):449–478
Richter S, Loesel R, Purschke G, Schmidt-Rhaesa A, Scholtz G, Stach T, Vogt L, Wanninger A, Brenneis G, Döring C, Faller S, Fritsch M, Grobe P, Heuer CM, Kaul S, Møller OS, Müller CHG, Rieger V, Rothe BH, Stegner MEJ, Harzsch S (2010) Invertebrate neurophylogeny: suggested terms and definitions for a neuroanatomical glossary. Front Zool 7:29
Sanders HL (1963) The Cephalocarida. Mem Conn Acad Arts Sci 15:1–80
Scholtz G (1992) Cell lineage studies in the crayfish *Cherax destructor* (Crustacea, Decapoda): germ band formation, segmentation, and early neurogenesis. Roux Arch Dev Biol 202(1):36–48
Scholtz G (2000) Evolution of the nauplius stage in malacostracan crustaceans. J Zool Syst Evol Res 38(3):175–187

Scholtz G, Wolff C (2013) Arthropod embryology: cleavage and germ band development. In: Minelli A, Boxshall GA, Fusco G (eds) Arthropod biology and evolution: molecules, development, morphology. Springer, Heidelberg, pp 63–90

Schrehardt A (1987) A scanning electron-microscope study of the post-embryonic development of *Artemia*. In: Sorgeloos P, Bengston DA, Decleir W, Jaspers E (eds) *Artemia* research and its applications, vol 1., Morphology, genetics, strain characterization, toxicologyUniversa Press, Wetteren, pp 5–32

Semmler H, Wanninger A, Hoeg JT, Scholtz G (2008) Immunocytochemical studies on the naupliar nervous system of *Balanus improvisus* (Crustacea, Cirripedia, Thecostraca). Arthropod Struct Dev 37(5):383–395

Smith KK (2001) Heterochrony revisited: the evolution of developmental sequences. Biol J Linn Soc 73:169–186

Stegner MEJ, Richter S (2011) Morphology of the brain in *Hutchinsoniella macracantha* (Cephalocarida, Crustacea). Arthropod Struct Dev 40:221–243

Stegner MEJ, Fritsch M, Richter S (2014a) The central complex in Crustacea. In: Wägele JW, Bartolomaeus T (eds) Deep metazoan phylogeny: the backbone of the tree of life. De Gruyter, Berlin, pp 361–384

Stegner MEJ, Brenneis G, Richter S (2014b) The ventral nerve cord in Cephalocarida (Crustacea): new insights into the ground pattern of Tetraconata. J Morphol 275(3):269–294

Stemme T, Iliffe TM, von Reumont BM, Koenemann S, Harzsch S, Bicker G (2013) Serotonin-immunoreactive neurons in the ventral nerve cord of Remipedia (Crustacea): support for a sister group relationship of Remipedia and Hexapoda? BMC Evol Biol 13:119

Strausfeld N (2012) Arthropod brains: evolution, functional elegance, and historical significance. Harvard University Press, Cambridge

Ungerer P, Scholtz G (2008) Filling the gap between identified neuroblasts and neurons in crustaceans adds new support for Tetraconata. Proc R Soc B Biol Sci 275(1633):369–376

Ungerer P, Eriksson BJ, Stollewerk A (2011a) Neurogenesis in the water flea *Daphnia magna* (Crustacea, Branchiopoda) suggests different mechanisms of neuroblast formation in insects and crustaceans. Dev Biol 357(1):42–52

Ungerer P, Geppert M, Wolff C (2011b) Axogenesis in the central and peripheral nervous system of the amphipod crustacean *Orchestia cavimana*. Integr Zool 6(1):28–44

Vilpoux K, Sandeman R, Harzsch S (2006) Early embryonic development of the central nervous system in the Australian crayfish and the Marbled crayfish (Marmorkrebs). Dev Genes Evol 216(4):209–223

Walley LJ (1969) Studies on the larval structure and metamorphosis of *Balanus balanoides* (L.). Phil Trans R Soc B Biol Sci 256:183–279

Walossek D (1993) The upper Cambrian *Rehbachiella kinnekullensis* and the phylogeny of Branchiopoda and Crustacea. Foss Strat 32:1–202

Walossek D, Müller KJ (1990) Upper Cambrian stem-lineage crustaceans and their bearing upon the position of *Agnostus*. Lethaia 23:409–427

Wheeler SR, Carrico ML, Wilson BA, Brown SJ, Skeath JB (2003) The expression and function of the achaete-scute genes in *Tribolium castaneum* reveals conservation and variation in neural pattern formation and cell fate specification. Development 130(18):4373–4381

Wildt A, Goergen EM, Benton JL, Sandeman DC, Beltz BS (2004) Regulation of serotonin levels by multiple light-entrainable endogenous rhythms. J Exp Biol 207(21):3765–3774

Williams T, Blachuta B, Hegna TA, Nagy LM (2012) Decoupling elongation and segmentation: Notch involvement in anostracan crustacean segmentation. Evol Dev 14(4):372–382

Schlussteil

14. Publikationen und Tagungsbeiträge

Publikationen

Stegner MEJ, Richter S: The nervous system in Cephalocarida. In: Structure and evolution of invertebrate nervous systems. Schmidt-Rhaesa A, Harzsch S, Purschke G (Hrsg). Oxford University Press (im Druck).

Stegner MEJ, Richter S (2015): Development of the nervous system in Cephalocarida: Early neuronal differentiation and successive patterning. Zoomorphology 134:183-209.

Stegner MEJ, Stemme T, Iliffe T, Richter S, Wirkner CS (2015): The brain in three crustaceans from cavernous darkness. BMC Neuroscience 16:19.

Stegner MEJ (2015): What can the brains of blind crustaceans tell us about evolving in the dark? BMC Series Blog, 7. April 2015.

Stegner MEJ, Fritsch M, Richter S (2014): The central complex in Crustacea. In: Deep Metazoan Phylogeny: The backbone of the Tree of Life. Wägele JW, Bartolomäus T (Hrsg). Berlin: de Gruyter. S. 361-384.

Stegner MEJ, Brenneis G, Richter S (2014): The ventral nerve cord of Cephalocarida (Crustacea): New insights into the ground pattern of Tetraconata. Journal of Morphology 275:269-294.

Stegner MEJ, Richter S (2011): Morphology of the brain in *Hutchinsoniella macracantha* (Cephalocarida, Crustacea). Arthropod Structure and Development 40: 221-243.

Richter S, Loesel R, Purschke G, Schmidt-Rhaesa A, Scholtz G, Stach T, Vogt L, Wanninger A, Brenneis G, Döring C, Faller S, Fritsch M, Grobe P, Heuer CM, Kaul S, Møller OS, Müller CHG, Rieger V, Rothe BH, Stegner MEJ, Harzsch S (2010): Invertebrate neurophylogeny: suggested terms and definitions for a neuroanatomical glossary. Frontiers in Zoology 7:29.

Tagungsbeiträge

Stegner MEJ, Richter S (2014): Development of the nervous system in Cephalocarida (Crustacea) – early neuronal differentiation and successive patterning. 3. International Congress on Invertebrate Morphology (ICIM3), Berlin, 3.-7. August 2014. (Vortrag).

Stegner MEJ, Richter S (2013): The nervous system in Cephalocarida – how complexity in an ancient crustacean helps unravel the phylogeny of Tetraconata. XXXII. Meeting der Willi Hennig Society, Rostock, 3.-7. August 2013. (Vortrag)

Stegner MEJ, Stemme T, Richter S (2011): The ventral nerve cord in Cephalocarida and Remipedia (Crustacea) – synapomorphic or symplesiomorphic within

Tetraconata? Deep Metazoan Phylogeny 2011 - new data, new challenges, München, 11.-14. Oktober 2011. (Poster)

Stegner MEJ, Stemme T, Richter S (2011): The nervous system in Cephalocarida and Remipedia – new implications for tetraconate phylogeny. 2nd International Congress on Invertebrate Morphology, Cambridge, Massachusetts (USA), 20.-23. Juni 2011. (Vortrag)

Stegner MEJ, Richter S (2011): The multilobed complex in Cephalocarida (Crustacea) – a secondary olfactory center with detailed correspondences to Insecta and Chilopoda. 15. Crustaceologentagung, Regensburg, 7.-10. April 2011. Jury-Preis für das beste Poster auf dem 2nd International Congress on Invertebrate Morphology, Cambridge, Massachusetts (USA), 20.-23. Juni 2011. (Poster)

Stegner MEJ, Richter S (2011): Morphologie des Nervensystems der Cephalocarida unter phylogenetischem Blickwinkel. 15. Crustaceologentagung, Regensburg, 7.-10. April 2011. (Vortrag)

Stegner MEJ, Richter S (2011): Das Nervensystem der Cephalocarida unter phylogenetischem Blickwinkel. DFG-Statusseminar, SPP Deep Metazoan Phylogeny, Hannover, 28.-29. Januar 2011. (Vortrag)

Stegner MEJ, Richter S (2010)**:** A phylogenetic perspective on the nervous system in Cephalocarida. 7th *International Crustacean* Congress, Qingdao (China), 20.-25. Juni 2010 (Vortrag)

Stegner MEJ, Brenneis G, Richter S (2009)**:** Brain anatomy in Cephalocarida. 102. Jahrestagung der Deutschen Zoologische Gesellschaft, Regensburg, 25.-28. September 2009. (Vortrag)

Stegner MEJ, Brenneis G, Richter S (2009)**:** The anatomy of the nervous system in Cephalocarida. Evolution of the arthropod nervous system, Jena, 6.-8. September 2009. (Vortrag)

Stegner MEJ, Richter S, Wirkner CS (2009)**:** Evolutionäre Morphologie des Gehirns der Peracarida. 14. Crustaceologentagung, Rostock, 2.-5. April 2009. (Vortrag)

Stegner MEJ, Brenneis G, Richter S (2009)**:** Immunohistochemical survey on the central nervous system in *Hutchinsoniella macracantha* (Cephalocarida). Celebrating Darwin: From *The Origin of Species* to Deep Metazoan Phylogeny, Berlin, 4.-6. März 2009. (Poster)

Stegner MEJ, Richter S, Wirkner CS (2008)**:** Evolutionary morphology of the brain in Peracarida. 1st International Congress on Invertebrate Morphology, Kopenhagen (Dänemark), 17.-21. August 2008. Jury-Preis für das beste Poster der Fachgruppe Morphologie auf der 101. Jahrestagung der Deutschen Zoologischen Gesellschaft, 19.-22. September 2008, Jena. (Poster)

15. Danksagung

Ganz besonders möchte ich mich bei Stefan Richter bedanken, der mich während meiner Doktorarbeit intensiv betreut und unterstützt hat. Auch bei detaillierten Fragen stand er mir mit großer Geduld und breitem morphologischen und evolutionstheoretischen Fachwissen zur Seite und gab viele hilfreiche Impulse. Einen großen Dank auch an Steffen Harzsch, dessen neurophylogenetischer Ansatz meinen Blick für die interessantesten Merkmalskomplexe schärfte. Seine Einladungen nach Greifswald ermöglichten mir einen inspirierenden Austausch mit seiner Arbeitsgruppe. Ich danke Georg Brenneis, der mir ein hervorragender Mentor in Sachen Immunhistochemie und konfokale Mikroskopie war und einige wunderschön gefärbte Cephalocariden hinterließ, die in meiner Arbeit Verwendung fanden. Ein dicker Dank an Jakob Krieger und Verena Rieger – sie wiesen mich in die Vibratomtechnik ein. Martin Fritsch war über viele Jahre mein Neuro-Bro in Rostock – ob methodisch im Labor, wohlbelesen im Seminar oder auf den unzähligen Dienstreisen, war er allzeit fritsch gelaunt und immer eine Riesenhilfe. Kerstin Schwandt danke ich für die großartige Semidünnschnittserie von *Hutchinsoniella*, die mir wichtige Erkenntnisse zum multilobierten Komplex lieferte, und Christin Wittfoth für die Konstruktion zweier eleganter Ganglien-3D-Modelle und die Vervollständigung von 3D-Rekonstruktionen im Rumpf. Einen vielfältigen und freudigen wissenschaftlichen Austausch habe ich auch meinen langjährigen Iglu-, Schach- und Rumblefreunden Günther Jirikowski, Martin Schwentner und Jonas Keiler zu verdanken. Für unzählige theoretische und praktische Hilfestellungen und manchen frechen Schüttelreim möchte ich Christian Wirkner danken.

Eine ganz wichtige Grundlage dieser Doktorarbeit waren die Sammelreisen nach New Bedford, die ohne Unterstützer an meiner Seite nie möglich gewesen wären. Ich bin George Hampson und Steve Aubrey mit ihrem Knowhow über geheime Cephalocariden-Standorte ebenso wie Simone Bourgeois und dem inzwischen verstorbenen Arthur Dutra, die uns ihr buntes SeaLab bereitgestellt haben, überaus dankbar. Ich danke auch meinen Rostocker Freunden und Kollegen Christian Wirkner, Günther Jirikowski, Jonas Keiler, Martin Fritsch und Basti Klußmann-Fricke für ihren

Sammeleifer, ihre Ausdauer und den nötigen Humor. Viele Mitglieder meiner Rostocker Arbeitsgruppe habe ich nun schon erwähnt. Namentlich möchte ich noch Helga Kreft, Susi Böx, Kati Huckstorf, Torben Göpel und den ehrwürdigen Scholle hinzufügen, die mich in vieler Weise unterstützten. Aber auch allen anderen Mitarbeitern am Zoologischen Institut danke ich für die herzliche Begleitung durch die vergangenen Jahre. Ein Gruß geht hinaus an alle auswärtigen Zoologen, die mir in vielen interessanten Diskussionen immer wieder Einblicke in ihre aktelle Forschung gaben und so besonders den vergleichenden Teil dieser Arbeit voranbrachten – Torben Stemme, Andy Sombke, Matthes Kenning, Joachim Haug, aber auch Ole Møller, Carsten Müller und viele andere.

Es hat etwas feierliches, dieses morphologische Brikett abzuschließen – es ist ja auch ein Lebensabschnitt, der nun vorübergeht. Ich bin sehr glücklich, dass ich in all den Jahren immer darauf vertrauen konnte, gute Freunde an meiner Seite zu haben – und liebe Eltern, Großeltern, Verwandte, die Anteil an meinem Leben nahmen und mir Kraft gaben. Vielen Dank Euch allen!